UNIVERSITE SCIENCES BRETAGNE DE LA MER LOIRE ET DU LITTORAL

UBO
Université de Bretagne Occidentale

THESE DE DOCTORAT DE

L'UNIVERSITE
DE BRETAGNE OCCIDENTALE
COMUE UNIVERSITE BRETAGNE LOIRE

ECOLE DOCTORALE N° 598
Sciences de la Mer et du littoral
Spécialité : *Microbiologie*

Par
Yang LU

Functional studies of new protein-protein interactions potentially involved in homologous recombination in hyperthermophilic archaea.

Study of interactions between PCNA and Mre11-Rad50 complex & Primase and RadA

Thèse présentée et soutenue à Brest, le 30 novembre 2018
Unité de recherche : Laboratoire de Microbiologie des Environnements Extrêmes (LM2E), UMR6197, Ifremer, CNRS, UBO

Rapporteurs avant soutenance :

Bruno FRANZETTI	Directeur de recherche, IBS, Grenoble
Tamara BASTA-LE BERRE	Maître de conférences, I2BC, Paris

Composition du Jury :

Président du Jury	
Marc BLONDEL	Professeur, UBO, Brest
Bruno FRANZETTI	Directeur de recherche, IBS, Grenoble
Tamara BASTA-LE BERRE	Maître de conférences, I2BC, Paris
Directeur de thèse	
Didier FLAMENT	Chercheur, LMEE/Ifremer/UBO, Brest
Invité(s)	
Mohamed JEBBAR	Professeur, LM2E/UBO, Brest

Acknowledgement

Firstly, I would like to express my sincere gratitude to my advisor Didier FLAMENT for the continuous support of my Ph.D study and related research, to thank him for his patience, motivation, and immense knowledge. His guidance helped me all throughout my research and my writing of this thesis. I could not have imagined a better advisor and mentor to have for my Ph.D study.

Besides my advisor, I would like to thank the other members of my thesis jury: Bruno FRANZETTI, Tamara BASTA-LE BERRE and Mohamed JEBBAR, special thanks for Marc BLONDEL for my thesis committee and my thesis jury, their insightful comments and encouragement, but also for the hard question which drove me to widen my research to various perspectives. Also thanks to another member of my thesis committee, Charlotte CORPOREAU. I would like to express my gratitude to all of the staff of laboratory LMEE for the last minute favors.

I am also grateful to Ifremer and Region de Bretagne for their financial support until the end of this thesis, and Elisabeth Bondu and Frédéric Jean of the EDSML for their administrative supports during these three years of thesis.

My sincere thanks also go to my “replication team”, who provided me with an opportunity to join their team as an intern, and who gave access to the laboratory and research facilities. Ghislaine, my internship supervisor of Master 2, thanks to her help and scientific guidelines, I opened the door of Archaeal World. I would like to thank Audrey BOSSE, who always gave me technical and moral support when I needed it. I would also like to thank Etienne, Sebastien, Remi, who gave me lots of valuable tips on their professional technics such as FRET, SPR and Genetic transformation *in vivo*, to realize different experiments in order to accomplish my research project. I would also like to thank Gaëlle, my important labmate, thanks for all the stimulating discussions, for the days we worked together, for all the helps before deadlines. Without their precious support it would not be possible to conduct this research. I would also like to thank my intern, Damien HUBERDEAU, who helped me to push my research forward. Also I’m grateful to group members from Clouet d’Orval group (LMGM, Toulouse) for all the help of several experimentations.

I am grateful to our secretaries, Christine and Christel, you were always there when I needed to process documents required for administration. Thank you also for all the organization for lab.

A super big thanks goes to all the past and present members of LMEE. In particular, I am grateful to Melanie and Charlene, we started as “office-mates” and finished as “family”, all of the precious memories and your support have been essential throughout these years. Thanks to Marion, thank you to have encouraged and supported me every time when I felt stressed out. A special thanks to my friends and colleagues, Sebastien, Simon, Caroline, Jordan, Sarah, Florian, Clarisse, Marc, Blandine, Johanne, Thomas, Dingding, Huan, Manman, thank you to have been with me in the most important moments of all lab’s life and outside the lab.

Last but not the least, I would like to thank my family: first, my husband, Francis, thank you for standing up for me and supporting me during all these years, to my parents, my grandparents, and my in-laws, Didier and Sylvie, for supporting me spiritually throughout writing this thesis and my life in general.

Table of contents

Abbreviation

°C: degree Celsius
6-MP: 6-methylpurine
A: adenine
ABC: ATP Binding Cassette
AD: ATPase domain
AEPs: Archaeo-eukaryotic primases
AFM: Atomic Force Microscopy
A. fu: *Archaeoglobus fulgidus*
Alt-EJ: Alternative Non-homologous End-joining
AP site: apurinic/apyrimidinic site
ATLD: Ataxia-telangiectasia-like disorder
ATP: adenosine triphosphate
BER: base excision repair
bp: base pair
C: cytosine
CoIP: Co-immunopreciptation
D. amylolyticus: Desulfurococcus amylolyticus
D. radiodurans: Deinococcus radiodurans
D-Loop: displacement loop
DNA: Deoxyribonucleic acid
DPANN: Diapherotrites, Parvarchaeota, Aenigmarchaeota, Nanoarchaeota, Nanohaloarchaea
DSBs: double-strand breaks
DTT: Dithiothreitol
E.coli: Escherichia coli
e.g.: for example
EDTA: Ethylenediaminetetraacetic acid
EM: electron microscope
etc.: *et cetera*
G: guanine
HA: Hyperthermophilic Archaea
HhH: helix-hairpn-helix
HR: homologous recombination
IDCL: Interacting Domain Connection Loop
LC-MS/MS: Liquid chromatography coupled to tandem mass spectrometry
LUCA: last universal common ancestor
MES: 2-(N-morpholino)ethanesulfonic acid
Mj: Methanoccocus jannaschii
MMEJ: microhomology-mediated end joing
MMR: mismatch repair
MOPS: 3-(N-morpholino)propanesulfonic acid
MPa: megapascal
Mpa: Methanocella paludicola
MR: Mre11-rad50
MRN: Mre11-ad50-Nbs1
MutS: Mutator S
NBDs: nucleotide binding domains
NBS: Nijmegen breakage syndrome
NBSLB: NBS-like disorder
NER: nucleotide excision repair
NHEJ: non-homologous end joining
OriC: origin of replicaiton
P. horikoshii: Pyrococcus horikoshii
P.abyssi: Pyrococcus abyssi
P.furiosus: Pyrococcus furiosus
Pab: Pyrococcus abyssi
PAGE: polyacrylamide gel electrophoresis
Pfu: Pyrococcus furiosus
pH: potential of hydronium ions
PIP: PCNA Interacting Protein
PM: Polymerization motif
RBD: Rad50 binding domains
RDR: recombination-dependent replication
RIR: Rev1 interacting region
RNA: Ribonucleic acid
rRNA: ribosomal RNA
S. acidocaldarius: Sulfolobus acidocaldarius
S. cerevisiae: *Saccharomyces cerevisiae*
S. pombe: Schizosaccharomyces pombe
S. solfatarucus: Sulfolobus solfataricus
S.islandicus: Sulfolobus islandicus
SD: subdomain
SDS: sodium dodecyl sulfate
SSA: single-strand annealing
SSBs: single-strand breaks
ssDNA: single-stranded DNA
Sso: Sulfolobus solfataricus
SUMO: small ubiquitin-related modifier
T: thymine
T. barophilus: Thermococcus barophilus
T. maritima: Thermotoga maritima
T.kodakarensis: Thermococcus kodakarensis
TACK: Thaumarchaeota, Aigarchaeota, Crenarchaeota and Korarchaeota
TBE: Tris Borate EDTA

TIP: Thermococcales inhibitior of PCNA
TLS: translesion synthesis
Tm: Thermotoga maritima
U: uracil
UV: Ultraviolet
WT: wild-type
Xp: *xeroderma pigmentosum*
β: bêta
δ: delta
η: êta
ι: iota
λ: lamda
μ: mu
μL: microliter
Mre11: meiotic recombination 11
MRX: Mre11-ad50-Xrs2
MutL: Mutator S
PCNA: proliferating cell nuclear antigen
Pol: polymerase
rad50: Radiation sensitive
RFC: replication factor C
RPA: replication protein A
SSB: single-stranded DNA binding protein
SSB: ssDNA-binding proteins

Amino acid

A: Ala, Alanine
F: Phe, Phenylalanine
I: Ile, Isoleucine
K: Lys, Lysine
L: Leu, Leucine
M: Met, Methionine
Q: Gln, Glutamine
R: Arg, Arginine
V: Val, Valine
W: Trp, Tryptophan
Y: Tyr, Tyrosine

Protein

ATPase: adenylpyrophosphatase
CDKs: cyclin-dependent kinases
EndoMS: endonuclease MS
Fen1: flap endonuclease 1
Fe-S: Iron-sulfur protein
GINS: go-ichi-ni-san, Japanese numbers 5-1-2-3
Hef: Helicase-associated endonuclease for fork-structured DNA
Hjc: Holliday junction cleavage
Hjm: Holliday junction migration
HMG-CoA: 3-hydroxy-3-methylglutaryl coenzymes A
Lig: ligase

List of Figures

List of Tables

INTRODUCTION

I. Hyperthermophilic archaea (HA)

1) Extremophiles

2) Hyperthermophiles

3) Archaea

II. Genomic integrity maintenance in HA

1) DNA replication and repair

2) Biological role of homologous recombination in the repair of DNA

a) DSBs Heat stress-induced DNA double-strand breaks (DSBs)

b) DNA repair

3) Biological role of homologous recombination in DNA replication

a) Replication restart after Fork arrest

b) Recombination-dependent replication (RDR)

III. Proteins interaction network in genome maintenance in HA

I. Hyperthermophilic archaea (HA)

1) Extremophiles

In the 1950s, Zobell's laboratory started the first study of microbiology under extreme conditions, leading to the discovery of barophiles (or piezophiles) (Zobell, 1952). Since then scientists have been intrigued by microorganisms that inhabit extreme environments.

What is an extreme environment? Gomez et *al.* gave us a definition: "*An extreme environment is a habitat characterized by harsh environmental conditions, beyond the optimal range for the development of humans"* (Gomez, 2014). On the planet Earth, life exists not just in a cozy and warm environment, but also under multiple hardest, surprising environments such as deep-sea hydrothermal vents, freezing cold Polar Regions or scorching hot geothermal pools. The extreme conditions may be divided into two categories: "physical extremes" conditions (e.g., temperature (from -20°C to 122°C), ionizing radiation (high energy radiation including X-ray, alpha particles) and pressure (up to 110 Mpa)) and "geochemical extremes" conditions (e.g., desiccation (water limitation), salinity (from 10% to 40%), pH (from 0 to 12.8), oxygen species or redox potential (oxygen content)) (Rothschild & Mancinelli, 2001; Rampelotto, 2010) (Figure 1).

Figure 1 : Examples of different extreme environments

The microorganisms that thrive in extreme conditions are named “extremophiles”. The extremophiles are classified according to the extreme conditions they are adapted to, such as hyperthermophiles (high temperature), psychrophiles (low temperature), acidophiles (low pH), alkaliphiles (high pH), xerophiles (very dry environement), piezophiles (high pressure), halophiles (high salt concentration) and osmophiles (high concentration of organic solutes) (Table 1). (Rothschild & Mancinelli, 2001; Bakermans, 2015).

Table 1 : Classification and examples of extremophiles (Rothschild & Mancinelli, 2001)

Environmental parameter	Type	Definition	Examples
Temperature	Hyperthermophile Thermophile Mesophile Psychrophile	Growth >80 °C Growth 60–80 °C 15–60 °C <15 °C	*Pyrolobus fumarii*, 113 °C *Synechococcus lividis* *Homo sapiens* *Psychrobacter*, some insects
Radiation			*Deinococcus radiodurans*
Pressure	Barophile Piezophile	Weight-loving Pressure-loving	Unknown For microbe, 130 MPa
Gravity	Hypergravity Hypogravity	>1*g* <1*g*	None known None known
Vacuum		Tolerates vacuum (space devoid of matter)	Tardigrades, insects, microbes, seeds
Desiccation	Xerophiles	Anhydrobiotic	*Artemia salina*; nematodes, microbes, fungi, lichens
Salinity	Halophile	Salt-loving (2–5 M NaCl)	Halobacteriaceae, *Dunaliella salina*
pH	Alkaliphile Acidophile	pH > 9 low pH-loving	*Natronobacterium, Bacillus firmus* OF4, *Spirulina* spp. (all pH 10.5) *Cyanidium caldarium*, *Ferroplasma* sp. (both pH 0)
Oxygen tension	Anaerobe Microaerophile Aerobe	Cannot tolerate O_2 Tolerates some O_2 Requires O_2	*Methanococcus jannaschii* *Clostridium* *H. sapiens*
Chemical extremes	Gases Metals	Can tolerate high concentrations of metal (metalotolerant)	*C. caldarium* (pure CO_2) *Ferroplasma acidarmanus* (Cu, As, Cd, Zn); *Ralstonia* sp. CH34 (Zn, Co, Cd, Hg, Pb)

Some microorganisms can be tolerant to multiple extremes, they are called “polyextremophiles”, for example, *Halobacterium salinarum* NRC-1, an archaea that is able to grow between 2.6 and 5.1 M NaCl, and is highly resistant to desiccation, UV radiation and oxygen limitation (Kottemann *et al*, 2005; Leuko *et al*, 2009).

The discovery of extremophiles has been applied in biotechnology e.g., the β-carotene of *Dunaliella salina* (halophilic micro-algae) in cosmetic products; DNA polymerase of *Pyrococcus furiosus* (hypertermophilic archaea) in genetic engineering, etc.) (Oren, 2010; Coker, 2016). Also the studies of their diversity and mechanisms of adaptation to extreme environmental conditions could also help to develop search in astrobiology on the origins of life, on the life outside the Earth and the dispersion of life in the universe (Rampelotto, 2010).

2) Hyperthermophiles

Although “Extremophiles” occur in all three domains of life: Eukarya, Bacteria and Archaea, thermophiles and hyperthermophiles are limited to the Archaea and Bacteria (Figure 2) (Stetter, 2006a).

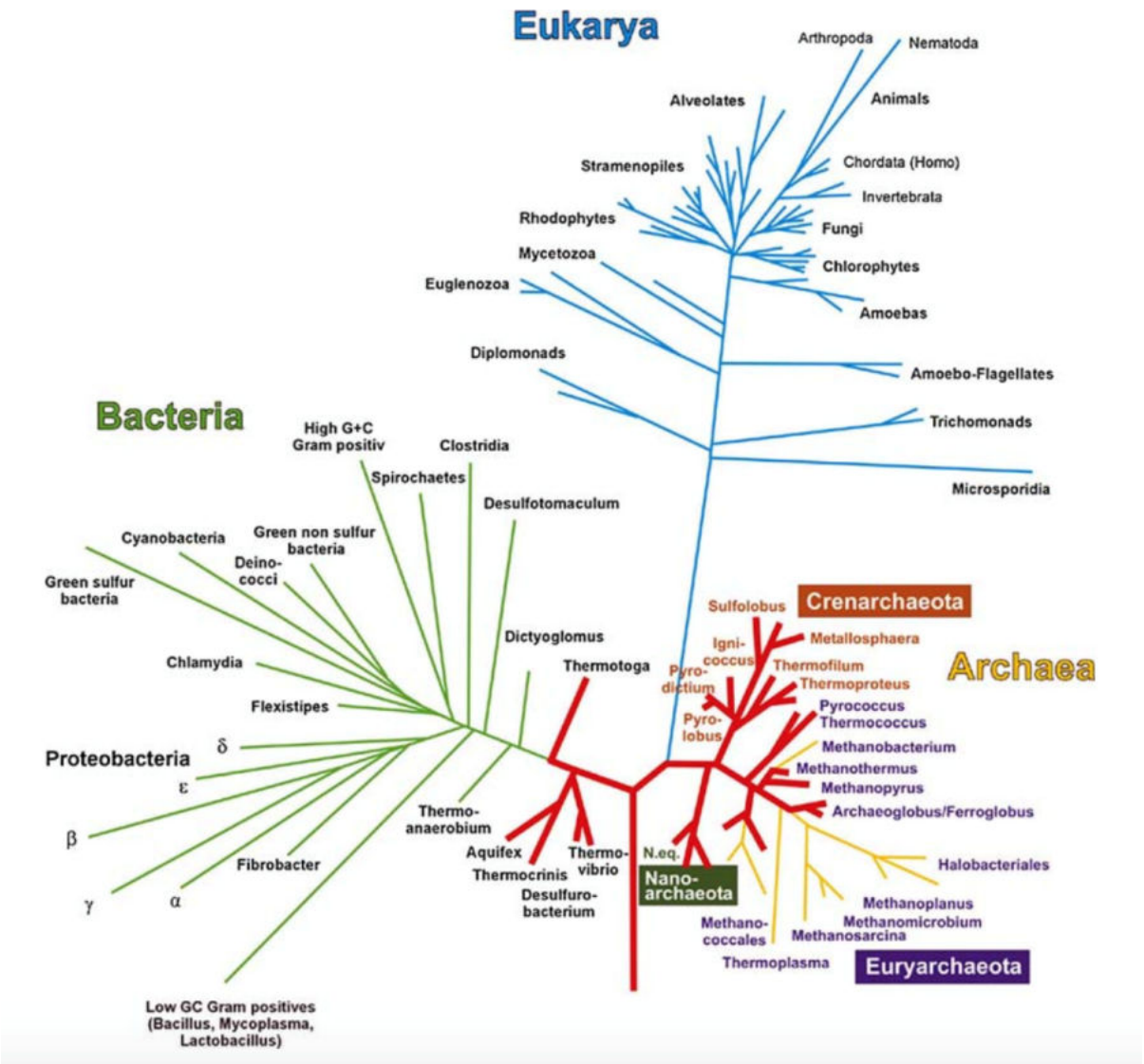

Figure 2 : Phylogenetic tree of the three domains of life inferred from small subunit rRNA sequence. The red bulky lineages represent hyperthermophiles **(Stetter, 2006a)**.

The thermophiles are defined as organisms able to grow in temperature between 45 °C and 80 °C, and the hyperthermophiles are organisms with an optimum growth temperature of 80 °C and above (Rampelotto, 2010), with *Methanopyrus kandleri* (Euryarchaeota), capable of growing at the highest temperature of 116 °C and tolerant up to 122°C (Takai *et al*, 2008). The first hyperthermophile was discovered in 1981 by Stetter and workmates (Stetter *et al*, 1981). The early 20th century, more than 70 species, 29 genera, and 10 orders of hyperthermophiles are known, only two of them are bacteria: *Thermotogales* and *Aquificales* (Vieille & Zeikus, 2001; Achenbach-Richter *et al*, 1987). In 2007, a third hyper/thermophilic bacteria was discovered by a Chinese group, *Fervidobacterium*, which grow between 55 °C and 90°C (optimum 75 °C – 80 °C) (Cai *et al*, 2007), the rest of hyperthermophiles are archaea (Vieille & Zeikus, 2001).

So far, water-containing terrestrial and marine high-temperature areas are two main environments where hyperthermophiles form complex microbial communities. Natural terrestrial biotopes of hyperthermophiles are mainly hot spring and solfataric fields; and marine biotopes of hyperthermophiles consist of various hydrothermal systems, located at shallow to abyssal depths, and at active seamounts (Table 2) (Stetter, 2002).

Table 2 : Biotopes of hyperthermophiles (modified from (Stetter, 2002))

	Type of thermal area	
Characteristics	**Terrestrial**	**Marine**
Location	Solfataric fields (steam-heated soils, mud holes, and surface waters); Deeply originating hot springs; Subterranean oil stratifications	Submarine hot spring, hot sediments and hydrothermal vents (“black smokers”) Active seamounts
Temperature	Surface, up to 100°C*; Depth, above 100°C	Up to ~400 °C (“black smokers”)
*: Depending on the altitude		

Normally, the high temperature generates fatal problems, such as protein and DNA denaturation. In addition the fluidity of membranes is increased leading up to the loss of cellular integrity.

To prevent all these lethal threats, hyperthermophiles present a variety of cellular adaptations. In comparison with proteins of mesophiles, the proteins of hyperthermophiles have shorter loops (Thompson & Eisenberg, 1999), an increased number of disulfide bonds (especially true for the Crenarchaea (Jorda & Yeates, 2011)), increased hydrophobic interactions (Lieph *et al*, 2006) and ionic interactions (Chan *et al*, 1995; Yip *et al*, 1998; Hashimoto *et al*, 1999; Karshikoff & Ladenstein, 2001). These features can render the hyperthermophilic proteins more flexible and stable at high temperatures. In addition, chaperoning activity in hyperthermophiles helps to refold denatured proteins (Kumar & Nussinov, 2001; Sterner & Liebl, 2001).

Some hypothesis of thermal adaptation supposed that guanine-cytosine (G-C) pair is important to thermostability, because a high C-G composition has been observed for several hyperthermophilic organisms, for example, *Pyrococcus abyssi*, a hyperthermophilic archaea, the chromosomal DNA contains a G-C content of 44,7% (Fukui *et al*, 2005). The G-C pairs in nucleic acids are more thermostable than the adenine-thymine (A-T) / A-U (adenine-uracil) pairs because of an additional hydrogen bond. However, the genomic analysis demonstrated that there is no correlation between genomic G-C content and optimal growth temperature (based on over 100 prokaryotes (Archaea or Bacteria genomes)). Conversely, the G-C content of structural RNA (16S and 23S) is strongly correlated with optimal temperature (Hurst & Merchant, 2001; Galtier & Lobry, 1997). Furthermore, certain hyperthermophiles exhibit very high intracellular salt concentration (Scholz *et al*, 1992; Hasan *et al*, 2002). Studies have reported that salt monovalent (like KCl) and divalent (like $MgCl_2$) ions can protect DNA not only against melting at high temperature (thermodenaturation), but also against heat-induced cleavage and depurination by protecting the purine N-glycosidic bond (thermodegradation) (Marguet & Forterre, 1998).

All of the thermophilic archaea have glycerol-ether lipids membranes, unlike those in bacteria that contain glycol-ester lipids. Ether bonds are chemically more stable than ester bonds, moreover, the presence of isoprenoid chains in archaeal membranes convery two thermostable properties: a high permeability barriers and a liquid crystalline state, to maintain vital functions of the cells (Koga, 2012).

The hyperthermophilic microorganisms are the key element to the research of the origin of life. The comparisons of 16S rRNA sequence have shown that, both hyperthermophilic bacteria and hyperthermophilic archaea are the deepest and shortest lineages in their respective branches in the phylogenetic trees (Figure 2). That means these hyperthermophiles are the most slowly evolving organisms within their domains, suggesting that the LUCA (last universal common ancestor) was hyperthermophile, and that the origins of life have first evolved facing the high temperature (Yamagishi *et al*, 1998; Woese, 1987; Pace, 1991; Stetter, 2006b; Di Giulio, 2000, 2003; Brooks *et al*, 2004; Akanuma *et al*, 2013). However, others theoretical studies have concluded that the LUCA was not thermophile/ hyperthermophile (Galtier *et al*, 1999; Becerra *et al*, 2007; Boussau *et al*, 2008).

3) Archaea

All living organisms were classified into two kingdoms at the beginning of the 20th century: Plants and Animals. But in the 1950s and 1960s, most biologists realized that this system of classification was now obsolete for the fungi, protists, and bacteria. By the 1970s, the two kingdoms were expanded to five kingdoms: which include the prokaryotic Monera and the eukaryotic Protista, Fungi, Plantae and Animalia (Cohen, 2014).

In 1977, Professor Carl Woese and his colleagues at the University of Illinois discovered a new group of living organisms: Archaea. They studied and compared the ribosomal RNA sequences (the 16S rRNAs of the prokaryotes and the 18S rRNAs of the eukaryotes) and then created another classification based on the phylogenetic relationships among the species. Initially, Woese had named this group of living organisms *Archaebacteria* as the 3rd domain of life (Woese & Fox, 1977). In 1990, he changed this name to *Archaea* (Woese *et al*, 1990).

The evolution of archaeal tree of life has never stopped since Archaea was recognized. Between 1990 and 2002, there were only two phyla of Archaea: Euryarchaeota and Crenarchaeota (Figure 3A1). Then between 2002 and 2011, Crenarchaeota was regrouped with Thaumarchaeota, Aigarchaeota and Korarchaeota in superphylum “TACK”, moreover, Nanoarchaeaota has been identified as another phylum (Figure 3A2). At present, according to the currently available genomic data, Archaea is divided into four major superphylums: Euryarchaeota, the new TACK (proteoarchaeota), Asgard and DPANN (Spang *et al*, 2017) (Figure 3A3).

The evolution of archaeal tree of life leads to of course the evolution of the tree of life. The evolutionary relationship between Eukarya and Archaea becomes a subject of debate, especially for the determination of the phylogenetic position of the novel Asgard lineages (Lokiarchaeota, Thorarchaeota, Odinarchaeota and Heimdallarchaeota) in relation to other archaea and to Eukarya. Recent studies favor a two-domain view of the tree of life where Eukarya were placed within the Archaea, as sister group to the TACK superphylum (Figure 3B1). Then another phylogenetic analysis placed Eukarya inside the Asgard superphylum with three different groups of markers (concatenated ribosomal proteins, conserved marker proteins and rRNA gene dataset) (Figure 3B2). However, different types of marker result in different positions

among four subgroups of Asgard, thereby if Lokiarchaeta is the closest phylum to eukaryotes is still a matter of debate (Eme *et al*, 2017; Zaremba-Niedzwiedzka *et al*, 2017). This "Two-domain" model was assumed that Eukarya originated from Archaea. However, Forterre has published a review article "*The Common Ancestor of Archaea and Eukarya was not an Archaeon"* to insist on Woesian Three-domain cellular world by suggesting the last common ancestor of Eukaya and Archaea was more complex than modern archea but simpler than modern eukaryotes (Forterre, 2013).

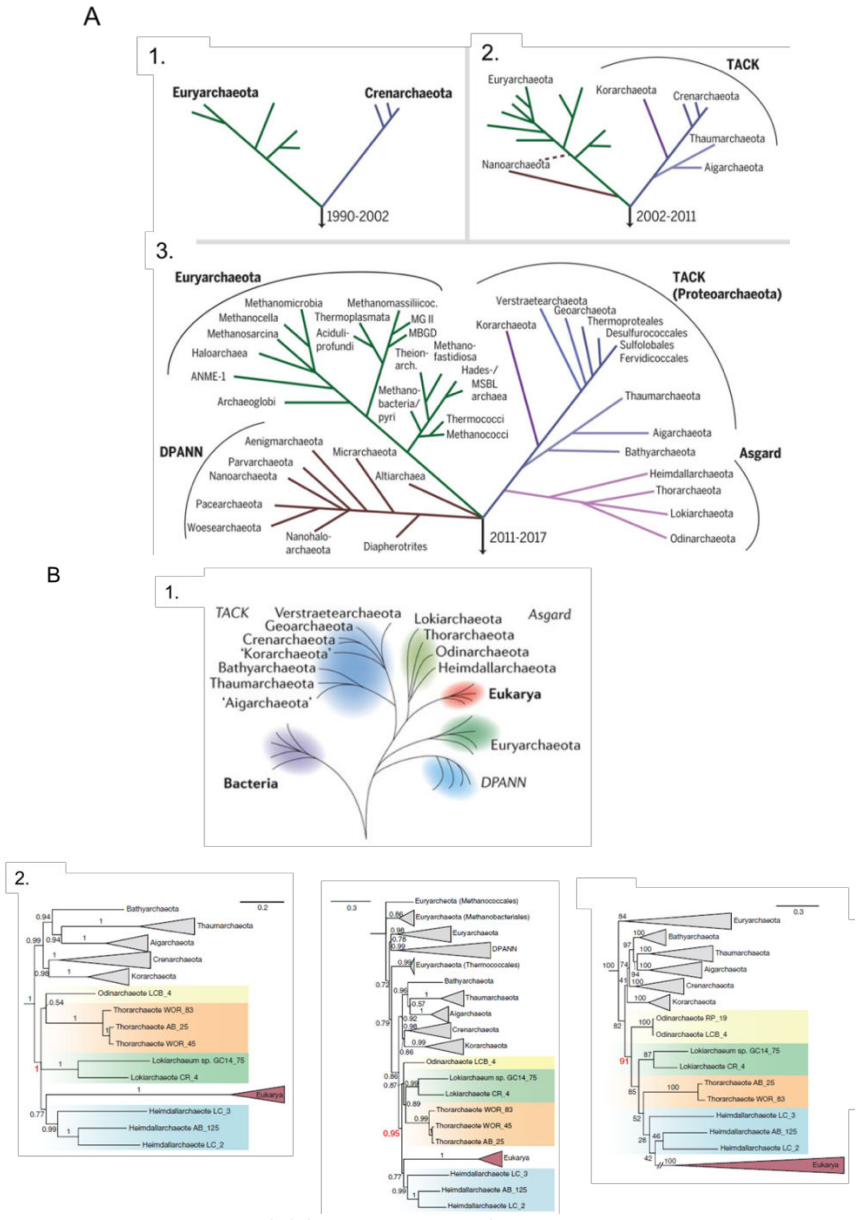

Figure 3 : The expanding archaeal diversity (A) (Spang *et al*, 2017) and evolutionary relationship between Archaea and Eukarya (B) (Eme *et al*, 2017; Zaremba-Niedzwiedzka *et al*, 2017) (A1) Archaea is classified into 2 groups from 1990 to 2002: Euryarchaeota and Crenarchaeota. (A2) Crenarchaeota is regrouped as "TACK", and a new group named Nanoarchaeota was identified between 2002 and 2011. (A3) So far, Archaea are divided into four major groups: Euryarchaeota, TACK, DPNAA and Asgard. (B1) Eukaryotes were placed outside of Asgard. (B2) Different phylogenetic analysis shown high support for the phylogenetic affiliation between Asgard arhaea and eukaryotes.

As mentioned, the majority of hyperthermophiles was found in the marine environment, that's why most of hyperthermophilic archaea have been isolated from shallow marine thermal springs (at depths < 200 m below sea level) or deep-sea hydrothermal vents (at a depth of 2000m or more below sea level) (Adams, 1998; Pichler, 2009). Archaea are now known to represent about 20% or more of all microbial cells in the oceans (Delong & Pace, 2001; Leigh *et al*, 2011).

In our laboratory (Laboratoire de Microbiologie des Environnements Extrêmes, LMEE, UMR 6197, Centre IFREMER de Brest), we use the species *Pyrococcus abyssi* (*P. abyssi*) and *Pyrococcus furiosus* (*P. furiosus*) as our study models, which are hyperthermophiles archaea that belong to the phylum of Euryarchaeota and order of Thermococcales (Table 3). *P. abyssi* was isolated from hydrothermal fluids in the North Fiji Basin at a depth of 2000m (Erauso *et al*, 1993), and *P. furiosus* was isolated from geothermally heated marine sediments collected at the beach of Porto Levante (Fiala & Stetter, 1986). In addition, bioinformatic comparison of *P. abyssi, P. horikoshii* and *P. furiosus* genomes have shown that these 3 *Pyrococcus* species have highly conserved DNA replication genes (Myllykallio *et al*, 2000).

Table 3 : Properties of two hyperthermophilic archaea

		Pyrococcus abyssi	***Pyrococcus furiosus***
		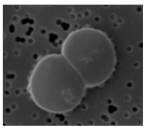	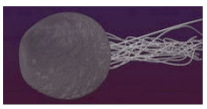
Identification	**Phylum / Order / Genus**	**Euryarchaeota / Thermococcales / *Pyrococcus***	
	Isolation	**Hydrothermal vent deep sea , -2000m Pacific**	**Geothermally heated marine sediment shallow marine , - 0,5m Italy**
Features	**Coccus**	**0,8 ~ 2 µm**	**0,8 ~ 2.5 µm**
	Growth condition	**Anaerobic**	
	Optimum Growth T°	**96°C**	**100°C**
	Optimum Growth P°	**20MPa**	**Atmospheric pressure**
	Optimum Growth [salt]	**3 %**	**2 %**
Genome	**Genomic size**	**1.76M bp**	**1,91M bp**
	Plasmid size	**pGT5: 3.44k bp**	**-**

Reference : (Fiala & Stetter, 1986; Erauso *et al*, 1993; Marteinsson *et al*, 1999; Cohen *et al*, 2003; Robb *et al*, 2001)

II. Genomic integrity maintenance in HA

1) DNA replication and repair

In comparison with Bacteria, Archaea not only share similar genomic structure but also mechanisms of genome duplication (Forterre *et al*, 2002). In addition, metabolic and cell division proteins in Archaea resemble those of Bacteria (Koonin *et al*, 1997; Jain *et al*, 2002). But since the first archaeal genome sequences have been completed, early bioinformatics studies have suggested that the machinery and functionality of the information processing systems (replication, recombination and repair) in Archaea are more similar to those in eukaryotes than to those in bacteria (Kelman & White, 2005). Therefore, some articles (Myllykallio *et al*, 2000; Grabowski & Kelman, 2003; Kelman & Kelman, 2014) suggest that DNA replication in Archaea is a process catalyzed by eukaryotic-like proteins in a bacterial context. We are particularly interested in DNA replication/repair mechanism in hyperthermophilic archaea because of its low rate of DNA replication error and fast speed of DNA repair under high temperature (detail below, Page 19).

DNA is a crucial component of all cellular life. The main role of DNA in the cell is the long-term storage of genetic information. All of genetic information is passed on by "DNA replication", the fundamental biological process of copying the DNA during S phase of cell division, involving dozens of proteins and enzymes. This process is functionally and often structurally conserved in all life forms (Grabowski & Kelman, 2003; Kelman & Kelman, 2014). DNA replication is divided into different stages (McGeoch & Bell, 2008; Sarmiento *et al*, 2014; Kelman & Kelman, 2014) (Table 4):

- Define origin: a origin of replication (OriC) must be defined initially (However recent studies in Archaea might question this ancient dogma ; see below)
- Recruit helicase: the replicative helicase is recruited on unwound DNA
- Pre-initiation: additional factors are recruited to help to form the pre-initiation complex in Eukaryote and Archaea (such as GINS) but not in Bacteria. However, following the pre-initiation complex formation, single-stranded DNA (ssDNA) is coated by SSB (single-stranded DNA binding protein) in order to prevent reannealing and protect the ssDNA. SSB or its homologous RPA (replication protein A) exist in all domains of life.

- Initiation (priming): Following the activation of helicase, formation of the replication bubble, loading of primase on exposed ssDNA and synthesis of a short RNA primer
- Elongation: RNA primers are subsequently extended by DNA polymerase in a replication-fork structure
- Maturation: the RNA primers will be removed in order to form a single, covalently close strand

Table 4 : Different stages in DNA replication and in the three domains of life (McGeoch & Bell, 2008)

Stage in DNA replication	Bacteria	Archaea	Eukaryotes
Define origin 	DnaA	Orc1/Cdc6, WhiP	Orc (Orc1, 2, 3, 4, 5 and 6)
Recruit helicase 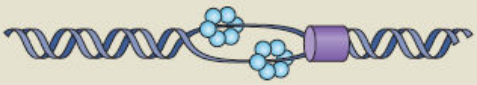	DnaC, DnaB	Orc1/Cdc6, MCM6	Cdt1, Cdc6, MCM (2–7)
Pre-initiation complex 	–	GINS (Gins23 and Gins15)	GINS (Psf1, 2, 3 and Sld5), MCM10, Cdc45, Sld2, Sld3, Dbp11
Priming 	DnaG	Primase (PriS and PriL)	Pol α/primase (PRIS, PRIL, β subunit, DNA polα)
DNA synthesis 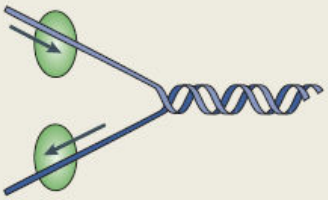	DNA pol III core τ-subunit, Clamp loader proteins (γ-complex), Sliding clamp proteins (β-clamp)	B family DNA pol, D family DNA pol*, Clamp loader proteins (RFC), Sliding clamp proteins (PCNA)	B family DNA pol (δ and ε), Clamp loader proteins (RFC), Sliding clamp proteins (PCNA)
Primer removal 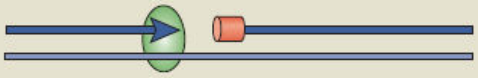	DNA pol I, RNaseH, DNA ligase (NAD-dep)	Fen1, Dna2, RNaseHII?, DNA ligase (ATP-dep)	Fen1, Dna2, RNaseHII?, DNA ligase (ATP-dep)

*Found in archaea only. dep, dependent; MCM, minichromosome maintenance; PCNA, proliferating cell nuclear antigen; pol, polymerases; RFC, replication factor C.

Unfortunately, both exogenous sources (UV and other radiation, chemicals etc.) and endogenous sources (reactive oxygen species, replicative errors, alkylation or hydrolysis) induce DNA damages. Including damages to DNA bases, bulky lesions, crosslinks, protein-DNA adducts, or others forms of base lesions such as pyrimidine dimers, AP sites (apurinic site) , as well as misincorporated DNA bases or single base insertions or deletions, or DNA strand breaks (SSBs or DSBs) (Shin *et al*, 2014; Shiloh, 2003). Several repair systems have been demonstrated, such as nucleotide excision repair (NER), base excision repair (BER), mismatch repair (MMR), homologous recombination repair (HR) and non-homologous end joining (NHEJ) (Sancar *et al*, 2004) (Figure 4). Moreover, during the replication, the polymerase-dependent translesion synthesis (TLS) is a pathway to respond to DNA damage (Lehmann, 2006b, 2006a; Kashiwagi *et al*, 2010), and recently, the findings of restarted replication forks suggest different pathways to rescue the stalled or damaged replication forks (such as HR, Fork remodeling etc.) (Jones & Petermann, 2012; Yeeles *et al*, 2013).

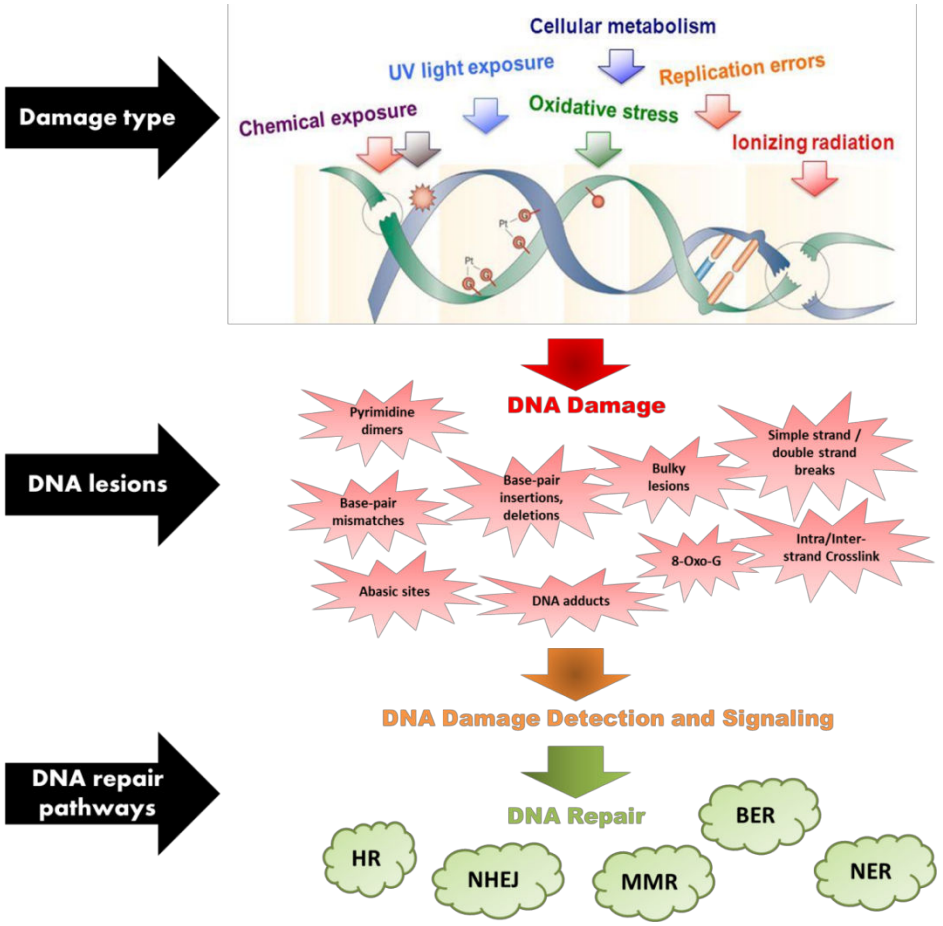

Figure 4 : DNA damage sources, lesions and repair pathways (modified from (Postel-Vinay *et al*, 2012)). Different types of DNA lesions are caused from both exogenous and endogenous sources. According to different DNA damages, different DNA repair pathways are in charge to fix them.

Many DNA repair protein homologous have been identified and characterized in Archaea (Table 5), so biologists have been trying to complete the different DNA repair pathways for years. NER seems to function in mesophilic archaea, but not in hyperthermophilic archaea because of the lack of the UvrABC endonuclease homologs, which is the only protein mediating NER in mesophilic archaea (Grogan, 2015; Rouillon & White, 2011). Archaeal BER is accomplished by the coordinated action of necessary enymes in hyperthermophilic archaea *Pyrobaculum aerophilum* (Sartori & Jiricny, 2003). Archaeal NHEJ system was recently elucidated in mesophilic archaeon *Methanocella paludicola* (Bartlett *et al*, 2013, 2016), but not yet found in hyperthermophilic archaea. Notably, the classical MMR mechanism is absent in most archaeal species, although the *MutS/MutL* homologous are mostly present in halophiles, methanogens, they are completely lacking in hyperthermophilic archaea (Lin *et al*, 2007; Sachadyn, 2010). It is worth mentioning that in 2016 a mismatch-specific endonuclease in hyperthermophilic archaea has been identified, called EndoMS/NucS (Ishino *et al*, 2016). In 2008, Hopkins and Pall have shown that the Mre11 and Rad50 from *P. furiosus* acted cooperatively with NurA and HerA to resect the 5' strand at a DNA end under physiologoical condition *in vitro*, and the 3' single-stranded DNA generated by these enzymes could be utilized by the recombinase RadA to catalyze strand exchange, suggesting that HR exists in Archaea for DSBs repair (Hopkins & Paull, 2008). In addition, recombinase RadA protein is essential for homologous recombination, several studies have shown that RadA proteins found in *H. volcanii, S. solfataricus, D. amylolyticus, P. islandicum, P. furiosus* are thougth to play a critical role in recombination and repair in hyperthermophilic archaea (Woods & Dyall-Smith, 1997; Seitz *et al*, 1998; Kil *et al*, 2000; Spies *et al*, 2000; Komori *et al*, 2000b). Furthermore, most of the genes involved in homologous recombination could not be deleted in HA, suggesting HR is an essential process in hyperthermophilic archaea (detail below, table 6, Page 24). In 2017, a new protein involved in HR has been identified in *Pyrococcus horikoshii*: MutS5, which can stabilize the Holliday junction and play a role in HR. This discovery could help to complete the whole molecular mechanism study of HR in Archaea (Ohshita *et al*, 2017).

As the structures and functions of genome maintenance proteins in Archaea are similar to those in eukaryotes (Kelman & White, 2005; Kelman & Kelman, 2014), studying genome maintenance in Archaea is very important to provide more insights into how homologous protein structures impact human health (Shin *et al*, 2014).

In this study, we focus on homologous recombination repair pathway in hyperthermophilic archaea. Hence, we will talk about biological roles of HR in the repair of DNA DSBs caused by high temperature, as well as in DNA replication for replication fork restart and ori-dependent replication.

Table 5 : Distribution of DNA repair protein homologues among the three domains of life

	Bacteria	Eukaryote	Archaea
NER	UvrA2B, RNAP UvrB UvrBC, Cho	Xpc-hr23B, RNAP TFIIH subunits, XPB, XPD XPF-ERCC1, XPG	SSB RNAP, **XPB, XPD** **XPF, Bax1, NucS**
BER	UDG (Family I – IV) EndoIII (Nth) Xth (ExoIII), Nfo (ExoIV) Pol II PCNA FEN1 Ligase	UDG (Family I – IV) Nth, OGG1 APE 1, Apn Pol β, Pol δ/ε PCNA FEN1 Ligase	UDG (Family II, **IV**, V VI) OGG, Nth, EndoIII, **EndoQ**, **KaeI** ExoIII, Xth, Endo IV, **APE (Nfo)** **PolB** (**1**, β), DNA primase **PCNA** (Family 1,2,3) **FEN1** (Not proven to ben involved in BER) **Ligase** (I, III)
MMR	MutS1, MutL, MutH PolII ExoI, RecJ UvrD	MutSα (MSH2/MSH6), MutSβ (MSH2/MSH3), MutL PCNA, RFC Exo1	 MutS (1, 4, 5) **EndoMS** (?)
HR	RecJ, SSB RecBCD SbcCD RecQ RecA RecF,O,R RuvAB, RecG RuvC MutS2	Exo1, RPA Spo11 Mre11/Rad50/Xrs2 (Nbs) SAE,Sgs1 Rad51, Rad52, 54 MutSγ (MSH4/MSH5)	**RPA**/SSB **Spo11** **MlaA/HerA/NurA** **Mre11/Rad50** Sgs1 **RadA (or Rad51), RadB** Rad 54 **Hjc** MutS5
NHEJ	Ku (30-40kDa) LigaseD SbcCD PoYahC family	Ku70/80, DNA-PKcs Ligase IV, XRCC4, XLF Mre11/Rad50/Nbs Artemis Pol μ / λ	Ku Ligase Polymerase phosphoesterase (PE)

* **Red:** proteins present in *Pyrococcus abyssi* or *Pyrococcus furiosus*

References: **NER:** (Rouillon & White, 2011)**; BER:** (Grasso & Tell, 2014; Shin *et al*, 2014; Krwawicz *et al*, 2007; Shiraishi *et al*, 2016; Sartori & Jiricny, 2003)**; MMR:** (Yang, 2000; Morita *et al*, 2010; Sachadyn, 2010; Shiraishi *et al*, 2016; Ohshita *et al*, 2017)**; HR:** (Seitz *et al*, 2001; Morita *et al*, 2010; Ohshita *et al*, 2017)**; NHEJ:** (Wilson *et al*, 2003; Lieber, 2010; Bartlett *et al*, 2013; Shin *et al*, 2014; Bowater & Doherty, 2006; Chiruvella *et al*, 2013)**.**

2) Biological role of homologous recombination in the repair of DNA

a) Heat stress-induced DNA double-strand breaks (DSBs)

Since 1953, James Watson and Francis Crick have uncovered the mystery of the structure of DNA. It is in the form of a three-dimensional double helix. DNA is composed of a series of “nucleotides”, and each nucleotide is made up of a deoxyribose sugar, a phosphate group, and one nitrogenous base which is composed of carbon and nitrogen rings. The number of rings in the base determines the type of base: “purine” base is with two fused rings, such as adenine (A) and guanine (G); while “pyrimidine” base is with a single ring, such as cytosine (C) and thymine (T).The linear chain of DNA is composed of alternating purine-pyrimidine nucleotides linked by “phosphodiester bonds” (between the deoxyribose sugar of one nucleotide and the phosphate group of the next). The two chains of DNA are connected by interactions (hydrogen bonds) between complementary base pairs (A-T or C-G), the DNA double strands are anti-parallel with one 5’ end (phosphate-bearing end) of one strand being paired with the 3’end (hydroxyl-bearing ends) of its partner, and vice versa (Dahm, 2005) (Figure 5).

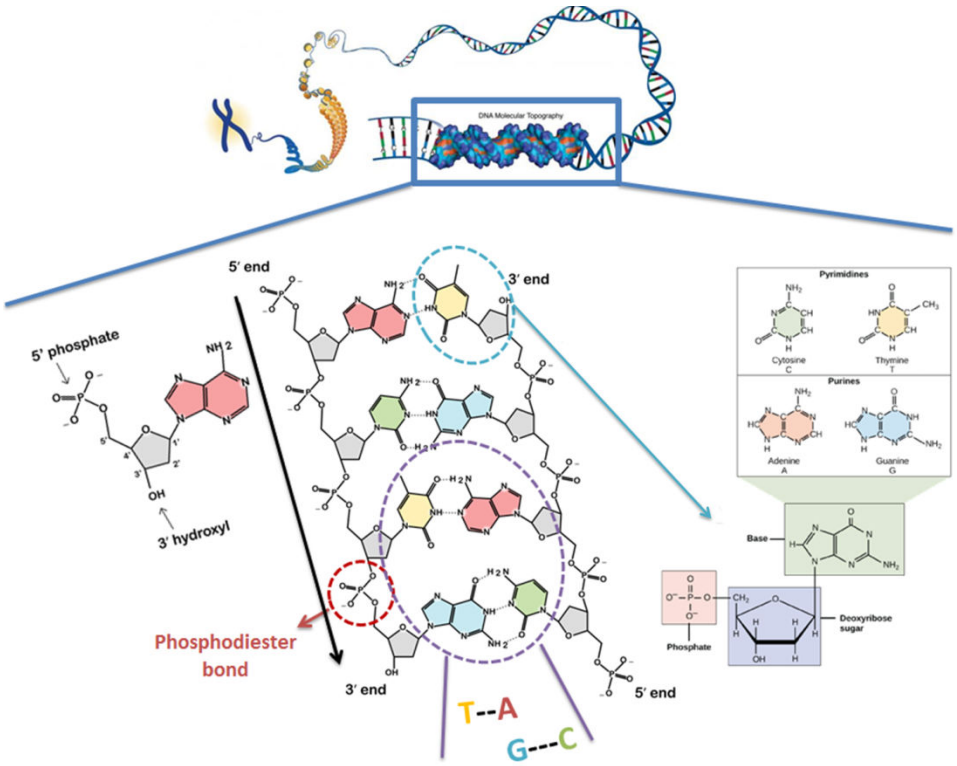

Figure 5 : The chemical structure of DNA (image modified from (Nucleic Acids - Biology - OpenStax CNX)). DNA is a double helix that consisted of two chains, and each strand is composed of four different nucleotides (A/T/C/G) linked together through the phosphodiester bonds. Adenine always binds with Thymine, and guanine always binds with cytosine, with hydrogen bonds.

Heat stress is one of the best-studied DNA stress factors. The high temperature leads to different damages on the DNA double helix:

- For the denaturation of DNA, the hydrogen bonds that hold the two strands together become weaker and weaker, and finally broken (Wang *et al*, 2014).
- The formation and accumulation of 8-oxoguanine (an oxidation product from guanine, which will pair with adenine if not repaired, could generate double-strand breaks) (Figure 6A) (Bruskov *et al*, 2002; Nakabeppu, 2014; Cheng *et al*, 1992); deaminated cytosine (becomes Uracil) (Figure 6B) (Lindahl & Nyberg, 1974) and apurinic DNA sites (AP-sites) (loss of purine from DNA sequence) (Figure 6C) (Warters & Brizgys, 1987).
- The induction of single-stranded DNA breaks (SSBs) or the formation of double-stranded DNA breaks (DSBs) because of breaking phosphodiester bonds, during the S-phase of the cell cycle. The SSBs could be converted into DSBs (Velichko *et al*, 2015; Kantidze *et al*, 2016).

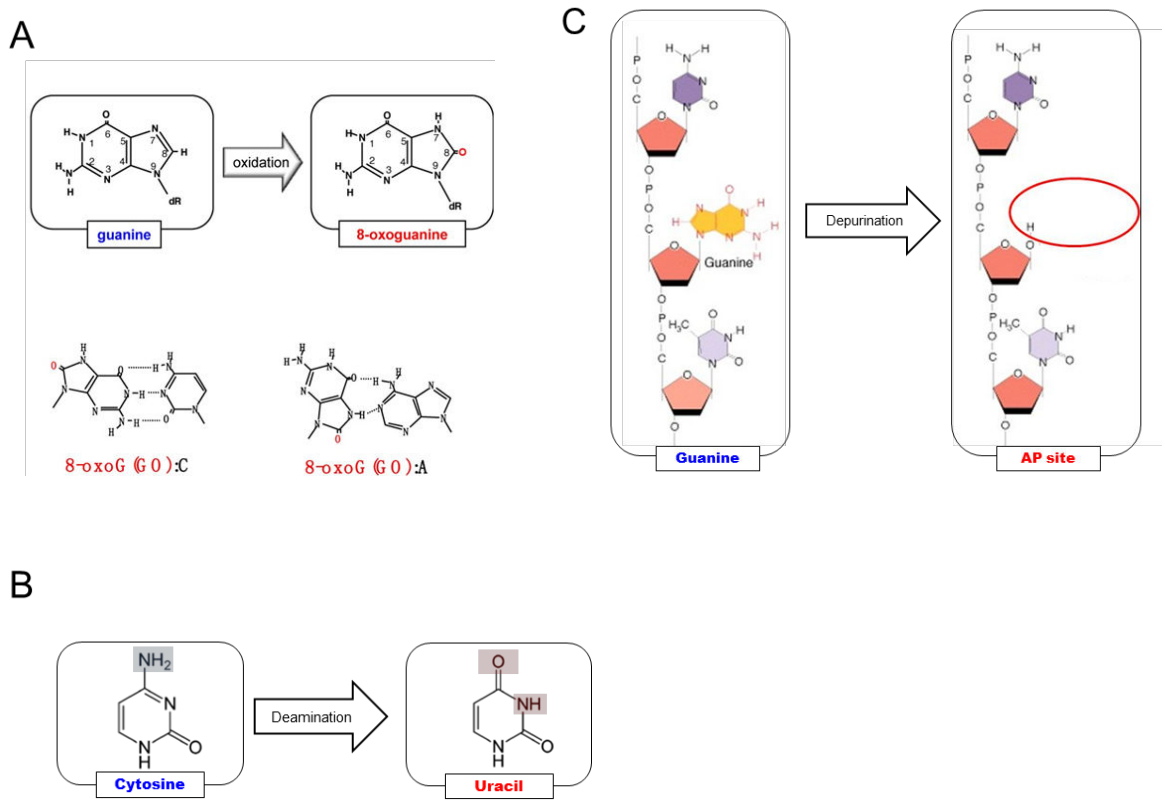

Figure 6 : Modifications of DNA base induced by heat-stress. (A) Formation of 8-oxoguanine from guanine resulting from reactive oxygen species **(Nakabeppu, 2014)**). (B) Transformation of uracil from cytosine due to deamination **(Lindahl & Nyberg, 1974)**. (C) Formation of AP site because of loss of purine from DNA sequence **(Warters & Brizgys, 1987)**.

Apart from the different DNA damages induced from high temperature, the heat stress can inhibit the activity of all repair systems such as BER, NER, NHEJ, HR and DNA mismatch repair systems (Figure 7) (Kantidze *et al*, 2016).

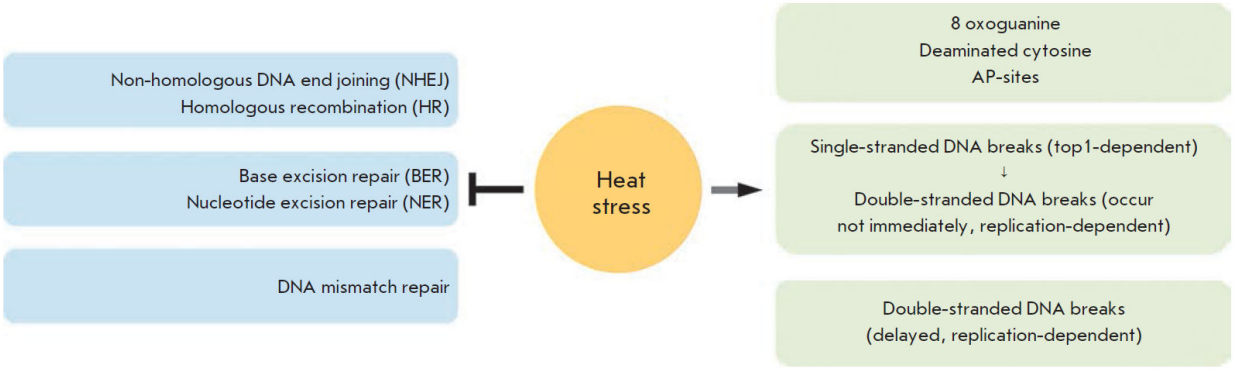

Figure 7 : The effect of heat stress on the integrity of DNA and the repair system (Kantidze *et al*, 2016). Heat stress causes the modification of base of DNA, ssDNA break and consequence of dsDNA break. It inhibits as well the DNA repair pathways.

Normally, the high temperature (such as 100 °C) accelerates the spontaneous degradation of DNA. However, in hyperthermophilic archaea *P.abyssi*, the level of AP sites was only 10-fold higher than in mesophilic bacteria *Escherichia coli* (*E.coli*). (Palud *et al*, 2008), and the spontaneous mutation rate in another hyperthermophilic archaea *Sulfolobus acidocaldarius* (*S. acidocaldarius*) was close to the standard rate for nealy all of other microbes (Grogan *et al*, 2001). Moreover, at 100°C, DNA damages in *E.coli* were increased about 3000-fold than at 37°C (Lindahl, 1993), while hyperthermophilic archaea *Pyrococcus furiosus* growing optimally at 100°C, is 20-fold more resistant to thermal breakage *in vivo* than the DNA from the *E. coli* (Peak *et al*, 1995). So Peak *et al.* supposed that "*this remarkable stability of DNA in a hyperthermophile is that this hyperthermophile possesses DNA-binding proteins that protect against hydrolytic damage, as well as other endogenous protective mechanisms and DNA repair enzyme systems*".

The following studies on hyperthermophiles radiation resistance have observed a similar rate of DNA double-stranded breaks produced by gamma irradiation in *P. abyssi*, *P. furiosus, E. coli* and *D. radiodurans* (*Deinococcus radiodurans*, a radioresistant bacteria), and proposed a hypothesis that there is no specific protection mechanisms against radiation of *P. abyssi* and *P. furiosus*, but there exists an efficient DNA repair system (Gérard *et al*, 2001). In 2003, Jolivet *et al.* showed that in the irradiated *P. abyssi* cells, the fragmented chromosomes were repaired quickly. Hence, they suggested that there is a highly efficient DNA repair system in hyperthermophilic microorganisms. Moreover, a set of proteins involved in DNA replication and repair (such as RadA, RPA, and RFC) bound chromatin before and after an extreme irradiation, suggesting that this efficient DNA repair system is continuously ready to restore the DNA damage caused by high temperature and/or ionizing radiation (Jolivet *et al*, 2003).

b) DNA repair

Among all the types of heat-stress induced DNA damage, DNA double-strand breaks due to thermal degradation via depurination are the most dangerous forms of stress for genome integrity (Marguet & Forterre, 1994; Shin *et al*, 2014).

DNA DSBs can be repaired by two main conserved mechanisms: classical Non Homologous End-joining (c-NHEJ) and Homologous Recombination (HR). Recently, two additional modalities of repair have come to be appreciated: Alternative Non-homologous End-joining (Alt-EJ, or named microhomology-mediated end joing (MMEJ)) and single-strand annealing (SSA) (Ceccaldi *et al*, 2016) (Figure 8).

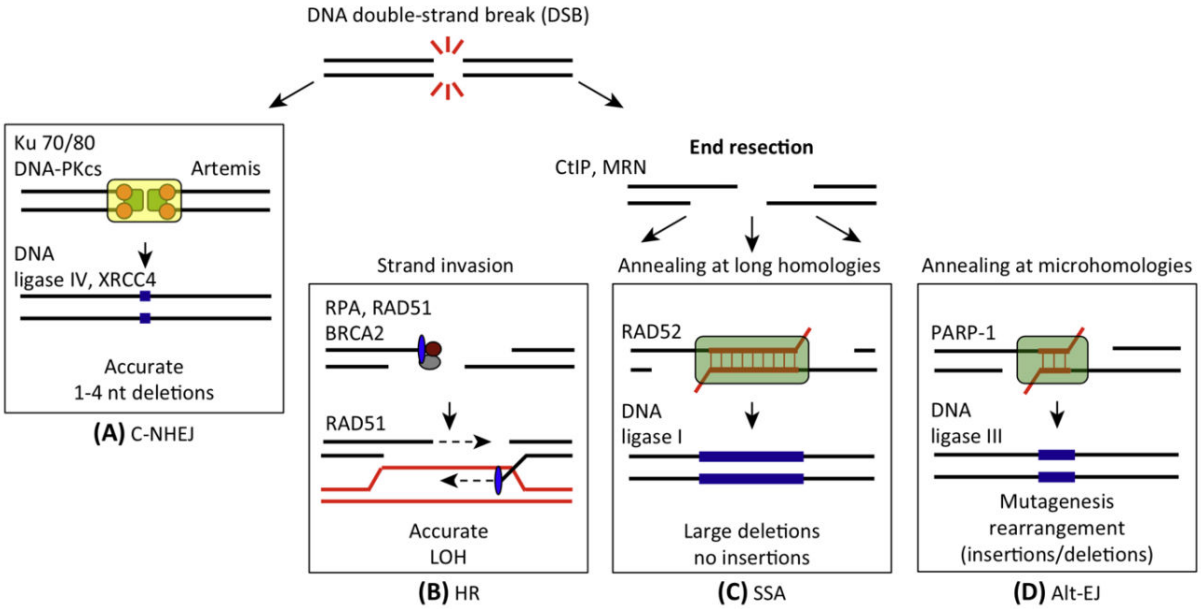

Figure 8 : Four pathways to repair DNA DSBs (Ceccaldi *et al*, 2016). When the DNA end resection is blocked, repair through c-NHEJ is favored (A). When the DNA end resection occurs, three pathways (HR, SSA and Alt-EJ) compete for the DSBs repair (B)-(D). c-NHEJ, classical nonhomologous end joining; HR, homologous recombination; SSA, single-strand annealing; alt-EJ, alternative end joining.

c-NHEJ is the major DNA DSBs repair pathway in mammalian cells. In this mechanism, the DSBs are repaired by direct ligation of the blunt ends, which does not require homologous sequences (Figure 8A). c-NHEJ is a fast but an error-prone mechanism because it operates small insertions and/or deletions of nucleotides, as well as translocations. While the three others repair mechanisms (HR, SSA and Alt-EJ) are initiated by a resection of double-strand DNA ends leaving a 3'-tailed single strand. However, HR requires an undamaged homologous sequence to repair the broken strands (Figure 8B), the HR mechanism is more complex than c-NHEJ, but it can restore any lost genetic information. The resected DNA ends may also serve for end-joining dependent machinery by annealing of two large homologous regions from 10 bp to several kilobases on both sides of the break (SSA) or by annealing of two short homologous sequences of only a few nucleotides (Alt-EJ) on separate ssDNA overhangs to align ends prior to ligation (Figure 8C and 8D). Nevertheless, SSA and Alt-EJ are also mutagenic repair pathways, because of its apparent predilection for joining two ssDNA overhangs of broken strands, that generates translocation or nucleotides deletions, resulting in loss of sequence information (Symington & Gautier, 2011; Chapman *et al*, 2012; Decottignies, 2013; Shibata & Jeggo, 2014; Aparicio *et al*, 2014; Ceccaldi *et al*, 2016).

NHEJ is a predominant repair pathway for DNA DSBs in eukaryote for G1 and G2 phases, while HR functions predominately during S phase of the cell cycle, following DNA replication while the sister chromatid is available as a template for repair (Symington & Gautier, 2011; Aparicio *et al*, 2014; Shibata & Jeggo, 2014; Ceccaldi *et al*, 2016; Shibata, 2017). In contrast to Eukaryotes, the proteins homologous involved in NHEJ mechanism are rarely present in Archaea, only a functional NHEJ pathway has been identified and characterized in 2013 in a mesophilic archaeon *Methanocella paludicola* (Bartlett *et al*, 2013).

It was thus supposed that the HR system is the prominent repair pathway in hyperthermophilic archaea to fix the DNA DSBs (Blackwood *et al*, 2013). In *P.abyssi*, protein RadA is continuously expressed, which plays an important role in homologous recombination (HR) to repair DNA DSBs (Jolivet *et al*, 2003). Since then, more and more homologs of several eukaryotic HR components have been identified in Archaea.

White *et al.,* proposed a homologous recombination pathway in the Archaea based on the described activities of eukaryotic homologous counterparts present in Archaea (Figure 9). The HR is initiated when the DSB is resected by co-operation of Mre11-Rad50/NurA-HerA (nuclease/helicase), to remove the 5'-strands, generating single-strand 3'-tails rapidly bound by SSB (ssDNA-binding proteins) / RPA (Replication protein A). The recombinase RadA removes SSB and assembles subsequently onto ssDNA to favor nucleoprotein filament formation. Then, the nucleoprotein filaments promote strand invasion and exchange with an undamaged homologous duplex DNA, which is used as a template for repair DNA synthesis. Meanwhile RadB (a paralogue of RadA) may modulate RadA activity. Hjm/Hel308 (a helicase) may perform branch migration to form a heteroduplex molecule and a Holiday junction (HJ). Finally, the HR mechanism is finished by cleavage of HJ by resolvase Hjc and ligated by ligase (White, 2011).

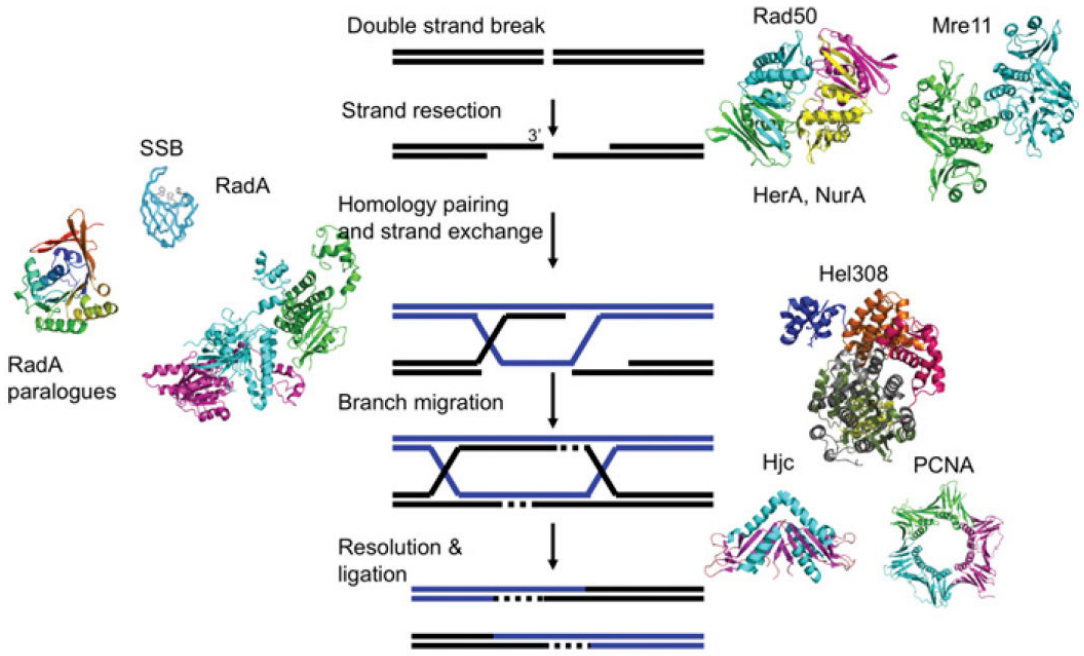

Figure 9 : HR pathway in the Archaea and involved proteins (White, 2011). The initial resectioning step is catalysed by the Rad50–Mre11–HerA–NurA complex, producing a 3'-end that is used for the strand invasion step, involving the RadA, RadA paralogues and SSBs. These results in the formation of an HJ that can branch migrate, possibly catalysed by the Hel308 helicase. Hel308 interacts with the junction-resolving enzyme Hjc, which can also form a functional complex with the sliding clamp PCNA. Finally, DNA ligase can seal the resultant nicked duplexes.

In the Archaea, gene deletions of proteins involved in homologous recombination, such as *mre11, rad50, radA,* as well as *nurA* and *herA* have been performed. These studies have demonstrated that these genes are essential in hyperthermophilic archaea (Table 6), meaning the HR pathway is very important in these hyperthermophiles, in contrast to the conclusions derived from similar genetic studies carried out on mesophilic archaea (Grogan, 2015).

Table 6 : HR pathway involving Gene-deletion studies in hyperthermophilic archaea (modified from **(Grogan, 2015)**)

Gene	organism	Predicted function	Phenotype	Reference
mre11	*T.kodakarensis* *S.islandicus*	Nuclease, DSB end-progressing	lethal	(Fujikane *et al*, 2010; Zhang *et al*, 2013; Huang *et al*, 2015b)
rad50	*T.kodakarensis* *S.islandicus*	Nuclease, DSB end-progressing	lethal	(Fujikane *et al*, 2010; Zhang *et al*, 2013; Huang *et al*, 2015b)
radA	*T.kodakarensis* *S.islandicus*	Recombinase	lethal	(Fujikane *et al*, 2010; Zhang *et al*, 2013)
herA	*T.kodakarensis* *S.islandicus*	Helicase, DSB end-progressing	lethal	(Fujikane *et al*, 2010; Huang *et al*, 2015b)
nurA	*T.kodakarensis* *S.islandicus*	Helicase, DSB end-progressing	lethal	(Fujikane *et al*, 2010; Zhang *et al*, 2013; Huang *et al*, 2015b)
hjc	*T.kodakarensis* *S.islandicus*	Holliday-junction resolvase	None observed	(Fujikane *et al*, 2010; Zhang *et al*, 2013)
hje	*S.islandicus*	Holliday-junction resolvase	None observed	(Zhang *et al*, 2013)
hje+hjc	*S.islandicus*	Holliday-junction resolvase	lethal	(Huang *et al*, 2015a)
hjm/hel308	*T.kodakarensis* *S.islandicus*	Helicase, DSB end-progressing	lethal	(Dorazi *et al*, 2007; Huang *et al*, 2015b; Hong *et al*, 2012)

3) Biological role of homologous recombination in DNA replication

a) Replication restart after Fork arrest

Faithful DNA replication is vital to the survival of all organisms. Usually, the replication forks formation speed is constant along the DNA (about 1000 bp/s in *E.coli* (Hirose *et al*, 1983), 10-50 bp/s in eukaryotes (Hyrien, 2000), 250-300 bp/s in hyperthermophilic archaea (Hjort & Bernander, 2001; Myllykallio *et al*, 2000)). However, different replication stresses can lead to arrest of replication fork progression, such as blocking lesion, accumulation of ssDNA gap or forks collapse. All the types of breakage of stressed replication forks is an important source of DSBs, generating either the two-ended DSB or the one-ended DSB. Studies in Bacteria and Eukaryotes have demonstrated that the HR proteins promote the repair of stalled and broken replication forks or escort replication forks. Different mechanisms have been proposed to explain how HR can promote restart of replication forks (example in Eukaryote, Figure 10). Hence, HR seems to play a multiple roles in fork-protection, fork-stabilization and restarting stressed replication forks (Gelot *et al*, 2015; Costes & Lambert, 2012; Prado, 2014; Michel, 2000).

The mysterious essentiality of recombination mechanism during replication in HA has been solved little by little. Due to a lack in HA of special, preventive-maintenance repair system like NER, which is a universal DNA repair mechanism to recognize and remove diverse DNA lesions before replication, the lesion-induced fork stalling should occur frequently. Grogan et *al.* have proposed two models of replication-fork collapse: a) if the lesion encountered is on the leading-strand, polymerase would be blocked before the lesion in order to create a partially single-stranded region near the junction of the fork, and the fork would be cleaved by some endonuclease in HA (such as Hef or Xpf) to leave the lesion on the resulting end (Figure 11A); b) if the lesion encountered is on the lagging-strand, the similar result would be obtained where the fork breakage was created by a 5'flap-endonuclease (such as Fen1or Xpg) (Figure 11B) (Grogan, 2015).

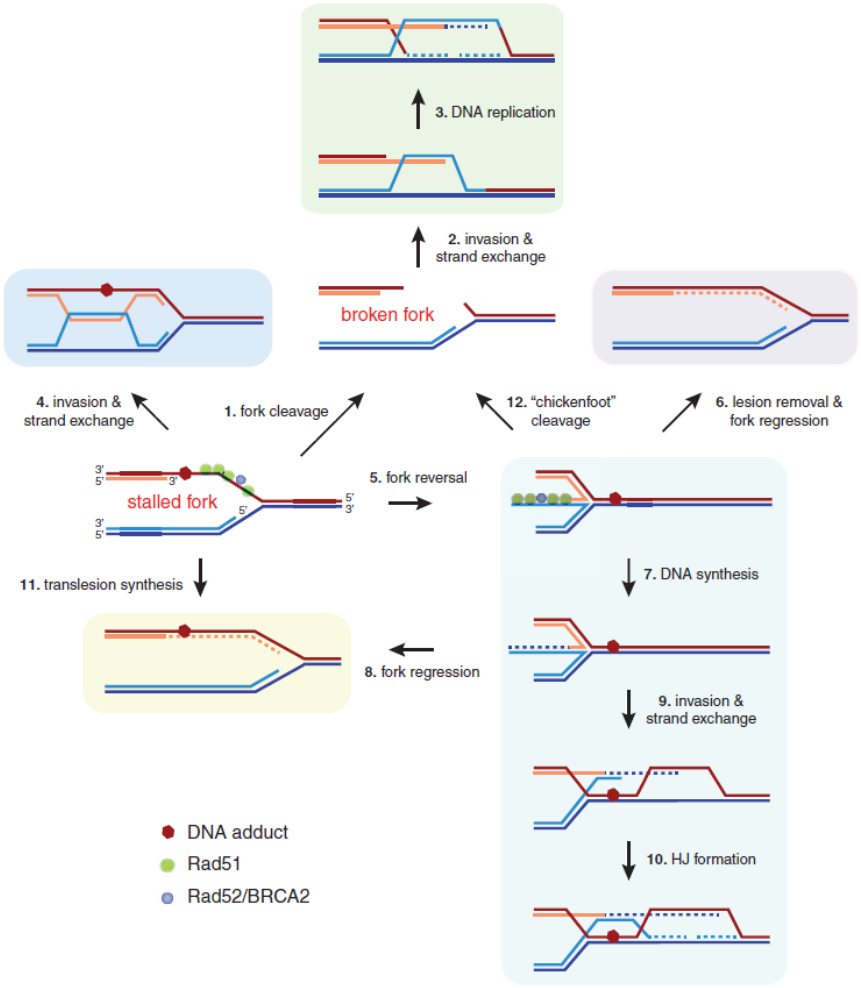

Figure 10 : Mechanisms of replication fork restart by homologous recombination (Prado, 2014). Stalled or broken replication forks can occur during DNA replication. At broken forks, the one-ended DSB might be resected, and then repaired by HR through sister chromatid invasion and strand exchange, leading to form HJ to reassemble replisome (step 1-3). At stalled fork, the 3'-ended nascent strand perform an invasion with its sister chromatid to generate: a. an HJ-like structure, resulting in a bypass of the blocking lesion (step 4), b. a "chicken-foot" structure resulting from fork reversal (step 5), repaired subsequently by lesion bypass during DNA synthesis and regression (step 6,7-8), or by DNA synthesis through DNA strand invasion and double HJ (step 9-10), c. a lesion bypass by recruiting translesion-synthesis polymerases (step 11), d. a "chicken-foot" structure cleavage by endonuclease to generate broken fork (step 12)

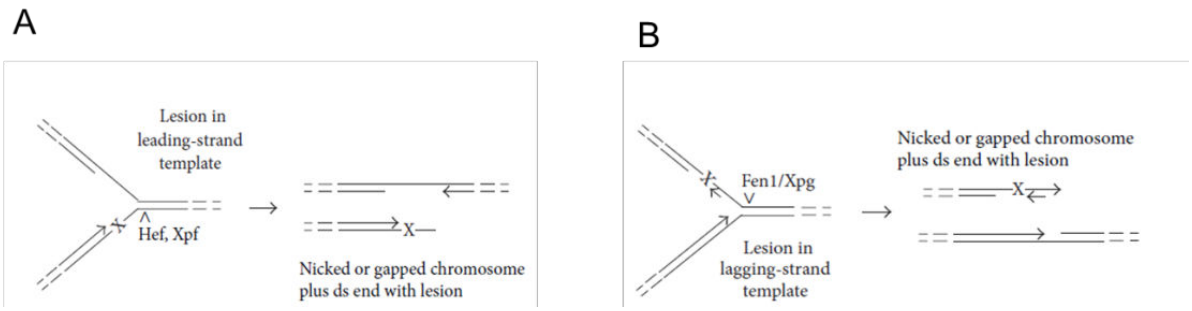

Figure 11 : Model of replication fork collapse in HA (Grogan, 2015). DNA lesions could be occurred during DNA replication. The endonucleolytic cleavage at downstream of lesion located both leading-strand (A) and lagging strand (B), generating one-ended double strand break, that result in replication fork collapse

In both two proposed models of replication-fork “collapse” in HA, the removal of DNA lesions by end-processing mechanism could be realized by unwinding and bidirectional nucleolytic activities, to leave a “clean” 3’-overhang products. Subsequently, the reassembling of replication fork could be carried out by HR using the “clean” 3’ tail on the double-strand end and an intact continuous duplex with which it can recombine (Figure 12) (Grogan, 2015).

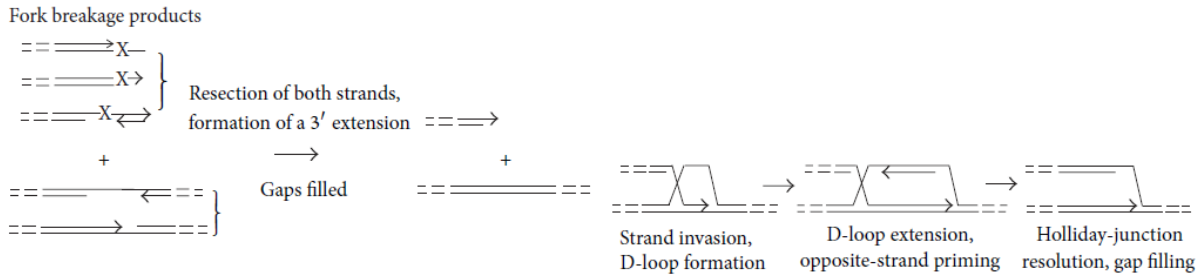

Figure 12 : Regeneration of broken replication forks by HR functions in HA (Grogan, 2015). Different types of replication fork collapse resulting DNA breakage (proposed in Figure 11) such as DNA lesion, gaps and overhang, could be repaired by HR pathways.

.

Taken together, in hyperthermophilic archaea, when replication forks are blocked at DNA lesions in either lagging strand or leading strand, HR is probably the major pathway for mediating and reassembling the stalled replication forks (Grogan, 2015).

b) Recombination-dependent replication (RDR)

Chromosomal DNA replication initiates at a specific region called an origin of replication ("ori"), which allows binding initiator proteins and then recruiting the replicative machinery. Although origins of replication differ in number, length and structure in the 3 domains of life, all share similar characteristics, most contain AT-rich elements as well as direct and inverted repeats (Kelman & Kelman, 2018). The putative single replication origin was initially identified *in silico* in several archaea (*Methanobacterium thermoformicicum*, *Pyrococcus horikoshii* and *Pyrococcus furiosus*) (Lopez *et al*, 1999). One year later, Myllykallio et *al.,* have reported identification *in vivo* of an origin of replication in a hyperthermophilic archaea *Pyrococcus abyssi* (Myllykallio *et al*, 2000). Until today, DNA replication origins have been mapped in about a dozen archaeal species, some archaea have only one origin as bacteria, whereas most archaea have multiple origins as all eukaryotes (Table 7). These "ori" were thought to be essential to replicate the archaeal chromosomes and for cell viability (Hawkins *et al*, 2013; Wu *et al*, 2014).

Table 7 : Summary of origins of replication in the three domains of life (Kelman & Kelman, 2018)

	Bacteria	Archaea	Eukarya
Chromosome	Circular	Circular	Linear
Number of origins	1	1 or multiple	Multiple
Can the origin be deleted?	Yes	Yes	Yes
Is a dormant origin then activated?[a]	Yes	Sometimes	Yes
Is the native origin used under laboratory growth conditions?	Yes	Not always[b]	Yes

[a]In many organisms, when the major origin of replication is deleted, secondary, dormant origins are activated. In some archaeal species, DNA replication in origin-deleted strains initiates along the chromosome and not at a specific site(s).
[b]At least in one archaeal species, the origin of replication is not utilized under laboratory growth conditions.

Recently, studies with the halophilic archaeon *Haloferax* have demonstrated that the strain with the deletion of all known origins or replication grew faster than the wild-type strain under laboratory growth conditions. This discovery leads to raising one question: "*Do Archaea need an origin of replication?*" (Hawkins *et al*, 2013; Kelman & Kelman, 2018).

In Eukaryote and Bacteria, it exists secondary dormant origins, which can be activated when the major origin of replication is deleted. But this is not the case in Archaea, at least, no secondary origin activation could be observed in *H.volcanii*. The result suggested that there is an origin-independent replication initiation mechanism in Archaea (Kelman & Kelman, 2018). Initiation mechanisms operated by homologous recombination have been observed in some bacteria, virus and eukaryotes, mediated by their respective Rad51 family proteins (Yang *et al*, 2001a). 20 years ago, Mosig has reported the first discovery of recombination-dependent replication (RDR) in bacteriophage T4. They found that recombination-dependent initiation is an essential pathway for DNA replication during development because origin initiation of DNA replication is inactivated (Mosig, 1998). Following the studies of replication restart machinery, DNA replication initiation from homologous recombination intermediate (D-Loop) has been described in both bacteria and yeast (Figure 13) (Xu & Marians, 2003; Michel & Bernander, 2014; Ravoitytė & Wellinger, 2017). Therefore, it was proposed that archaeal origin-less cells initiate essentially replication at dispersed sites along chromosome via RDR for viability.

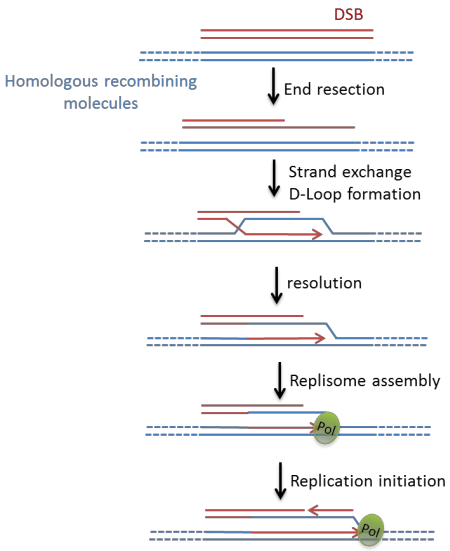

Figure 13 : Model of possible mechanism involved in origin-independent replication initiation (adapted from (Michel & Bernander, 2014; Ravoitytė & Wellinger, 2017). In the case of the deletion of DNA replication origins, HR is potentially used for initiation of replication.

Overall, HR pathway appears to be crucial in Archaea, and particularly for hyperthermophilic archaea, to repair DNA double strand breaks and possibly to restart or initiate DNA replication in the context of stalled replication fork and deletion of replication origins.

III. Proteins interaction network in genome maintenance in HA

At the molecular level, study of proteins of interest and their interaction landscapes is one of the strategies to better understand molecular mechanisms at work within a particular biological pathway. Two proteins interacting with each other could probably function in the same cellular process.

In order to get a better understanding of key proteins and protein-protein interactions involved in genomic integrity in HA, our laboratory has applied the strategy "Co-immunoprecipitation (CoIP) coupled to mass spectrometry (LC-MS/MS)" to identify the proteins and their partners (known and/or unknown) implicated in different DNA mechanisms (DNA replication/recombination/repair ; RNA metabolisms; methylation/modification and unknown functions), leading to the description of a protein-protein interaction network in genome maintenance in hyperthermophilic archaea *Pyrococcus abyssi* (Pluchon *et al*, 2013). There are four main protein clusters in this network: PCNA (in blue), RPA (in green), RNAP_rpoa2 (in yellow) and DNA primase p41 (in red).

From the network, we have noted that several proteins involved in HR interact with proteins involved in DNA replication. These findings encourage us to dig deep into biological role of HR not only in DNA DSBs repair, but also in DNA replication, improving our knowledge on genomic maintenance mechanisms of DNA repair, replication and recombination processes.

It was noteworthy for two new interactions:

1) PCNA (Recruitment platform for various DNA enzymes, see table 9, Page 42) could interact with Mre11-rad50 (MR) complex (initiator of homologous recombination) (Figure 14 left)
2) P41(leader for *de novo* DNA synthesis) and RadA (mediator for strand exchange during homologous recombination) (Figure 14 right)

Why we chosen these two interactions as the subjects of this study?

Firstly, decades of biochemical studies on Mre11-Rad50 complex, emblematic key player of this pathway, have emphasized its importance as a central hub that senses, processes, and signals double-strand breaks. However, we still have much more to learn about the complex and its regulation *in vivo*, most notably the regulation of the different enzymatic activities of this complex.

RadA, a member of recombinase RecA family, plays a central role in the homologous recombination. It has multifunction as homologous sequence searching, repairing and strand exchange, which are the core of HR mechanism. Biochemical functions of their bacterial and eukaryotic homologues have been well documented, but knowledge of archaeal RadA is much more incomplete.

In addition, the interactions between these key players of genomic integrity have not been described yet. And understanding the role of these associations might shed light on the corresponding eukaryotic homologs.

The aim of this thesis is to bring about a more precise characterization of these two protein-protein interactions, in order to explore the physiological role of this partnership in genome maintenance in Archaea. First of all, their physical interactions in different conditions will be confirmed with Co-IP and biophysical technics. Then the change of various activities of the protein in the presence of their potential partner will be determined by using different functional approaches. Finally, a study *in vivo* will be carried out to test the effect of this interaction in biological condition.

According to the two interactions that will be studied, this thesis is composed of two chapters: (1) PCNA/Mre11-rad50 and (2) Primase/RadA. Each chapter begins with a description of proteins that can help us to understand their stuctural and biochemistry characteristics. The results and discussion of the first chapter “PCNA/Mre11-rad50” will be clearly presented through our published article “Physical and functional interplay between PCNA DNA clamp and Mre11–Rad50 complex from the archaeon *Pyrococcus furiosus*”, and this chapiter will be complemented with a supplementary genetic experiments *in vivo*. For the second chapter, it is followed by the experiment and the results. The ensuing sections discuss the obtained results. The end of this manuscript will be one general conclusion from all of the research and perspectives.

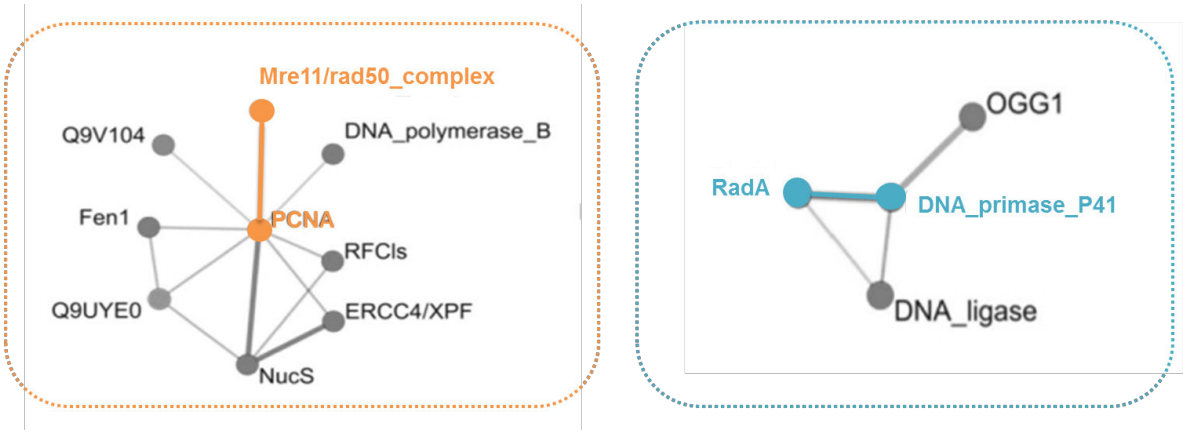

Figure 14 : Protein-protein interaction network in genome maintenance in the Hyperthermophilic archaea *Pyrococcus abyssi* (Pluchon *et al*, 2013). The study of thesis is focusing mainly on two interactions: Mre11-rad50 complex and PCNA (left: in orange square) & DNA primase-P41 and RadA (right: in blue square)

Chapter 1: PCNA & Mre11-rad50

I. Presentatio of studied proteins

1) PCNA

2) Mre11-rad50 complex

3) Aim

II. Article

Physical and functional interplay between PCNA DNA clamp and Mre11–Rad50 complex from the archaeon *Pyrococcus furiosus*

III. Supplementary study: genetic study *in vivo*

1) Context

2) Materials & methods

3) Results and discussion

a) Verification of mre11_Δpip gene sequence

b) Construction of the mre11_Δpip recombination plasmid

c) Deletion of mre11_Δpip is potentialy essential for viability in *Thermococcus*

I. Presentation of studied proteins

1) PCNA

a) "Clamp-loaders" in all three domains of life

Proliferating cell nuclear antigen (PCNA) is a DNA sliding clamp, which is globally conserved in all three domains of life (Moldovan *et al*, 2007), and sometimes could be found in virus (Kuriyan & O'Donnell, 1993). Although PCNA is a common multimeric ring-shaped complex in eukaryotes, bacteria, archaea and virus, the individual clamps exist in different oligometric states. Eukaryotic PCNA and T4 bacteriophage clamps (gp45) are formed by three identical monomers (homotrimeric complex) (Figure 15a and 15e). Archaeal PCNA complexes are divided into two groups: in the euryarchaea, as in eukaryotes, PCNA is homotrimeric (from *e.g. Archaeoglobus.fulgidus, Pyrococcs furiosus* and *Haloferax volcanii*) (Figure 15b); in crenarchaeal organisms, PCNA complexes potentially form both homo- and hetero-trimeric complexes (*e.g. Sulfolobus solfataricus*) (Figure 15c). In bacteria, the β subunit of *Eschericha coli* Polymerase III holoenzyme acts as the DNA clamp and is active as a dimer (Figure 15d) (MacNeill, 2016; Shin *et al*, 2014; Yao *et al*, 1996; Mueser *et al*, 2010; Trakselis & Benkovic, 2001; Matsumiya *et al*, 2001). In almost all euryarchaeal, there is only one gene encoding PCNA as in eukaryotes, except for *Thermococcus kodakarensis,* that has two PCNA homologous. In contrast, the majority of crenarchaea for which genome sequences are available have multiple PCNA homologues. In *S. solfataricus,* there are three PCNA homologs (Barry & Bell, 2006).

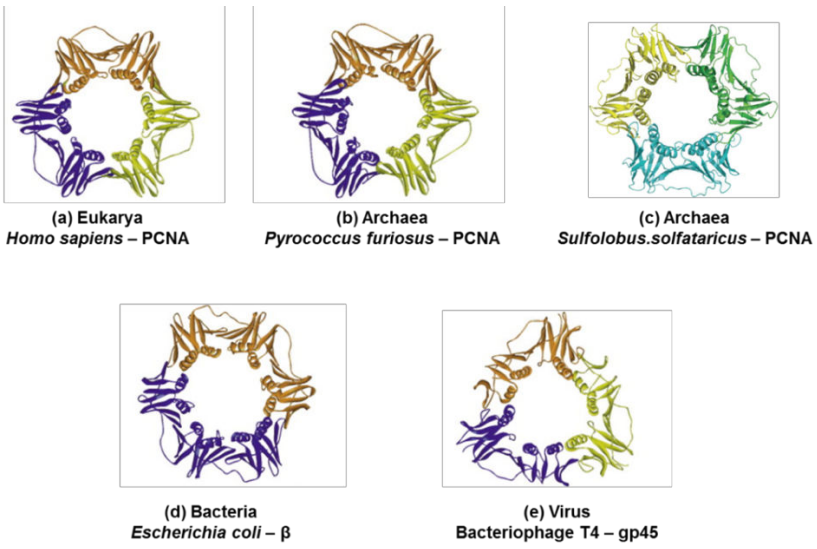

Figure 15 : X-ray structure of the Clamp from different organisms (study from (Shin *et al*, 2014; Trakselis & Benkovic, 2001). (a) *H. sapiens*; (b) *P. furiosus*; (c) *S. solfataricus*; (d) *E. coli*; and (e) Bacteriophage T4

The crystal structure of *Pfu*PCNA has been characterized in 2001. As mentioned, PCNA from *P. furiosus* forms homotrimers, each monomer is composed of two structurally similar domains: N-terminal domain and C-terminal domain (Figure 16a). Three monomers are connected in a head-to-tail manner by a long loop (named "IDCL" for Interacting Domain Connection Loop), to form a circular fashion in pseudo six-fold symmetry (Figure 16b) (Matsumiya *et al*, 2001; Xu *et al*, 2016). These two domains and IDCL are in the "front" side of PCNA, while the "back" side of PCNA contains several pronounced loops that protrude into the solvent (Naryzhny, 2008).

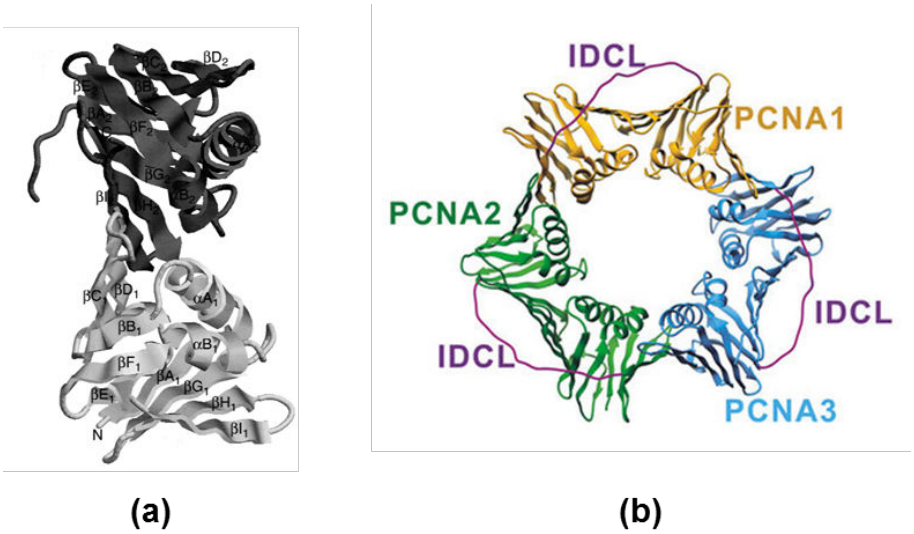

Figure 16 : Structure of *Pfu*PCNA. (a) monomer of *Pfu*PCNA, N-terminal domain is shown in light gray, and C-terminal domain is shown in dark gray **(Matsumiya *et al*, 2001)** (b) homotrimers of *Pfu*PCNA, three identical monomers are shown in yellow, green and blue, and IDCL are shown in purple **(Xu *et al*, 2016)**.

PCNA is called a “DNA sliding clamp” because it encircles dsDNA in its central cavity (with its inner positively charged surface) and can slide freely bi-directionally along it (Kelman & Kelman, 2014). PCNA has no enzymatic activities when it is free in solution without encircling DNA, however, it cannot assemble independently around the duplex. So one “loader” which is capable of assembling PCNA around the DNA is necessary: RFC (Replication factor C). RFC can use its ATPase activity to open the PCNA ring and assemble it around the primer synthetized by primase in the beginning of replication (Figure 17) (Indiani & O’Donnell, 2006; Dionne *et al*, 2008; Tainer *et al*, 2010). In several archaea, PCNA can load upon DNA itself without ATP hydrolysis, even if RFC could reinforce the DNA clamping (Cann *et al*, 1999; Henneke *et al*, 2002; Rouillon *et al*, 2007).

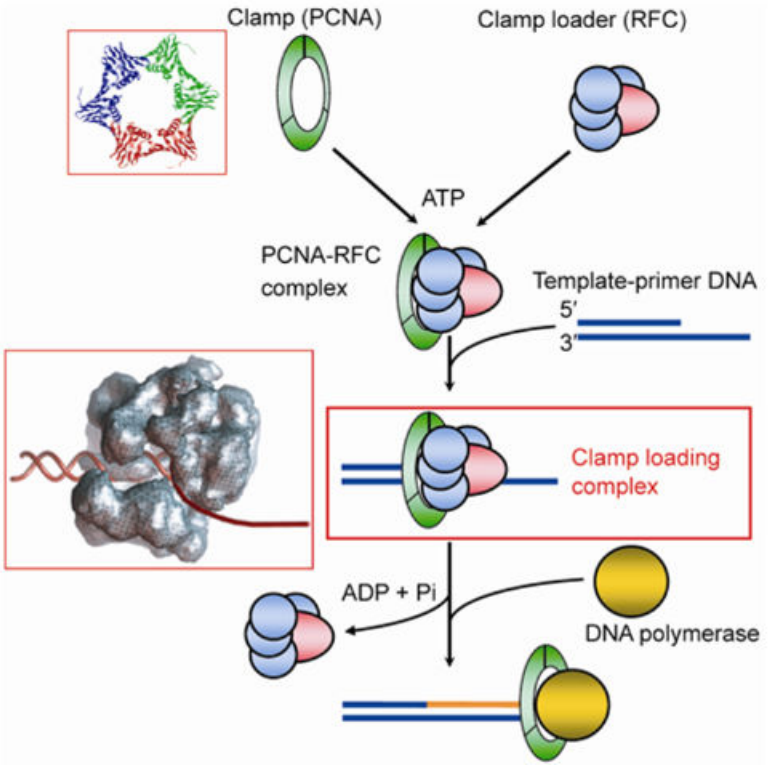

Figure 17 : Schematic representation of the clamp loader function using RFC and PCNA in Archaea. ATP hydrolysis by RFC allows RFC to bind and open PCNA. In the presence of a primer template, RFC places PCNA onto DNA and then replaced by DNA polymerase. The crystal structure of *P. furiosus* PCNA (PDB code 1GE8) (Top left) and the structure of the clamp loading complex (PCNA-RFC-DNA complex) (Bottom left) are represented respectively **(Ishino & Ishino, 2012)**.

b) "Dancer" with many partners

PCNA functions as a molecular platform which recruits several proteins in DNA replication (enhancing the activity of polymerases in leading and lagging strands formation, and also in Okazaki fragments processing), DNA repair (coordinating different replication-coupled repair reactions) (Figure 18), cell cycle control & survival (mediated via interaction with cyclins and CDKs Chromatin assembly & chromatid cohesion, transcription (remodeling factors involved in transcription) and other miscellaneous functions (such as in immune response, proteolysis, translocation etc.). In 2008, Naryzhny has listed more than 100 proteins which interact directly with PCNA in eukaryotes (Naryzhny, 2008).

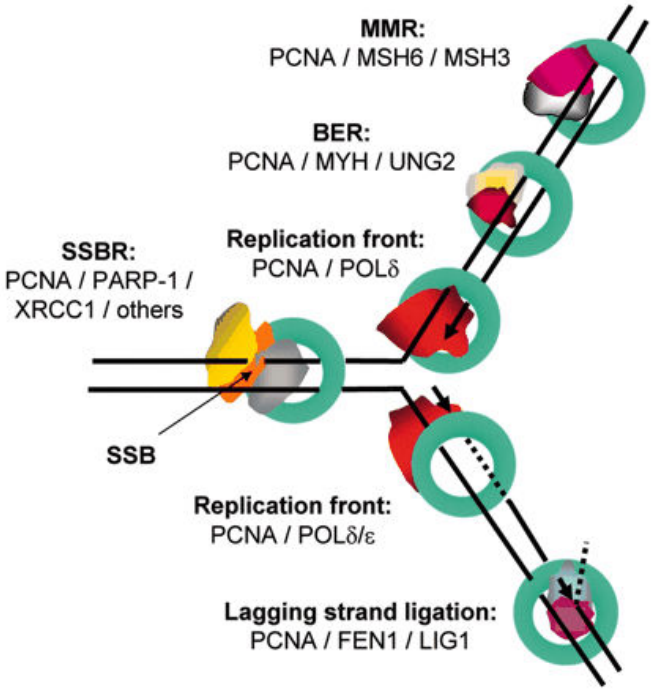

Figure 18 : Several PCNA-Protein interaction functions in DNA repair and DNA replication in Eukaryotes. PCNA can interact with the protein involved DNA replication (leading/lagging strand), in different DNA repair mechanism such as MMR, BER SSBR **(Fan *et al*, 2004)**.

In most of these recruited proteins, a common motif has been identified, called "PCNA Interacting Protein (PIP)-box". It has the consensus sequence: Q-XX-Φ-XX-ΩΩ (Jónsson *et al*, 1998; Warbrick, 2000), where X is any residue, Φ represents hydrophobic residues Leu (L), Met (M) or Ile (I), and Ω stands for aromatic residues Phe (F) or Tyr (Y) (Naryzhny, 2008). Several non-consensus PIP motifs have been determined also (Table 8) (Hishiki *et al*, 2009; Armstrong *et al*, 2012). In 2016, Boehm and Washington have shown that PIP motif is no longer considered specific. This study suggests that two adjacent aromatic residues from PIP motif are mainly responsible for interacting with target proteins. However these two adjacent aromatic residues are conserved also in other specific motifs, such as RIR motifs (which bind the translesion synthesis protein Rev1). Several proteins containing "PIP motif" can bind to Rev1, or several proteins containing "RIR motif" can bind to PCNA. In fact, the interactions are mediated by the conserved aromatic residues inserting into hydrophobic pockets on target proteins (Boehm & Washington, 2016).

Table 8 : Comparison of Consensus PIP motif and Non-consensus PIP motif (adapted from (Hishiki *et al*, 2009; Armstrong *et al*, 2012; Boehm & Washington, 2016))

		Example	
		Protein	sequence
Consensus PIP motif	Q-XX-Φ-XX-ΩΩ	*h*p21	**Q**TS**M**TD**FY**
Non-consensus PIP motif		*h*polη	**M**QT**L**ES**FF**
		*h*polι	**K**GL**I**DY**Y**L
		*y*Srs2	**Q**MD**I**FS**QL**

*Bold black: consensus residues in PIP motif;
*Bold red: different residue in non-consensus PIP motif from consensus PIP motif
*underline: adjacent aromatic residues

In 2001, a novel PCNA binding motif, K-A-(A/L/I)-(A/L/Q)-XX-(L/V), has been identified and called “KA box”, it is also present in several PCNA interacting proteins (Xu *et al*, 2001; Maga & Hübscher, 2003). In 2009, the third PCNA-interacting motif has been found in more than 200 human proteins, termed the AlkB homologous 2 PCNA interacting motif (APIM), which is characterized by the sequence: K/R-F/Y/W-$[L/I/V/A]_{X2}$-K/R, this motif is not only conserved in higher eukaryotes (Gilljam *et al*, 2009), but also conserved in yeast (Olaisen *et al*, 2018). Not all the known PCNA-interacting proteins contain PIP-box motif, some of them bind to PCNA through the PIP-related sequence QLXLF, or interact with PCNA independently of any of these motifs (Naryzhny, 2008). The majority of PCNA-interacting proteins bind to PCNA at IDCL and C-terminal tail. It exists another binding site on PCNA located at the N-terminal region comprising the inner α-helices, which was shown to form the binding site for cyclin D (Figure 19) (Matsuoka *et al*, 1994; Maga & Hübscher, 2003; Naryzhny, 2008).

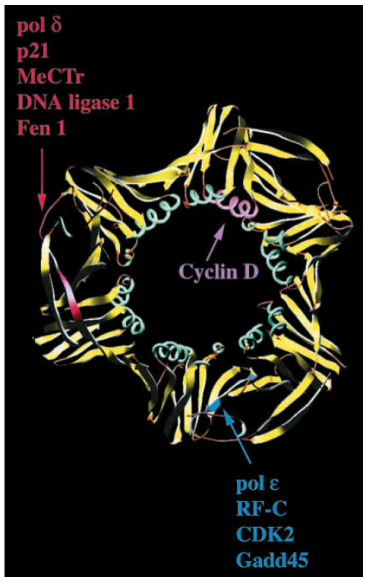

Figure 19 : Binding sites on PCNA for many of its partners in eukaryote (Maga & Hübscher, 2003). 3 main regions of the PCNA ring involved in protein-protein interactions with the relevant partners: IDCL (red); the inner side α-helices at then N-terminus (pink) and C-terminal tail (blue). Each monomer of PCNA contains these 3 protein binding regions

Most of the PCNA-binding proteins have the PIP-box, and all of these proteins will not bind to the same sites on PCNA at same time. Hence binding of different PIP-box proteins to PCNA occurs normally in a competitive manner even if PCNA is a homotrimer that can bind to more than one PCNA partners (Naryzhny, 2008). How multiple binding events to PCNA are temporally and spatially orchestrated to achieve ordered enzymatic reactions is not fully understood. One mutagenesis study suggested that the hierarchical binding of PCNA partners occurs according to their PCNA affinities. For example, p21 has dramatically higher PCNA affinity than other PIP-box proteins and when it binds to PCNA, the replication and other PCNA-linked functions are inhibited (Bruning & Shamoo, 2004). Modification of binding partners is another means to control their interactions with PCNA. Such as the phosphorylation of PCNA partners allows removing specific binding factors from PCNA, or the PCNA-coupled ubiquitylation of binding proteins could prevent their re-association. Moreover, the post-modification of PCNA by ubiquitin and SUMO (*small ubiquitin-related modifier*) is also a principal means of regulation of interactions between PCNA and its binding partners. These modifications could influence PCNA-binding properties of PCNA partners, leading to either recruitment or inhibition of cofactor binding. The new binding partners can then bind to unmodified or modified PCNA. Finally, PCNA unloading mediated by RFC and PCNA degradation triggered by dephosphorylation-induced ubiquitylation are the two last ways to affect PCNA and its binding partners. In these cases, newly bound PCNA molecules can engage in interaction with new cofactors (Moldovan *et al*, 2007; Mailand *et al*, 2013).

Several studies in archaea have identified that the PIP-box motif is conserved in a larger numbers of PCNA-interacting proteins (Warbrick, 2000; Meslet-Cladiére *et al*, 2007). In archaea *Sulfolobus solfataricus*, PCNA is a heterotrimer (3 subunits: PCNA1, PCNA2 and PCN3), and each subunit can distinctively bind Flap endonuclease 1 (Fen-1), replicative DNA polymerase and DNA ligase 1 (Lig1), respectively, during Okazaki fragment-processing (Figure 20) (Cannone *et al*, 2015). In addition, the post-modifications of PCNA in archaea have been suggested to participate in turn over regulation of the archaeal PCNA (Kirkland & Maupin-Furlow, 2009). In 2014, Li *et al*. have characterized one small protein TIP (Thermococcales inhibitor of PCNA) in *T. kodakarensis*, which is capable to bind to PCNA, although without PIP motif, and prevent PCNA trimerization. The disruption of a DNA clamp by a small protein, like

TIP, represents a new mechanism for PCNA regulation (Li *et al*, 2014). It contrasts with previously described inhibitors of eukaryotic PCNA, such as the cell cycle regulator p21, that function as competitive inhibitors at the PIP site (Gibbs *et al*, 1997).

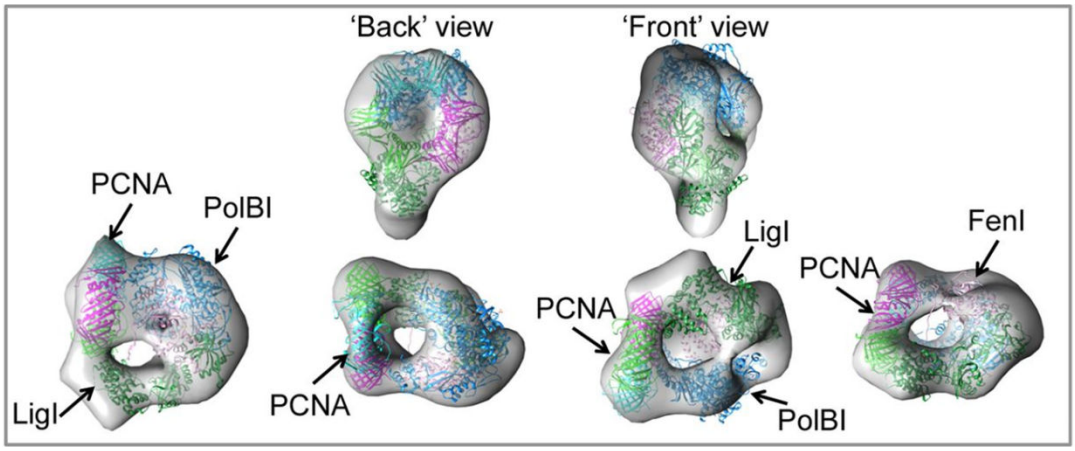

Figure 20 : 3D-EM model of complex PCNA-PolB-Fen1-Lig1-DNA involved in Okazaki fragment maturation in *Sulfolobus solfataricus* (Cannone *et al*, 2015). Each subunit of PCNA has it preferential interacting proteins.

Importantly, PCNA in archaea plays not only a "recruiter" role, but also serves as an accessory factor to increase the processivity of some of its partners involved in DNA replication (Table 9). For example, archaeal PCNA can provide replicative polymerases with the high processivity required to replicate genome, as in eukaryotes. In addition to the role of PCNA in replication, archaeal PCNA interacts as well with several proteins involved in DNA repair and recombination. Several studies in archaea have reported that PCNA serves to stimulate the enzymatic activities of some of its partners (*e.g.* Hjc, Hjm/Hel308 *etc.*) (Pan *et al*, 2011), however, the role of PCNA in these processes is less well understood.

Overall, all of these findings suggest that PCNA play a key role in DNA replication, repair and recombination (Pan *et al*, 2011; MacNeill, 2011). In this chapter, we will discover the effect of PCNA on the activity of Mre11-rad50 in *P. furiosus*.

Table 9 : Archaeal PCNA-interaction proteins in DNA replication and repair.
(Adapted from (Pan *et al*, 2011; MacNeill, 2016; Pluchon *et al*, 2013; Bubeck *et al*, 2011; Meslet-Cladiére *et al*, 2007; Henneke, 2012))

	Proteins	effect	Organisms in which interactions has been demonstrated
DNA Replication	PolB	Increase polymerase processivity	*Aeropyrum pernix; A. fulgidus; Methanobacterium thermoautotrophicum; Methanosarcina acetivorans; P. abyssi; P. furiosus; S. solfataricus*
	PolD	Increase polymerase processivity	*A. fulgidus; P. abyssi; P. furiosus; Pyrococcus horikoshii*
	RFC	Loads PCNA on to DNA	*A. pernix; A. fulgidus; M. thermoautotrophicus; P. abyssi; P. furiosus; S. solfataricus*
	DNA Ligase	Stimulates ligase activity	*A. pernix; P. furiosus; S. solfataricus*
	Fen-1	Stimulates nuclease activity	*A. pernix; P. aerophilum; S. solfataricus*
DNA Repair & Recombination	PolY	Increases polymerase processivity	*M. acetivorans; S. solfataricus*
	RNase HII	Modulates activity*[1]	*A. fulgidus; P. abyssi*
	XPG (Rad2)	?	*A. fulgidus*
	UDG	Stimulates activity*[2]	*P. aerophilum; P. furiosus; S. solfataricus*
	XPF	Stimulates nuclease activity	*S. solfataricus*
	AP endonuclease	Stimulates nuclease activity	*P. furiosus*
	NucS	Increases nuclease cleavage specificity	*P. abyssi; A. fulgidus*
	Hjc	Stimulates nuclease activity	*S. solfataricus*
	Hjm	Stimulates helicase activity	*P. furiosus*
	NreA	?	*A. fulgidus*
	NreB	?	*A. fulgidus*
	Mre11-rad50	?	*P.abyssi*

Note: UDG: uracil-DNA glycosylase
XPF/XPG: Xeroderma pigmentosum complementation group F / G
AP: Apurinic/apyrimidinic

*[1]Enhancing activity *on A. fulgidus* RNaseHII (Bubeck *et al*, 2011); in *P. abyssi,* PCNA can inhibited activity of RNase HII (Meslet-Cladiére *et al*, 2007), however, Henneke observed that there was no effect of PCNA on RNase HII (Henneke, 2012)

*[2]Stimulatory effect *on P. furiosus* UDG, but no effect was observed on *P. aerophilum* and *S. solfataricus UDG.*

2) Mre11-rad50 complex

From the previous study of PCNA in archaea, we have noted an interaction between PCNA and Mre11-rad50 complex (MR complex) from *Pyrococcus abyssi*, the aim of this chapter is to discover the functional role of this interaction using *Pyrococcus furiosus* proteins, a close relative of *P. abyssi*. Before the study of the interaction, we will present the characteristics of Mre11-rad50.

Mre11-rad50 complex is a key player in homologous recombination for the response to double-strand breaks, which are caused by exogenous or endogenous agents, and are one of the most lethal forms of DNA damage that lead to chromosomal rearrangements, genome disruption, oncogenesis and even cell death.

a) Conserved in all three domains of life and virus

The Mre11 (Meiotic recombination 11)-rad50 (Radiation sensitive) complex is a critical enzyme involved in different cellular processes of genome maintenance such as double-strand break repair (in sensing, binding, resecting and tethering DNA ends), telomere maintenance (Lamarche *et al*, 2010), replication stabilization (Tittel-Elmer *et al*, 2009), and meiotic recombination in eukaryote (in triggering signal pathway by interaction with checkpoint kinase ATM) (Borde, 2007).

MR complex is composed of Mre11 endo/exonuclease dimer and two Rad50 ATP-binding cassette proteins. This complex is conserved in all kingdoms of life: Mre11(M)-Rad50(R) in Eukaryotes (Paull & Gellert, 1998) and Archaea (Hopfner *et al*, 2000a), SbcD(M)-SbcC(R) in Bacteria (Sharples & Leach, 1995) and gp47 (M)-gp46(R) in bacteriophage T4 (Leach *et al*, 1992). MR complex in eukaryotes is particularly combined to a third protein partner: Nbs1(Nijmegen breakage syndrome) in mammalian (formed in MRN) (Paull & Gellert, 1999), or Xrs2 in yeast (formed in MRX) (Trujillo *et al*, 2003). All of these MR complexes share the same organizational arrangement. The M subunit of MR complexes contains phosphoesterases motifs that are required for nuclease activities of M subunit. While in the R subunit, Walker A and Walker B nucleotide-binding motifs are found in N- and C- terminal regions, respectively (Connelly & Leach, 2002).

b) Structural analysis of the Mre11-rad50 complex

- structure of Mre11-rad50

The crystal structures of both Mre11 subunit and Rad50 subunits from *Pyrococcus furiosus* have been reported in 2001 (Hopfner *et al*, 2001), its structure generally resembles that of its eukaryotic and bacterial homologs (Figure 21A-C). Two Mre11 and two rad50 in *P. furiosus* form a conserved heterotrimeric complex M_2R_2. The MR complex is composed of three parts: the globular DNA-binding head formed by a dimer of the Mre11 and the ABC (ATP binding cassette)-ATPase domains of Rad50, which serve as catalytic domain of the complex; the elongated mobile Rad50 coiled-coils, which links the N-terminal and C-terminal ATPase domains of Rad50; and the distal Rad50 hook domain, which is a dimerization domains and binds a Zn^{2+} cation. The structure of *h*MRN complex in solution has been reveled by AFM (Atomic Force Microscopy) (Figure 21D) (Moreno-Herrero *et al*, 2005).

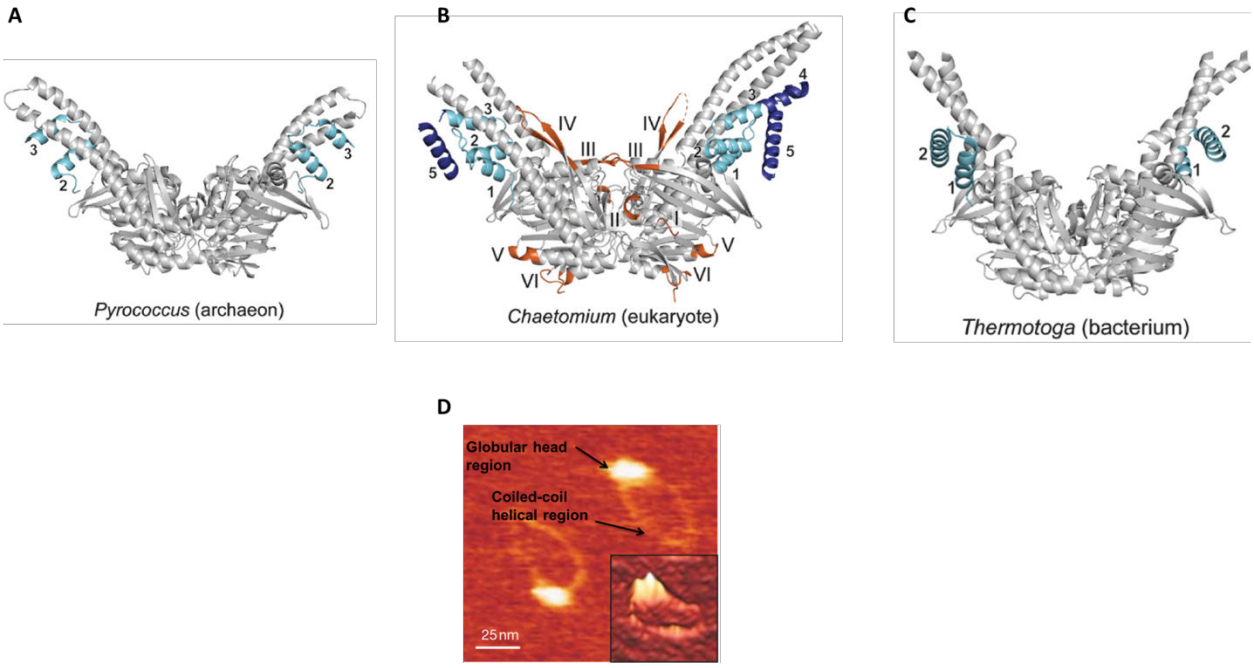

Figure 21 : Comparison of archaeal, eukaryotic and bacterial Mre1-Rad50. A-C: Crystal structures of *Pyrococcus furiosus* (A), *Chaetomium thermophilum* (B) and *Thermotoga maritima* (C) Mre11-rad50 complexes are shown (PDB codes: 3QKU, 5DA9, 3QF7) **(Seifert *et al*, 2016)**. D: AFM image of hMRN complex **(Moreno-Herrero *et al*, 2005)**.

*Pfu*Mre11 has a size of 426 amino acid residues compared to 708 residues for human or 649 residues for *Schizosaccharomyce pombe*. The conserved Mre11 core contains a nuclease domain (five conserved phosphodiesterase motifs at N-terminal of protein, which form the nuclease active site), a capping domain and a C-terminal Rad50 binding domains (RBD). The two last domains are bridged by a flexible linker. Apart from these 3 domains, Mre11 possesses also several DNA-binding recognition loops (Hopfner *et al*, 2001; Williams *et al*, 2008; Assenmacher & Hopfner, 2004; Taylor *et al*, 2004) (Figure 22A).

Within the nuclease activity area of *Pfu*Mre11, two Mn^{2+} ions are coordinated by seven conserved residues of the phophodiesterase motifs. When Mn^{2+} ions are replaced by Mg^{2+}, a significantly weaker affinity was observed, such that only one Mg^{2+} ions could be bound to active site (Hopfner *et al*, 2001). The mutations of endonuclease activity site of Mre11 in *S. pombe* result in an augmentation of cells sensibility to different genotoxic agents (Williams *et al*, 2008). Capping domain is involved in discriminating between ssDNA and dsDNA, DNA binding and restricting dsDNA access (Williams *et al*, 2008; Das *et al*, 2010; Shibata *et al*, 2014). Recently, a structural study in *S. cerevisiae* has identified a residue located in capping domain which play a key role in mediating the interaction of Mre11 with both Rad50 and DNA (Cassani *et al*, 2018). The rad50-binding-domain was mapped at the C-terminal of Mre11 protein (Figure 22A), the mutation of RBD leads to a severe diminution of interaction between Mre11 and Rad50 *in vivo* (Williams *et al*, 2011).

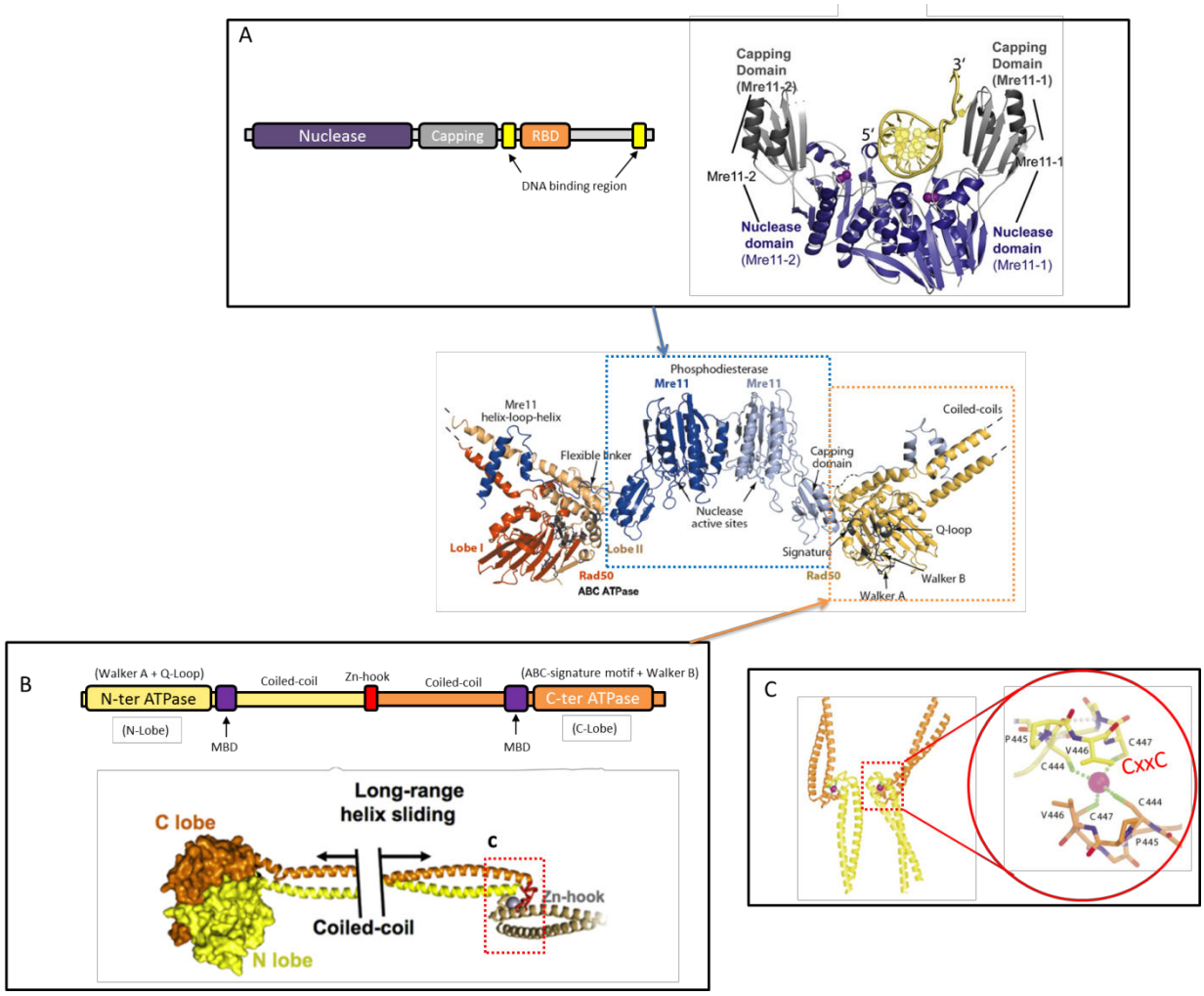

Figure 22 : Domain architecture and crystal structures of Mre11-rad50 complex (Lammens *et al*, 2011; Lafrance-Vanasse *et al*, 2015; Hopfner *et al*, 2002). (A) Mre11 consists of a conserved N-terminal nuclease domain with a capping domain, and a C-terminal Rad50-binding domain which is flanked by two DNA binding regions. Crystal structure of Mre11 nuclease dimers (purple and grey) from hyperthermophilic archaea *Pyrococcus furiosus* with DNA (yellow). (B) Rad50 is made up from a bipartite ABC-ATPase cassette with adjacent Mre11-binding domain, which is separated by a long coiled-coil region and a Zn-hook in the center of coiled-coil region. Crystal structure of Rad50 from eukaryote is build up from head domain (N-lobe (yellow) and C-lobe (orange)) and two coiled-coils which are linked by Zn-hook, respectively. (C) Crystal structure of Zn-hook from hyperthermophilic archaea *Pyrococcus furiosus*, two *Pfu*Rad50-CXXC molecules (orange and yellow) form a dimer interface serving as Zn2+ binding site.

Rad50 is a member of the structural maintenance of chromosome (SMC) proteins family (Hopfner *et al*, 2001). In *P. furiosus*, Rad50 is composed of 882 residues (Hopfner *et al*, 2000a). The Rad50 bipartite ABC-ATPase globular domains consist of an N-terminal (ABC-N) and a C-terminal (ABC-C) segment. ABC-N has the Walker A motif, and ABC-C has the Walker B and a conserved "signature motif". The Walker A motif binds ATP and forms the nucleotide binding domains (NBDs); the Walker B hydrolyses ATP and binds one active Mg^{2+} ion and participates in dimerization; the "signature motif" is as well essential to ATP binding and plays a key role in ATP-dependent Rad50 dimerization (Moncalian *et al*, 2004; Hopfner *et al*, 2000b, 2001). There is also a Q-loop in Rad50 which serves for the binding of Mn^{2+} ions (Hopfner *et al*, 2000b; Szalkai *et al*, 2014) (Figure 22B). The Mre11 binding site is on the Rad50 coiled-coil region, adjacent to the ABC domain, it allows to flexibly form Mre11-rad50 complex with Rad50 binding domain of Mre11 (Hopfner *et al*, 2001; Williams *et al*, 2011; Szalkai *et al*, 2014).

In eukaryotes, zink-hook of Rad50 is located at the terminal part of the coiled-coil region, formed by two conserved cysteine residues (Cys-X-X-Cys motif), which bind one Zn^{2+} ion. The dimerization of Rad50 is mediated by Zn^{2+} (figure 22C), this Rad50 zinc-hook structure could serve as a joint between two MR complexes in DNA recombination and repair (detail below, page51) (Hopfner *et al*, 2002). Recently, a study of MR complex from bacteriophage T4 has shown that the Zn^{2+} binding ability by Zinc-hook is critical for the function of MR complex. The mutation of the Zinc-hook leads to abolish the ATPase activity of Rad50 and reduce repetitive exonuclease activity of MR complex (Barfoot *et al*, 2015).

- DNA binding/tethering activity

At first the crystal structures of Mre11-rad50 complex from eukaryote have revealed that the conformation of *h*MRN is changed upon DNA binding. AFM data showed that, in the absence of DNA, the coiled-coil region is opened with an interaction between two apexes of coiled-coils tails within the same complex. After DNA binding, the coiled-coils of *h*MRN complex adopt a parallel conformation. Indeed, in the presence of DNA, the coiled-coil apex interaction converted from intra-complex to inter-complex (Figure 23). This conformational change could be implicated in DNA-end tethering (Moreno-Herrero *et al*, 2005). Notably, all of the experiments realized in this study are in presence of a non-hydrolysable ATP analogous, AMP-PNP. On the one hand this ATP analog is necessary because MR complex binds especially to DNA in an ATP-dependent manner. On the other hand, this observed switch of conformation of MR complex was not due to ATP hydrolysis, but whether ATP binding is in charge of this conformational change was not clear. Moreover, the observations were with MRN complex, which part of the complex is mainly responsible for DNA binding and the change of conformation was not completely understood.

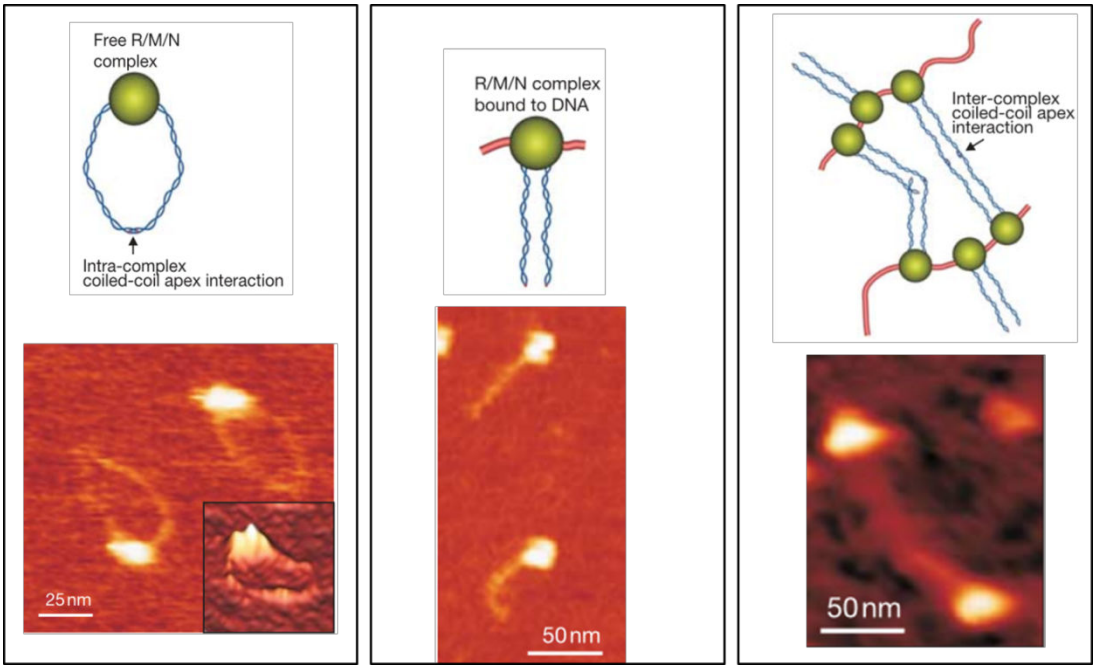

Figure 23 : AFM images of hMRN complex in the absence and presence of DNA (Moreno-Herrero *et al*, 2005). Left figure: *h*MRN in free solution (without DNA), its coiled-coils tails are in "open" state. Middle figure: *h*MRN conformation in the presence of DNA, the coiled-coils are oriented in a parallele conformation. Right figure: inter-complex coiled-coil apex interaction mediated by the interaction of zinc-hook domain of *h*MRN complex.

In 2008, a structural study has analyzed how the Mre11 domain of *P.furiosus* binds to DNA lesions : either Mre11 dimers align and tether two DNA ends with a short 3' overhang (Figure 24 left), or Mre11 dimers binds cooperatively to one branched DNA ends (Figure 24 right) (Williams *et al*, 2008). This study suggested that Mre11 dimers can distinguish different DNA substrates. Another structural, biochemical and genetic findings of Mre11 from archaea *Methanococcus jannaschii* indicate that Mre11 dimer is required to bind extended B-form DNA near the end of broken chromosomes to facilitate DNA repair (Sung *et al*, 2014). Single-molecule imaging of human MRN complex also suggested that Mre11 is in charge of DNA end recognition and then nuclease activities (Myler *et al*, 2017).

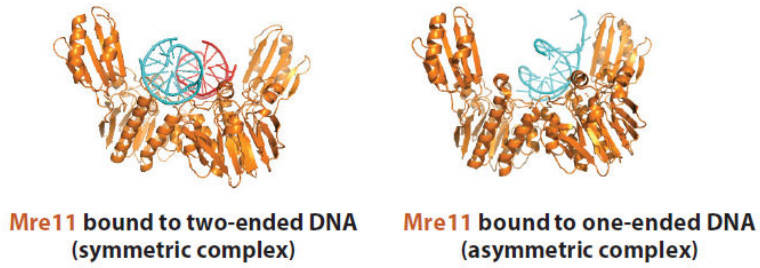

Figure 24 : X-ray structures for two Mre11-DNA binding models (Syed & Tainer, 2018),adapted from (Williams *et al*, 2008). (Left) Mre11 dimers (orange) bind two DNA ends (blue and red), they can align and tether two DNA ends. (Right) Mre11 dimers bind one dsDNA.

Structural studies form Bacteria and Archaea have discovered that ATP binding to the two NBDs of the Rad50 subunits induces MR complex conformational change. MR complex adopts from a flexible "open" form with a central Mre11 nuclease dimer and two separated Rad50 NBDs to a more rigid conformation ("closed" form) (Figure 25). In *Thermotoga maritima*, an increase of DNA affinity of the complex has been observed in ATP-binding induced "closed" form (Lammens *et al*, 2011; Lim *et al*, 2011; Möckel *et al*, 2012; Williams *et al*, 2011).

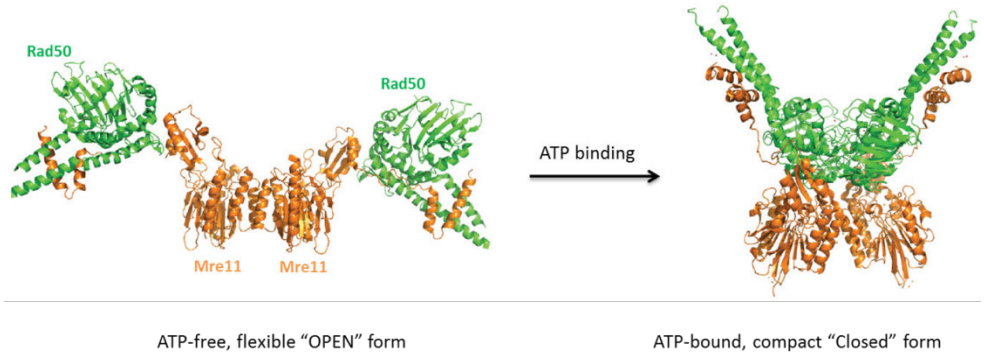

Figure 25 : Structural model for MR complex conformation (Syed & Tainer, 2018). In ATP-free "Open" state (*T. martima* MR, PDB: 3QG5) and in ATP-bound "closed" state" (*M. jannaschii* MR, PDB: 3AV0).

In 2014, Rojowska et *al* have shown that dsDNA could bind to coiled-coil domain of *Tm*Rad50 with AMPPNP (Rojowska *et al*, 2014) (Figure 26A). The recent studies have shown that Mre11 is also physically separated from the DNA duplex. A central positively charged groove is formed when ATPs bind to Rad50, which promotes dsDNA binding. And this dimerization of Rad50 recognizes approximately 18 bp long DNA duplex (Figure 26B) (Liu *et al*, 2016; Seifert *et al*, 2016).

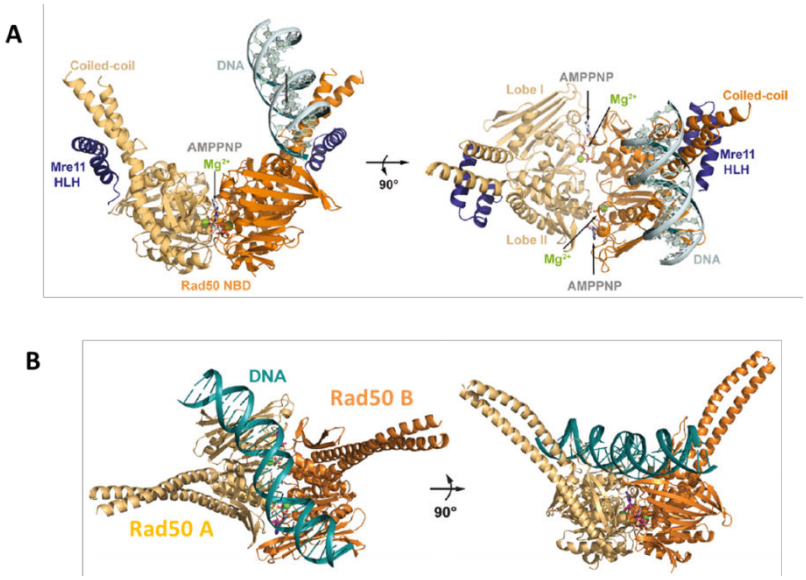

Figure 26 : Rad50 dimerization induced DNA binding and Zn-hook formation (Seifert *et al*, 2016; Rojowska *et al*, 2014). ATP-induced dimerization stimulates DNA binding to MR complex on coiled-coil (A) or in the central grooves (B).

A recent study using fluorescence imaging of the human MRN complex has revealed that the subunits Rad50 of the complex is responsible of binding dsDNA and facilitating diffusion along chromatin, whereas Mre11 is required for DNA end recognition and nuclease activities (Myler *et al*, 2017). Hence, Paull proposed a model of Mre11/Rad50 after ATP hydrolysis with Mre11 accessing DNA for nuclease attack. ATP binding to Rad50 promotes DNA binding to central groove, hydrolysis of ATP by Rad50 stimulates conformational change of MR complex, allowing the core Walker A / B ATP-binding domains of Rad50 presumably detaching from the ATP-binding domians of the other Rad50 monomer and entering of DNA to Mre11 nuclease site (Figure 27) (Paull, 2018). However, the mechanism for DNA end recognition by Mre11 within MRN or MR complex and how Mre11 engages a DNA end within its active site are not elucidated.

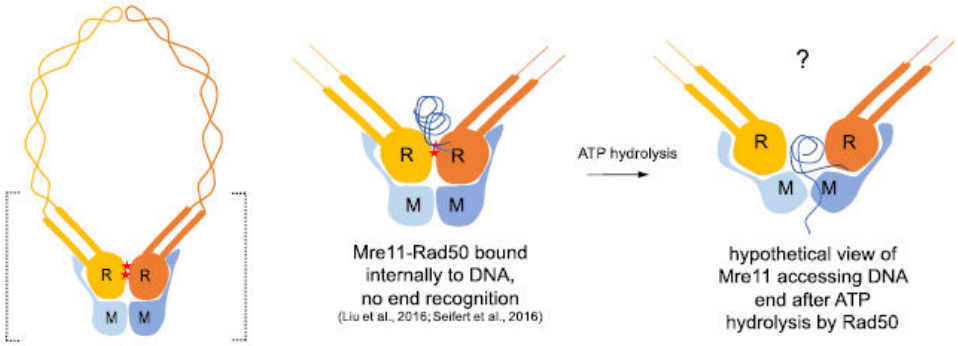

Figure 27 : Schematic representation of an Mre11-Rad50 Complex bound to DNA (Paull, 2018). Left: ATP binding (two red stars) MR complex is in "closed" form. Middle: DNA binding on the top surface of Rad50, based on structures of MR complex **(Liu *et al*, 2016; Seifert *et al*, 2016)**. Right: hypothetical model of Mre11 accessing DNA end after ATP hydrolysis by Rad50.

Furthermore, since 2001, SFM (scanning force microscopy) revealed that MR complex is used to tether DNA ends. Subsequent biochemical, EM (electron microscope) image and X-ray data of Rad50 from human and *P. furiosus* show that ATP-binding to Rad50 induced closed conformation and formed Zn^{2+}-coordinating complex either intra-complex (as a rod-shape form) with a novel interaction interface within the coiled-coil, or inter-complex (two Rad50 molecules interact between dimeric complexes) for tethering two distant DNA sites (Figure 28) (de Jager *et al*, 2001; Hopfner *et al*, 2002; Hopfner & Tainer, 2003; Williams *et al*, 2010; Deshpande *et al*, 2014; Lafrance-Vanasse *et al*, 2015; Park *et al*, 2017). Therefore, both Zn-hook and Rad50 coiled-coil domain are important for DNA binding and tethering.

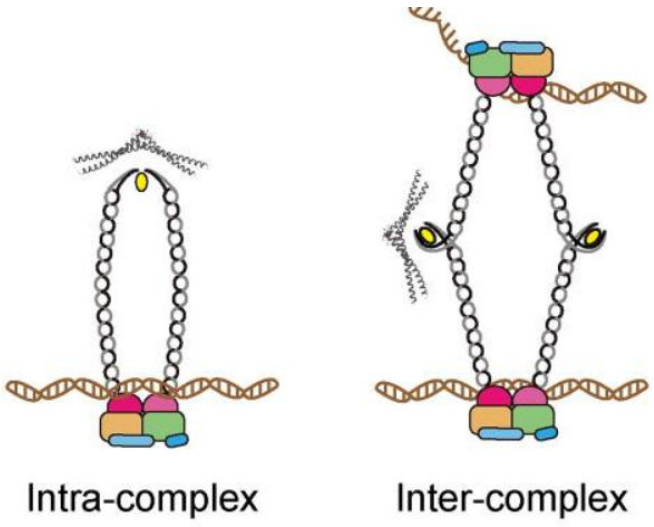

Figure 28 : ATP-binding to Rad50 induced Zn-hook formation in either intra-complex (left) or inter-complex (right) (Park *et al*, 2017). The crystal structrure of the *Pfu*Rad50 hook domain (PDB: 1L8D) is shown on top of the ring-shaped intra-complex and to the left of the intercomplex.

- ATP binding / ATP hydrolysis induced nuclease activity switch

Some biochemical studies in yeast and virus have shown that the 3'→5' dsDNA exonuclease activity of MR complex is inhibited in the presence of ATPγS due to its slow ATP hydrolysis, whereas its endonuclease activity was stimulated or unaffected in the same condition (Trujillo & Sung, 2001; Herdendorf *et al*, 2011). ATP hydrolysis inducing a conformational change of MR complex from "closed" conformation to "Open" conformation was observed (Lim *et al*, 2011; Möckel *et al*, 2012). So that Majka *et al.* proposed that this "open-closed" conformational transition by ATP hydrolysis by Rad50 can probably switch Mre11 from an endonuclease to an exonuclease, that is, Mre11 is an endonuclease under ATP-binding induced "closed" confirmation condition, and ATP-hydrolysis promotes conformational change to "open" state and switches Mre11 from an endonuclease to an exonuclease (Figure 29A) (Majka *et al*, 2012).

However, several studies demonstrated that "ATP-binding" is not sufficient for DNA end resection. They proposed that, at the beginning of ATP hydrolysis, dsDNA could be partially opened so that ssDNA may access the Mre11 active site (detail below, Page 54). It is suggested that at this moment, the Rad50 intermediates promote Mre11 ssDNA endonuclease activity while blocking the access of dsDNA and Mre11 exonuclease activity. Then, after ATP hydrolysis, the Rad50 dimers are totally disengaged to expose the Mre11-binding site, this hydrolysis-induced MR complex more open state allows DNA access to Mre11 3'→5' exonuclease activity site (Figure 29B) (Liu *et al*, 2016; Deshpande *et al*, 2014; Syed & Tainer, 2018), these observations explain why MR complex exonuclease activity is always ATP-dependent, which are shown by biochemical studies (see below, Page 56).

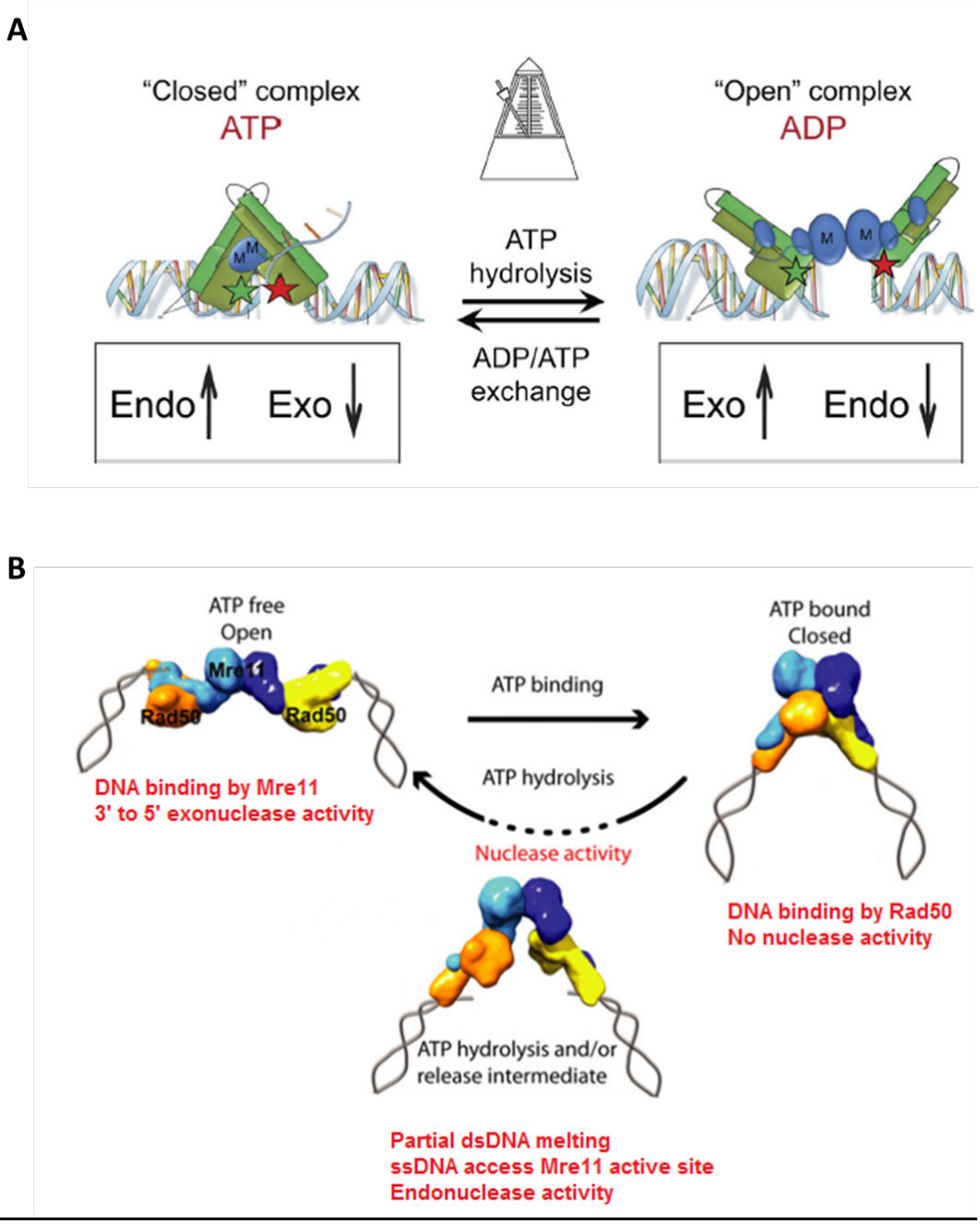

Figure 29 : Two models of ATP-induced conformation changes in MR and its associated nuclease activity. (A) ATP binding and ATP hydrolysis induced MR complex conformational states change switches the nucleolytic activity of Mre11 between endonuclease and exonuclease functions **(Majka *et al*, 2012)**. (B) ATP binding cannot induce MR endonuclease activity and DNA binding by Rad50, beginning of ATP hydrolysis induce MR intermediate for endonuclease activity on ssDNA, and complete ATP hydrolysis is necessary for DNA binding by Mre11 and exonuclease activity (modified from **(Deshpande *et al*, 2014)**).

- DNA melting activity and hypothetical related endonucleasic activity

Structural and biophysical studies gave some new insights for DNA unwinding by MR complex. One study has demonstrated that human MRN complex can realize a local DNA unwinding using FRET (Fluorescence Resonance Energy Transfer), in an ATP and Mg^{2+} dependent manner. The unwound DNA (15~20 nt) could be hold for minutes *in vitro* (Cannon *et al*, 2013) and was not observed in absence of Nbs1, consistant with biochemical observation that DNA duplex could be partially unwind (~10%) by MR complex from human, but just only in the presence of the third partner Nbs1 and ATP (Paull & Gellert, 1999). Prokaryotes lack the additional Nbs1/Xrs2 subunit, raising the question whether they also possess DNA unwinding activities? In archaea *P. furiosus*, Williams et *al*. have revealed that DNA duplex melting is linked to capping domain rotation following DNA binding. A structural study in thermophilic archaea *Methanoccocus jannaschii* has indicated that once DNA symmetrically binds to both monomer of *Mj*Rad50, ATP hydrolysis promotes the rotation of the lobes of Rad50, which induces local DNA melting during the change of conformation. This rotation allows also to open the gate for Mre11 (Liu *et al*, 2016). The same author has confirmed this DNA unwinding mechanism in bacteria *T. maritima*, showing a weak ATP-dependent DNA unwinding activity (~8%).

Several structural studies have proven that the DNA melting and endonuclease activity are coordinated by the conformational changes in both DNA and the MR complex. Their studies in *Methanococcus jannaschii* revealed that DNA symmetrical binding by both monomer of *Mj*Rad50 occurs particularly at two different minor grooves and could induce DNA melting. The interaction minor grooves are ~9-13nt and ~20-24nt away from one end of the DNA, this region of the DNA is likely to be melted by Rad50. Therefore, they suggested the hypothesis that Rad50 recognizes the terminal ends of the intact dsDNA and binds to the minor grooves, this initial recognition of the DNA results in a partial deformation of the DNA, the dsDNA is then melted. The unwound DNA could access the Mre11 active site for DNA cleavage. That is why the DNA binding sites are close to the endonuclease activity cleavage sites (Figure 30) (Liu *et al*, 2016). This hypothetical model could explain why endonucleolytic cleavage by MR complex occurs always around dozen nucleotides, which are shown by biochemical studies (Table 10).

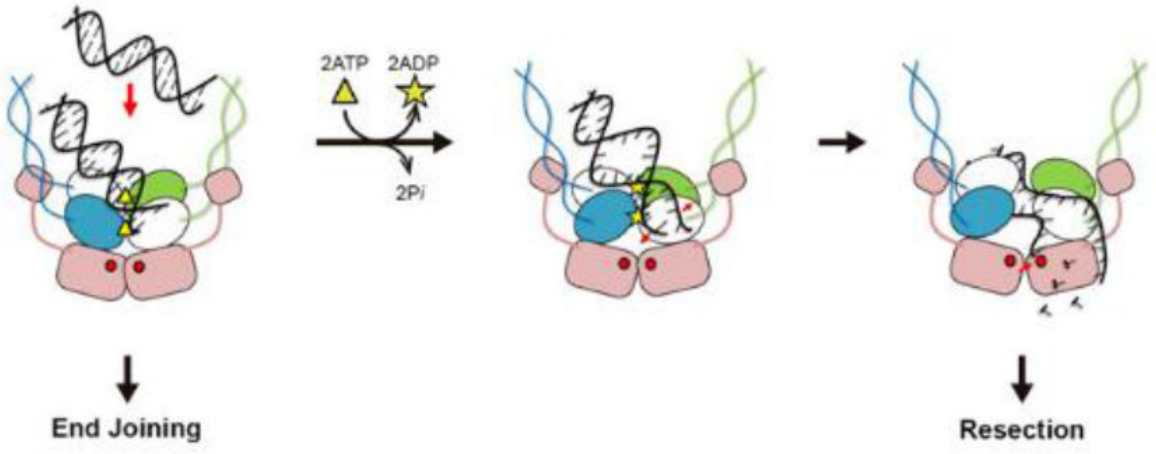

Figure 30 : A model for the ATP-dependent DNA binding, melting, and endonuclease activities of the *Mj*MR complex (Liu *et al*, 2016). Initial recognition of DNA by ATP-bound MR results in partial deformation of the DNA. ATP hydrolysis induces a lobe rotation of Rad50NBDs that melts both the internal segment and ends of the DNA, which subsequently access the Mre11active site.

Table 10 : Studies of MR complex endonuclease activity in different microorganisms

organisms	MR(N/X) complex endonucleasic resection sites	Reference
P. furiosus	~12 - 25 nt	(Hopkins & Paull, 2008)
S. cerevisiae	~ 15 - 25 nt	(Cannavo & Cejka, 2014; Shibata *et al*, 2014)
M. jannaschii	~ 9 – 13nt / ~ 20-24 nt	(Liu *et al*, 2016)
E. coli	~ 12 nt / ~22 nt	(Lim *et al*, 2015)

c) Biochemical *in vitro* activities of Mre11-rad50 complex

- Nuclease activity

In vitro, Mre11 exhibits three major nuclease activities: single-strand and double-strand endonuclease activities, double-strand exonuclease activity with a 3'-to-5' polarity, observed in all of the domains of life and virus; the third activity is DNA hairpin loops opening activity which exist in prokaryotes and eukaryotes (Table 11). Nuclease activities are Mn^{2+} or Mg^{2+}-dependent, but the nuclease activity of Mre11 is much stronger in the presence of Mn^{2+} than in presence of Mg^{2+} (Hopfner *et al*, 2002; Hopkins & Paull, 2008).

From the table 11, we note that ATP hydrolysis by Rad50 is required for MR-mediated nuclease activity on double-stranded DNA, but not for single-stranded DNA with secondary structure (such as M13 phage), and eukaryotic Mre11 exhibits 3'→5' exonuclease activity in the absence of Rad50 (Paull & Gellert, 1998; Trujillo *et al*, 1998). Moreover, viral Mre11 (gp47) of T4 bacteriophage needed ATP hydrolysis by Rad50 (pg46) for exonuclease activity, but not for the removal of the first nucleotide (Herdendorf *et al*, 2011). All above was suggesting that the requirement of ATP hydrolysis by Rad50 in not essential for all Mre11 nuclease activity, but rather for the conformation of the active site on DNA. And in several conditions, this DNA accessing to Mre11 active site is related by Rad50 (Paull, 2018).

Table 11 : Summary of biochemical nuclease activities of MR complex in Bacteria (SbcCD), Eukaryotes (MRN/X), Archaea (MR) and virus (gp46/47) *in vitro*

DNA resection	DNA substrate	Cofactor		MR complex				References
		Mn^{2+}	ATP	SbcCD	MRN/X	MR	gp46/47	
3'→5' exonuclease activity		+	+					(Connelly *et al*, 1997, 1999; Herdendorf *et al*, 2011; Hopfner *et al*, 2000a; Trujillo & Sung, 2001; Trujillo *et al*, 1998)
ssDNA endonuclease activity	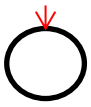	+	-					(Connelly & Leach, 1996; Connelly *et al*, 1999; Herdendorf *et al*, 2011; Hopkins & Paull, 2008; Trujillo & Sung, 2001; Trujillo *et al*, 1998)
dsDNA endonuclease activity	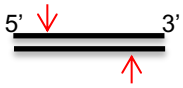	+ *	+					(Herdendorf *et al*, 2011; Trujillo *et al*, 1998; Hopkins & Paull, 2008; Cannavo & Cejka, 2014; Lim *et al*, 2015)
Hairpin degradation activity		-	+					(Connelly *et al*, 1999; Paull & Gellert, 1998; Trujillo & Sung, 2001)

* (Hopkins & Paull, 2008) has revealed an Mg^{2+}/ATP dependent endonuclease activity of MR complex on dsDNA.

- ATPase activity

According to structural studies, the cycle of ATP-binding and ATP-hydrolysis is crucial for degradation of DNA end. Biochemical studies have shown that all of the MR complexes in different organisms (Eukaryote, Bacteria, Archaea and virus) are capable to hydrolyze ATP (Bhaskara *et al*, 2007; Herdendorf *et al*, 2011). However, this ATP-hydrolysis activity is negligible in the absence of DNA, even if a DNA-independent ATPase activity has been observed once in *Pyrococcus furiosus* (Majka *et al*, 2012). In bacteriophage T4, ATP hydrolysis rate by Rad50 subunit is relatively low, while in the presence of Mre11 subunit and dsDNA, this ATPase activity had a 20-fold augmentation (Herdendorf *et al*, 2011).

The MR complex from eukaryotes show a weaker ATP hydrolysis rate (from 0,03 to 0,1 mol ATP/ mol MR/ min) than other organisms: virus, bacteria and archaea (from 1 to 4 mol ATP/ mol MR/ min) (Bhaskara *et al*, 2007; de Jager *et al*, 2002; Deshpande *et al*, 2014; Herdendorf *et al*, 2011; Lammens *et al*, 2011; Majka *et al*, 2012). Different DNA lengths and types (ssDNA, dsDNA, circular DNA) can influence the ATP hydrolysis capacity of MR complex, as well as the DNA ends structure (blunt, 5'/3'-overhang, free/blocked end) (Table 12.1, 12.2). Normally, ATP-hydrolysis capacity of MR complex is stronger with the longer linear DNA than shorter DNA or circular DNA. With the same DNA length, ATPase activity is stimulated with either 3'-overhang or 5'-overhang of dsDNA. Also, blocked DNA end reduce the ATP-hydrolysis activity of MR complex (Deshpande *et al*, 2017; Herdendorf *et al*, 2011; Majka *et al*, 2012; Trujillo *et al*, 2003).

Table 12: Studies of ATP hydrolysis activity of MR complex in different organisms

12,1: ATP hydrolysis activity rate is dependent DNA type and DNA length

MR complex	No DNA	ssDNA		dsDNA						Circular DNA
		50 bp	5 kb	40 bp	50 bp	83 bp	197 bp	1 kb	3,8 kb	
Yeast	----	NA	+++	NA	NA	++	NA	+++	NA	NA
Human	----	X	NA		++		+++	+++	+++	+
P. furiosus	----	NA		NA	NA			++	+++	NA
	+++			+++				NA		NA
virus	----	X	NA	NA	++++	NA		NA		X

12,2: ATP hydrolysis activity rate is dependent of DNA end structure

MR complex	dsDNA						
	Blunt (197 bp, B-strept)				3,8 kb		
Human	No Biotin	5' Biotin	5' Biotin+strep		Blunt	5' overhang	3' overhang
	+++	++	+		+++	++++	++++

NA: Not available

d) Third component of the MR complex in eukaryotes

In eukaryotes, MRN/X complex possesses a third partner: Nbs1 (Nibrin) in mammals and fission yeast and Xrs2 in budding yeast. The role of this third component is to regulate the catalytic activities of Mre11-rad50. Human Nbs1 is required to stimulate both Mre11 endonucleases activity on blocked DNA ends / hairpin substrates and Rad50 ATP hydrolysis activity (Deshpande *et al*, 2016, 2017; Paull & Gellert, 1999). Notably, MR-catalyzed 3'→5' exonuclease activity is inhibited on open DNA ends, but promoted at protein-blocked ends (Deshpande *et al*, 2016). In addition, Nbs1 plays an essential role via its Mre11-interacting interface for cell viability (Kim *et al*, 2017). In contrast, the yeast Xrs2 is less important in budding yeast than Nbs1 in human cells. Xrs2 is normally required for Mre11 nuclear localization, while Oh et *al* have demonstrated that in the absence of Xrs2, localizing Mre11 to the nucleus keeps the MRX-mediated functions such as DNA end resection, hairpin resolution, meiotic recombination and DNA damage survival (Oh *et al*, 2016).

e) The Mre11-rad50 complex in double-strand break repair and replication fork

As a response to DNA damage such as DNA double-strand breaks, the Mre11-rad50 complex regulates DSB repair, through the HR, c-NHEJ or Alt-EJ pathways and via the initiation of the repair mechanism, by promoting the resection of DSB ends. Mre11-rad50 is implicated also in replication fork restart. So this protein is critical to sustain the viability of proliferating cells and maintain the genomic integrity.

- The Mre11-rad50 complex in DSB repair

All of the MR(N/X) complexes have a 3'→5' exonuclease activity, that means the exonucleasic products of MR complex are 5' overhang ssDNA. During HR processes, a 3' overhang ssDNA is necessary for the following strands exchange step. How MR(N/X) can initiate the HR with a opposite exonuclease activity?

Initially, during meiosis in *S. cerevisiae*, the DSB ends are terminally blocked by covalently bound Spo11 protein (topoisomerase), Mre11 endonuclease activity was observed and also subsequent 3'→5' exonuclease activity toward the blocked DNA ends (Garcia *et al*, 2011). Thus, an « endo-cut followed by exo-cut » model was proposed for explaining how 3' overhang ssDNA can be obtained. In other words, MR complex initiated an endonucleolytic incision at DNA ends, and exonucleolytic degradation occurs subsequently. This model is always observed *in vitro* and only with protein-blocked ends (Connelly *et al*, 2003; Anand *et al*, 2016; Deshpande *et al*, 2016; Reginato *et al*, 2017; Wang *et al*, 2017). In eukayotic model, the endonuclease activity of MRX results in DNA nick, other 5'→3' exonuclease enzymes (ExoI or Helicase/nuclease Sgs1-Dna2) will be recruited at DNA nick and resect away from the DNA nick site to generate an extended 3' overhang ssDNA for HR (Figure 31B) (Cannavo & Cejka, 2014; Mimitou & Symington, 2008; Cejka, 2015; Anand *et al*, 2016). In human cells, this cooperation of the bidirectional resection is capable to free a 3' overhang single-strand up to 3,5 kb in length (Zhou *et al*, 2014). In addition, several MRN/X complex co-factors, such as Sae2 in yeast and CtIP in mammalian cells, are required to promote endonuclease activity of the MRN/X complex at ~200–300 nt away from the 5'end of DNA duplex. Recent study has shown that Sae2 in yeast can stimulate MRX endonuclease activity also at DNA nick site (Sartori *et al*, 2007; Anand *et al*, 2016; Cannavo & Cejka, 2014; Nicolette *et al*, 2010; Wang *et al*, 2017) Nevertheless, end resection by MRX complex could be bypassed when MRN

recognizes a DNA free end, Sgs-Dna1 or Exo1 was recruited by MRX to generate a 3' tailed ssDNA unsing its 5'→3' exonuclease activity (Figure 31A) (Cejka, 2015).

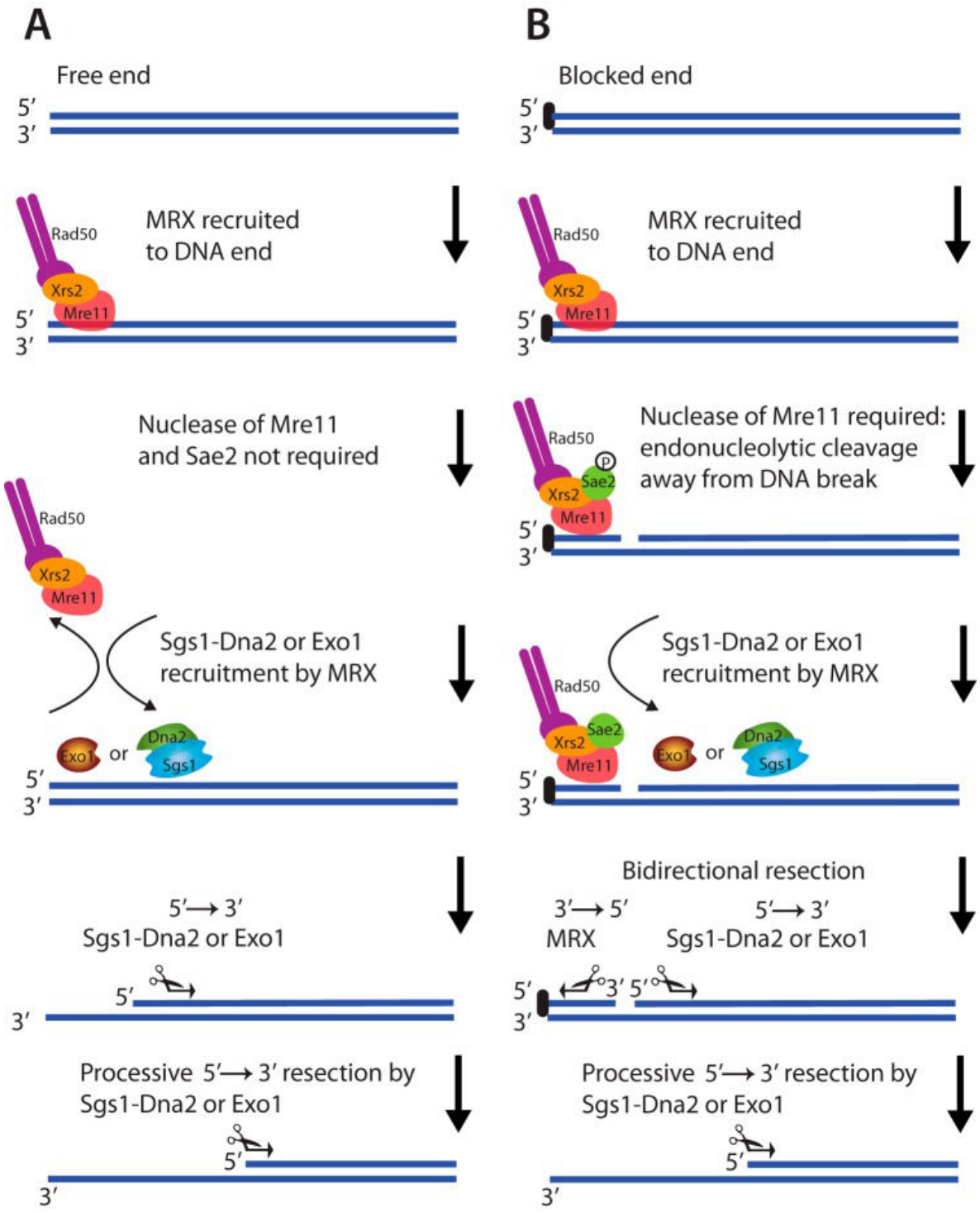

Figure 31 : Model of DNA end resection by MRX in yeast (Cejka, 2015). (A) Resection of free DNA ends. The MRX complex nuclease activity can be bypassed, Exo1 or Sgs-Dna2 are recruited to resect the ends in direction 5'→3'. (B) Bidirectional resection of blocked DNA ends. Phosphorylated Sae2 stimulates endonuclealytic activity of MRX. Then, MRX resect the ends from 3' to 5', and Exo1 or Sgs-Dna2 degrade the strand in direction 5'→3'

In Archaea, functional analogs of the eukaryotic helicase/nuclease Sgs1-Dna2 or Exo1 have been identified, that is helicase/nuclease HerA/NurA complex (Constantinesco *et al*, 2002, 2004; Zhu *et al*, 2008; Mimitou & Symington, 2008; Cannavo *et al*, 2013; Huang *et al*, 2015b; Rzechorzek *et al*, 2014). HerA is a helicase which can unwind the DNA and exhibits ATPase activity, while NurA is a nuclease which has 5'→3' ssDNA/dsDNA exonuclease and ssDNA endonuclease activities (Constantinesco *et al*, 2002, 2004; Manzan *et al*, 2004; Zhang *et al*, 2008) (Figure 32A). In archaea *Sulfolobus acidocaldarius* and *Pyrococcus furiosus*, genes *mre11*, *rad50*, *herA* and *nurA* are encoded in the same operon. Moreover, several *in vitro* experiments have demonstrated that Mre11-rad50 and HerA/NurA co-operate to resect the 5' strand at a DNA double strand break, generating a 3' ssDNA suitable for the recombinase RadA (Figure 32B) (Hopkins & Paull, 2008; Constantinesco *et al*, 2002, 2004; Blackwood *et al*, 2012).

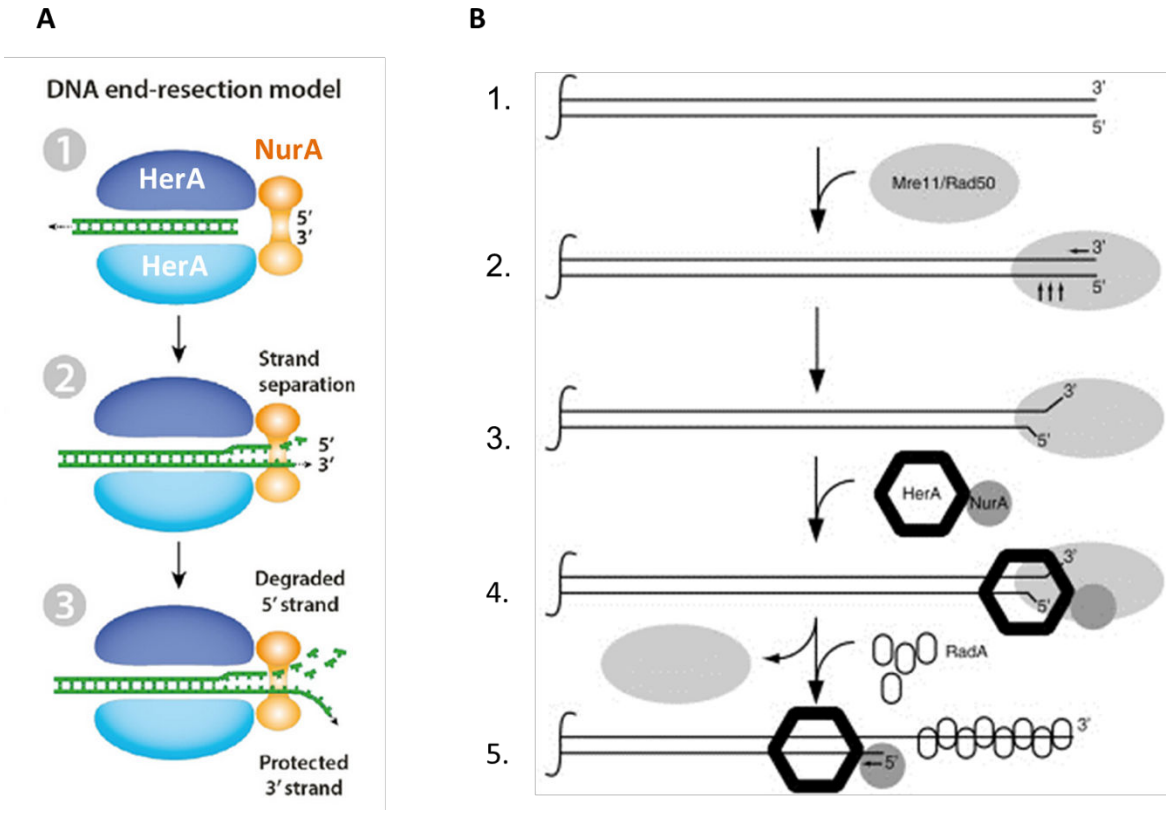

Figure 32 : DNA end-resection model of MR complex coupled with HerA/NurA. (A) HerA-NurA performs a degradation of DNA strand from 5'end to 3'end **(Ahdash *et al*, 2017)**. (B) Model of DNA end resection with cooperation of Mre11-rad50 and HerA/NurA in *Pyrococcus furiosus*. MR complex initiates the DNA end resection, the HerA/NurA is recruited subsequently and then degrade the DNA strand at 5'end to generate a long 3'-overhang ssDNA which will be coated by RadA (Hopkins & Paull, 2008).

- The Mre11-rad50 complex in replication fork dynamics

MR complex is involved not only in DSB repair, but also in the repair of stalled replication forks. Several evidences *in vivo* have been shown to support this suggestion: Yeast cells with a depletion of MRX complex cannot survivre under the stress resulting in replication blocage condition (Tittel-Elmer *et al*, 2009); MRN complex in mammals is required for cells viability (Adelman *et al*, 2009; Errico & Costanzo, 2012); Additionally, an increase of both ssDNA and dsDNA breaks during S-phase has been observed in Mre11 knockdown cells (Kondratova *et al*, 2015), which is consistent with the observation using *Xenopus* extracts, that the depletion of Mre11 leads to impaired fork restart and replication-dependent DSB accumulation (Trenz *et al*, 2006; Costanzo *et al*, 2001). Moreover, recombination factors Mre11 and Rad51 are required for reloading of replisome components (which were lost upon fork collapse) at broken replication forks to restore a functional replisome in eukayotes (Hashimoto *et al*, 2011). In Archaea, Delmas et *al* has shown that the MR complex from *H. volcanii* favors the reassembly of nucleoid under cellular stress which generated DNA damages or interferred with DNA replication (Delmas *et al*, 2013).

In a yeast model, MRX complex is recruited to forks stalled in a nuclease-independent manner. It stabilizes paused replisomes and promotes an MRX mediated sister-chromatid tethering during replication stress, to facilitate replication recovery through HR mediated mechanisms (Mirzoeva & Petrini, 2003; Tittel-Elmer *et al*, 2009). A similar model was proposed in human cells with MRN complex and proposes that this sister-chromatids tethering function of MRN is to prevent branch migration that leads to fork reversal (Kondratova *et al*, 2015). In addition, the cohesin loading at replication sites to promote fork restart is influenced by the neighboring Zn-hook sequence of Rad50. The role of cohesin proteins is to maintain the DNA neo-strand of chromatid (Tittel-Elmer *et al*, 2012). Together, it strongly suggests that MRN complex plays a role in the protection of replication forks during DNA replication (Figure 33A). This DNA end tethering role can be also involved in DSBs repair (Williams *et al*, 2008).

Although MRN complex is needed to prevent fork reversal, one-ended replication-associated DSBs is possibly formed, and under this condition, DNA end-resection processing by MRN complex is required to initiate HR function (Petermann & Helleday, 2010; Kondratova *et al*, 2015) (Figure 33B). This fork restart via HR-mediated repair of

the DSB is similar to analogous mechanism BIR (break-induced replication) which is well-characterized in yeast (Lydeard *et al*, 2010).

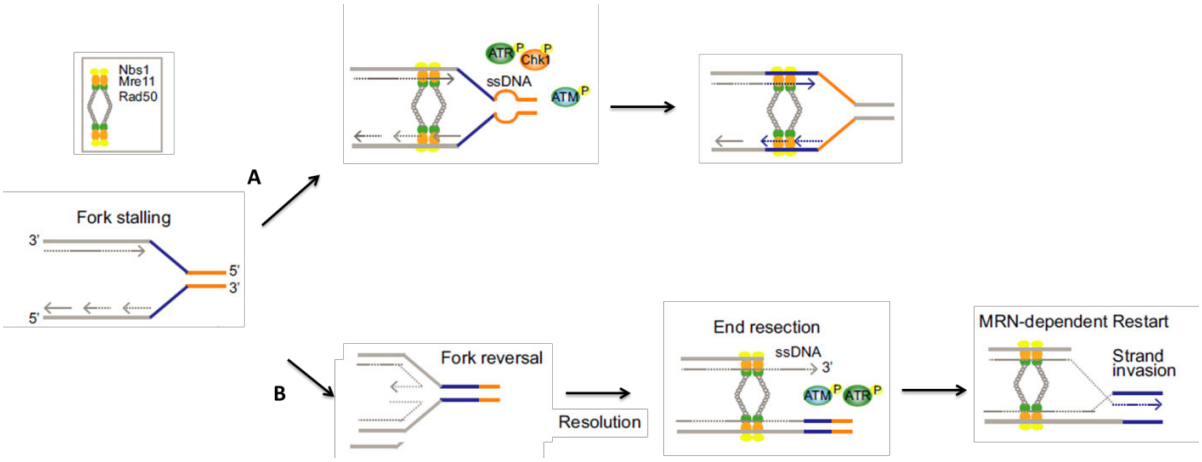

Figure 33 : Model of MRN complex orchestrates replication fork in fork protection (A) and fork restart (B) (Adapted from **(Kondratova *et al*, 2015))**. (A) MRN complex facilitates fork restart before fork reversal by sister chromatid tethering activity. (B) MRN complex facilitates also fork restart from one-ended breaks by en resection activity

However, Kondratova et *al* have observed that *mre11-null* cells could still proliferate with broken forks, suggesting that there might be an alternative, MRN-independent fork restart mechanism from broken fork (Kondratova *et al*, 2015).

f) Diseases linked with mutations in Mre11-rad50

Null mutations of the gene encoding MRN induce different heredity diseases in humans. Ataxia-telangiectasia-like disorder (ATLD), Nijmegen breakage syndrome (NBS) or NBS-like disorder (NBSLB) are caused by the germinal mutations in *mre11, nbs1* or *rad50* genes, respectively (Taylor *et al*, 2004; Stracker & Petrini, 2011; Waltes *et al*, 2009). All of these diseases have a common consequence that the chromosome in cells from patients is instable and sensible to radiation. Moreover, the mutated gene of these 3 components of MRN are found in more than 50 cancers (Syed & Tainer, 2018) and the absence of MRN gene is frequently found in patients with epithelial ovarian cancer (Brandt *et al*, 2017). Neuropathology studies indicated that ATLD, NBS or NBSLB diseases are characterized by microcephaly, mental retardation and growth defects, and proposed that the mutations of MRN affecting the DNA DSB signaling are responsible for these diseases (Uchisaka *et al*, 2009; Shull *et al*, 2009).

Overall, MR(N) complex proteins is a key player in sensing, signaling and response at DNA double-strand breaks.

3) Aim

The MR complex is involved in various aspects of DSB repair, including sensing the DSB triggering signal pathways and facilitating the DSB repair through different pathways. Among hyperthermophilic archaea, gene deletions of mre11 and rad50 are lethal for cell arguing for their apparent essentiality distinguishable HA from all other cellular organisms, including mesophilic archaea (Grogan, 2015). Protein-protein interaction network in hyperthermophilic archaea has revealed that MR complex has a partner PCNA, but we don't know the role of PCNA on MR complex. Several studies have shown that PCNA participates in DSB repair in eukaryotes, serving as a processivity factor for Exo1 or stimulator for the potential 3'-5' exonuclease activity of exonuclease domain of a RecQ-like helicase. In archaea, PCNA can interact with other proteins involved in HR pathway (such as Hjc and Hel308) (Chen *et al*, 2013; Lebel *et al*, 1999; Dorazi *et al*, 2006; Fujikane *et al*, 2006).

Furthermore, the level of Mre11 peaks on chromatin during S-phase, as well as its colocalization with PCNA at replication foci, and also MRN(X) could stabilize replisome and is required upon fork collapse (Mirzoeva & Petrini, 2003; Maser *et al*, 2001; Tittel-Elmer *et al*, 2009; Hashimoto *et al*, 2011; Maga & Hübscher, 2003). Together, with a burning desire, we want to explore the role of MR complex in replication fork and the role of PCNA in recombination processes in archaea.

As mentioned above, a previous study from the lab has provided an interaction network with proteins involved in genomic maintenance in the archaea *Pyrococcus abyssi*. Gaëlle Hogrel (PhD in Ifremer) and his colleagues have revealed *in vitro* a physical association between the MR complex and the DNA clamp PCNA using the homologous proteins from *P. furiosus.* Based on these results of physical interaction between the MR complex and PCNA of *Pyrococcus furiosus,* the first aim of my PhD was devoted to the completion of the characterization of this association, in nuclease activity, DNA binding/unwinding activity and ATPase activity of Mre11-rad50 complex from *P. furiosus*.

After two-years study, we have published the article "*Physical and functional interplay between PCNA DNA clamp and Mr11-Rad50 complex from the archaeon Pyrococcus furiosus*" (Hogrel *et al*, 2018). We demonstrated both physical and functional interplay between PCNA and MR, a complex involved in recombination process.

A variation of the PCNA Interacting Protein motif (PIP-like motif) was identified in Mre11: *Pfu*MR directly interacts with *Pfu*PCNA through a peptide in the C-terminal region of *Pfu*Mre11. We identified a new non-canonical PIP box in this C-ter segment of *Pfu*MR11: [PK]-5X-[LI]-2X-W-[LIV]. This motif is different to the classical canonical PIP motif because of the absence of the well conserved glutamine residue. This PIP-like motif was also revealed among all sequences of Thermococcales Mre11. Deletion of this identified PIP-like motif effaces totally the interaction between these two proteins.

Then we investigate also functional interplay of MR complex and PCNA at physiological ionic strength and show that PCNA activates MR nuclease activities and promotes an endonucleolytic incision proximal to 5' strand of double strand DNA break. Although MR complex alone doesn't have DNA melting activity, the endonucleasic cleavage product could be displaced via MR/PCNA strand opening activity. Furthermore, we have demonstrated that *Pfu*PCNA does not have influence on ATP hydrolysis activity by Rad50.

Finally, we completed biochemical results with a genetic study, in which the PIP motif was deleted, suggesting that PIP motif is probably essential in cells growth in HA.

II. Article

Nucleic Acids Research, 2018 1
doi: 10.1093/nar/gky322

Physical and functional interplay between PCNA DNA clamp and Mre11–Rad50 complex from the archaeon *Pyrococcus furiosus*

Gaëlle Hogrel[1,2,3,†], Yang Lu[1,2,3,†], Sébastien Laurent[1,2,3], Etienne Henry[1,2,3], Clarisse Etienne[4], Duy Khanh Phung[4], Rémi Dulermo[1,2,3], Audrey Bossé[1,2,3], Pierre-François Pluchon[1,2,3], Béatrice Clouet-d'Orval[4] and Didier Flament[1,2,3,*]

[1]Ifremer, UMR6197, Laboratoire de Microbiologie des Environnements Extrêmes, 29280 Plouzané, France, [2]Université de Bretagne Occidentale, UMR6197, Laboratoire de Microbiologie des Environnements Extrêmes, 29280 Plouzané, France, [3]CNRS, UMR6197, Laboratoire de Microbiologie des Environnements Extrêmes, 29280 Plouzané, France and [4]Université de Toulouse; UPS, 118 Route de Narbonne, F-31062 Toulouse, France; CNRS; LMGM; F-31062 Toulouse, France

Received January 12, 2017; Revised April 11, 2018; Editorial Decision April 12, 2018; Accepted April 18, 2018

Nucleic Acids Research, 2018 **1**
doi: 10.1093/nar/gky322

Physical and functional interplay between PCNA DNA clamp and Mre11–Rad50 complex from the archaeon *Pyrococcus furiosus*

Gaëlle Hogrel[1,2,3,†], Yang Lu[1,2,3,†], Sébastien Laurent[1,2,3], Etienne Henry[1,2,3], Clarisse Etienne[4], Duy Khanh Phung[4], Rémi Dulermo[1,2,3], Audrey Bossé[1,2,3], Pierre-François Pluchon[1,2,3], Béatrice Clouet-d'Orval[4] and Didier Flament[1,2,3,*]

[1]Ifremer, UMR6197, Laboratoire de Microbiologie des Environnements Extrêmes, 29280 Plouzané, France, [2]Université de Bretagne Occidentale, UMR6197, Laboratoire de Microbiologie des Environnements Extrêmes, 29280 Plouzané, France, [3]CNRS, UMR6197, Laboratoire de Microbiologie des Environnements Extrêmes, 29280 Plouzané, France and [4]Université de Toulouse; UPS, 118 Route de Narbonne, F-31062 Toulouse, France; CNRS; LMGM; F-31062 Toulouse, France

Received January 12, 2017; Revised April 11, 2018; Editorial Decision April 12, 2018; Accepted April 18, 2018

ABSTRACT

Several archaeal species prevalent in extreme environments are particularly exposed to factors likely to cause DNA damages. These include hyperthermophilic archaea (HA), living at temperatures >70°C, which arguably have efficient strategies and robust genome guardians to repair DNA damage threatening their genome integrity. In contrast to Eukarya and other archaea, homologous recombination appears to be a vital pathway in HA, and the Mre11–Rad50 complex exerts a broad influence on the initiation of this DNA damage response process. In a previous study, we identified a physical association between the Proliferating Cell Nuclear Antigen (PCNA) and the Mre11–Rad50 (MR) complex. Here, by performing co-immunoprecipitation and SPR analyses, we identified a short motif in the C- terminal portion of *Pyrococcus furiosus* Mre11 involved in the interaction with PCNA. Through this work, we revealed a PCNA-interaction motif corresponding to a variation on the PIP motif theme which is conserved among Mre11 sequences of Thermococcale species. Additionally, we demonstrated functional interplay *in vitro* between *P. furiosus* PCNA and MR enzymatic functions in the DNA end resection process. At physiological ionic strength, PCNA stimulates MR nuclease activities for DNA end resection and promotes an endonucleolytic incision proximal to the 5′ strand of double strand DNA break.

INTRODUCTION

Extremophile organisms provide remarkable study systems for understanding cellular processes that allow them to live in conditions likely to cause a high rate of DNA damage. Several archaeal species prevalent in extreme environments are particularly exposed to such stressors, including hyperthermophilic archaea (HA) living at temperatures >70°C. However, several studies have shown that HA such as *Pyrococcus furiosus and Sulfolobus solfataricus* can fully restore their genomes if they are fragmented by γ-radiation (1–3). They arguably have efficient strategies and robust genome guardians to repair DNA damage threatening genome integrity. These guardians are proteins working and interacting together in a carefully orchestrated ballet. Archaea employ 'eukaryotic' DNA replication and repair complex proteins (4), but several DNA repair protein families that are broadly conserved among Bacteria and Eukarya have not been found in Archaea (5). Using *in silico*, genetic or biochemical approaches, several studies revealed new actors or new complexes involved in genomic integrity in Archaea (6–15), leading to the characterization of new helicases and nucleases, like Hel308/Hjm, GAN, NucS/EndoMS and more recently NerA, thus, improving our understanding of genomic maintenance processes in Archaea. To contribute to this effort to discover new actors or new complexes involved in archaeal genomic integrity, we characterized a protein-protein interaction network sustaining genome maintenance in *Pyrococcus abyssi* (15). In this previous study, we identified a physical association between the Proliferating Cell Nuclear Antigen (PCNA) and the Mre11–Rad50 (MR) complex: the characterization of this association is addressed in the present study.

*To whom correspondence should be addressed. Tel: +33 298 224 527; Email: dflament@ifremer.fr
† The authors wish it to be known that, in their opinion, the two first authors should be regarded as joint First Authors.

Structurally conserved between Archaea and Eukarya, PCNA is a multimeric, ring-shaped factor that encircles DNA duplex. Archaeal Replication Factor C complex (RFC), which functions as a clamp loader, stimulates PCNA assembly around DNA even though archaeal PCNA can spontaneously load *in vitro* onto DNA (16,17). First reported as a processivity factor for DNA polymerases, PCNA is essential for cell viability. As a DNA-clamp, PCNA is a moving platform for numerous partners involved in DNA replication and repair pathways (18). Extensive lists of PCNA partners have been given in reviews (19–21).

The MR complex has a broad influence on the DNA damage response network, especially on repair of DNA Double-Strand Breaks (DSB) (22). As DSBs are a particularly threatening type of DNA damage, induced by external agents as well as by internal molecular events, cells have evolved a highly sophisticated DNA damage response system. For the recognition and repair of DNA breaks, the two major mechanisms are Homologous Recombination (HR) and Non-Homologous End-Joining (NHEJ). In HR, the broken ends are resected into 3′ single-strand tails and then used as templates for a homology search; whereas in NHEJ, the broken ends are directly rejoined (for reviews see (23–25)). In Eukarya, DSBs are repaired by either HR or NHEJ depending on the cell cycle (26). NHEJ was assumed to be absent from Archaea until Bartlett *et al*. reconstituted an archaeal NHEJ apparatus *in vitro* similar to that of bacterial machinery (27). In contrast to eukaryotes and other archaea, HR appears to be a vital pathway in HA, since genetic analyses have shown that the *mre11*, *rad50* and *radA* genes are essential for *Thermococcus kodakaraensis* and *Sulfolobus islandicus* (28,29).

The eukaryotic macromolecular machine MR(N/X) is composed of two core proteins, Mre11 and Rad50, with an additional component: Nbs1 for higher eukaryote or Xrs2 for yeast, which are found in neither Bacteria nor Archaea. Both Mre11 and Rad50 are highly conserved in all three domains and even exist as gp46/47 in some virus such as T4 phage (30). The MR complex engages the HR pathway by tethering and resecting DNA ends through a combination of nuclease and ATPase activities tightly related to conformational changes (31). However, the MR complex nuclease functions, 3′→5′ double strand (ds) DNA exonuclease activity and single strand (ss) DNA endonuclease activity, are not sufficient to generate a long 3′ ssDNA tail and require additional partners to catalyse efficient DSB resection (32). Moreover, the MR complex appears to be essential in replication fork restart in eukaryote cells, but to date the biochemical and regulation mechanisms remain partially understood.

Given the role of PCNA to orchestrate DNA replication and other DNA processes, we wondered whether this newly discovered interaction with the MR complex would regulate MR enzymatic functions in the DNA end resection process. By performing co-immunoprecipitation and SPR analyses, we demonstrated physical association between *P. furiosus (Pfu)* PCNA and the MR complex and identified a short motif in the C terminal portion of *Pfu*Mre11 that interacts with *Pfu*PCNA and corresponds to a variation on the PCNA-Interaction Peptide (PIP) motif theme. Enzymatic assays, at physiological ionic strength, showed that *Pfu*PCNA stimulates nuclease activity of the *Pfu*MR complex on dsDNA substrates and promotes an endonucleolytic incision proximal to the 5′ strand of a DNA double strand break in a manner still consistent with HR process requirements.

MATERIALS AND METHODS

Proteins and peptides

A gene coding for *P. furiosus* PCNA was inserted into pET19b to add an N-terminal 10xHis-tag (plasmid provided by B. Connolly (33)) and expressed in *Escherichia coli* Rosetta pLysS. The *P. furiosus* MR complex was co-expressed from a bicistronic pET27b vector (gift from J. Tainer and T. Paull (34)) in BL21 DE3 codonplus *E. coli* adding a 6xHis-tag in the N-terminal region of Mre11. This *P. furiosus Mre11–Rad50* plasmid was used to build a *P. furiosus Mre11–Rad50 ΔPIP* mutant (1–411) using Q5® Site-Directed Mutagenesis Kit (BioLabs). *P. furiosus* Mre11–Rad50^{link1}, Rad50^{link2} and Mre11^{core} proteins were provided by G. Williams and J. Tainer.

Cells were grown at 37°C to an OD_{600} 0.7–0.8, and expression was induced by addition of 1 mM IPTG (final concentration). Four hours after induction, cells were harvested by centrifugation and re-suspended in a buffer containing (i) for *Pfu*PCNA proteins: 10 mM Tris–HCl pH 7.4, 500 mM NaCl, 20 mM imidazole, 1 mM DTT, (ii) for *Pfu*MR wt and *Pfu*MR ΔPIP: 20 mM Tris–HCl pH 8.0, 500 mM NaCl, 10 mM imidazole, 1 mM DTT, supplemented by EDTA-free protease inhibitor (Roche). Cells were lysed by applying 1.9 kbar pressure (One shot, Constant Systems). *Pfu*PCNA, *Pfu*MR wt and ΔPIP supernatants were incubated overnight with DNase I at 37°C and then heated at 75–80°C for 20 min. After centrifugation, soluble fractions were loaded onto a HisPrepFF 16/10 (GE Healthcare) nickel resin column. After a wash step, elution was performed with a linear gradient from 10 to 500 mM imidazole. Peak fractions were run on 15% SDS-PAGE gels (Bio-Rad), then pooled and concentrated using Vivaspin columns (10 or 30 MWCO) before running on a Superdex 200 10/300 GL column (GE Healthcare). *Pfu*PCNA was eluted in 10 mM Tris–HCl pH 7.4, 200 mM NaCl, 1 mM DTT and *Pfu*MR wt and ΔPIP in 20 mM Tris–HCl pH 8.0, 150 mM NaCl, 1 mM DTT complemented with 20% glycerol and stored at −20°C. Proteins were quantitated using DC protein assay (BioRad) for *Pfu*PCNA, and absorbance measurement at 280 nm for *Pfu*MR wt and ΔPIP complexes. All molar concentrations indicated in this study corresponded to the homotrimeric PCNA and to the heterotetrameric form of the M_2R_2 complex.

Peptides to be used as competitors for PCNA-binding in pull-down assays were synthesized and purified (>90% purity) by Genepep (St-Jean-de-Védas, France). The PIP-like Mre11 peptide was derived from the *Pfu*Mre11 sequence (412–424): Ac-KKKRGTLDSWLGG-NH_2. The peptide used as the negative control (PIP–) was: Ac-KEVKEEYKRFLEE-NH_2 (12).

Co-immunoprecipitation experiments

To study the physical interaction between *Pfu*PCNA and *Pfu*MR wt or ΔPIP, 8.33 μg of anti-*P. abyssi* (*Pab*) PCNA polyclonal antibody was immobilized onto 1.5 mg of magnetic Dynabeads Protein A (ThermoFischer). Subsequently, antibodies were covalently anchored using 57 μg of BS3 crosslinker (Thermo Scientific); such an amount of beads was determined in order to specifically bind 1 μg of *Pfu*PCNA input (data not shown). In a 20 μl reaction volume, 1 μg *Pfu*PCNA was incubated for 30 min at 4°C with 10 μg *Pfu*MR wt or ΔPIP complexes in binding buffer (25 mM HEPES pH 7.0, 150 mM NaCl, 1 mM DTT, 0.05% Tween 20). The resulting protein complexes were trapped by anti-PCNA Dynabeads over 10 min at 4°C. Beads were washed three times with binding buffer (100 μl) before final elution for 10 min at 95°C in denaturating XT loading buffer (Bio-Rad). Proteins were then separated on SDS-PAGE (4–20% Pierce) and visualized using Coomassie Blue dye. Pull-down assays were performed following the same procedure for the three *Pfu*MR constructs, with the exception that protein complexes were formed during 1 h at 4°C and incubated with the bead-antibody complex for 5 min at 4°C and then washed three times at 25°C. A 1:3 molar ratio *Pfu*PCNA:*Pfu*MR proteins was used. As input controls, 1 μg of proteins was loaded onto SDS-PAGE.

For co-immunoprecipitation experiments in presence of PIP-like peptide, in 20 μl reaction, 1 μg *Pfu*PCNA was incubated with a 100 molar excess of competitor peptide or negative control peptide at least 1 h at 4°C in binding buffer. Then, 10 μg *Pfu*MR complex was added to the PCNA/peptide solution for 5 min at 4°C. The resulting protein complexes were trapped by anti-PCNA Dynabeads, washed three times with 50 μl binding buffer at 4°C and eluted as described above. After SDS-PAGE separation, proteins were transferred onto a PVDF membrane (Thermo Scientific). *Pfu*PCNA and *Pfu*Mre11 were simultaneously probed using anti-His monoclonal antibody (Invitrogen). Proteins were revealed by immunofluorescence using an ECL 2 blot kit (Thermo Scientific). Image acquisition was done with a ChemiDoc XRS+ (BioRad) and quantifications carried out using QuantityOne software (Bio-Rad).

DNA substrates

Oligonucleotides were purchased from Eurogentec and purified by RP-HPLC for S50/50, S50/50s, S50s/50s, S87/87s and S87s/87s or by PAGE for substrates containing reporter-quencher pairs, RQ-S87s/87s and RQ23-S87s/87s (Sequences in supplementary data). DNA substrates were annealed, at a 1:1 primer:template ratio, in presence of 10 mM HEPES pH 7.5 and 100 mM NaCl by heating at 95°C for 5 min and cooling to room temperature.

Nuclease assays

Nuclease activities of *Pfu*MR wt and ΔPIP complexes on linear dsDNA substrates was followed in 10 μl reactions containing 25 nM DNA in 25 mM HEPES pH 7.0, 1 mM DTT, 0.5 mg/ml BSA complemented with 1 mM ATP, 5 mM $MgCl_2$, 5 mM $MnCl_2$ and 150 or 300 mM NaCl, as indicated in the figure captions. Pre-incubation was performed with 25 nM dsDNA substrates and the indicated concentrations of *Pfu*PCNA at ambient temperature for 5 min followed by an incubation with the indicated concentrations of *Pfu*MR wt or ΔPIP complexes at 70°C for different times as indicated in the figures. Reactions were stopped by addition of 85% deionized formamide, 0.01 N NaOH, 10 mM EDTA, 2 μM Trap (RC50 or RC87) and by heating samples at 95°C for 5 min. DNA products were separated by electrophoresis on a gel composed of 15% or 18% polyacrylamide 19:1, 7 M urea, 16% deionized formamide and 1× Tris Borate EDTA (TBE). Labeled fragments were analysed with a fluorimager Typhoon 9500 (GE Healthcare) and quantified with Image Quant software.

Real time fluorescence DNA unwinding assays

Unwinding assays were carried out at 55°C using dsDNA RQ-S87s/87s and RQ23-S87s/87s, which contain a fluorophore-quencher pair (6-FAM, 6-carboxyfluorescein/DDQI, Deep Dark Quencher I or BHQ-1, Black Hole Quencher 1) positioned at the DNA end or 23 nt from the extremity. Emission of fluorescence was triggered by unwinding quenched DNA duplex substrates. Unwinding assays were performed in 50 μl of 25 mM HEPES pH 7.0 buffer containing 25 nM DNA, 300 mM NaCl, 1 mM DTT, 0.5 mg/ml BSA, 5 mM $MgCl_2$ and 500 nM Trap 3′ 87RC, complemented with 1 mM ATP and 5 mM $MnCl_2$ when indicated. 50 nM *Pfu*PCNA were pre-incubated with the DNA mix for 5 min at ambient temperature before adding 25 nM *Pfu*MR wt or ΔPIP. Fluorescence emission was monitored using Q-PCR equipment (StepOnePlus™ Real Time PCR System Thermo Fisher Scientific). After 30 min, the temperature was increased to 95°C to induce complete unwinding to determine the maximum fluorescence intensity (100% unwinding signal, Q_{max}).

Unwinding percentage was calculated as follows: $\text{Unwinding } \% = \frac{Q}{(Q_{max}-Q_0)} \times 100$, where Q was the real-time detected fluorescence and Q_0 corresponds to the fluorescence measured at the beginning of the reaction. Unwinding assays were repeated at least three times.

SPR experiments

Data were obtained using a Reichert SR7000DC spectrometer instrument (Reichert Inc., Buffalo, NY, USA). The running buffer was 25 mM HEPES pH 7.0, 300 mM NaCl, 1 mM DTT and 0.05% Tween 20, and flow rate was 25 μl/min. *Pfu*PCNA was immobilized on a mixed self-assembled monolayer (10% C11-(OEG)6-COOH: 90% C11-(OEG)3-OH), Reichert Inc.) via classic amine coupling chemistry and 25 nM of *Pfu*MR wt or ΔPIP complexes were injected over the *Pfu*PCNA surface at 25°C. The chip was regenerated after serial injections of 100 mM H_3PO_4 (3 × 30 s). Each curve displayed was double referenced with a set of blank buffer injections.

Figure S1

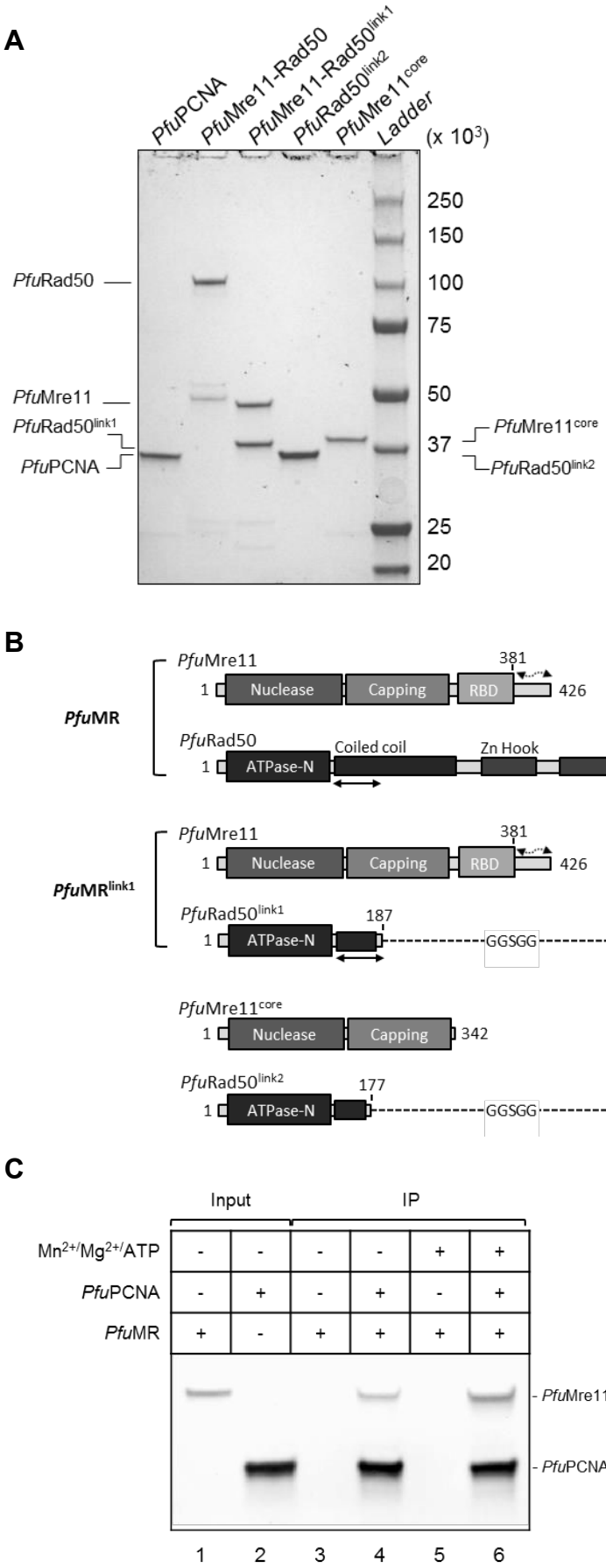
A
PfuPCNA
PfuMre11-Rad50
PfuMre11-Rad50link1
PfuRad50link2
PfuMre11core
Ladder
(x 10³)
250
150
100
75
50
37
25
20
PfuRad50
PfuMre11
PfuRad50link1
PfuPCNA
PfuMre11core
PfuRad50link2
B
PfuMR
PfuMre11
381
1
Nuclease
Capping
RBD
426
PfuRad50
Coiled coil
Zn Hook
Coiled coil
ATPase-N
ATPase-C
882
PfuMRlink1
187
716
GGSGG
PfuMre11core
342
PfuRad50link2
177
726
C
Input
IP
Mn2+/Mg2+/ATP
PfuPCNA
PfuMR
- PfuMre11
- PfuPCNA
1
2
3
4
5
6

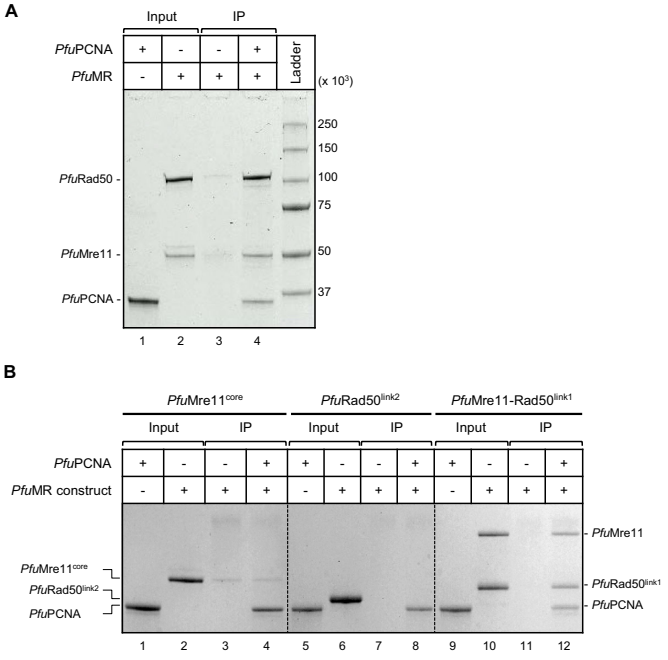

Figure 1. Physical association of *P. furiosus* PCNA and Mre11–Rad50. Protein-protein interactions were determined, *in vitro,* using a bead-based co-immunoprecipitation assay. (**A**) Full length *Pfu*MR co-immunoprecipitated with *Pfu*PCNA, (**B**) co-immunoprecipitation assays with *Pfu*PCNA and different *Pfu*Mre11 and *Pfu*Rad50 protein constructs (details given in Supplementary Figure S1B). 1 μg of protein was loaded on SDS-PAGE as Input. IP corresponds to the immunoprecipitation assays in presence of beads coated with PCNA antibodies. Fraction bound to the beads were analysed by Coomassie blue staining. Assays were performed in buffer with 150 mM NaCl.

RESULTS

P. furiosus PCNA physically interacts with the MR complex

We first considered using the homologous system with *P. abyssi* recombinant proteins but failed to achieve a proper level of production of the MR complex. As an alternative we used the recombinant proteins from the close species *Pyrococcus furiosus*. Complexes of *Pfu*PCNA and *Pfu*MR from *P. furiosus* were produced and purified (Supplementary Figure S1A). Using co-immunoprecipitation, we demonstrated that these two components also formed a complex in *P. furiosus*, as shown by the co-precipitation of the *Pfu*MR complex with *Pfu*PCNA (Figure 1A). We then explored some conditions where this association could take place. As illustrated in Supplementary Figure S1C, the complex could form in presence or absence of a metallic co-factor and ATP. As protein samples were DNA free after DNase I treatment, we assumed that the interaction between *Pfu*MR complex and *Pfu*PCNA is not dependent on DNA substrates.

To investigate the surface of interaction, we were able to use three *Pfu*Mre11 and *Pfu*Rad50 deletion constructs (35). *Pfu*Mre11^{core} (residues 1–342) lacks 84 C-terminal residues including its Rad50 binding domain (RBD); *Pfu*Rad50-link2, an untagged version of *Pfu*Rad50 with shortened coiled coils (unable to bind Mre11) connected by an intramolecular Gly-Gly-Ser-Gly-Gly sequence; and *Pfu*Mre11–Rad50-link1 a complex of another shortened version of *Pfu*Rad50 (able to bind Mre11 RBD) purified with full-length *Pfu*Mre11 (Supplementary Figure S1B). Only the *Pfu*Mre11–Rad50-link1 construct could form a complex with *Pfu*PCNA in solution (Figure 1B, compare lanes 4, 8 and 12). These data indicated that *Pfu*PCNA does not interact directly with *Pfu*Rad50 and that the coiled-coil domain of *Pfu*Rad50 is not required for recruitment of the MR complex onto *Pfu*PCNA. On the other hand, these observations raised two non-exclusive hypotheses: *Pfu*PCNA/MR interaction requires prior *Pfu*MR complex formation and/or is mediated by the C-terminal region of *Pfu*Mre11 absent in the Mre11^{core} construct. With the exception of a domain interacting with the base of *Pfu*Rad50's coiled-coils (348–381), the C-terminal domain of *Pfu*Mre11 is predicted to be disordered or flexible and is thought to be responsible for protein-protein and protein–DNA interactions (31).

The C-terminal region of *P. furiosus* Mre11 contains a putative PCNA interacting motif

PCNA-binding partners generally possess a PCNA-Interaction Peptide (PIP) motif, usually located at the extreme N- or C-terminus (36). The results obtained prompted us to look for a potential PIP motif at the C-terminal portion of *Pfu*Mre11. The core element of the archaeal PIP-box is a peptide with a sequence Qxxϕ (ϕ being hydrophobic residues L, M or I), which in most cases is C-terminally flanked by the sequence xxΩΩ (Ω being aromatic residues F or W) (37). Based on the alignment of PIP-Box like sequences (QXXϕXXΩΩ) from a subset of *Pyrococcus sp.* proteins whose affinity for PCNA has already been described (19), we identified a candidate PCNA-interacting peptide in the C-terminal region of *Pfu*Mre11 (Figure 2A). Located in the extreme C-terminal portion of *Pfu*Mre11 (positions 412–422) the motif exhibits the conserved hydrophobic residues but lacks the otherwise conserved glutamine residue. In addition, N-terminal extension from the motif is composed of a stretch of basic residues known to interact with the positively charged outer surface of PCNA (38). As Meslet-Cladiere *et al.* described, high affinity peptides for PCNA tend to be positively charged (12). Here the identified peptide has a predicted Isoelectric Point (p*I*) of 10.29 consistent with this property. 3D structure of the complete C-terminal Mre11 region has not been resolved to date; however, Hydrophobic Cluster Analysis identified this motif as a globular region and showed that the hydrophobic residues clustered with a similar shape to that observed for canonical PIP motif sequences (data not shown). Although this motif lacks the glutamine conserved residues, these features strongly suggest that it could act as a hydrophobic anchor on PCNA.

We then looked at occurrence of this motif in Mre11 sequences among species of the order Thermococcales. Remarkably, all available sequences displayed this putative PCNA-interacting motif in the C-terminal region (Supplementary Figure S2). From this alignment, we could derive a pattern [PK]-x-[KRNA]-x-[GSPNK]-x(1,3)-[IL]-x(2)-[WFY]-[ILV]) for a motif search using Scanprosite on archaeal protein sequences from Swiss-prot and

Figure S2

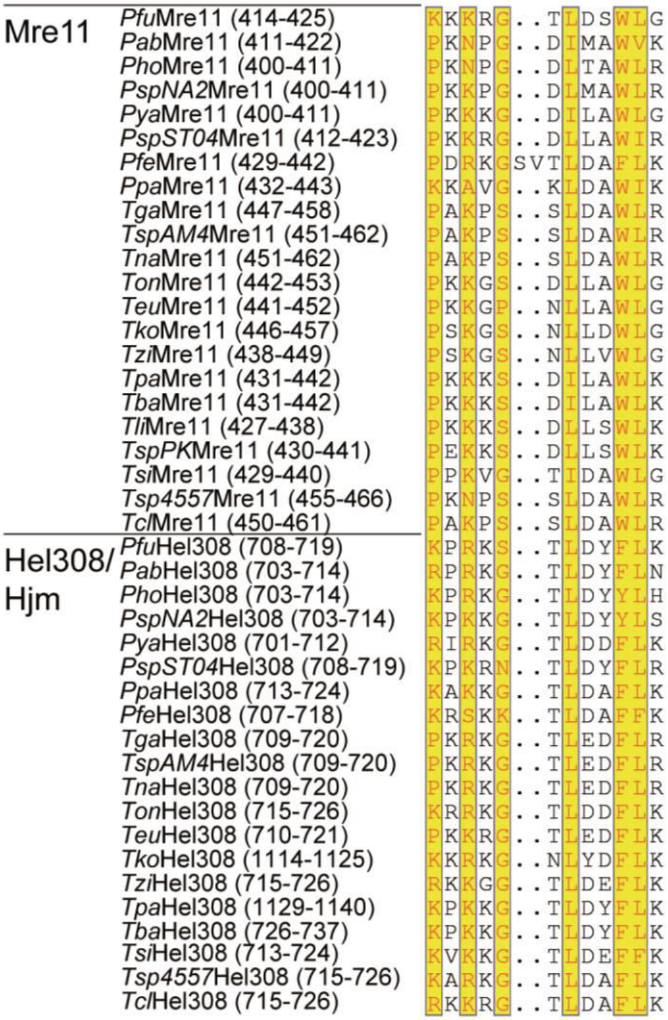
Mre11
PfuMre11 (414-425) KKKRG..TLDSWLG
PabMre11 (411-422) PKNPG..DIMAWVK
PhoMre11 (400-411) PKNPG..DLTAWLR
PspNA2Mre11 (400-411) PKKPG..DLMAWLR
PyaMre11 (400-411) PKKKG..DILAWLG
PspST04Mre11 (412-423) PKKRG..DLLAWIR
PfeMre11 (429-442) PDRKGSVTLDAFLK
PpaMre11 (432-443) KKAVG..KLDAWIK
TgaMre11 (447-458) PAKPS..SLDAWLR
TspAM4Mre11 (451-462) PAKPS..SLDAWLR
TnaMre11 (451-462) PAKPS..SLDAWLR
TonMre11 (442-453) PKKGS..DLLAWLG
TeuMre11 (441-452) PKKGP..NLLAWLG
TkoMre11 (446-457) PSKGS..NLLDWLG
TziMre11 (438-449) PSKGS..NLLVWLG
TpaMre11 (431-442) PKKKS..DILAWLK
TbaMre11 (431-442) PKKKS..DILAWLK
TliMre11 (427-438) PKKKS..DLLSWLK
TspPKMre11 (430-441) PEKKS..DLLSWLK
TsiMre11 (429-440) PPKVG..TIDAWLG
Tsp4557Mre11 (455-466) PKNPS..SLDAWLR
TclMre11 (450-461) PAKPS..SLDAWLR
Hel308/ Hjm
PfuHel308 (708-719) KPRKS..TLDYFLK
PabHel308 (703-714) RPRKG..TLDYFLN
PhoHel308 (703-714) KPRKG..TLDYYLH
PspNA2Hel308 (703-714) KPKKG..TLDYYLS
PyaHel308 (701-712) RIRKG..TLDDFLK
PspST04Hel308 (708-719) KPKRN..TLDYFLR
PpaHel308 (713-724) KAKKG..TLDAFLK
PfeHel308 (707-718) KRSKK..TLDAFFK
TgaHel308 (709-720) PKRKG..TLEDFLR
TspAM4Hel308 (709-720) PKRKG..TLEDFLR
TnaHel308 (709-720) PKRKG..TLEDFLR
TonHel308 (715-726) KRRKG..TLDDFLK
TeuHel308 (710-721) PKKRG..TLEDFLK
TkoHel308 (1114-1125) KKRKG..NLYDFLK
TziHel308 (715-726) RKKGG..TLDEFLK
TpaHel308 (1129-1140) KPKKG..TLDYFLK
TbaHel308 (726-737) KPKKG..TLDYFLK
TsiHel308 (713-724) KVKKG..TLDEFFK
Tsp4557Hel308 (715-726) KARKG..TLDAFLK
TclHel308 (715-726) RKKRG..TLDAFLK

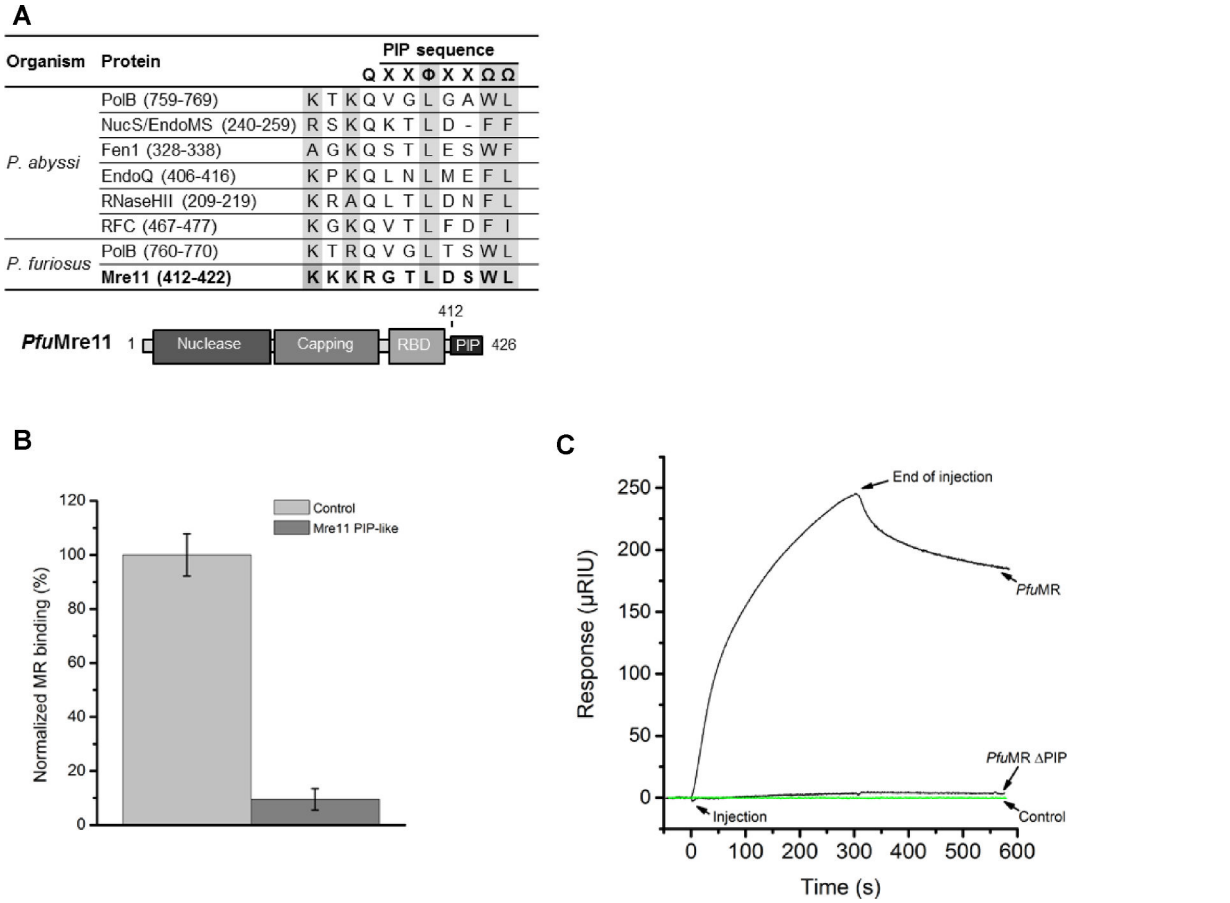

Figure 2. Identification of a putative PCNA binding motif in the C-terminal region of *Pfu*Mre11. (**A**) *Pfu*Mre11 displays a C-terminal PIP-like motif when compared with the consensus sequence (x, any residues; Φ, hydrophobic; Ω, aromatic or hydrophobic) and various sequences of proteins from *Pyrococcus sp.* known to interact with PCNA through the PIP motif. Positions within the sequences are indicated and *Pfu*Mre11 domains are illustrated below the table. (**B**) The interaction *Pfu*PCNA/MR is inhibited by an excess of Mre11 C-terminal peptide in competitive co-immunoprecipitation assays. Western blot signals of *Pfu*Mre11 were normalized with corresponding signals obtained with a peptide control. Experiments were performed in binding buffer containing 150 mM NaCl. Error bars represent standard deviation of three independent reactions. (**C**) Surface plasmon sensograms obtained after injection of 25 nM *Pfu*MR wt or ΔPIP over an immobilised *Pfu*PCNA surface. The running buffer contained 300 mM NaCl.

TrEMBL databases. This pattern was detected in Mre11 sequences from the order Thermococcales and from an Archeoglobale, *Archeoglobus fulgidus*. We also identified that Hel308/Hjm archaeal members of helicase superfamily 2 possessed a similar motif in the extreme C-terminal region (Supplementary Figure S2). Presence of this PIP-like motif in Hel308/Hjm sequences showed similar repartition as in sequences of Mre11, as only Thermococcale Hel308/Hjm helicases harboured the motif, with the exception of *Thermococcus litoralis*. In addition, alignment of the C-terminal region of Hel308/Hjm and Mre11 proteins showed a strong conservation of hydrophobic residues in the C-terminal extension of the motif (Supplementary Figure S2), suggesting that this structural element could also serve as a hydrophobic plug on PCNA surface. Most noticeably, interaction between PCNA and Hel308/Hjm from *P. furiosus* has already been described. Using a deletion mutant lacking the 20 residues at the extreme C-terminal region (39), the authors proposed that this portion could mediate interaction with PCNA which is consistent with our analysis.

Mre11 C-terminus region is essential for *Pfu*PCNA/MR interaction

Taken together, these observations prompted us to verify the assumption that the C-terminus of *Pfu*Mre11 contributes to *Pfu*PCNA/MR complex formation. To this aim, we performed pull-down competitive assays with the Mre11 peptide corresponding to the revealed motif (412-KKKRGTLDSWLGG-424). Figure 2B shows that an excess of the Mre11 peptide (Mre11 PIP-like) significantly blocked *Pfu*PCNA/MR interaction compared with the control peptide. As shown in the graph, the amount of immunoprecipitated Mre11 decreased drastically in the assay with the competitive peptide suggesting that this peptide inhibits assembly of the *Pfu*PCNA/MR complex. To test whether the C-terminal sequence of *Pfu*Mre11 could mediate interaction of the *Pfu*MR complex with *Pfu*PCNA, we used Surface Plasmon Resonance (SPR) with *Pfu*PCNA immobilized on a chip. SPR measurements indicated that the Mre11 peptide physically interacts with *Pfu*PCNA at a micromolar range of concentrations (Supplementary Fig-

Figure S3

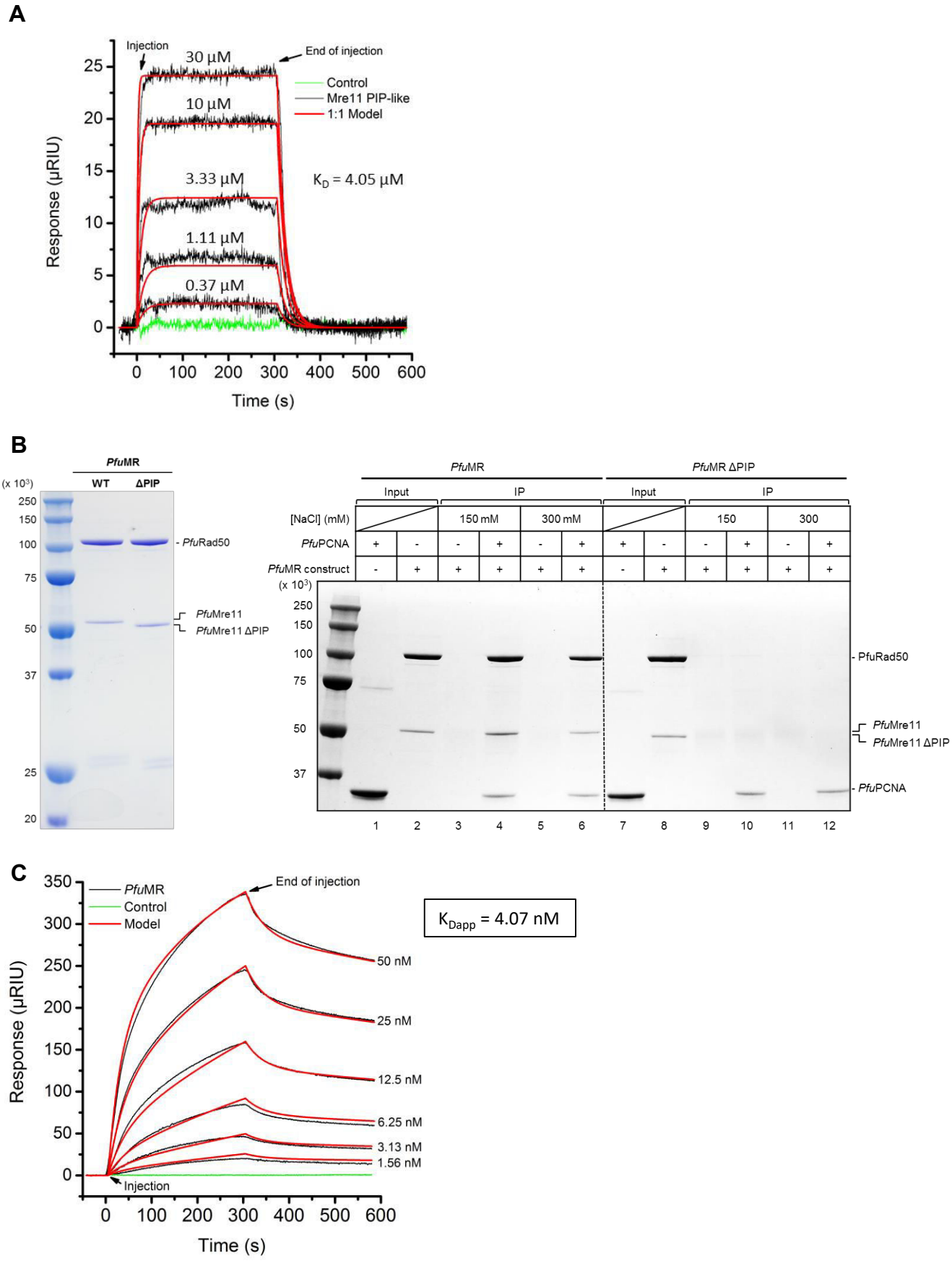
A
Injection
End of injection
30 µM
10 µM
3.33 µM
1.11 µM
0.37 µM
Control
Mre11 PIP-like
1:1 Model
K_D = 4.05 µM
Response (µRIU)
Time (s)
B
PfuMR
WT
ΔPIP
(x 10^3)
PfuRad50
PfuMre11
PfuMre11 ΔPIP
PfuMR
PfuMR ΔPIP
Input
IP
[NaCl] (mM)
150 mM
300 mM
PfuPCNA
PfuMR construct
PfuRad50
PfuMre11
PfuMre11 ΔPIP
PfuPCNA
C
PfuMR
Control
Model
End of injection
K_Dapp = 4.07 nM
50 nM
25 nM
12.5 nM
6.25 nM
3.13 nM
1.56 nM
Injection
Response (µRIU)
Time (s)

ure S3A). It is interesting to note that the binding value (4.05 μM) correlates with K_D value obtained with a canonical PIP motif peptide derived from the sequence of another nuclease, *P. abyssi* NucS (40). Together, these results suggest that the primary docking site of *Pfu*Mre11 on *Pfu*PCNA could be similar to that described for PIP-motif containing proteins.

To confirm the essentiality of the PIP-like motif for the interaction, we produced a deleted version of the *Pfu*MR complex lacking the last 15 amino acids of the *Pfu*Mre11 subunit (Supplementary Figure S3B, left panel). The co-IP experiments clearly showed that the mutant *Pfu*MR ΔPIP complex did not bind to *Pfu*PCNA (Supplementary Figure S3B, right panel, compare lanes 4 and 10), providing conclusive evidence that this variation in the PIP motif mainly contributes to the interaction of the *Pfu*MR complex with *Pfu*PCNA. We then looked at the stability of the interaction at a higher salt condition to test specificity and to get closer to the reported physiological ionic strength of *Pyrococcus furiosus* (41). Supplementary Figure S3B indicates that the interaction between *Pfu*MR and *Pfu*PCNA is stable at 300 mM NaCl (lanes 5–6) and that the mutant *Pfu*MR ΔPIP complex did not interact with *Pfu*PCNA under the same conditions (lanes 11–12). As a final point on the physical interaction, the direct association between *Pfu*PCNA and the full length *Pfu*MR complex was confirmed by SPR analysis at 300 mM NaCl. *Pfu*MR specifically bound to *Pfu*PCNA anchored on a sensor chip, while the *Pfu*MR ΔPIP complex did not bind under the same conditions (Figure 2C). In addition, we conducted a kinetic experiment over the full range of *Pfu*MR complex concentrations and determined an apparent dissociation constant value (K_{Dapp}) of ∼4.07 ± 1.46 nM (Supplementary Figure S3C).

*Pfu*PCNA stimulates *Pfu*MR activity for dsDNA cleavage

In archaea, as in some other organisms, the MR complex is implicated in early steps of the HR pathway. Thanks to a combination of Mre11 nuclease and Rad50 ATPase activities, the MR complex initiates DNA end resection to provide suitable DNA template used by subsequent HR components. In several *in vitro* studies, *Pfu*Mre11 displayed distinct activities: 3′→5′ dsDNA exonuclease, ssDNA endonuclease and endonucleolytic cleavage on the 5′ strand at a break (30,34,42–44). Given PCNA preference for dsDNA substrate, we tested influence of the *Pfu*PCNA on *Pfu*MR complex nuclease activities to resect synthetic dsDNA oligonucleotides.

To this end, we performed nuclease assays on a linear blunt-end dsDNA substrate (S50/50s). The unlabeled complementary strand has phosphorothioate bonds at its 3′ end to block 3′→5′ exonuclease activity, in order to characterize exo- and endonuclease activities on the top strand irrespective of exonuclease degradation of the complementary strand (Figure 3A). We first confirmed that the nuclease activities of the *Pfu*MR complex were in accordance with previously reported activities at low salt conditions (Supplementary Figure S4A) and observed DNA products as already described on the same dsDNA substrates (42). Intracellular salt concentration was determined to be ∼350 mM in *P. furiosus* (41), we then decided to test the activity of the *Pfu*MR complex and impact of *Pfu*PCNA at 300 mM NaCl, close to the reported ionic strength. Increased concentrations of *Pfu*MR complex were incubated for 30 min at 70°C with dsDNA substrate. DNA fragments from the 5′-labeled strand was revealed by fluorescence (Figure 3B). As shown in lanes 6–7, the 5′-labeled strand was degraded by the *Pfu*MR complex, although to a much lesser extent than at low salt condition (compare with Supplementary Figure S4A), and defined products ranging from 15 to 37 nt were generated.

From a *Pfu*MR:DNA ratio of 1:1, conditions in which *Pfu*MR was inactive, we tested increased concentrations of *Pfu*PCNA and observed strong activation of DNA degradation activity (Figure 3C, lanes 7–9) with about 94% of the substrate used. Moreover, addition of *Pfu*PCNA, changed the degradation pattern and increased the specificity of the enzyme towards generation of major products ranging from 27 to 29 nucleotides (compare lanes 7 in Figure 3B and Figure 3C). A time course experiment confirmed that the products accumulated over time and were the major end products of the reaction (Supplementary Figure S4C). As expected, this activation was not observed in presence of the mutant *Pfu*MR ΔPIP (Figure 3D, compare lanes 3 and 5). To confirm that the interaction of *Pfu*PCNA with the *Pfu*MR complex is responsible of nuclease activation, we demonstrated that the ΔPIP mutant is not affected in its nuclease activity (compare Figure 3B and C with Supplementary Figure S4 D and E), indicating that direct interaction was necessary to stimulate *Pfu*MR nuclease activity. However, faint bands at 27–29 nt could still be observed on Figure 3D when *Pfu*MR ΔPIP was in presence of *Pfu*PCNA, indicating that the secondary domain of interaction might account for a weak resilient interaction with *Pfu*PCNA.

At 150 mM NaCl, we also a noticed change in the degradation pattern of DNA caused by *Pfu*PCNA, but this shift came with a strong inhibition of substrate utilization by *Pfu*MR, contrary to what was observed at 300 mM NaCl, and most importantly, we found no significant differences between *Pfu*MR wt and ΔPIP activities in presence of *Pfu*PCNA (Supplementary Figure S4B). These led us to test, for both salt concentrations, the ability of *Pfu*MR to bind dsDNA. By performing EMSA experiments, we confirmed its binding onto DNA at 150 and 300 mM NaCl and noticed no significant change caused by *Pfu*PCNA (Supplementary Figure S5), indicating that nuclease inhibition or activation effect was not due to an improvement or a blockage of *Pfu*MR fixation onto DNA substrates. This demonstrated the relevance of characterizing the functional interplay between *Pfu*MR and *Pfu*PCNA in higher salt concentration conditions than for previous reported characterizations of the MR complex from *P. furiosus*, especially as we were approaching physiological ionic strength with this treatment (41).

We also explored the effect of *Pfu*PCNA on metal dependence of nucleolytic degradation. Mre11 has two metal binding sites for which manganese has a higher affinity (43) whereas Rad50 needs magnesium to hydrolyse ATP (45). Supplementary Figure S6A showed that at 70°C, dsDNA

Figure S4

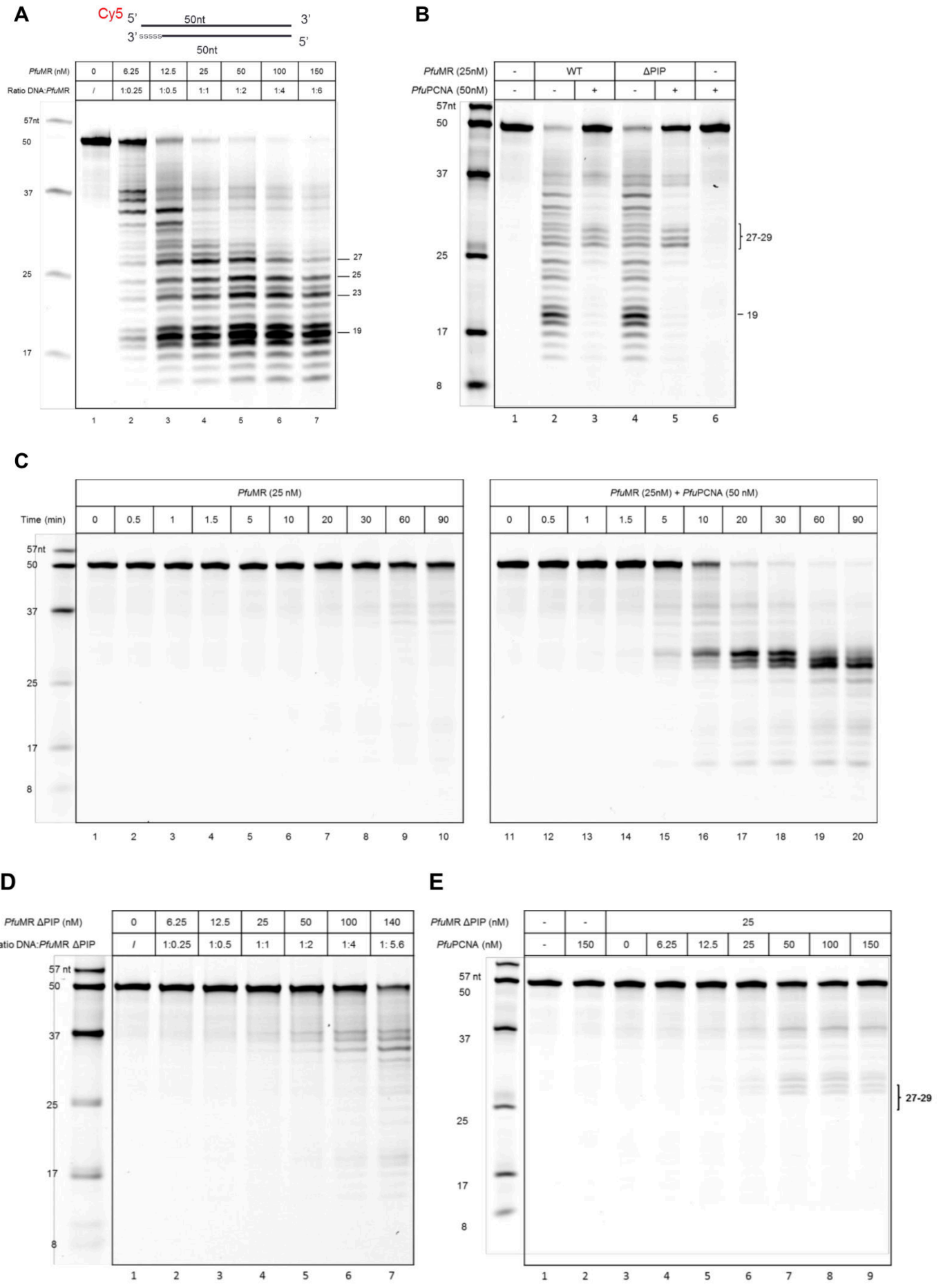
A
Cy5 5' 50nt 3'
3' sssss 5'
50nt
PfuMR (nM) 0 6.25 12.5 25 50 100 150
Ratio DNA:PfuMR / 1:0.25 1:0.5 1:1 1:2 1:4 1:6
57nt
50
37
25
17
27
25
23
19
1 2 3 4 5 6 7
B
PfuMR (25nM) - WT ΔPIP -
PfuPCNA (50nM) - - + - + +
57nt
50
37
25
17
8
27-29
19
1 2 3 4 5 6
C
PfuMR (25 nM)
Time (min) 0 0.5 1 1.5 5 10 20 30 60 90
57nt
50
37
25
17
8
1 2 3 4 5 6 7 8 9 10
PfuMR (25nM) + PfuPCNA (50 nM)
0 0.5 1 1.5 5 10 20 30 60 90
11 12 13 14 15 16 17 18 19 20
D
PfuMR ΔPIP (nM) 0 6.25 12.5 25 50 100 140
Ratio DNA:PfuMR ΔPIP / 1:0.25 1:0.5 1:1 1:2 1:4 1: 5.6
57 nt
50
37
25
17
8
1 2 3 4 5 6 7
E
PfuMR ΔPIP (nM) - - 25
PfuPCNA (nM) - 150 0 6.25 12.5 25 50 100 150
57 nt
50
37
25
17
8
27-29
1 2 3 4 5 6 7 8 9

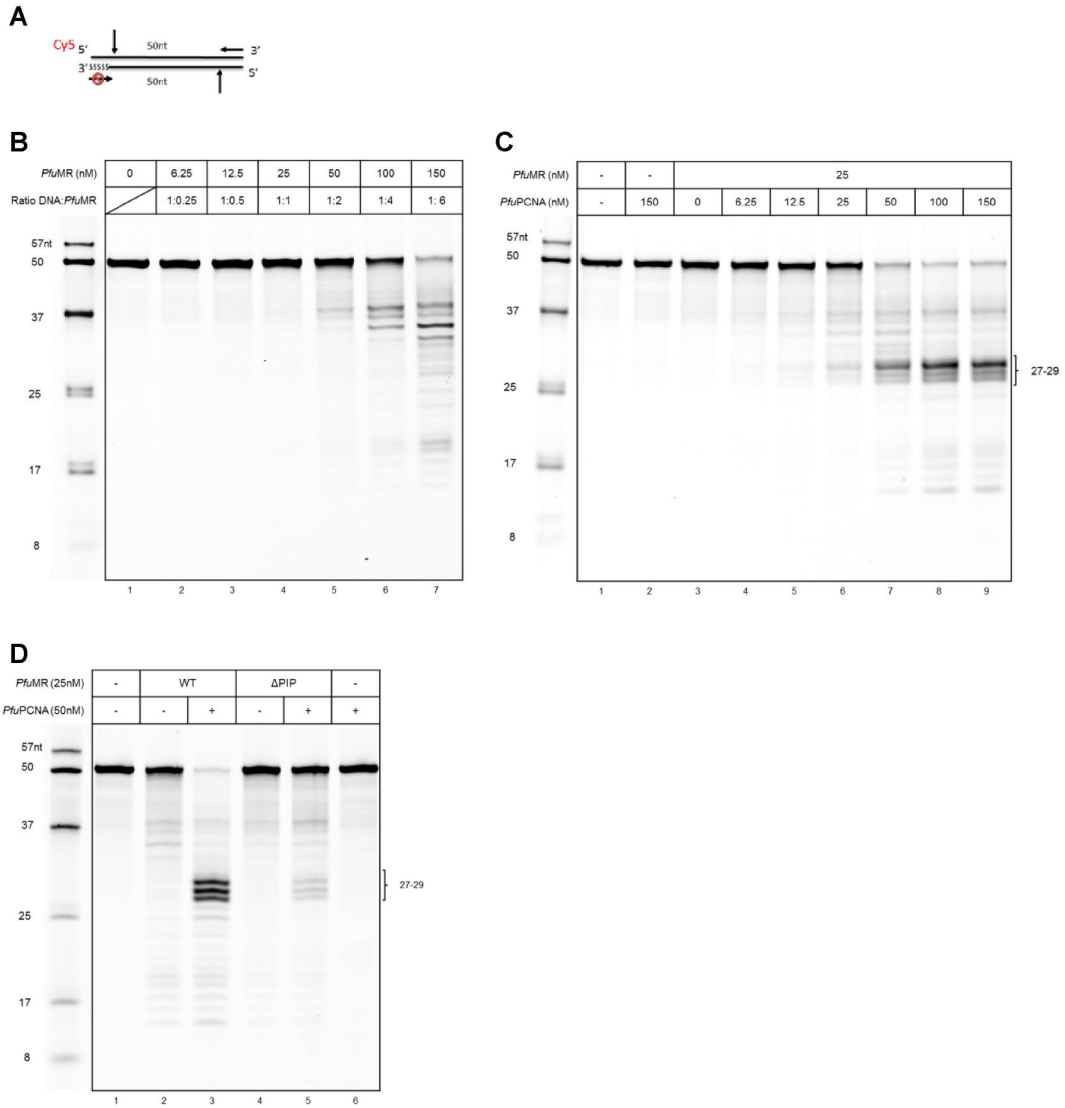

Figure 3. *Pfu*PCNA stimulates DNA degradation activity of *Pfu*MR. *In vitro* nuclease assays (**A**) 5′-labeled 50bp dsDNA substrate used. SSSSS represents phosphorothioate bonds. Black arrows indicate potential endo- and exo-nuclease cleavage activities. (**B**) 25 nM of DNA substrate were incubated at 70°C for 30 min with increasing concentrations of *Pfu*MR wt. (**C**) 25 nM of DNA substrate were pre-incubated with indicated concentrations of *Pfu*PCNA at room temperature for 5 min before adding 25 nM *Pfu*MR wt. Reactions were performed for 30 min at 70°C. (**D**) 25 nM of DNA substrate were pre-incubated with 50 nM *Pfu*PCNA at room temperature for 5 min before adding 25 nM *Pfu*MR wt or ΔPIP. Reactions were performed for 30 min at 70°C in 300 mM NaCl. DNA products were resolved in 18% PAGE and fluorescence revealed using Typhoon 9500 (GE Healthcare).

nucleolytic cleavage strongly required both ATP and manganese and that change in cleavage specificity observed in presence of *Pfu*PCNA was not dependent on the presence or absence of magnesium. Hereinafter we focus on our data obtained at 300 mM NaCl, with 10 mM ATP, 5 mM $MgCl_2$ and 5 mM $MnCl_2$ (similar results were obtained with KCl instead of NaCl, data not shown).

From the degradation pattern observed, it is tempting to speculate that this product occurred through endonucleolytic cleavage, which might be promoted upon association with *Pfu*PCNA. However, at this point it is not possible to conclude whether *Pfu*PCNA had an effect on the exonuclease, the endonuclease or regulated both activities of the *Pfu*MR complex.

Cleavage of the 5′-terminated DNA strand is promoted by *Pfu*PCNA/MR association

To address this question, we used dsDNA substrates protected against exonuclease activity at both 3′ ends (S50s/50s), which consequently could be only degraded by endonuclease activity. As observed previously, major DNA products of 27–29 nt were generated from blocked 3′ end substrate (Figure 4A), confirming that the pattern observed stems from the initial endonuclease cut. To question whether phosphorothioates bonds in synthetic oligonucleotides may have an impact on *Pfu*PCNA effect, we used unprotected blunt dsDNA substrate. Supplementary Figure S7A clearly shows that addition of *Pfu*PCNA generated a similar change of cleavage specificity in that it led to the

Figure S5

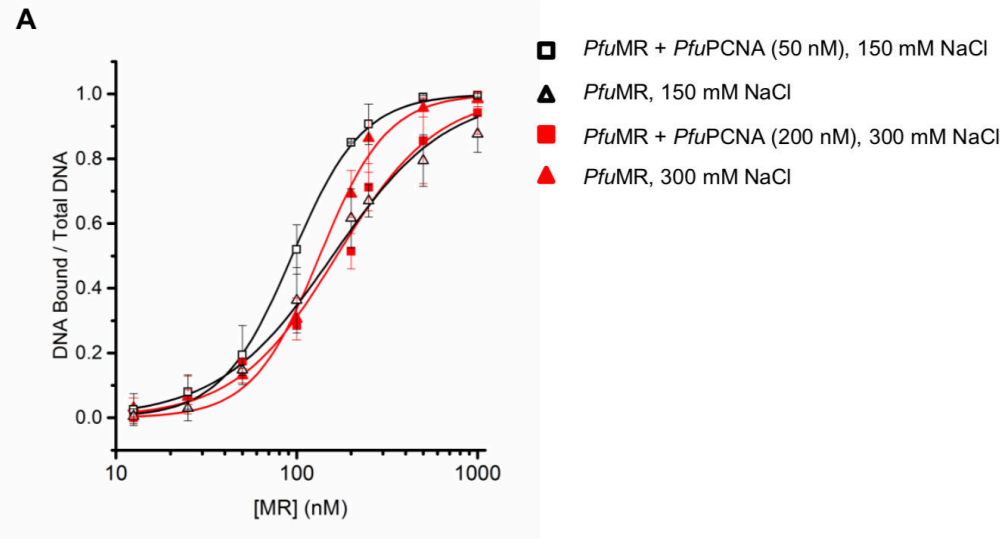

Figure S6

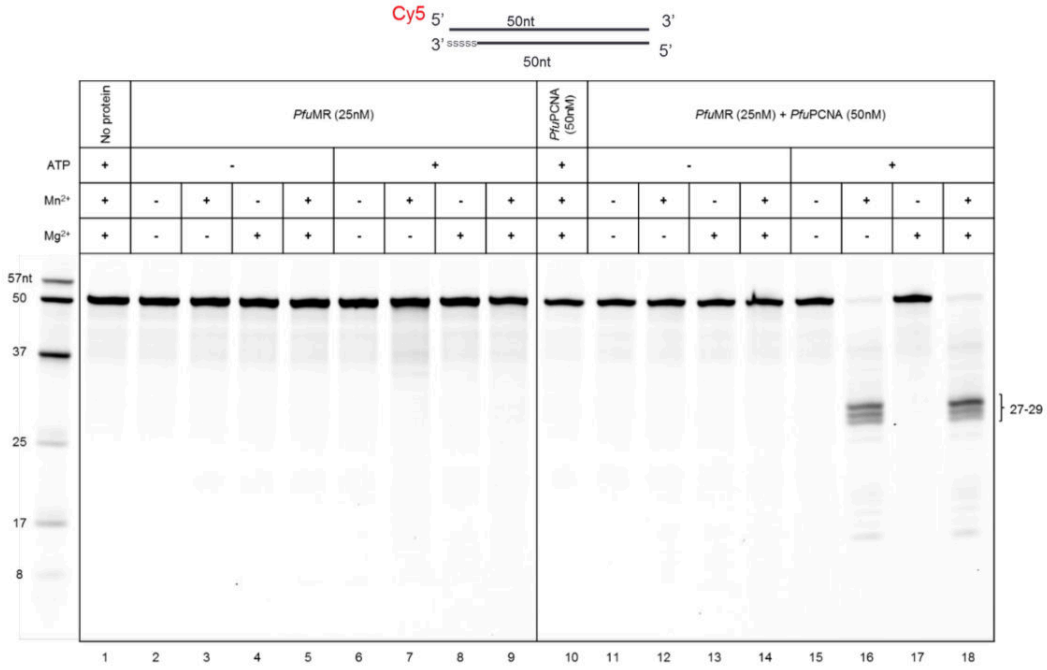

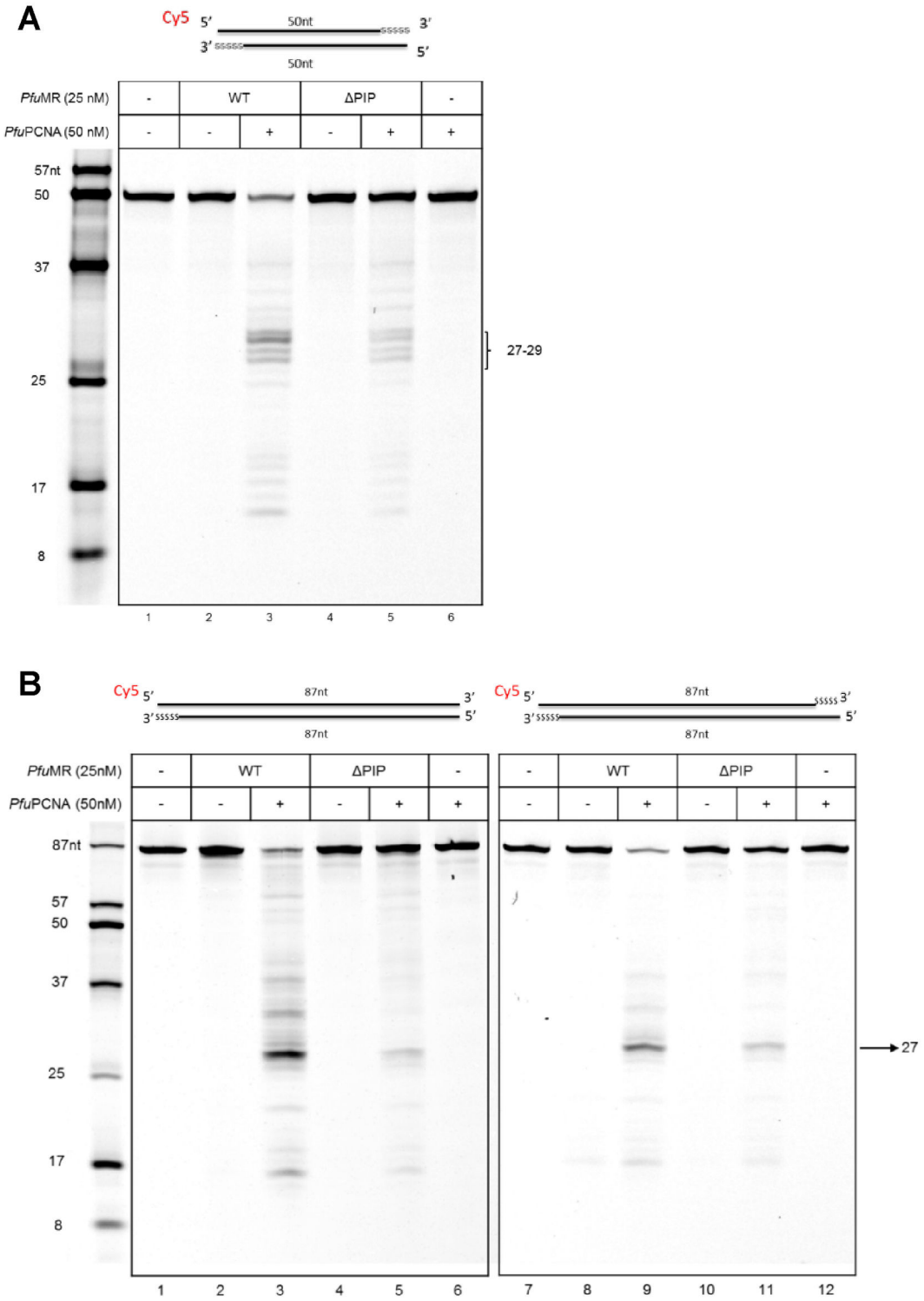

Figure 4. *Pfu*PCNA/MR interaction generates endonucleolytic cleavage at dsDNA ends. *In vitro* nuclease assays. 25 nM of DNA substrate were pre-incubated with 50 nM *Pfu*PCNA at room temperature for 5 min before adding 25 nM *Pfu*MR wt or ΔPIP. Reactions were performed for 30 min at 70°C. DNA products were resolved in 18% PAGE and fluorescence revealed using Typhoon 9500 (GE Healthcare). DNA substrates used are indicated at the top of the panels. (**A**) 50 bp DNA substrate with a phosphorothioate stretch at both 3′ ends and (**B**) 87 bp DNA substrate with protected (right panel) or unprotected (left panel) 3′ end.

Figure S7

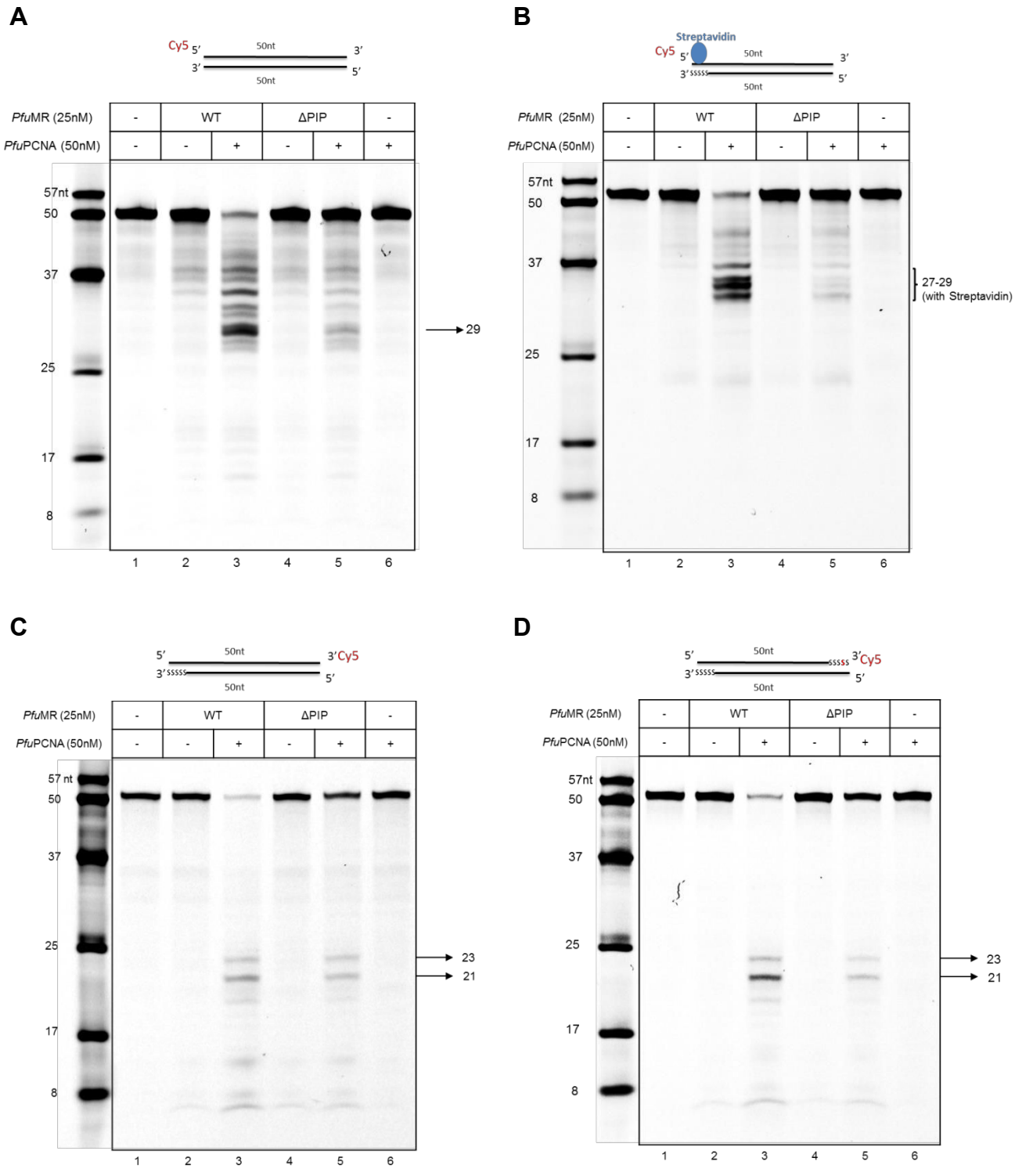
A
Cy5 5′ 50nt 3′
3′ 50nt 5′
PfuMR (25nM) - WT ΔPIP -
PfuPCNA (50nM) - - + - + +
57nt
50
37
25
17
8
29
1 2 3 4 5 6
B
Streptavidin
Cy5 5′ 50nt 3′
3′ sssss 50nt 5′
PfuMR (25nM) - WT ΔPIP -
PfuPCNA (50nM) - - + - + +
57nt
50
37
25
17
8
27-29
(with Streptavidin)
1 2 3 4 5 6
C
5′ 50nt 3′Cy5
3′ sssss 50nt 5′
PfuMR (25nM) - WT ΔPIP -
PfuPCNA (50nM) - - + - + +
57 nt
50
37
25
17
8
23
21
1 2 3 4 5 6
D
5′ 50nt sssss 3′Cy5
3′ sssss 50nt 5′
PfuMR (25nM) - WT ΔPIP -
PfuPCNA (50nM) - - + - + +
57nt
50
37
25
17
8
23
21
1 2 3 4 5 6

accumulation of main products around 27–29 nt. We then asked whether a non-specific protein, such as streptavidin, bound to the 5′ end might bring about a change in cleavage pattern or efficiency. To this end, we tested a biotinylated synthetic oligonucleotide with streptavidin to block the 5′ end (Supplementary Figure S7B) and noticed no cleavage pattern difference on this particular substrate. Finally, we looked at cleavage products from 3′ end labeled substrates. The generated fragment sizes (21–23 nt) were complementary to 5′ end labeled products (27–29 nt) confirming the specificity of the endonucleolytic cut (Supplementary Figure S7C and D).

Next, we set out to examine whether there was any sequence and/or length dependence concerning the DNA substrate. To address this, we used blunt end dsDNA substrate of 87 bp that differed in sequence from the shorter substrate. Comparison of nuclease activity of the *Pfu*MR complex in presence of *Pfu*PCNA clearly showed a similar activation on this longer substrate, either blocked or accessible from the 3′ end (Figure 4B). Regardless of the size and sequence of the DNA substrates, *Pfu*PCNA stimulated the nuclease activity of the *Pfu*MR complex at the 5′ end of a DNA break to generate major 27–29 nt products through its direct interaction via the PIP-like motif. This suggests that alteration of nuclease activity by *Pfu*PCNA seems to be promiscuous and independent of length or sequences of substrates. These results are in agreement with the mechanism by which the endonuclease activity of *Pfu*Mre11 acts to incise the 5′ strand DNA close to the DSB ends (46). Taken together, these data suggest that upon association with *Pfu*PCNA, *Pfu*MR could promote endonucleolytic activity to process DNA ends.

After cleavage, the endonucleolytic product is released *via Pfu*MR/PCNA strand opening activity

Next, we investigated whether the endonucleolytic cleavage was coupled with DNA melting by the *Pfu*MR complex. As ATP-dependent DNA unwinding activity has already been reported for both prokaryotic and eukaryotic MR complexes (47–50), we made a fluorescence-based helicase assay to monitor the activity of *Pfu*MR and assess the influence of *Pfu*PCNA. We used modified S87s/87s substrate with reporter-quencher pair at the 5′ end to monitor emission of fluorescence during double strand opening in real time. To prevent partial DNA melting at high temperature, we performed unwinding assays at 55°C on the 3′ end protected substrate. In the previous cited studies (47,48,50,51), authors showed that addition of ATP/$MgCl_2$ was sufficient to detect a limited DNA unwinding activity of the MR complex. Yet, in our case, *Pfu*MR did not exhibit bona-fide DNA unwinding activity dependent on ATP/$MgCl_2$ cofactors (Figure 5A, compare lanes 1 and 4). However, in presence of *Pfu*PCNA and $MnCl_2$, conditions for which *Pfu*MR also displayed nuclease activity, strand opening activity was detected (Figure 5A, compare lanes 4 and 8). We obtained similar results with the same substrate but containing the reporter-quencher pair located at internal position 23 nt from 5′ end of the top strand (Figure 5B), indicating that local DNA melting extended from the cleavage site down to the 5′ extremity and suggesting that this DNA fragment was displaced by the *Pfu*PCNA/MR complex. To confirm this, we performed nuclease assays using the same substrates in similar conditions and resolved DNA products in native PAGE (Supplementary Figure S8). Data showed generation of a single strand DNA fragment of about 30 nt, corresponding to the displaced FAM-labeled fragment from the 5′ end. From these results, we can propose that coordination of endonuclease and local strand opening activities of *Pfu*PCNA/MR complex leads to the release of a small 5′ end ssDNA fragment to generate a DNA product with a 3′ ssDNA overhang of about 30 nt exposed.

*Pfu*PCNA does not interfere with ATP hydrolysing cycle of *Pfu*Rad50

At this point, we demonstrated that *Pfu*PCNA stimulates *Pfu*MR nuclease activity depending on ATP presence. A member of the ATP Binding Cassette (ABC) protein superfamily, Rad50 contains a conserved Nucleotide Binding Domain (NBD) that dimerizes upon two ATP molecules binding at dimer interface (45). By binding and hydrolysing ATP, Rad50 drives dynamic structural transitions of the MR complex controlling DNA unwinding and nuclease activities (49,52–56). To examine effect of the *Pfu*PCNA/MR complex interaction on ATPase activity, we measured radioactive phosphate released by ATP hydrolysis in conditions where *Pfu*MR complex was deficient in nuclease activity (without $MnCl_2$). As observed in several other studies, *Pfu*MR alone exhibited weak ATPase activity that was not stimulated by the addition of dsDNA substrate (Supplementary Figure S9). In addition, we showed that *Pfu*PCNA did not significantly regulate ATPase activity of *Pfu*MR and hence may have no effect on *Pfu*MR conformational change; similar data (not shown) were obtained in presence of $MnCl_2$.

DISCUSSION

MR complex is involved in various aspects of DSB repair, including sensing DSB triggering signal pathways and facilitating DSB repair through different pathways. Among hyperthermophilic archaea, gene deletions of *mre11* and *rad50* are lethal for cells arguing for their apparent essentiality, which distinguishes HA from all other cellular organisms, including mesophilic archaea (for a review, see (5)). Here we revealed *in vitro* physical association and functional interplay between the DNA clamp PCNA and the recombination MR complex of *P. furiosus*. To support this conclusion, we found that (i) *Pfu*MR directly interacts with *Pfu*PCNA via a PIP-like motif and (ii) *Pfu*PCNA regulates *Pfu*MR ATP-dependent nuclease activity to promote endonucleolytic cleavage about 30 nt from 5′-terminated dsDNA.

We demonstrated that PCNA binds directly to the Mre11–Rad50 complex of *P. furiosus* and that the interaction is mediated by a non-canonical PIP motif located in the C-terminal region of *Pfu*Mre11. The conspicuous difference between the *Pfu*Mre11 motif and the canonical PIP motif is the absence of the well-conserved glutamine residue. For several PCNA-interacting partners, the PIP motif contains a glutamine residue involved in multiple interactions

Figure S8

A

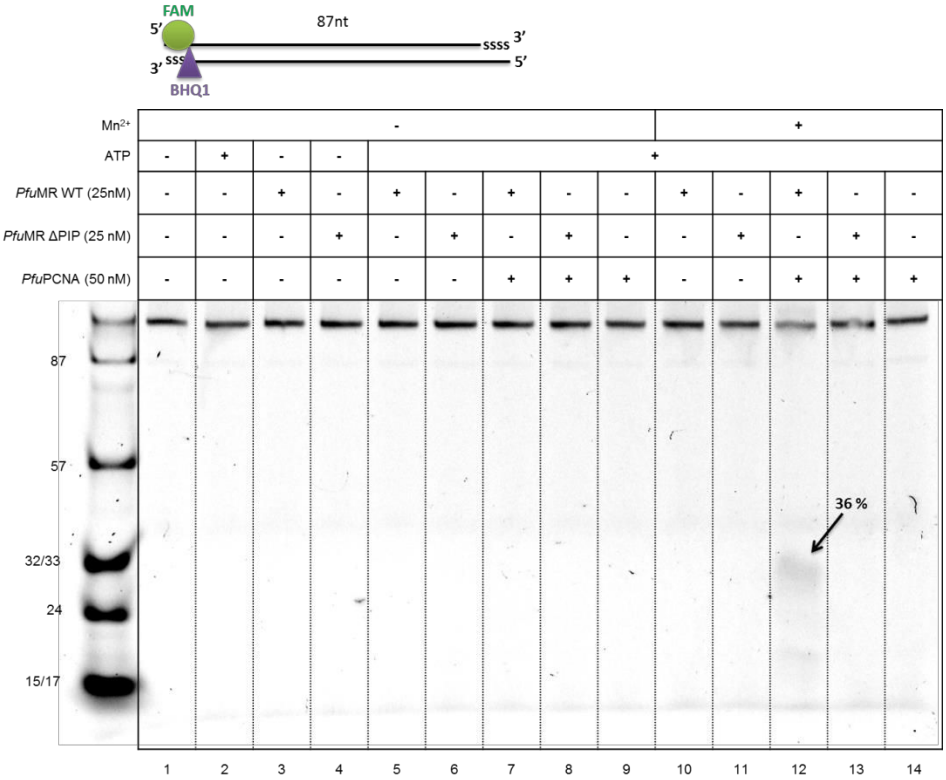
FAM
5′
87nt
ssss 3′
3′ sss
5′
BHQ1
Mn2+
ATP
PfuMR WT (25nM)
PfuMR ΔPIP (25 nM)
PfuPCNA (50 nM)
87
57
32/33
24
15/17
36 %
1 2 3 4 5 6 7 8 9 10 11 12 13 14

B

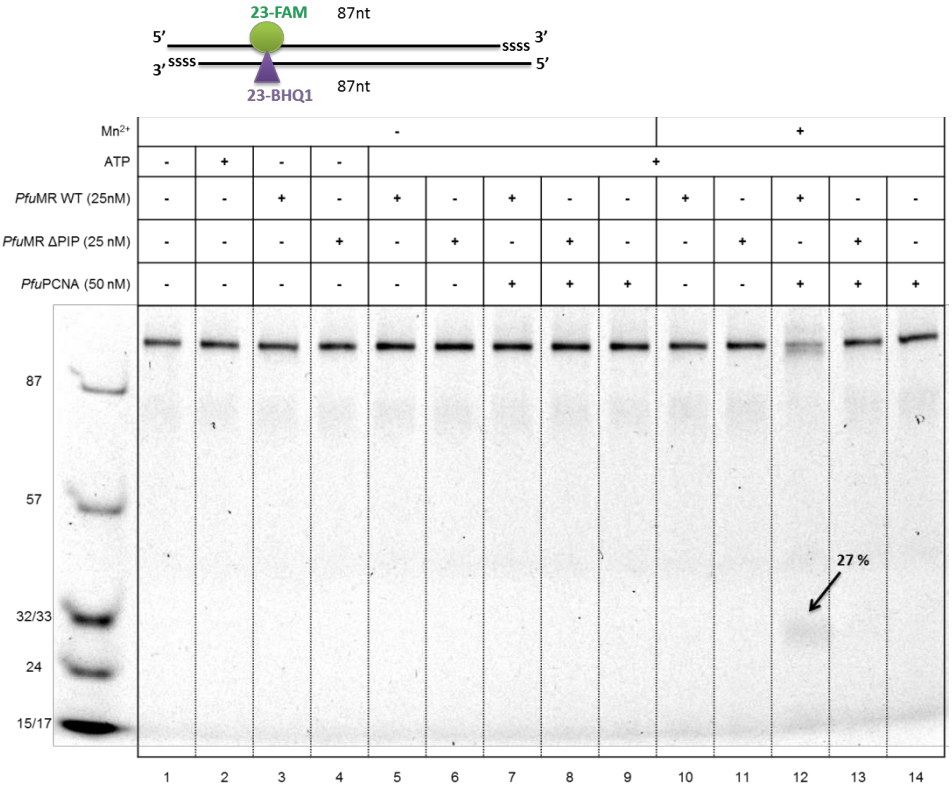
23-FAM
87nt
5′
ssss 3′
3′ ssss
5′
87nt
23-BHQ1
Mn2+
ATP
PfuMR WT (25nM)
PfuMR ΔPIP (25 nM)
PfuPCNA (50 nM)
87
57
32/33
24
15/17
27 %
1 2 3 4 5 6 7 8 9 10 11 12 13 14

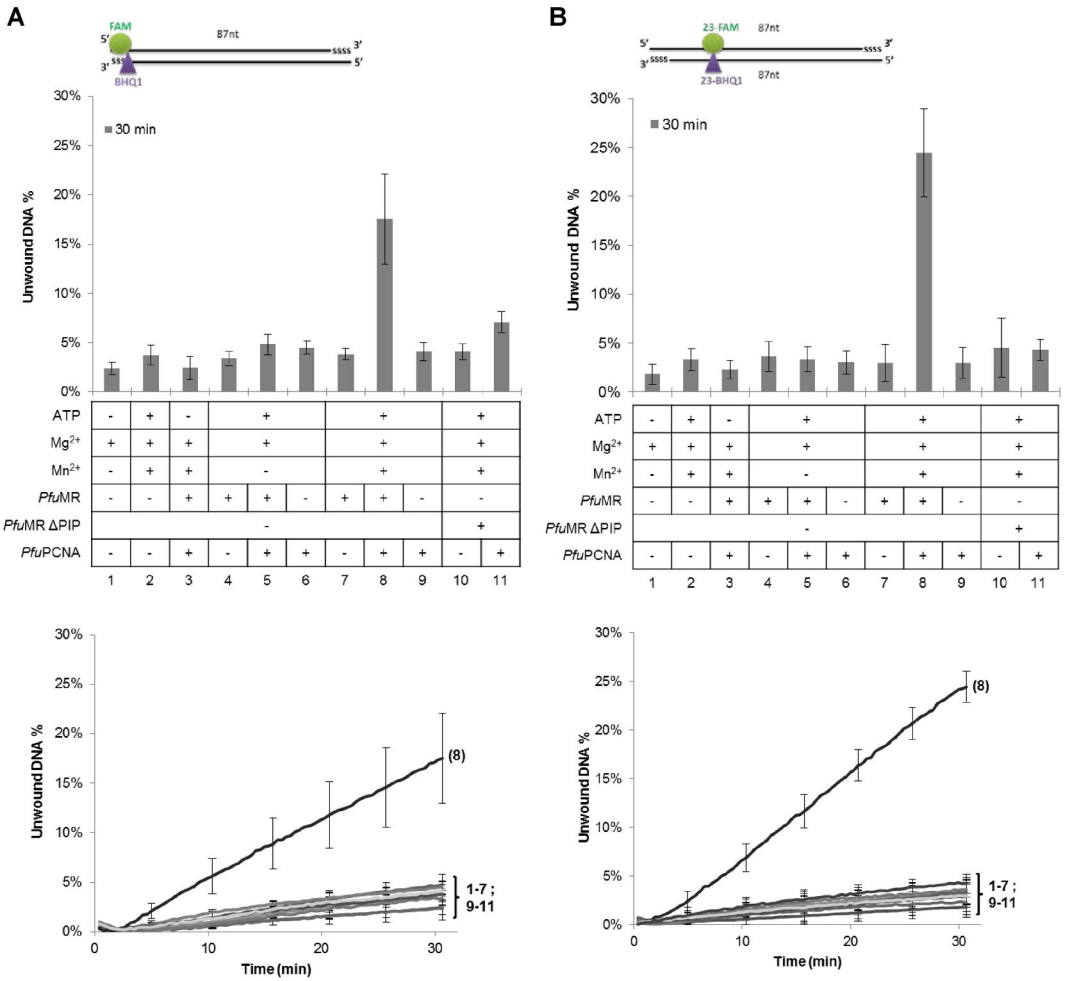

Figure 5. The endonucleolytic product from *Pfu*PCNA/MR activity is displaced from dsDNA. Results from real-time fluorescence DNA unwinding assays are presented on histogram chart with the percentage of unwound quenched substrates at 55°C after 30 min of time reaction. The dsDNA substrates used are illustrated above each histogram: RQ-S87s/87s substrate (**A**) contained a reporter-quencher pair at one extremity (+5 of the 3′ strand) consisting of dsDNA duplex; (**B**) RQ23-S87s/87s substrate had the reporter-quencher pair located at internal position 23 of dsDNA. Kinetics of DNA unwinding assays are displayed in the panels below, curves numbering corresponds to the histogram lane number (from 1 to 11). 25 nM DNA substrate were pre-incubated with 50 nM *Pfu*PCNA at room temperature for 5 min before adding 25 nM *Pfu*MR wt or ΔPIP. Reactions were performed for 30 min at 55°C in buffer with 300 mM NaCl, 5 mM $MgCl_2$ complemented with 1 mM ATP and 5 mM $MnCl_2$ as indicated in the table below histograms (see 'Materials and methods' for complete protocol). Experiments were performed in triplicate and error bars correspond to standard deviation.

with PCNA surface residues (38). Recently, a number of additional proteins that bind to PCNA have been reported (reviewed in (19–21,57)). Among them, some PCNA partners showed a PIP motif lacking this glutamine residue, and its absence has also been observed for homologue proteins, such as RFC in Archaea (58). Interestingly, the N-terminal part of the *Pfu*Mre11 peptide contains a basic region composed mainly of lysine (K) amino acids. As described for the PIP motif of RFC from *P. furiosus,* these residues could establish electrostatic interactions with the negatively charged surface of the PCNA C-terminal tail and compensate for the absence of glutamine residue (59,60). These results suggest that the peptide detected on *Pfu*Mre11 sequences is a variation on a theme of the canonical PIP motif, lacking the otherwise conserved glutamine residue, and mediates interaction between *Pfu*PCNA and the *Pfu*MR complex

Remarkably, the putative PCNA interacting motif is conserved among Mre11 sequences of all Thermococcales species and of *Archaeoglobus fulgidus*. Similar PCNA interaction motifs were not found in other archaea or in eukaryotic Mre11 sequences. However, a search for a canonical PIP motif (Q-x(2)-[LIVM]-x(2)-[FYW]-[FYWLIVM]) in generic databases Swiss-Prot and TrEMBL, using Mre11 as description filter, identified Mre11 sequences from the orders Methanosarcinales and Halobacteriales as potentially harbouring a canonical PIP motif at the extreme C-terminus region (data not shown). This suggests that the interaction between PCNA and the MR complex could be a more general feature, not only restricted to these phylogenetic branches. In addition, proteins may use additional regions to interact with the DNA clamp and novel PCNA interacting motifs have been identified since the classic PIP-box discovery (21,61). In this context, this hypothesis deserves to be tested, particularly for eukaryotic Mre11 for which a co-localisation with PCNA was observed in human during the S phase of the cell cycle (62).

Figure S9

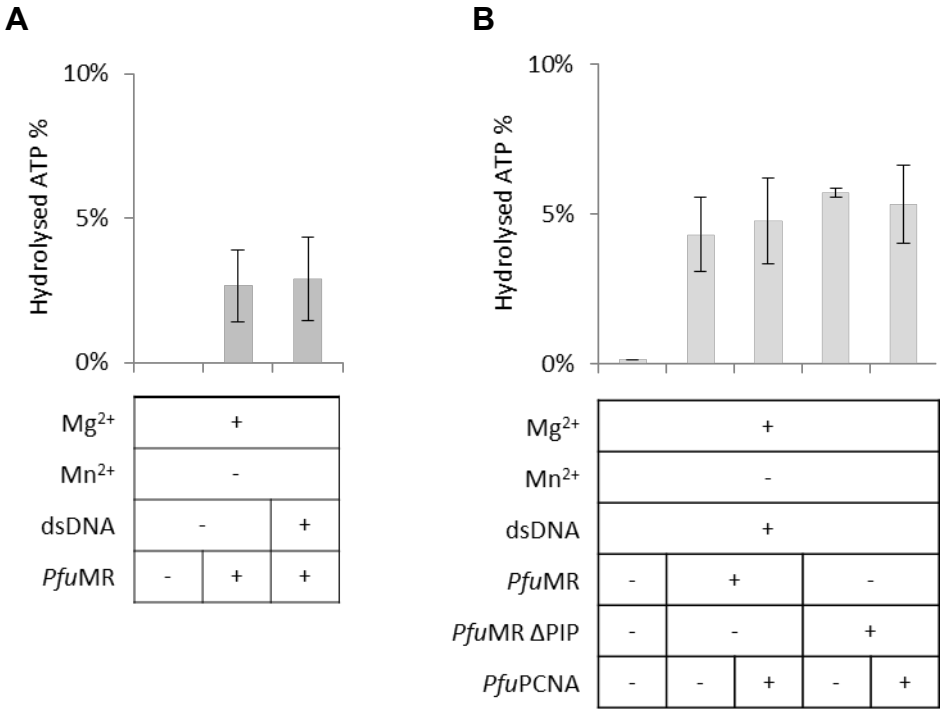
A
B
10%
5%
0%
Hydrolysed ATP %
Mg2+
Mn2+
dsDNA
PfuMR
PfuMR ΔPIP
PfuPCNA

Besides the physical interaction, we described a functional interplay between the recombination complex and *Pfu*PCNA. First, we demonstrated that *Pfu*MR is weakly active at moderate ionic strength, the condition prevailing in *P. furiosus* cells. We also demonstrated that, in these particular conditions the DNA sliding clamp stimulates and modulates nuclease activity of *Pfu*MR complex. Our data thus indicate that DNA resection initiated by *Pfu*MR could be regulated by the DNA sliding clamp. We showed that upon association with *Pfu*PCNA, the *Pfu*MR complex generates a major internal incision in the 5′ strand proximal to DSB ends. Our findings are consistent with recent study in budding yeast, wherein a distinct MR complex partner, Sae2, influenced the activity of MR in a comparable manner, by activating only the endonuclease activity of the Mre11–Rad50–Xrs2 complex (46). In addition, it was shown that the 5′ strand cleavage by eukaryotic MR was strongly enhanced by a protein block mimicking a covalently bound topoisomerase-like protein (46). While MR nuclease activities are dispensable for the resection of 'clean' DSBs (63), endonuclease activity is essential to clear obstructed DNA ends (64). Consistent with this property, we also demonstrated that *P. furiosus* MR complex was able to cleave ds break DNA intermediates with a streptavidin block at the 5′ end or with both ends blocked with phosphorothioate residues. The reported behaviour of T4 phage system gp46/47 (MR homologues) in presence of the protein factors gp32 and UvsY was also comparable to what we observed for the archaeal *Pfu*PCNA/MR complex, since the degradation profile of gp46/47 was shifted towards the generation of endonuclease products between 15 and 25 nt (30). More recently, Deshpande *et al.*, demonstrated for human proteins the role of Nbs1, the third component of the MR/N complex, in regulating MR activities by inhibiting exonuclease activity on clean ends, whereas phosphorylated CtIP, the orthologue of Sae2, stimulates endonucleolytic cleavage (65).

These different reports emphasize the importance of regulating endo- and exonuclease activities of Mre11 within the MR complex for DSB repair and that this regulation is tightly coupled with ATP-dependent conformational changes of the MR complex. A major contribution of the present study is that we revealed *Pfu*PCNA as a new interacting partner stimulating nuclease activity of the *Pfu*MR complex. The molecular mechanisms that would explain how *Pfu*PCNA triggers this internal incision by *Pfu*MR remain to be determined.

As mentioned earlier, the cycle of ATP binding and hydrolysis is associated with conformational changes of the MR complex, with transition between ATP-bound and ATP-hydrolysed states, where the ATP-bound form mediates DNA end binding, whereas ATP-hydrolyzed state renders the Mre11 nuclease active site accessible. Here, we showed that the endonucleolytic cleavage induced by the *Pfu*PCNA/MR complex is ATP-dependent, but that *Pfu*PCNA had no effect on ATP hydrolysis or DNA binding activities of *Pfu*MR. Interestingly, the PIP-like motif in *Pfu*Mre11 is located close to the RBD domain involved in binding of the Rad50 subunit. PCNA and the Rad50 subunit slide or diffuse along DNA whereas Mre11 is required for DNA end recognition and nuclease activities (66). Further structural and biochemical analysis would be required to determine if one of the two proteins has an effect on its partner's diffusion along the DNA or if *Pfu*PCNA interacts preferentially with a conformation of the *Pfu*MR complex. In support of the latter hypothesis, we showed by SPR that a more stable *Pfu*PCNA/MR complex was formed in presence of ATP, and in the case of the *Pfu*MR construct with truncated *Pfu*Rad50, the complex was faster to dissociate from *Pfu*PCNA (data not shown), indicating that the *Pfu*Rad50 coiled-coil domain also has a role in the stabilisation of the interaction. Structural determination of the *Pfu*PCNA/MR complex with DNA would be important for understanding how *Pfu*PCNA controls or binds a specific conformational state of *Pfu*MR complex.

According to bidirectional resection model of DNA DSB, upon the initial endonuclease cleavage, the Mre11 exonuclease proceeds back towards the DNA end *via* its 3′→5′ exonuclease activity (model discussed in (32,67). Astonishingly, in our results no 5′-products shorter than 15 nt were observed in the nuclease assays, suggesting an absence of extensive 3′→5′ resection for the second step. The most likely explanation for this observation is that archaeal *Pfu*MR displaced the 5′ end through a combination of melting and endonuclease activities. This explanation is consistent with the reported ability of the eukaryotic MR(N/X) complex to open the DNA helix on ∼20 base pairs at the end of the duplex in an ATP-dependent manner (47,50).

In our conditions, the *Pfu*PCNA/MR complex did not display genuine DNA helicase activity dependent on ATP and Mg^{2+}. To date, ATP-dependent DNA unwinding activity has only been reported for bacterial MR and eukaryotic MRN complexes. This finding suggests that this unwinding activity is not conserved in the archaeal MR complex. However, in conditions suitable for DNA cleavage, the 5′ labeled product (27–29 nt) was displaced from the initial dsDNA substrate. We thus propose that *Pfu*PCNA stimulates *Pfu*MR DNA end processing leading to an internal cleavage coupled with 5′ end removal. As described by Liu and collaborators, ATP-dependent DNA melting facilitates the access of Mre11 for DNA cleavage (49). Here, we cannot elucidate which, from the cleavage or the DNA opening event, occurs first. Altogether, we assume that the short-range processing by *Pfu*PCNA/MR would generate 3′-tailed substrate that could be suitable for additional partners responsible for extended resection. The helicase/nuclease HerA/NurA complex was found in all thermophilic archaea, clustered in the operon encoding Mre11 and Rad50 (68), and *in vitro* experiments demonstrated that Rad50, Mre11, HerA and NurA co-operate for resection of the 5′ strand at a DNA double strand break, generating a 3′ ssDNA suitable for the recombinase RadA (42). In *Pyrococcus abyssi,* at least 20 nt are required to bind one RPA trimer onto DNA efficiently (unpublished data). Here, the *Pfu*PCNA/MR interplay generates a 3′ overhang of 27–29 nt suitable for RPA loading and thus for 3′ tail protection from degradation by NurA, while the complex HerA/NurA can still extend 5′ strand resection. Taken together, our findings indicate that *Pfu*MR interacts with *Pfu*PCNA physically and functionally in a manner consistent with an end resection process for the HR pathway.

This study leads to questions about the role of PCNA/MR interplay in hyperthermophilic archaea. The precise employment of the different process components in cases of either DSB damage or replication fork stalling remains to be clarified. Deciphering the role of PCNA/MR interplay in HA will require further genetic and structural studies, with the hope that it might provide clues to improve understanding of recombinational repair processes in archaea.

SUPPLEMENTARY DATA

Supplementary Data are available at NAR Online.

ACKNOWLEDGEMENTS

We thank Tanya Paull, John Tainer and Bernard Connolly for sending clones and we are grateful to Gareth Williams for providing proteins and for helpful discussions.
Author Contributions: G.H., L.Y., S.L., E.H., B.C.O., D.F. designed the experiments; G.H., Y.L., S.L., R.D., D.K.P., A.B., P.F.P. performed the experiments; G.H., D.F., Y.L., S.L. analysed the data; G.H., D.F., Y.L. wrote the paper; and D.F. conceived and directed the study.

FUNDING

Ifremer; CNRS; University of Western Britany. This work was supported by the French "Agence Nationale pour la Recherche" [ANR-16-CE12-0016 to B.C.O. and D.F.]. Funding for open access charge: Ifremer.
Conflict of interest statement. None declared.

REFERENCES

1. Gerard,E., Jolivet,E., Prieur,D. and Forterre,P. (2001) DNA protection mechanisms are not involved in the radioresistance of the hyperthermophilic archaea Pyrococcus abyssi and P. furiosus. *Mol. Genet. Genomics*, **266**, 72–78.
2. Peak,M.J., Robb,F.T. and Peak,J.G. (1995) Extreme resistance to thermally induced DNA backbone breaks in the hyperthermophilic archaeon Pyrococcus furiosus. *J. Bacteriol.*, **177**, 6316–6318.
3. Larmony,S., Garnier,F., Hoste,A. and Nadal,M. (2015) A specific proteomic response of Sulfolobus solfataricus P2 to gamma radiations. *Biochimie*, **118**, 270–277.
4. Kelman,L.M. and Kelman,Z. (2014) Archaeal DNA replication. *Annu. Rev. Genet.*, **48**, 71–97.
5. Grogan,D.W. (2015) Understanding DNA repair in hyperthermophilic Archaea: persistent gaps and other reasons to focus on the fork. *Archaea*, **2015**, 942605.
6. Shiraishi,M., Ishino,S., Yamagami,T., Egashira,Y., Kiyonari,S. and Ishino,Y. (2015) A novel endonuclease that may be responsible for damaged DNA base repair in Pyrococcus furiosus. *Nucleic Acids Res.*, **43**, 2853–2863.
7. Giroux,X. and MacNeill,S.A. (2016) A novel archaeal DNA repair factor that acts with the UvrABC system to repair mitomycin C-induced DNA damage in a PCNA-dependent manner. *Mol. Microbiol.*, **99**, 1–14.
8. Tori,K., Ishino,S., Kiyonari,S., Tahara,S. and Ishino,Y. (2013) A novel Single-Strand specific 3′-5′ exonuclease found in the hyperthermophilic archaeon, pyrococcus furiosus. *PLoS One*, **8**, e58497.
9. Li,Z., Pan,M., Santangelo,T.J., Chemnitz,W., Yuan,W., Edwards,J.L., Hurwitz,J., Reeve,J.N. and Kelman,Z. (2011) A novel DNA nuclease is stimulated by association with the GINS complex. *Nucleic Acids Res.*, **39**, 6114–6123.
10. Li,Z., Santangelo,T.J., Cubonova,L., Reeve,J.N. and Kelman,Z. (2010) Affinity purification of an archaeal DNA replication protein network. *MBio*, **1**, e00221.
11. Ren,B., Kuhn,J., Meslet-Cladiere,L., Briffotaux,J., Norais,C., Lavigne,R., Flament,D., Ladenstein,R. and Myllykallio,H. (2009) Structure and function of a novel endonuclease acting on branched DNA substrates. *EMBO J.*, **28**, 2479–2489.
12. Meslet-Cladiere,L., Norais,C., Kuhn,J., Briffotaux,J., Sloostra,J.W., Ferrari,E., Hubscher,U., Flament,D. and Myllykallio,H. (2007) A novel proteomic approach identifies new interaction partners for proliferating cell nuclear antigen. *J. Mol. Biol.*, **372**, 1137–1148.
13. Guy,C.P. and Bolt,E.L. (2005) Archaeal Hel308 helicase targets replication forks in vivo and in vitro and unwinds lagging strands. *Nucleic Acids Res.*, **33**, 3678–3690.
14. Fujikane,R., Komori,K., Shinagawa,H. and Ishino,Y. (2005) Identification of a novel helicase activity unwinding branched DNAs from the hyperthermophilic archaeon, Pyrococcus furiosus. *J. Biol. Chem.*, **280**, 12351–12358.
15. Pluchon,P.F., Fouqueau,T., Creze,C., Laurent,S., Briffotaux,J., Hogrel,G., Palud,A., Henneke,G., Godfroy,A., Hausner,W. *et al.* (2013) An extended network of genomic maintenance in the archaeon pyrococcus abyssi highlights unexpected associations between eucaryotic homologs. *PLoS One*, **8**, e79707.
16. Henneke,G., Gueguen,Y., Flament,D., Azam,P., Querellou,J., Dietrich,J., Hubscher,U. and Raffin,J.P. (2002) Replication factor C from the hyperthermophilic archaeon Pyrococcus abyssi does not need ATP hydrolysis for clamp-loading and contains a functionally conserved RFC PCNA-binding domain. *J. Mol. Biol.*, **323**, 795–810.
17. Cann,I.K., Ishino,S., Hayashi,I., Komori,K., Toh,H., Morikawa,K. and Ishino,Y. (1999) Functional interactions of a homolog of proliferating cell nuclear antigen with DNA polymerases in Archaea. *J. Bacteriol.*, **181**, 6591–6599.
18. Maga,G. and Hubscher,U. (2003) Proliferating cell nuclear antigen (PCNA): a dancer with many partners. *J. Cell Sci.*, **116**, 3051–3060.
19. Pan,M., Kelman,L.M. and Kelman,Z. (2011) The archaeal PCNA proteins. *Biochem. Soc. Trans.*, **39**, 20–24.
20. Moldovan,G.L., Pfander,B. and Jentsch,S. (2007) PCNA, the maestro of the replication fork. *Cell*, **129**, 665–679.
21. Gilljam,K.M., Feyzi,E., Aas,P.A., Sousa,M.M., Muller,R., Vagbo,C.B., Catterall,T.C., Liabakk,N.B., Slupphaug,G., Drablos,F. *et al.* (2009) Identification of a novel, widespread, and functionally important PCNA-binding motif. *J. Cell Biol.*, **186**, 645–654.
22. Stracker,T.H. and Petrini,J.H. (2011) The MRE11 complex: starting from the ends. *Nat. Rev. Mol. Cell Biol.*, **12**, 90–103.
23. Daley,J.M., Niu,H., Miller,A.S. and Sung,P. (2015) Biochemical mechanism of DSB end resection and its regulation. *DNA Repair*, **32**, 66–74.
24. Goodarzi,A.A. and Jeggo,P.A. (2013) The repair and signaling responses to DNA double-strand breaks. *Adv. Genet.*, **82**, 1–45.
25. White,M.F. (2011) Homologous recombination in the archaea: the means justify the ends. *Biochem. Soc. Trans.*, **39**, 15–19.
26. Huertas,P. (2010) DNA resection in eukaryotes: deciding how to fix the break. *Nat. Struct. Mol. Biol.*, **17**, 11–16.
27. Bartlett,E.J., Brissett,N.C. and Doherty,A.J. (2013) Ribonucleolytic resection is required for repair of strand displaced nonhomologous end-joining intermediates. *PNAS*, **110**, E1984–E1991.
28. Fujikane,R., Ishino,S., Ishino,Y. and Forterre,P. (2010) Genetic analysis of DNA repair in the hyperthermophilic archaeon, Thermococcus kodakaraensis. *Genes Genet. Syst.*, **85**, 243–257.
29. Huang,Q., Liu,L., Liu,J., Ni,J., She,Q. and Shen,Y. (2015) Efficient 5′-3′ DNA end resection by HerA and NurA is essential for cell viability in the crenarchaeon Sulfolobus islandicus. *BMC Mol. Biol.*, **16**, 2.
30. Herdendorf,T.J., Albrecht,D.W., Benkovic,S.J. and Nelson,S.W. (2011) Biochemical characterization of bacteriophage T4 Mre11–Rad50 complex. *J. Biol. Chem.*, **286**, 2382–2392.
31. Lafrance-Vanasse,J., Williams,G.J. and Tainer,J.A. (2015) Envisioning the dynamics and flexibility of Mre11–Rad50-Nbs1 complex to decipher its roles in DNA replication and repair. *Progr. Biophys. Mol. Biol.*, **117**, 182–193.
32. Paull,T.T. (2010) Making the best of the loose ends: Mre11/Rad50 complexes and Sae2 promote DNA double-strand break resection. *DNA Repair*, **9**, 1283–1291.

33. Emptage,K., O'Neill,R., Solovyova,A. and Connolly,B.A. (2008) Interplay between DNA polymerase and proliferating cell nuclear antigen switches off base excision repair of uracil and hypoxanthine during replication in archaea. *J. Mol. Biol.*, **383**, 762–771.
34. Hopfner,K.P., Karcher,A., Shin,D., Fairley,C., Tainer,J.A. and Carney,J.P. (2000) Mre11 and Rad50 from Pyrococcus furiosus: cloning and biochemical characterization reveal an evolutionarily conserved multiprotein machine. *J. Bacteriol.*, **182**, 6036–6041.
35. Williams,G.J., Williams,R.S., Williams,J.S., Moncalian,G., Arvai,A.S., Limbo,O., Guenther,G., SilDas,S., Hammel,M., Russell,P. *et al.* (2011) ABC ATPase signature helices in Rad50 link nucleotide state to Mre11 interface for DNA repair. *Nat. Struct. Mol. Biol.*, **18**, 423–431.
36. Winter,J.A. and Bunting,K.A. (2012) Rings in the extreme: PCNA interactions and adaptations in the archaea. *Archaea*, **2012**, 951010.
37. Warbrick,E. (1998) PCNA binding through a conserved motif. *Bioessays*, **20**, 195–199.
38. Gulbis,J.M., Kelman,Z., Hurwitz,J., ODonnell,M. and Kuriyan,J. (1996) Structure of the C-terminal region of p21(WAF1/CIP1) complexed with human PCNA. *Cell*, **87**, 297–306.
39. Fujikane,R., Shinagawa,H. and Ishino,Y. (2006) The archaeal Hjm helicase has recQ-like functions, and may be involved in repair of stalled replication fork. *Genes Cells*, **11**, 99–110.
40. Creze,C., Ligabue,A., Laurent,S., Lestini,R., Laptenok,S.P., Khun,J., Vos,M.H., Czjzek,M., Myllykallio,H. and Flament,D. (2012) Modulation of the Pyrococcus abyssi NucS endonuclease activity by replication clamp at functional and structural levels. *J. Biol. Chem.*, **287**, 15648–15660.
41. Hasan,M.N., Hagedoorn,P.L. and Hagen,W.R. (2002) Pyrococcus furiosus ferredoxin is a functional dimer. *FEBS Lett.*, **531**, 335–338.
42. Hopkins,B.B. and Paull,T.T. (2008) The P. furiosus mre11/rad50 complex promotes 5′ strand resection at a DNA double-strand break. *Cell*, **135**, 250–260.
43. Hopfner,K.P., Karcher,A., Craig,L., Woo,T.T., Carney,J.P. and Tainer,J.A. (2001) Structural biochemistry and interaction architecture of the DNA double-strand break repair Mre11 nuclease and Rad50-ATPase. *Cell*, **105**, 473–485.
44. Paull,T.T. and Gellert,M. (1998) The 3′ to 5′ exonuclease activity of Mre 11 facilitates repair of DNA double-strand breaks. *Mol. Cell*, **1**, 969–979.
45. Hopfner,K.P., Karcher,A., Shin,D.S., Craig,L., Arthur,L.M., Carney,J.P. and Tainer,J.A. (2000) Structural biology of Rad50 ATPase: ATP-driven conformational control in DNA double-strand break repair and the ABC-ATPase superfamily. *Cell*, **101**, 789–800.
46. Cannavo,E. and Cejka,P. (2014) Sae2 promotes dsDNA endonuclease activity within Mre11–Rad50-Xrs2 to resect DNA breaks. *Nature*, **514**, 122–125.
47. Cannon,B., Kuhnlein,J., Yang,S.H., Cheng,A., Schindler,D., Stark,J.M., Russell,R. and Paull,T.T. (2013) Visualization of local DNA unwinding by Mre11/Rad50/Nbs1 using single-molecule FRET. *PNAS*, **514**, 122–125.
48. Chen,L., Trujillo,K.M., Van Komen,S., Roh,D.H., Krejci,L., Lewis,L.K., Resnick,M.A., Sung,P. and Tomkinson,A.E. (2005) Effect of amino acid substitutions in the rad50 ATP binding domain on DNA double strand break repair in yeast. *J. Biol. Chem.*, **280**, 2620–2627.
49. Liu,Y., Sung,S., Kim,Y., Li,F., Gwon,G., Jo,A., Kim,A.K., Kim,T., Song,O.K., Lee,S.E. *et al.* (2016) ATP-dependent DNA binding, unwinding, and resection by the Mre11/Rad50 complex. *EMBO J.*, **35**, 743–758.
50. Paull,T.T. and Gellert,M. (1999) Nbs1 potentiates ATP-driven DNA unwinding and endonuclease cleavage by the Mre11/Rad50 complex. *Gene Dev.*, **13**, 1276–1288.
51. Liu,Y., Sung,S., Kim,Y., Li,F., Gwon,G., Jo,A., Kim,A.K., Kim,T., Song,O.K., Lee,S.E. *et al.* (2016) ATP-dependent DNA binding, unwinding, and resection by the Mre11/Rad50 complex. *EMBO J.*, **35**, 743–758.
52. Deshpande,R.A., Williams,G.J., Limbo,O., Williams,R.S., Kuhnlein,J., Lee,J.H., Classen,S., Guenther,G., Russell,P., Tainer,J.A. *et al.* (2014) ATP-driven Rad50 conformations regulate DNA tethering, end resection, and ATM checkpoint signaling. *EMBO J.*, **33**, 482–500.
53. Mockel,C., Lammens,K., Schele,A. and Hopfner,K.P. (2012) ATP driven structural changes of the bacterial Mre11:Rad50 catalytic head complex. *Nucleic Acids Res.*, **40**, 914–927.
54. Majka,J., Alford,B., Ausio,J., Finn,R.M. and McMurray,C.T. (2011) ATP hydrolysis by RAD50 protein switches MRE11 enzyme from endonuclease to exonuclease. *J. Biol. Chem.*, **287**, 2328–2341.
55. Lim,H.S., Kim,J.S., Park,Y.B., Gwon,G.H. and Cho,Y. (2011) Crystal structure of the Mre11–Rad50-ATPgammaS complex: understanding the interplay between Mre11 and Rad50. *Gene Dev.*, **25**, 1091–1104.
56. Lammens,K., Bemeleit,D.J., Mockel,C., Clausing,E., Schele,A., Hartung,S., Schiller,C.B., Lucas,M., Angermuller,C., Soding,J. *et al.* (2011) The Mre11:Rad50 structure shows an ATP-Dependent molecular Clamp in DNA Double-Strand break repair. *Cell*, **145**, 54–66.
57. Pedley,A.M., Lill,M.A. and Davisson,V.J. (2014) Flexibility of PCNA-Protein interface accommodates differential binding partners. *PLoS One*, **9**, e102481.
58. Warbrick,E. (2000) The puzzle of PCNA's many partners. *Bioessays*, **22**, 997–1006.
59. Matsumiya,S., Ishino,Y. and Morikawa,K. (2001) Crystal structure of an archaeal DNA sliding clamp: proliferating cell nuclear antigen from Pyrococcus furiosus. *Protein Sci.*, **10**, 17–23.
60. Matsumiya,S., Ishino,S., Ishino,Y. and Morikawa,K. (2002) Physical interaction between proliferating cell nuclear antigen and replication factor C from Pyrococcus furiosus. *Genes Cells*, **7**, 911–922.
61. Xu,H., Zhang,P., Liu,L. and Lee,M.Y. (2001) A novel PCNA-binding motif identified by the panning of a random peptide display library. *Biochemistry*, **40**, 4512–4520.
62. Maser,R.S., Mirzoeva,O.K., Wells,J., Olivares,H., Williams,B.R., Zinkel,R.A., Farnham,P.J. and Petrini,J.H. (2001) Mre11 complex and DNA replication: linkage to E2F and sites of DNA synthesis. *J. Mol. Cell Biol.*, **21**, 6006–6016.
63. Llorente,B. and Symington,L.S. (2004) The Mre11 nuclease is not required for 5′ to 3′ resection at multiple HO-induced double-strand breaks. *J. Mol. Cell Biol.*, **24**, 9682–9694.
64. Shibata,A., Moiani,D., Arvai,A.S., Perry,J., Harding,S.M., Genois,M.M., Maity,R., van Rossum-Fikkert,S., Kertokalio,A., Romoli,F. *et al.* (2013) DNA double-strand break repair pathway choice is directed by distinct MRE11 nuclease activities. *Mol. Cell*, **53**, 7–18.
65. Deshpande,R.A., Lee,J.H., Arora,S. and Paull,T.T. (2016) Nbs1 converts the human Mre11/Rad50 nuclease complex into an Endo/Exonuclease machine specific for protein–DNA adducts. *Mol. Cell*, **64**, 593–606.
66. Myler,L.R., Gallardo,I.F., Soniat,M.M., Deshpande,R.A., Gonzalez,X.B., Kim,Y., Paull,T.T. and Finkelstein,I.J. (2017) Single-Molecule imaging reveals how Mre11–Rad50-Nbs1 initiates DNA break repair. *Molecular Cell*, **67**, 891–898.
67. Cejka,P. (2015) DNA end resection: nucleases team up with the right partners to initiate homologous recombination. *J. Biol. Chem.*, **290**, 22931–22938.
68. Constantinesco,F., Forterre,P. and Elie,C. (2002) NurA, a novel 5′ -3′ nuclease gene linked to rad50 and mre11 homologs of thermophilic Archaea. *Embo Rep*, **3**, 537–542.

III. Supplementary study: genetic study *in vivo*

1) Context

Homologous recombination is a fundamental cellular process that plays a key role in rearrangement of genes both within and between chromosomes, also in promoting repair of damaged DNA and underpins replication. Since most archaeal species are difficult to cultivate due to their extremophilic growth conditions, large amount of current knowledge of recombination in the archaea is obtained from comparative genomics *in silico* and biochemistry studies *in vitro*. In our laboratory, we have developed a gene disruption system using hyperthermophilic Archaeon *Thermococcus barophilus* as a model organism, as it can be cultivated in the laboratory, to realize the studies of genes *in vivo*.

Thermococcus barophilus (*T. barophilus*) is a hyperthermophilic, piezophilic archaeon. It was isolated from a deep-sea hydrothermal vent in 1993. It grows optimally at 85°C and within a range of pressure from atmospheric pressure (0,1 Mpa) to 85 Mpa, with an optimum of 40MPa (Marteinsson *et al*, 1999). Moreover, *T. barophilus* is phylogenetically related to *P. furiosus* (Thiel *et al*, 2014).

This gene deletion system consists of a double-selection system: a positive selection using simvastatin and following by a counter-selection by 6-methylpurine (6-MP) (Birien *et al*, 2018).

Simvastatin is a positive selection marker developed in genetic manipulation system in different hyperthermophilic archaeal species such as *Thermococcus kodararensis* (*T. kodararensis*) (Matsumi *et al*, 2007; Hileman & Santangelo, 2012), *Pyrococcus furiosus* (Lipscomb *et al*, 2011), *Sulfolobus* isladicus (Zheng *et al*, 2012), *T. barophilus* (Thiel *et al*, 2014) and *Pyrococcus yayanossi* (Li *et al*, 2015). Why antibiotic simvastatin is used for the screen for transformed cells? The *hmg* gene (coding for the 3-hydroxy-3-methylglutaryl coenzymes A (HMG-CoA) reductase) in selection cassette can be overexpressed in strain and demonstrated to confer simvastatin resistance in different organism. Hence, *P. furiosus* (hmg_{pf}) can be used as a positive marker (Thiel *et al*, 2014).

6-MP is counter-selective marker developed in *T. kodararensis*. It is a toxic compound (an adenine analog) that inhibits cell growth. In *T. kodararensis,* an encoding gene *TK0664* (hypoxanthine-guanine phosphoribosyl-transferase) was identified and the gene product was shown to possess 6-MP resistance competence (Santangelo *et al*, 2010). In *T. barophilus*, the homologous gene to *T. kodakarensis TK0664* has been found, called "*T. barophilus TERMP_00517*". Birien *et al*. have shown that *TK0664* gene confers sensitivity to 6-MP in mutant Δ*TREMP_00517 T. barophilus*. Therefore, $TK0664_{tk}$ is chosen as a negative marker (Birien *et al*, 2018).

In brief, the gene deletion system (*Pop-in /pop-out*) is started by a construction of a vector (pUPH) containing the selection cassette (hmg_{pf} gene and $TK0664_{tk}$ gene) and the target gene was not in this constructed vector. Then this $pUPH_{\Delta target\_gene}$ will be transformed in Δ*TREMP_00517 T. barophilus* followed by the double selections. Finally, we performed an extraction of DNA from living cells after double crossing-over, and a PCR using primers located within (or downstream of) target gene and upstream of target gene, to confirm if the target gene was deleted. If the cells could grow without target gene, it means that the target gene is not essential; if not, target gene is essential for cells survival.

With this genetic tool, we have investigated the function of *mre11* gene deleted from the PIP motif of Mre11-rad50 complex (or the function of interaction between PCNA and Mre11-rad50 complex) in genomic maintenance.

2) Materials & methods

a) Strains and Growth media

T. barophilus strain MP: TBΔ*TREMP_00517* was used in this study (reference in (Birien *et al*, 2018)). *T. barophilus* strain was grown under anaerobic conditions at 85 °C in *Thermococcales* Rich Medium (TRM), which was made up as follows: 1 L of demineralized water was supplemented with 23 g NaCl, 5 g $MgCl_2.6H_2O$, 3.46 g PIPES disodium salt, 4 g Tryptone, 1 g yeast extract, 0.7 g KCl, 0.5 g $(NH_4)_2SO_4$, 0.05 g NaBr, 0.01 g $SrCl_2.6H_2O$, and 1 drop of resazurin 1%. The pH was adjusted to 6.6–6.7 and the medium autoclaved for 20 min at 121 °C. Once cooled, 1 mL of each of the following solutions was added: 5% K_2HPO_4, 5% KH_2PO_4, 2% $CaCl_2.2H_2O$, 10 mM $Na_2O_4W.2H_2O$, 25 mM $FeCl_3.6H_2O$. The liquid medium was dispensed in 50 or 100 mL vials, sulfur was added (2 g/L), and all vials were sealed with butyl-rubber stoppers, vacuum and N_2 gas addition steps were required to remove O_2 and to maintain the culture media under anaerobic conditions. The liquid phase was reduced by 0.1 mL of a Na_2S.9H20 solution. TRM was used in liquid or solid form and, for the latter case, 10 g/L of phytagel (Sigma-Aldrich Chimie, L'Isle D'Abeau Chesnes, St Quentin Falavier, France) were added to the TRM liquid medium.

After cell transformation, the transformants were selected on TRM supplemented with 2.5 µg/mL of simvastatin (Sigma) or 100 µM of 6-MP (Sigma).

b) Construction of gene deletion vector

The pUPH plasmid was used for the construction of our new suicide vector (Thiel *et al*, 2014). This plasmid bears the ampicillin resistance gene and two selection markers: the *HMG-CoA* gene of *P. furiosus* with its putative promoter region, and the *TK0664* gene of *T.kodakarensis*. It is a replicative plasmid in *E. coli* (Figure 34).

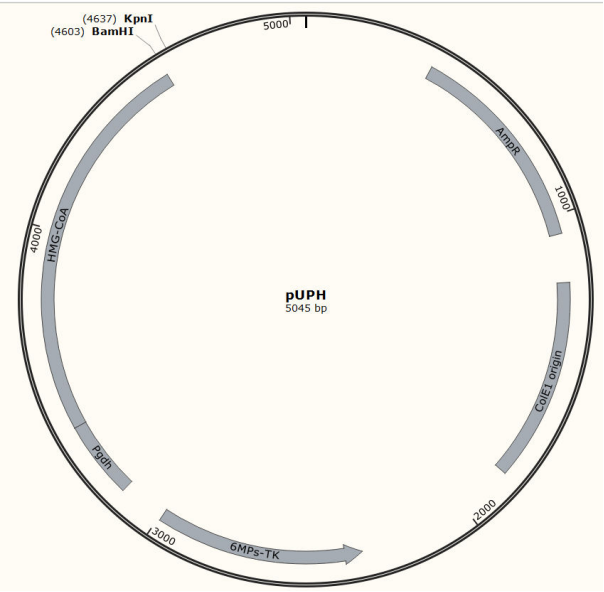

Figure 34 : Schematic representation of plasmid pUPH (5045 bp). The major elements in the plasmid follow as such: Pgdh (promoter)+HMG-CoA gene, enzymatic restriction sites BamHI and KpnI, AmpR gene, ColE1 origin and 6Mps-TK gene.

The *mre11_Δpip* gene (indicates *mre11* gene without PIP motif) was obtained by 3 PCR amplifications on the *T. barophilus* genome wild-type (WT) with the primers MRE11_1Up_KpnI, MRE11_1Do, PIP_2Up, PIP_2Do_BamHI (see table 13 and Figure 35). The resulting PCR product was sequenced by "Eurofin" to verify that the PIP motif has been deleted. Then this PCR product bears the KpnI and BamHI restriction enzyme sites at its extremities. The *mre11_Δpip* amplicon was cloned in the pUPH plasmid digested by the restriction enzymes KpnI and BamHI, and after ligation between the pUPH plasmid and the *mre11_Δpip* PCR-amplified gene (using T4 ligase; Promega), a plasmid named pP_Δ_MRE11_PIP was constructed (Figure 36). PCR products were loaded in 0,8% agar gel followed by a migration at 100V during 40 min, and purified by "QIAquick Gel Extraction Kit". Then the pP_Δ_MRE11_PIP plasmid was transformed in *E.coli* DH5α, and then clones were extracted and stocked at -80°C.

Table 13 : List of primers used in this study

Primers used for amplification of flanking regions of targeted gene	Sequence (5'-3')	Tm (°C)
MRE11_1Up_KpnI	AAAAAAGGTACCCCAGCTCCTCGAGTCTTTCCTTG	64,8
MRE11_1Do	GCTGAGAAAAAAGTGAAAAAAGCTCCCTGAGAATATGAGAATTGAAA AAATCATTGTGAGG	65,5
PIP_2Up	AAAAAAGGATCCCCCAGAAGAAGATCTCCGCCTATCA	65,0
PIP_2Do_BamHI	CCTCACAATGATTTTTTCAATTCTCATATTCTCAGGGAGCTTTTTTCAC TTTTTTCTCAGC	65,5
Primers used to check mutants	Sequence (5'-3')	
MRE-PIP-Verif-YM_up	ATCAAGCCCCAACACTTTCCTCAC	59,6
MRE-PIP-Verif-YM_Do	AAGAAGAAATCTGATATTTTGGCTTGGTTGAAGG	59,2
MRE-PIP-Verif-YM_2_Do	CCACGGGCGGAAAGGGA	60,9

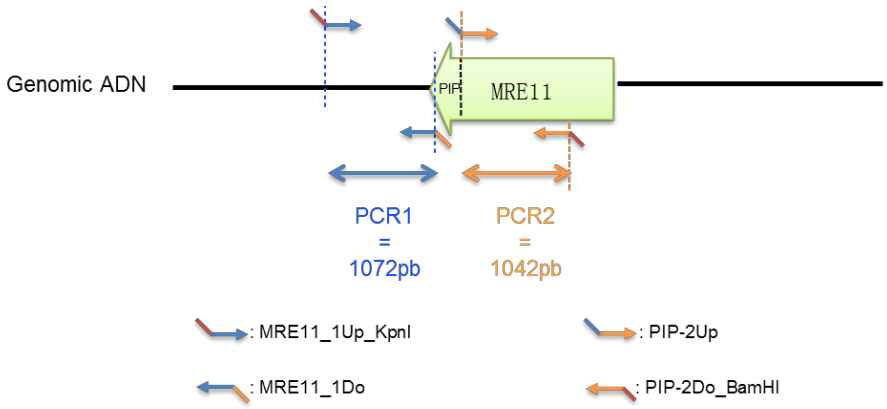

Overlap extension PCR between the PCR1 products and the PCR2 product= PCR3 (=2063bp).

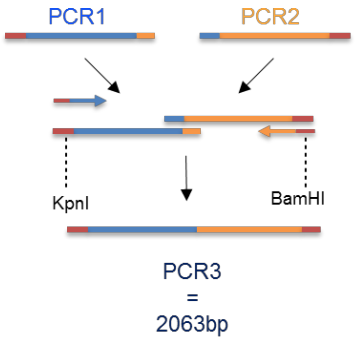

Figure 35 : Construction of mre11_Δpip gene by PCR amplification. Primers Mre11_1Up_KpnI and Mre11_1Do were used to amplify the zone before pip motif, and primers PIP_2Up and PIP_2Do_BamHI were used to amplify zone the after pip motif. Primers Mre11_1Up_KpnI and PIP_2Do_BamHI were used to amplify the resulting PCR1 and PCR2 products, to obtain *mre11_Δpip* gene (PCR3).

A

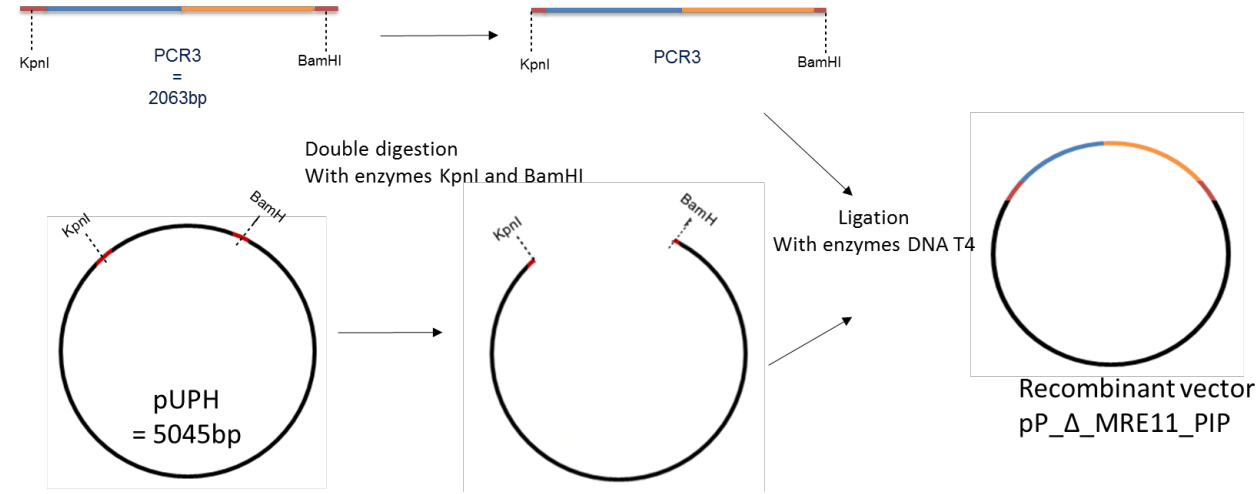

B

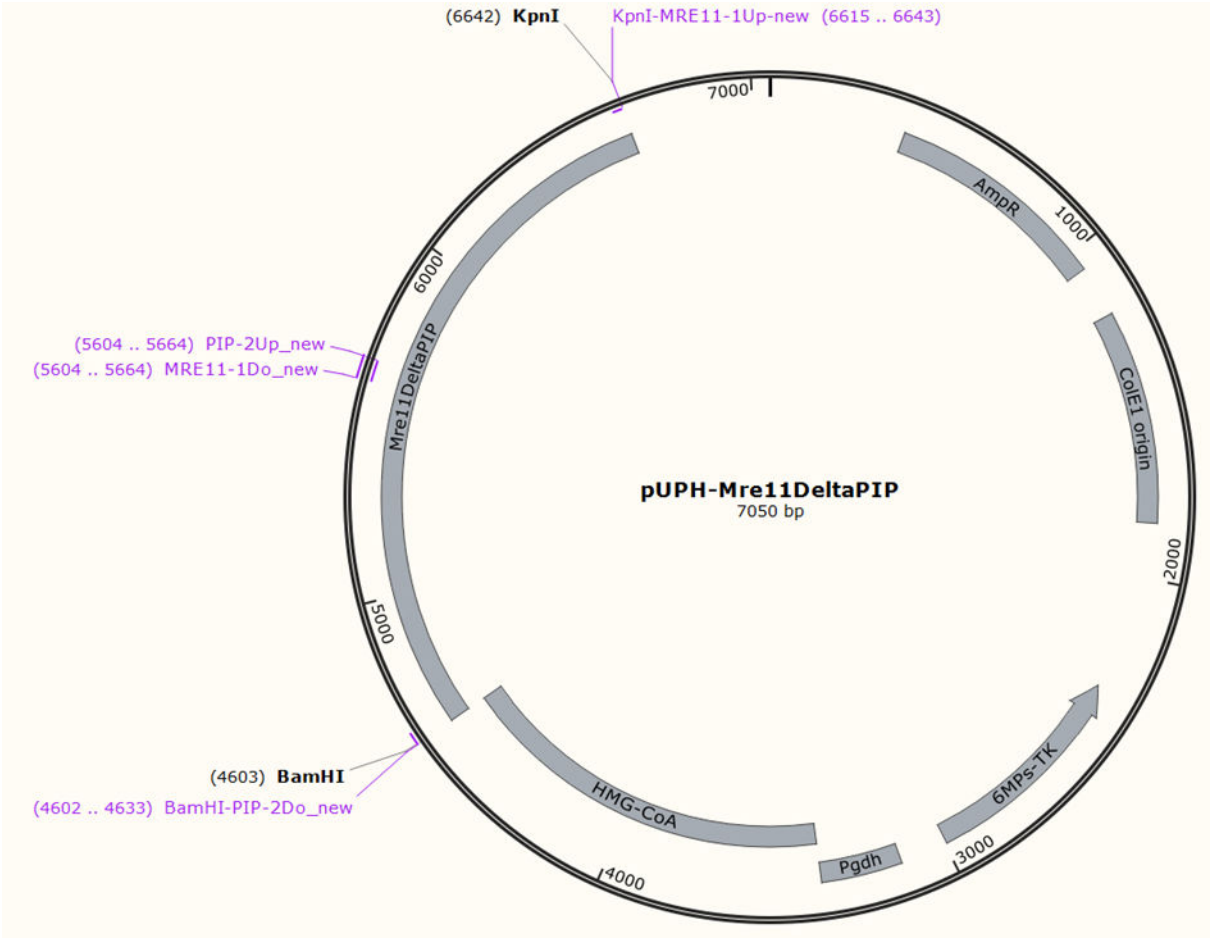

Figure 36 : Construction of pP_Δ_MRE11_PIP plasmid. pUPH plasmid and mre11_Δpip gene were digested by KpnI-HF and BamH-HF and were then ligated to obtain the plasmid pP_Δ_MRE11_PIP. (A) Schematic representation of construction steps. (B) Schematic representation of plasmid pP_Δ_MRE11_PIP (7050 bp). The restriction enzyme sites BamHI (B) and KpnI (K) were conserved to enable cloning of the homologous regions in pUPH plasmid.

c) Transformation of *Thermococcus barophilus*

The transformation protocol used in this study was identical to that described by (Birien *et al*, 2018). The $CaCl_2$ cell treatment was not required for the transformation. Cells were pre-cultivated in TRM medium with sulfur for 6 h at 85 °C at atmospheric pressure. Then, the cells were harvested by centrifugation (8000xg, 6 min, 4°C) concentrated in 200 µL of fresh TRM without sulfur; and kept on ice for 30 min. An aliquot of 4–5 µg of plasmid DNA (Recombinant vector pP_Δ_MRE11_PIP) was added to the cells, and the mixture was incubated for 1 h on ice. The heat shock step was carried out at 85 °C for 10 min and was followed by an incubation of 10 min on ice. Finally, the transformants were used to inoculate 20 mL of fresh TRM medium supplemented with sulfur and incubated at 85 °C for 18 h.

After transformation, the cells that had integrated the plasmid into their chromosome were selected on solid medium (Phytagel (Sigma, 10 g/L) maintains TRM plates in a solid state at 85°C (Pop-in recombination, Figure 37A&B). The cells were harvested by centrifugation (8000xg, 6 min, 4°C), resuspended in 50 µL of fresh TRM before spreading on plates containing simvastatin (final concentration 2,5 µg/mL). The plates were then incubated for five days at 85 °C.

A second step was needed to excise the targeted gene (pop-out recombination, Figure 37C). This counter selection was performed on plates containing TRM, supplemented with 6-MP (final concentration 100 µM). The strains growing on these plates were resistant to 6-MP and sensitive to simvastatin, since the plasmids had been excised. A PCR was performed to examine the mutant.

A. WT *T.barophilus* genome and pP_Δ_MRE11_PIP plasmid

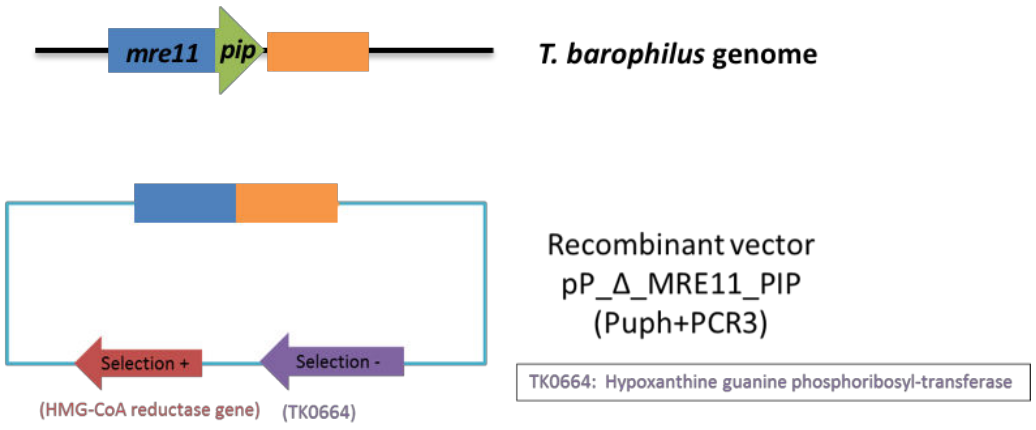

B. *Pop-in recombination*

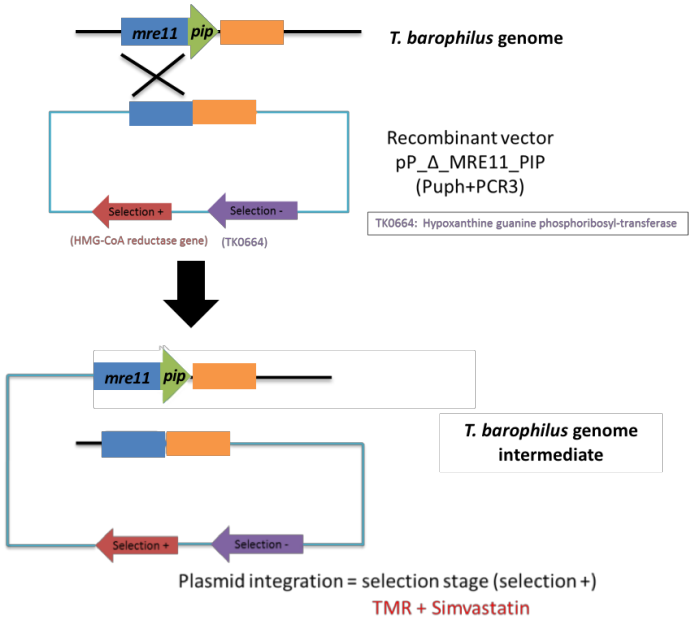

C. *Pop-out recombination*

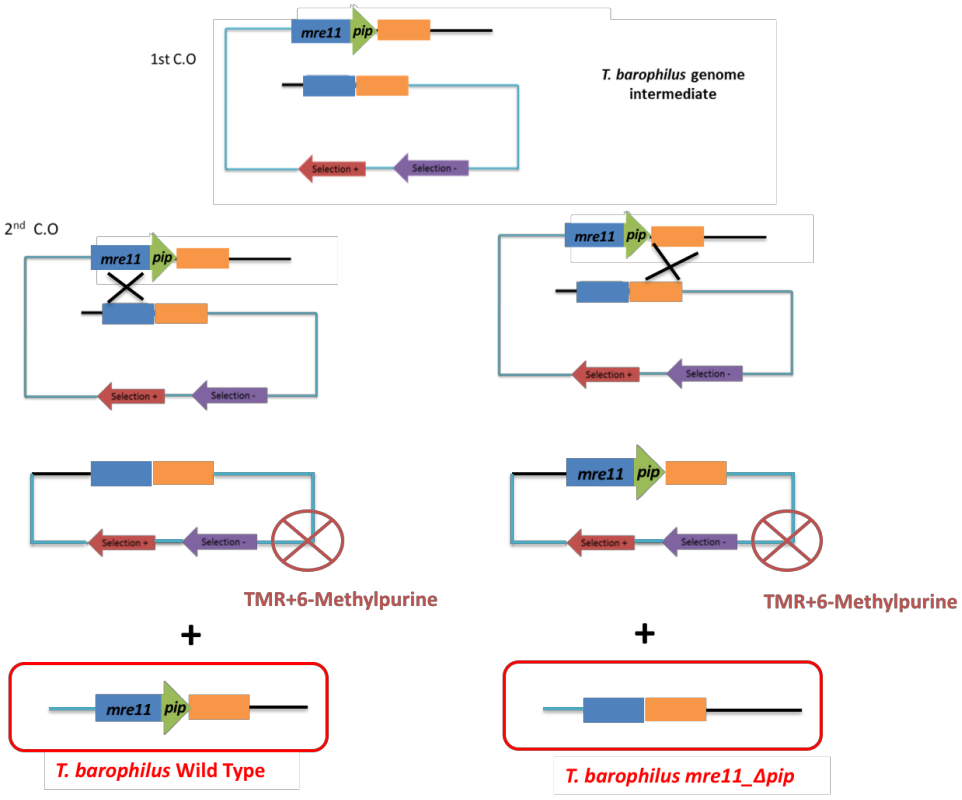

Figure 37 : Schematic deletion diagram of pip motif. (A) Schematic representation of recombinant plasmid pP_Δ_MRE11_PIP and intact genome from *T. barophilus* MP. The recombinant plasmid was constructed by ligation of homologous region (HR) localized in flanking mre11_Δpip and in inside pUPH (B) Recombinant plasmid is used to transform *T. barophilus* MP. The first "pop-in" step is the homologous recombination between plasmid recombination and intact genome from T. barophilus. After the "pop-in", cells containing the integrated plasmid were selected with simvastatin. (C) Intermediated cells were spread on 6-MP to get the second recombination event (pop-out), resulting in plasmid excision. This could lead either to gene deletion or to a WT genotype, depending on the recombination site. Primers "MRE-PIP-Verif-YM_up + MRE-PIP-Verif-YM_Do" and "MRE-PIP-Verif-YM_up + MRE-PIP-Verif-YM_2_Do" were used to validate successful creation of a mutatnt strain.

d) DNA extraction and purification

Plasmid DNA was extracted from an *E. coli* DH5α strain with a plasmid extraction kit "QIAquick Miniprep KIT" supplied by Thermofisher. *E. coli* DH5α cultures (5 ml) at exponential growth phase were harvested after centrifugation (6,000xg, 6 min, 4°C) and then used to extract DNA vectors with a final concentration of 160 to 200 ng/µL.

Genomic DNA extraction of *T. barophilus* was performed using "GeneJET Genomic DNA Purificaiton Kit" (ThermoFisher Illkirch, France). Different colonies from plates were chosen and inoculated in distinct fioles containing 20 mL TRM with sulfur and incubated at 85°C during 24h. Overnight cultures were centrifuged at 8000xg for 8 min. Then, the pellet was suspended in 300 µL of TE (100 mM of Tris-HCl pH8, 50 mM of NaCl, 50 mM of EDTA pH 8). To ensure cell lysis, 40 µL of SDS (10%), 40 µL of Sarkosyl (10%) and 20 µL of proteinase K (20 mg/mL Kit) were added. The cell suspension was incubated for 1 h at 55 °C. Then, 20 µL of RNase A (50 mg/mL, Kit) and 200 µL of lysis buffer (Kit) were added. The mix was incubated for 5-30 min at room temperature, and then put into a purification column (silica-based membrane spin column) and centrifuged at 8000xg for 1 min. Two successive cleaning steps were carried out, with 500 µL of Wash Buffer (with ethanol) and 1 min of centrifugation at 12,000xg. To remove any trace of ethanol, the suspension was centrifuged (12,000xg, 3 min). Then, the column was placed in a clean tube and 200 µL of sterile water used for elution after centrifugation at 8000x g for 1 min.

e) PCR conditions

Mre11_Δpip gene was obtained using *Pfu* polymerase (Promega) for PCR1 or Phusion Polymerase HF (Biolabs) for PCR2 and PCR3. Routine tests by PCR amplification were performed using *Taq* Polymerase (Promega). Different PCR programs are described below:

PCR1: 95°C for 5 min; 30 cycles of 95°C for 50 s, 55°C for 50 s, and 72°C for 2 min 30 s; 72°C for 7 min.

PCR2 /3: 98°C for 30 s; 30 cycles of 98°C for 10 s, 50°C for 30 s, and 72°C for 40 s; 72°C for 7 min.

Routine PCR: 95°C for 10min; 35 cycles of 95°C for 30 s, 53°C for 30 s, and 72°C for 2 min 10 s; 72°C for 7 min

3) Results and discussion

a) Verification of *mre11_Δpip* gene sequence

The amplification of gene *mre11_Δpip* was performed with three PCR (Polymerase chain reaction) reactions from genome of *T. barophilus*. Two pairs of primers designed with KpnI and BamHI specific restriction sequences localized upstream and downstream of PIP motif in *mre11* gene were used in the first time to produce two amplicons with some common sequences. These common sequences will serve as an overlap area to combine two amplicons in the third PCR, in order to generate an about 2000 bp PCR3 product (*mre11_Δpip* gene). The PCR3 product was sequenced (Eurofins Scientific) and did not contain sequencing errors.

b) Construction of the *mre11_Δpip* recombinant plasmid

To verify if the *mre11_Δpip* gene was integrated in plasmid pUPH, enzymatic digestion with BamHI and KpnI was used to cleave free plasmid (pUPH) and recombinant plasmid (pUPH+ gene). After separation by electrophoresis (Figure 38), only one fragment was observed for the digestion of pUPH vector (~ 5000 bp), while two fragments were seen on gel for the digestion of the recombinant plasmid, the smaller band corresponded to the size of the insert (*mre11_Δpip* gene).

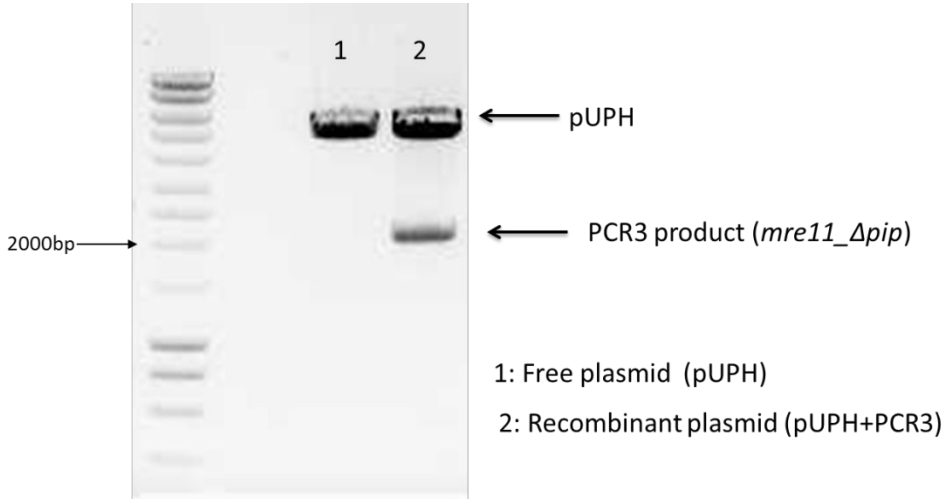

Figure 38 : Gel migration of plasmid pUPH and recombinant plasmid pP_Δ_MRE11_PIP after enzymatic digestion by BamHI and KpnI.

c) Deletion of PIP motif is potentialy essential for viability in *Thermococcus barophilus*

According to biochemical study *in vitro* on interaction between Mre11-rad50 complex and PCNA form hyperthermophilic archaea *Pyrococcus furiosus*, PCNA is capable to stimulate the endonuclease activity of Mre11-rad50 complex *in vitro*. To characterize this interaction further, we sought to determine the function of this interaction *in vivo*.

The PIP motif in *mre11* gene was targeted for deletion in *T. barophilus*, with primers designed (Table 13). Plasmid containing *mre11_Δpip* gene was inserted into plasmid pUPH, then submitted to "*pop-in*" and "*pop-out*" selections. After the counter-selection on 6-MP, 20 clones resistant to 6-MP were isolated. We used two pairs of primers, locating both downstream and upstream of *pip* domain of *mre11* gene (Figure 39, Pair A: blue and orange arrows) or in center of *pip* domain of *mre11* (Pair B: blue and red arrows), to verify the living cells containing or not *pip* motif with PCR (Primes sequences seen in Table 13). With the pair A, we could obtain amplified fragments in WT (*mre11* gene contains always PIP motif) and mutant (*mre11* gene don't contain PIP motif) with a difference size. With the pair B, only chromosome WT can be amplified.

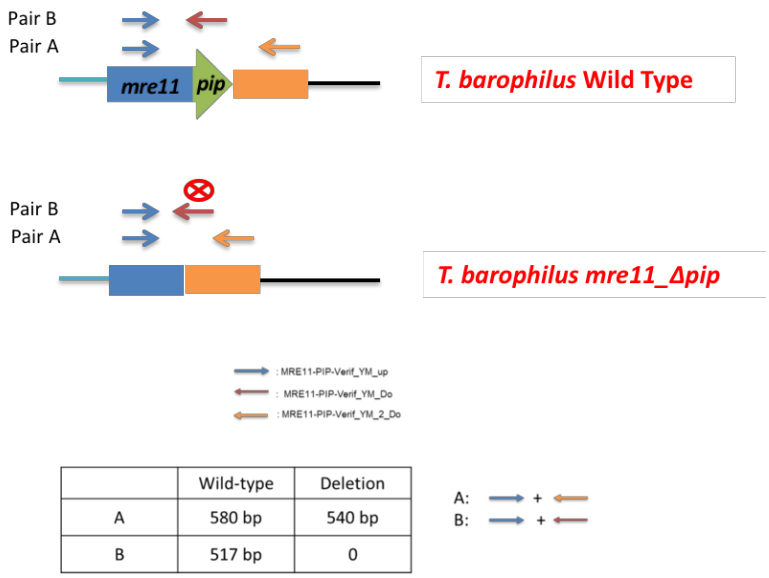

	Wild-type	Deletion
A	580 bp	540 bp
B	517 bp	0

Figure 39 : Schematic representation of verification of pip motif deletion using PCR. 2 pairs of primers used for verification. Pair A: Primer located upstream of pip motif (Blue arrow) + Primer located downstream of pip motif (orange arrow); Pair B: Primer located upstream of pip motif (Blue arrow) + Primer located in center pip motif (orange rouge). Different amplifications with different pairs of primers will be used to differ wild-type strain and gene deletion strain.

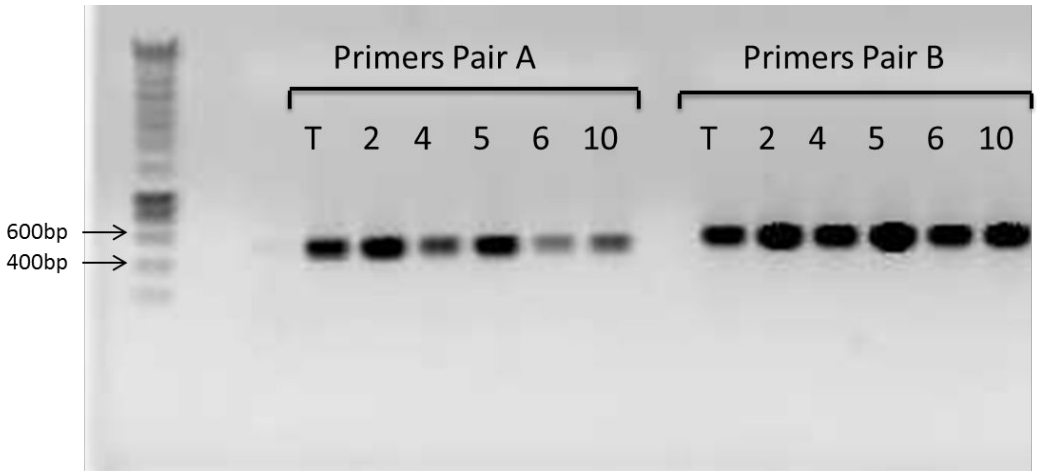

Figure 40 : Example of gel migration of amplification of fragments with Primers Pair A and Pair B. T: genome WT from *T. barophilus*; N° 2,4,5,6,10 corresponded to selected colonies.

Figure 40 show that all the amplified fragments with primers pair A are the same size very close to 600 bp, we cannot conclude whether the genome WT was deleted or not because there is only 40 bp different between genome WT and genome *mre11_Δpip.* However, the result with primers pair B was more evident to interpret. There was an amplification of fragments with primers pair B in all the colonies, that means strains carrying deletion of PIP motif can not grow.

The object of this study was to discover the effect of the interaction between Mre11-rad50 and PCNA *in vivo*.

Preliminary results indicated that the deletion of PIP motif from *mre11* gene in T. barophilus cells is not viable. This apparent essentiality of PIP domain in *mre11* gene was only obtained once and the number of clones tested is not sufficient enough to confidently draw robust conclusions. Due to lack of time, I could not reiterate these experiments and that the reason why we did not incorporate this genetic part in the published paper.

This is yet an interesting result that might emphasize the biological importance of the association between PCNA and MR complex for HR pathway. This result is to be brought closer to the observation that, at physiological ionic strength, MR complex seems to be inactive at stoichiometric condition with DNA substrate and needs association with PCNA to be activated. In other words, this could reflect a particular type of regulation for DNA enzymes driven by the association with PCNA recruitment platform at high intracellular salt concentration. It is well known that some hyperthermophilic archaea contain strikingly high intracellular potassium ion concentrations (Scholz *et al*, 1992). In addition, the same phenomena of activation of DNA enzymes upon association with PCNA at high salt concentration as already been described for archaeal thermosable DNA ligases (Sriskanda *et al*, 2000; Rolland *et al*, 2004). In this regard, Kiyonari and collaborators reported that: "*Each protein involved in DNA replication and repair has to work at a certain time in the successive processes at the appropriate site. To control the specific timing and the position for each related protein factor to access the target DNA in vivo, the salt concentration, which prevents nonspecific binding of protein factors in the cells, is especially important, and in the case of replication fork progression, for example, PCNA probably functions as a platform to control the order and the sites of interacting proteins involved in this successive reaction process*" (Kiyonari *et al*, 2006). It is thus tempting to speculate that hyperthermostable archaea might have evolved a regulation mechanism based on recruitment and activation of DNA enzymes by PCNA on specific DNA structures under physiological ionic conditions. This may also explain why we mainly found occurences of PIP-like motif on thermococcales Mre11 proteins. However, up to now, it has never

been reported any preferential binding of archaeal PCNA onto physiological DNA substrates for Mre11 or DNA ligase.

Chapter 2: Primase & RadA

I. Presentation of studied proteins

1) Primase

2) RadA

II. Hypotheses for biological functions of primase/recombinase association

III. Materials & methods

IV. Results and discussion

1) Protein purification

2) Biochemical characterization

3) Could RadA help Primase to perform TLS

4) Which DNA polymerase promotes DNA synthesis from strand invasion intermediates of HR

The last year of my PhD was devoted to the study of an intriguing association, detected in the interaction network, revealed in the laboratory by Pierre-Francois Pluchon and collaborators (Pluchon *et al*, 2013), concerning the catalytic subunit p41 of DNA primase recombinase RadA, its modulator RadB and DNA ligase (Figure 41). RadA is a recombinase that is essential for homologous recombination, so that its interaction with DNA primase and DNA ligase raises the possibility that these two proteins could also be implicated in recombinational repair of DNA double-strand breaks. In support to this hypothesis, the primase from *S. solfatarucus* was shown to be able to realize a template-dependent polymerization across discontinuous DNA templates (Hu *et al*, 2012). This property is indeed relevant to a potential implication in recombinational repair pathway. Due to lack of time, I could not achieve a complete functional characterization of this potential complex in order to propose a role or at least to target a pathway in which this complex could be involved. However, I started to set up production and purification of RadA as well as recombinase assays. Protocols for production and purification of DNA primase holoenzyme and p41 subunit were already available in the laboratory. Thereby I could have the recombinant proteins at my disposal to initiate the study of this complex, concentrating first on RadA and DNA primase. In the next sections, I will first introduce the current knowledge on functions of RadA and primase. Then I will argue for the hypothesis regarding the potential biological implication of this complex before presenting the preliminary data obtained.

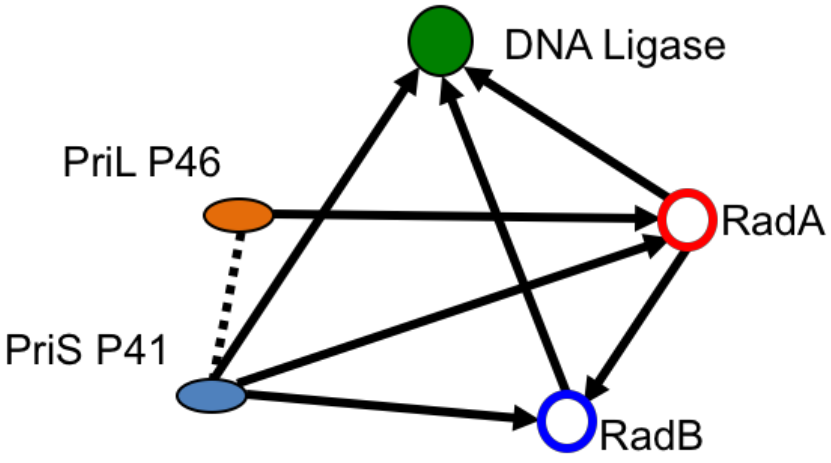

Figure 41 : Protein interaction cluster linking DNA primase, DNA igase and recombinase RadA and RadB from *Pyrococcus abyssi* (Pluchon *et al*, 2013). Each protein indicated here was used as a bait in pull-down/MS experiments. Black arrows point out the partners found after MS identification. The significance ratio gave confident scores even with sample treated by nuclease.

I. Presentation of studied proteins

1) Primase

Several studies have shown that genes encoding the primase in archaea are essential for cell viability (Berquist *et al*, 2007; Le Breton *et al*, 2007; Sarmiento *et al*, 2013; Liu *et al*, 2015), as well as for its bacterial (Kobayashi *et al*, 2003) and eukaroytic homologs (Arezi & Kuchta, 2000). Hence, DNA primase is an important player in replication.

During DNA replication, *de novo* DNA synthesis of DNA strand cannot be initiated by polymerase, DNA primase is required and capable of the synthesis of a short RNA, as a primer on template DNA, which is subsequently extended by DNA polymerase (Figure 42) (Frick & Richardson, 2001).

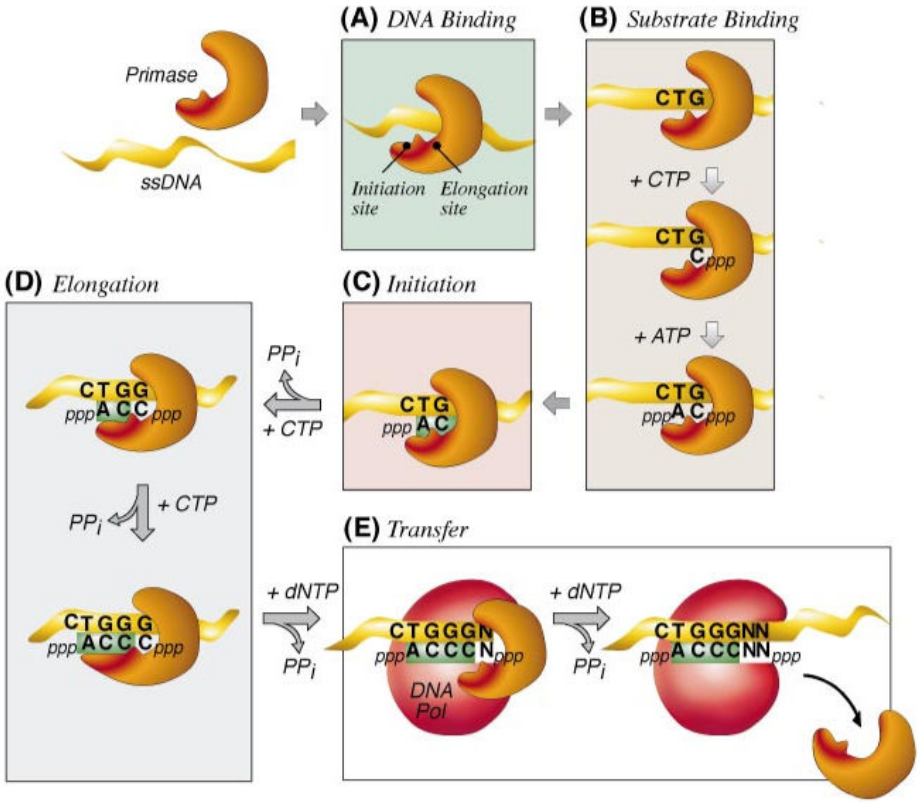

Figure 42 : Synthesis of primer by Primase (Frick & Richardson, 2001). Example of primer synthesis by T7 primase. DNA primase (orange) binds to ssDNA template (yellow) (A), then two NTP (ribonucleotide) substrates bind to the elongation site and the initiation site (B) to catalyze the formation of a dinucleotide and inorganic pyrophosphate (C). The growing oligonucleotide is transferred to the initiation site while addinitional NTPs bind to the elongation site and is ncorporated at the 3'end of the pirmer (D). Finally, primer RNA is transferred to the replicative DNA polymerase which adds deoxyribonucleotides (dNTPs) to their 3'ends.

DNA primase is an essential component of the DNA replication, this specialized DNA-dependent RNA polymerase is conserved in the all kingdoms of life. DNA primases belong to two distincts protein families: DnaG type and AEPs (Archaeo-eukaryotic primases). All of DNA primase in Bacteria are single subunit protein, termed DnaG, which binds to the DNA helicase, to form a complex called the primosome. Bacterial primases are activated by helicase and synthetis an RNA primer. In *E. coli*, one primer (10-12 nucleotides) is synthetized every second, and around 2000 to 3000 primers are synthetized (Keck *et al*, 2000; Frick & Richardson, 2001). AEPs are structurally distinct from the bacterial DnaG primases, in both Eukaryote and Archaea, and constitute a two-subunit primase, that means the AEPs typically consists of a small catalytic subunit (PriS) and a large regulatory subunit (PriL). In eukaryotes, the PriS-PriL primase complex is associated with DNA polymerase α and its accessory B subunit, to form a heterodimeric enzyme: DNA polymerase α-primase complex. In this complex, the primase catalytic subunit (PriS) is able to synthetize a short RNA primer approximately from 8 to 12 nt, which is elongated by Polα to about 30 nt to form the pre-Okazaki fragement (Frick & Richardson, 2001; Grabowski & Kelman, 2003). The first archaeal primase was identified from *Methanococcus jannaschii*, which has a sequence similar to eukaryotic primase-like subunit p48 (Desogus *et al*, 1999). Later, proteins (p41 and p46) with homology to the eukaryal PriS and PriL subunits were found in several *Pyrococcus* species (Bocquier *et al*, 2001; Liu *et al*, 2001; Matsui *et al*, 2003; Ito *et al*, 2007; Le Breton *et al*, 2007), as well as in other Euryarchaeota *Thermococcus kadakaraensis* (Chemnitz Galal *et al*, 2012) and *Archaeoglobus fulgidus* (Jozwiakowski *et al*, 2015), and in Crenarchaeote *Sulfolobus solfataricus* (Lao-Sirieix & Bell, 2004; Lao-Sirieix *et al*, 2005b). Recently, a third primase subunit was identified in archaeon *Sulfolobus solfatarcus*, called “PriX”, which is essential for primer synthesis (Liu *et al*, 2015). Moreover, primase exists also in virus *Bacteriophage T4*, called gp46, and also coupled with a helicase gp41 in order to optimize its activity (Frick & Richardson, 2001) (Table 14).

Table 14 : Example of architecture of primase from the three domains of life (study from (Lao-Sirieix *et al*, 2005b; Rowen & Kornberg, 1978; Holzer *et al*, 2017)

	Eukaryotes		Archaea		Bacteria
	Human	*S.cerevisiae*	Sulfolobus	Pyrococcus	*E.coli*
Pol α	p165	Pol1 (180 kDa)	-	-	-
B subunit	p77	Pol12 (79 kDa)	-	-	-
Small Primase	p50	Pri1 (48 kDa)	PriS (38 kDa)	*Pfu*p41 (41 kDa)	DnaG (60 kDa)
Large Primase	P59	Pri2 (58 kDa)	PriL (36 kDa)	*Pfu*p46 (46 kDa)	
Third subunit			PriX		

These p41-p46 (PriS-PriL) complexes are called “classic archaeal DNA primases” and exist in most archaea (Figure 43A). A conserved Fe-S cluster-binding domain is identified in PriL subunit, which modulates the activity of primase in archaea, and the PriS contains an N-terminal catalytic domain with a conserved motif, that plays its primase function. Another form of archaeal DNA Primase has been described, called “fused archaeal DNA Primases”. This type of primase contains a single gene encoding a fused PriS/PriL. In other words, this short atypical primase consists in a fusion of the catalytic domain of PriS and the Fe-S cluster-binding domain of PriL (Figure 43B) (Raymann *et al*, 2014). Fused archaeal DNA primase are has been found in *Nanoarchaeum equitans* (Iyer *et al*, 2005), in Nanoarchaeote Nst1 (Podar *et al*, 2013) and in an uncultured nanoarchaeon (Rinke *et al*, 2013). Whereas, in 2014, Gill *et al,* have identified a similar fused primase encoded by pTN2 plasmid from the hyperthermophilic archaeon *Thermococcus nautili,* named “PolpTN$_2$”, that is without sequence similarity with the primases found in nanosized archaea. This archaeal primase PolpTN$_2$ harbors both primase and DNA polymerase activity thanks to a fusion of domains homologous of two subunits (Soler *et al*, 2010; Gill *et al*, 2014).

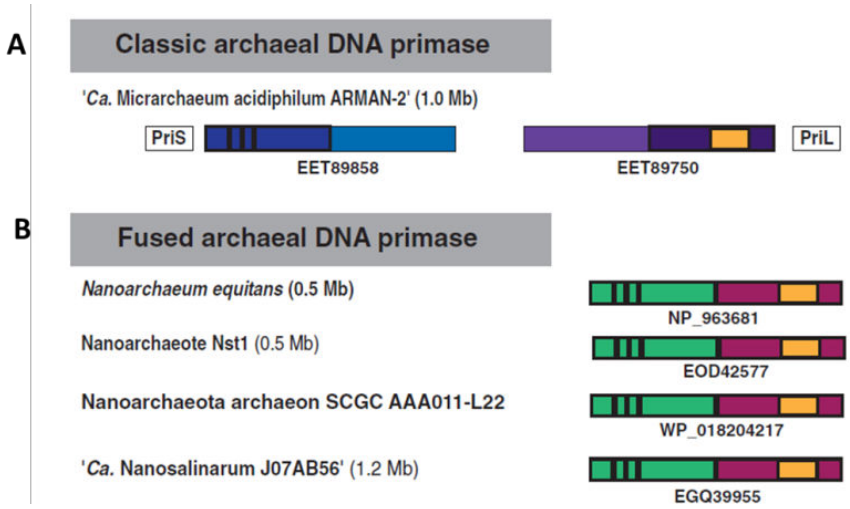

Figure 43 : Schematic representation of two types of archaeal primase (Raymann *et al*, 2014). (A) Classic archaeal DNA primase, consisting of two subunits PriS and PriL. (B) Fused archaeal DNA primase, containing a fused primase which are found in some nanosized lineages. Conserved motif in N-terminal catalytic domain in PriS subunit is represented in black bars, and Fe-S cluster-binding domain in PriL subunit is represented with yellow box. “Ca.” is shorter for “*Candidatus*”.

The crystal structure of the catalytic subunit (p41) from *P. furiosus* has been reported (Figure 44). The small subunit p41 of *Pfu*Primase is a two-domain structure: a large primase domain, which contains the catalytic part with conserved residues within eukaryote and archaea (Figure 44, right) and Zinc-finger motif (indicated in blue); and a small helical domain (indicated in red) which has a species-specific fold, highly variable in length and sequence (Augustin *et al*, 2001; Lao-Sirieix *et al*, 2005b). The role of Zinc-finger motif in archaeal primase is not clear, but Zinc-finger motifs of DNA primase of bacteriophage T7 and bacteria *Bacillus* are responsible for template or single-stranded DNA recognition and binding (Kusakabe *et al*, 1999; Pan & Wigley, 2000). Moreover, Lao-Sirieix and his group have shown that mutant *Sso*Primase lacking PriS-Zn had always a high activity that could synthetize shorter products compared with the wild-type enzyme (Lao-Sirieix *et al*, 2005a). Thus, it was proposed that Zinc motif of archaeal primase possibly has a similar role that allows the interaction of the primase with the DNA template (Lao-Sirieix *et al*, 2005a).

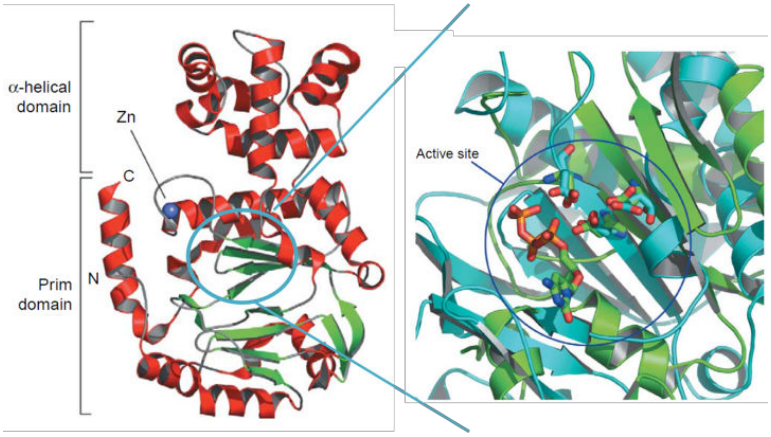

Figure 44 : Structure of the small subunit (PriS) from archaea (Lao-Sirieix *et al*, 2005b). Cystallographic sturcture for the catalytic subunit of *P. furiosus* primase (PDB: 1G71) **(Augustin *et al*, 2001)** , and closed view of position of active site residues for the *P. horikoshii* primase (PDB: 1V33) **(Ito *et al*, 2003)**.

The archaeal large subunit (p46) is composed of two structural domains, the N-terminus (PriL^{NTD}), which is able to interact with PriS, and the C-terminus (PriL^{CTD}), which has an ssDNA binding function. The crystal structure of PriL^{NTD} alone from *P. horikoshii* (Figure 45A) and a complex of the PriL^{NTD} and PriS from *S .solfataricus* (Figure 45B) have been determined. As shown in Figure 47A, the PriL^{NTD} consists of two subdomains, SD1 (blue part) and SD2 (yellow part). SD1 subdomain is named also as "PriL^{NTD}-α", because this is an entirely α-helical domain. It is suggested that this PriL^{NTD}-α domain in *S .solfataricus* might be implicated in the DNA-dependent RNA synthesis mechanism. While SD2 in PriL^{NTD} is responsible for mediating the PriS binding, that's why it is called also "PriL^{NTD}-SBD" (Figure 45B). This PriS-PriL interface is conserved in eukaryotic primases (Ito *et al*, 2007; Lao-Sirieix *et al*, 2005a). PriS from *P. horikoshii* alone do not have an efficient primer synthesis activity, *Pho*PriS-PriL complex is required, suggesting that PriL^{NTD} serves as an arm that links catalytic subunit PriS to the DNA binding domain located at PriL^{CTD} (Matsui *et al*, 2003; Ito *et al*, 2007). The PriL^{CTD} is found at the C-terminal end of the *S. solfataricus* but is absent from the *Pyrococcus* proteins (Lao-Sirieix *et al*, 2005a). The role of PriL^{CTD} is unclear but it has been suggested that this may play a role maintaining structure that forms the stem of the zinc-binding motif (Lao-Sirieix *et al*, 2005a). In 2007, Klinge and his colleagues have shown that *Sso*PriL^{CTD} contains an iron-sulfur domain which is essential for RNA primer synthesis. However, 10 years later, Holzer et *al* have revealed that the Fe-S cluster is not required for primer synthesis (Holzer *et al*, 2017). The role of this Fe-S domain in maintaining the correct 3D structure of PriL^{CTD} has been demonstrated in Eukaryote (Pellegrini, 2012).

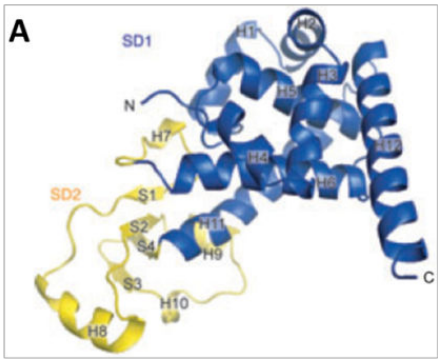

Subunit p46 (PriL^{NTD}) from *Pyrococcus horikoshii*

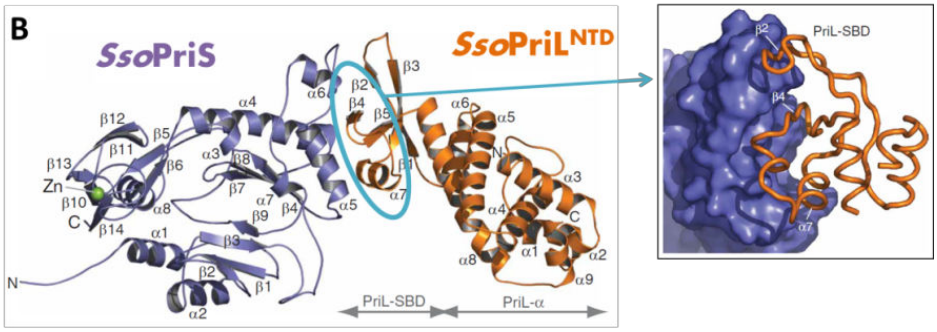

Complex PriL^{NTD}-PriS from *Sulfolobus solfataricus*

Figure 45 : Structure of the large subunit (PriL) and complex PriL-PriS from Archaea. (A) Subunit PriL^{NTD} from *Pyrococcus horikoshii* (PDB: 2DLA). Subdomain SD1 is indicated in blue and SD2 is indicated in yellow **(Ito *et al*, 2007)**. (B) Complex PriL^{NTD}-PriS from *Sulfolubus solfataricus* (PDB: 1ZT2). Purple: small subunit; orange: large subunit; green sphere: zinc atom. For PriL-SBD closed view, Purple molecular surface: PriS; orange tube: PriL-SBD **(Lao-Sirieix *et al*, 2005a)**.

Taken together, a mechanism of DNA-dependent RNA primer synthesis by archaeal primase has been proposed (Figure 46). In this model, the 5'end of DNA template (lagging strand) is recognized by PriS-Zn domain, which is near the Prim domain for the subsequent polymerization, whereas the 3'end of DNA template is recognized by PriL^{CTD}, in the direction of the replication fork. This model suggests that the DNA-RNA helix is positioned toward the PriL, and its phosphate backbones interact with two solvent-exposed arginines (Arg84 and Arg 85). The double mutation of these two arginines causes a reduction in the both size and amount of RNA product. Therefore, the interactions between RNA primer and PriL is possibly used to adjust the length of RNA primer to a 7-14 nt (Lao-Sirieix *et al*, 2005a).

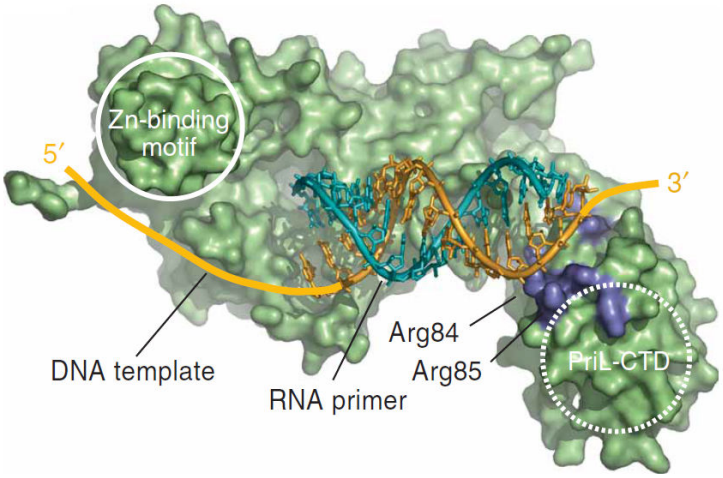

Figure 46 : Model of the core Primase-DNA template-RNA primer complex in Archaea (Lao-Sirieix *et al*, 2005a). The *Sso*PriS-PriL complex is represented as a molecular surface (in green). The phosphate backbones of DNA and RNA are orange and cyan tubes, and the position of PriS-Zn and putative position PriL^{CTD} are indicated by white circle, respectively. The position of residues Arg84 and Arg85 within PriL are indicated in purple.

In addition to RNA primer synthesis activity during replication of the chromosome; AEPs may have additional functions in the DNA/plasmid replication, in DNA double-strand break repair and in DNA damage tolerance.

- AEPs involved in DNA/plasmid replication

DNA primase from eukaryote and bacteria can utilize only ribonucleotides (rNTPs) to form RNA primer. In contrast, *in vitro* studies with p41 subunit or the p41-p46 complex from *Pyrococcus furiosus* have demonstrated that this archaeal primase had the ability to synthesize both DNA and RNA primers. Indeed, p41 subunit alone preferentially utilizes deoxyribonucleotides (dNTPs) to synthesize long DNA fragments (~7 kb), but in combination with p46 subunit, DNA polymerase activity is reduced, and RNA polymerase activity is increased with short length fragments (Liu *et al*, 2001).

Furthermore, some archaea have extra-chromosomal plasmids that encodes additional AEPs. These AEPs are possibly playing a role in both the initiation and replication of these small circular plasmids. For example, enzyme ORF904 encoded by plasmid of *Sulfolubus islandicus*. The crystal structure of the N-terminal domain of ORF904 shows that it is strongly similar to *Pyrococcus* archaeal primase, so we call this N-terminal domain as “AEP domain”. The study has demonstrated that ORF904 has both DNA-dependent DNA/RNA primase and DNA polymerase activity. Similar to p41 subunit of archaeal DNA primase, ORF904 preferentially generates DNA primers and could extend these primers until several thousand nucleotides in length (Iyer *et al*, 2005; Lipps *et al*, 2003; Beck & Lipps, 2007). Moreover, another primase/helicase has been identified from an integrated prophage in bacteria *Bacillus cereus* genome, termed *Bc*MCM. The N-terminal domain of *Bc*MCM is weakly similar to AEPs, but it harbors Primase and DNA-dependent DNA polymerase activities (McGeoch & Bell, 2005; Samuels *et al*, 2009; Sanchez-Berrondo *et al*, 2012).

- AEPs involved in DNA repair

Several studies have demonstrated that AEP genes coding enzymes are frequently involved in DNA double-strand breaks repair through NHEJ pathway in co-operating with protein Ku (a protein implicated in binding to the ends of DSBs) in bacteria. It was shown that in mycobacteria, the Ligase D (LigD) is a fusion protein composed of AEPs (large domain), nuclease and ligase domains. It is capable of primase activity, and is involved in NHEJ DNA repair in complex with Ku (Aravind & Koonin, 2001; Koonin *et al*, 2000; Weller & Doherty, 2001; Doherty *et al*, 2001). Recently, this AEPs related DSB repair mechanism has been discovered in mesophilic archaeon, *Methanocella paludicola* (*Mpa*), named Archaeo-Prokaryotic (AP) NHEJ model (Bartlett *et al*, 2013). Bartlett group has identifed that *Mpa* DNA Polymerase (*Mpa*Pol) contains three key conserved AEP catalytic motifs and is capable of incorporating either dNTPs or NTPs, even preferentially insert NTPs rather than dNTPs onto a DNA primer strand. In the model, *Mpa*Pol incorporated ribonulcleotides in to gaps and displace annealed bases followed by recruitement by *Mpa*Ku (Figure 47) (Bartlett *et al*, 2013, 2016).

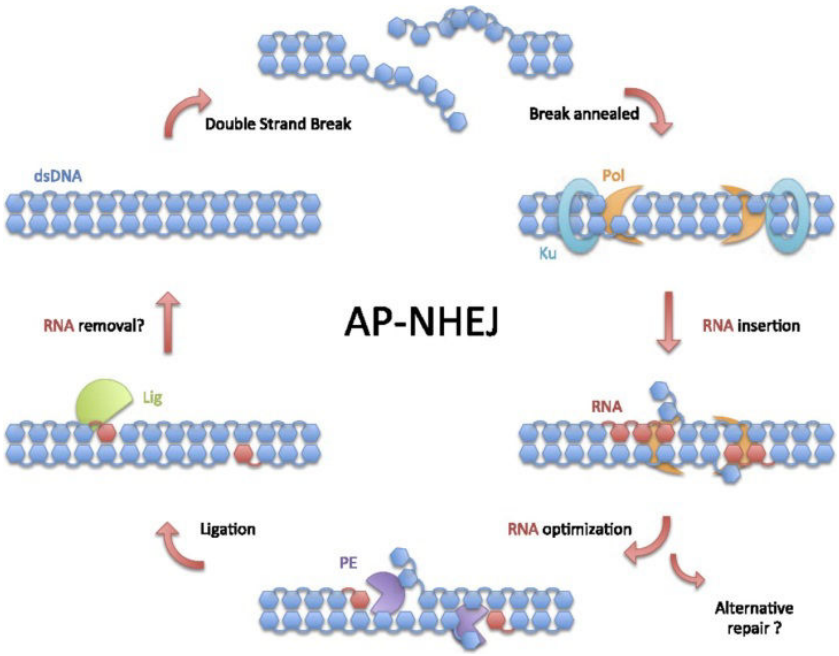

Figure 47 : Model of AP-NHEJ in archaeon *M. paludicola* (Bartlett *et al*, 2013). Ku and Pol proteins initially bind broken ends and promote to anneal the break. Pol fills in any resulting gaps by a template-dependent RNA synthesis and may displace several bases of downstream DNA. Strand-displacement RNA synthesis by Pol is regulated by PE, which can remove unnecessary NMPs and allow the displace DNA to realign with the template. Lig is finally required for seal the nicked substrate.

In addition to DNA DSBs repair by NHEJ, archaeal primase is suggested to be involved in other DNA repair mechanisms thanks to the structural similarity between small subunit of primase and the X family of DNA polymerases. This family encompasses specialized DNA polymerases involved in repair mechanisms like Terminal Transferase and DNA polymerase β, λ and μ (Yamtich & Sweasy, 2010). For example, the structure of *Sso*PriS is similar to the catalytic mechanism of DNA Polymerase X and accordingly the terminal transferase activity (template-independent addition of nucleotides to the 3'end of a DNA strand) was detected in *Sso*Primase (Lao-Sirieix & Bell, 2004; De Falco *et al*, 2004; Hu *et al*, 2012). This terminal transferase activity has been found also in bacterial LigD and archaeal primase PolpTN$_2$ (Keen *et al*, 2014; Lao-Sirieix *et al*, 2005b; Sanchez-Berrondo *et al*, 2012; Gill *et al*, 2014). It was suggesting that the terminal transferase activity was important for several DNA repair mechanism such as MMEJ (microhomology-mediated end joining), in which terminal transferase adds some nucleotides in the end of ssDNA and promotes the association of the two 3'-protruding ends containing a micro-homology base pair (Hu *et al*, 2012; Gouge *et al*, 2015).

In addition, Le Breton et *al* have shown that *Pab*Primase displays gap-filling and strand-displacement activities, as do polymerases β and λ in DNA repair, suggesting that *Pab*Primase could fulfill the role of the DNA Polymerase X which has not been detected in *Pyrococcus* genome (Le Breton *et al*, 2007; Ramadan *et al*, 2004).

- AEPs involved in DNA damage tolerance

Eukayotic cells possess several DNA translesion synthesis (TLS) polymerases (Prakash *et al*, 2005). In 2013, a new primase in human cells has been described, termed PrimPol (García-Gómez *et al*, 2013). It is a competent trans-lesion synthesis DNA polymerase that can bypass a number of replicase-blocking DNA lesions, such as 8-oxo-guaninine, deoxyruacile (García-Gómez *et al*, 2013; Bianchi *et al*, 2013; Keen *et al*, 2014; Stojkovič *et al*, 2016), but does not bypass lesion with AP site (Bianchi *et al*, 2013; Keen *et al*, 2014; Stojkovič *et al*, 2016). Additionally, DNA repriming activity by PrimPol was detected in 2016, it is critical for DNA replication restart downstream of lesions (Kobayashi *et al*, 2016)

In contrast to eukaryotes which possess specialized polymerases that allow DNA lesion bypass, most of archaea lack this type of polymerase that performs TLS (Kelman & White, 2005). However, the PriS or PriS/L of archaeal primase from *A. fulgidus* and the primase holoenzyme PriS/L of *P. furiosus* are capable of traversing blocking DNA lesions induced by UV, such as 8-oxo-dG and templating uracil bases, but are strongly blocked by AP site (Jozwiakowski *et al*, 2015). Although not confirmed by genetic analyses, archaeal primase could hence be involved in tolerance to DNA damage and in genome instability maintenance (participating in replication fork process maintaining).

Finally, the different enzymatic activities associated with AEP members (Primase or AEP-like molecules) and its biological functions are summarized in table 15. From the summary table, we found that the archaeal primase could be a promiscuous primase, suggesting that it might have crucial role not only in DNA replication, but also in DNA repair in the Archaea, as already reported (Lao et *al.,* 2005b)

Table 15: Summary of enzymatic activities of AEPs and its biological functions in 3 domains of life

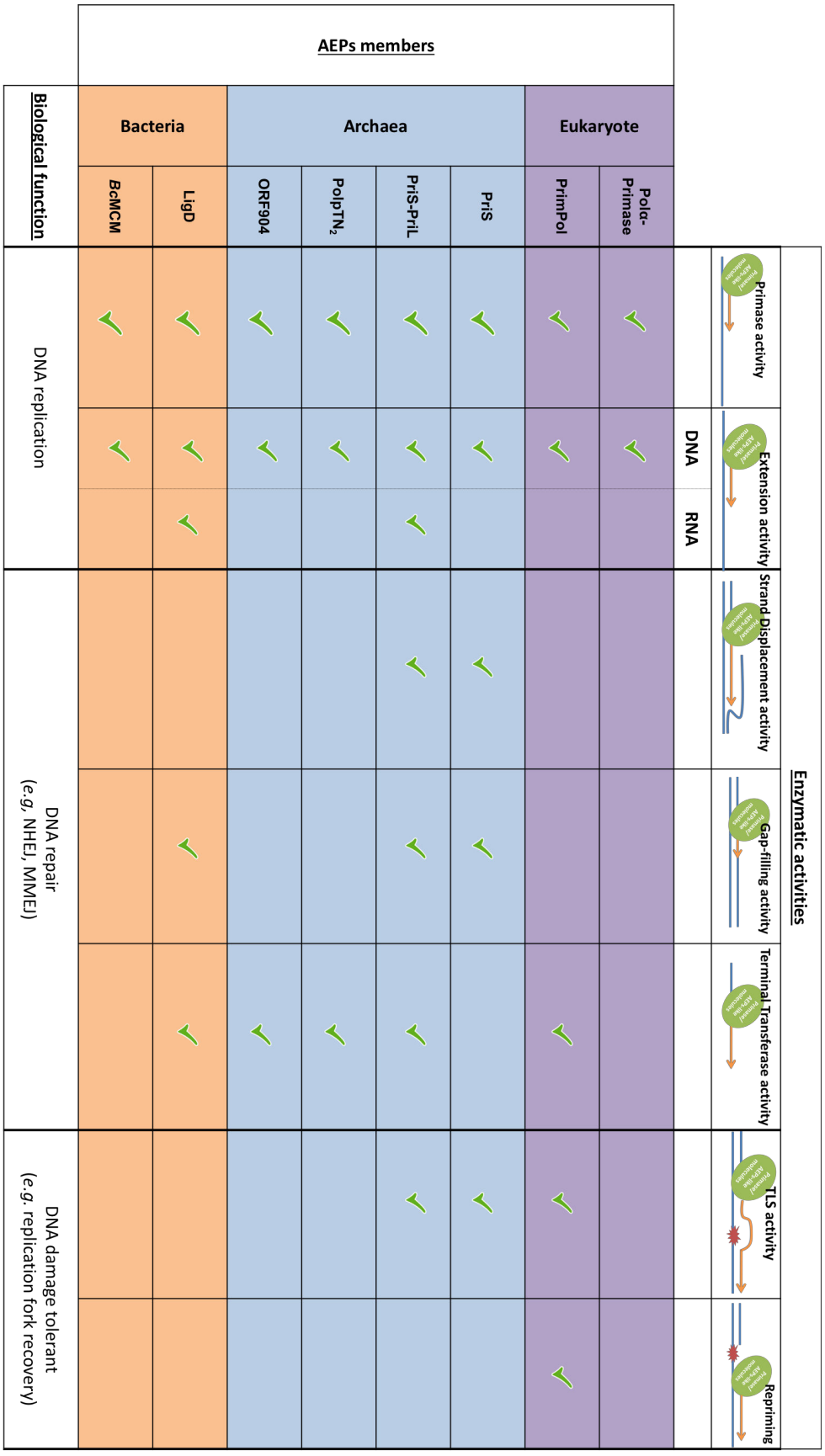

2) RadA

As mentioned, homologous recombination (HR) is an essential mechanism involved in repairing double-strand DNA breaks, the restart of stalled replication forks and maybe the initiation of replication. The central step of HR is homologous base-paring and strand exchange, which are catalyzed by RecA-family recombinases: Rad51/Dmc1 in Eukaryote, RecA in Bacteria and RadA in Archaea. Since the first discovery of RecA from *E. coli* in 1965, the studies of deletion of recombinase genes have shown an HR defect and an increased sensitivity to DNA-damaging agents (like UV irradiation) (Clark & Margulies, 1965; Woods & Dyall-Smith, 1997). *In vivo*, an accumultation of Rad51 at nuclear foci in dividing cells before or after exposure to DNA-damaging agents was observed (Pellegrini *et al*, 2002).

- Structure of archaeal RadA

RecA-family recombinases are conserved in the 3 domains of life. RadA from *Pyrococcus furiosus* consists of two domains: a small N-termnial domain (NTD), which is conserved in eukaryote and archaea, but not in bacterial; a large C-terminal domain, also called “ATPase domain (AD)”, which is a core domain conserved in Eukaryote, Archaea and Bacteria (Figure 48A) (Shin *et al*, 2003).

NTD domain of *Pfu*RadA possesses helix-hairpin-helix (HhH motif, which is responsible for DNA phosphate backbone binding (blue box)). The AD of *Pfu*RadA has the Walker A and B motifs (dark green), which are required for ATP binding and hydrolysis, and DNA-binding domains Loop1 (yellow) and Loop2 (light purple). Polymerization motif (PM) (dark purple) is located between the NTD and the core ATPase domain, a key linker for tethering individual two domains together and mediating filament formation. The crystal structure of PfuRadA is represented in Figure 49B. A hydrophobic amino acid “phenylalanine” (Phe) in RadA, Rad51 and DMC1; or “isoleucine” (Ala) in RecA from PM is crucial for its subunits contact, the mutation of this hydrophibic residue can cause an abolished filament formation (Pellegrini *et al*, 2002; Shin *et al*, 2003).

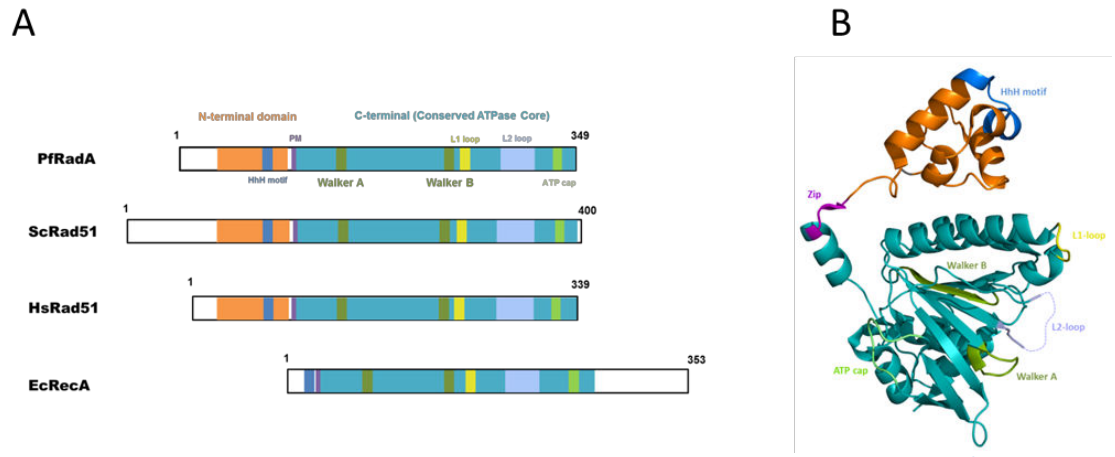

Figure 48 : Organization of the the RecA family protein sequence and crystal structure of *Pfu*RadA (adapted from (Shin *et al*, 2003; Wu *et al*, 2004)). (A) Conserved structure of RadA homolologs from *P. furiosus* (PfRadA), *S. cerevisiae* (ScRad51), *H. sapiens* (HsRad51) and *E. coli (*EcRecA). N-terminal domain and ATPase domain are colored orange and cyan, respectively. HhH motif is in blue, PM motif is in dark purple, Walk A and B motif are in dark green, loop1 is in yellow, loop2 is in light purple and ATP cap is light green. (B) Cystal structure of RadA from *Pyrococcus furiosus* (PDB: 1PNZ). The main motifs are colored in the same manner as in caption left.

In solution, without DNA, *Pfu*RadA proteins stay in heptameric ring structure, and can be assembled as dimer of heptamers (Figure 49A) (Shin *et al*, 2003; Komori *et al*, 2000b). In presence of DNA, *Pfu*RadA is able to form a helical filament on ssDNA (normally one monomer for three nucleotides, as observed for both bacterial RecA and eukaryotic Rad51 proteins) (Figure 49B) (Seitz *et al*, 1998; Shin *et al*, 2003; Komori *et al*, 2000b). The helical filament formed by archaeal RadA proteins are mainly right-handed with 3-6 monomers per helical turn in the presence of DNA, but archaeal *Sso*RadA can form also left-handed filament with four monomers per helical turn without DNA (Chen *et al*, 2007a). *Sso*RadA was reported as octamers in the solution without DNA and nucleotide cofactor (Figure 50A). Surprisingly, in addition to helical filament formation on ssDNA, *Sso*RadA can also bind to circular ssDNA in the absence of nucleotide cofactor as octameric rings (Figure 50C). Furthermore, *Sso*RadA can form an extended helical filaments on dsDNA in the presence of ATP (Figure 50B), and a compressed helical filaments in the presence of ATPγs (Figure 50D) (Yang *et al*, 2001b).

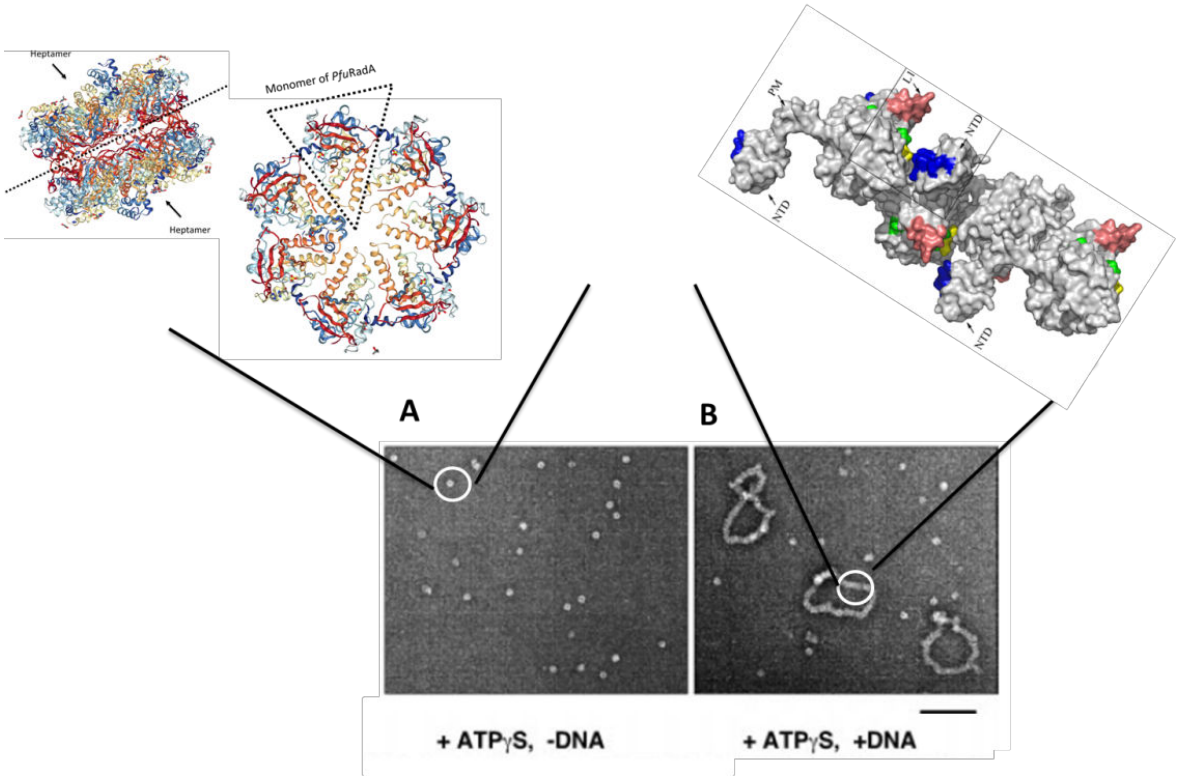

Figure 49 : Electron micrographs of archaeal RadA in different states and its crystal structure (study from **(Chen *et al*, 2007b; Komori *et al*, 2000b; Shin *et al*, 2003)**. (A) In the absence of DNA, PfuRadA is a bi-heptameric ring structure (consisting of 7 monomers) (PDB: 1PZN). (B) In the presence of DNA, PfuRadA proteins bind to ssDNA and form nucleoprotein filament. The crystal structure of nucleoprotein filament is modeled with SsoRadA.

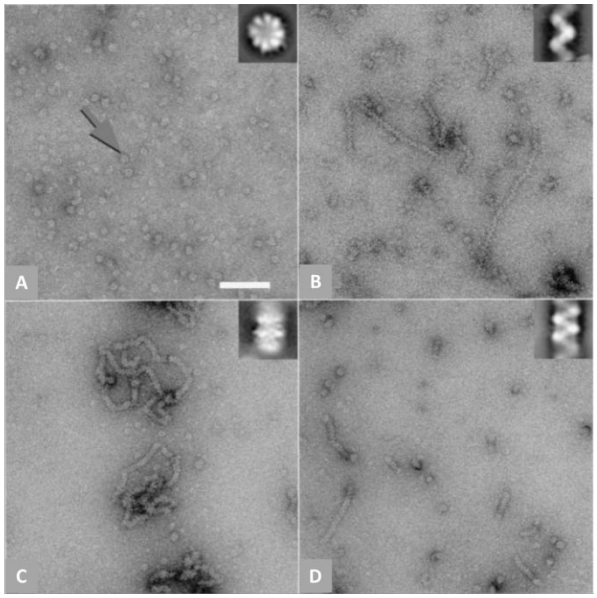

Figure 50 : Electron micrographs of different states of the RadA protein (Yang *et al*, 2001b). (A) Octameric ring state in the absence of DNA and nucleotide cofactor; (B) extended helical filaments on dsDNA in the presence of ATP and aluminum fluoride; (C) rings bound to circular ssDNA molecules in the absence of nucleotide cofactor; (D) compressed helical filaments on dsDNA in the presence of ATPγS.

- RecA family protein-mediated strand exchange

Typically, the strand exchange by RecA family proteins in HR is realized in three phases (Figure 51):

1) Presynaptic phase. Earlier in this phase, RecA family proteins load onto ssDNA to form filament as nucleation (4-5 recombinase proteins) with gaps between different clusters. Even if nucleation does not need ATP hydrolysis, ATP binding could stabilize the interaction with DNA. And then the recombinase filament extension is due to additional RecA to cover DNA (Holthausen *et al*, 2010; van der Heijden *et al*, 2007; van Loenhout *et al*, 2009). This extended filament facilitates the homologous alignment of two DNA molecules and the strand exchange in the following step (Chen *et al*, 2008; Klapstein *et al*, 2004).

2) Synaptic phase. All RecA family proteins possess DNA-dependent ATPase activities. They catalyze ATP-dependent DNA pairing and strand exchange between homologous DNA molecules (Sigurdsson *et al*, 2001; Chi *et al*, 2006; Seitz *et al*, 1998; Komori *et al*, 2000b). In the first time, the presynaptic helical filament bind to duplex DNA to from synaptic complex (three-stranded intermediate), then the ssDNA invades into the homologous region of duplex DNA to form a DNA joint (also called Displacement loop, or D-Loop) and here, RadA-dsDNA filaments are formed, and finally effect strand exchange (Chi *et al*, 2006; Sung & Klein, 2006; Sung *et al*, 2003). Several studies in both bacterial RecA and eukaryotic Rad51 have shown that homologous pairing and strand exchange function upon ATP binding, but not hydrolysis (Chi *et al*, 2006; Sung & Stratton, 1996; Cox, 2007; Bugreev & Mazin, 2004; Sigurdsson *et al*, 2001). A recent FRET experimentation using Rad51 has confirmed that ATP binding by Rad51, but not ATP hydrolysis, is sufficient for the formation of three-strand intermediate, ATP hydrolysis is crucial for ssDNA release and strand-exchange competition (Ito *et al*, 2018).

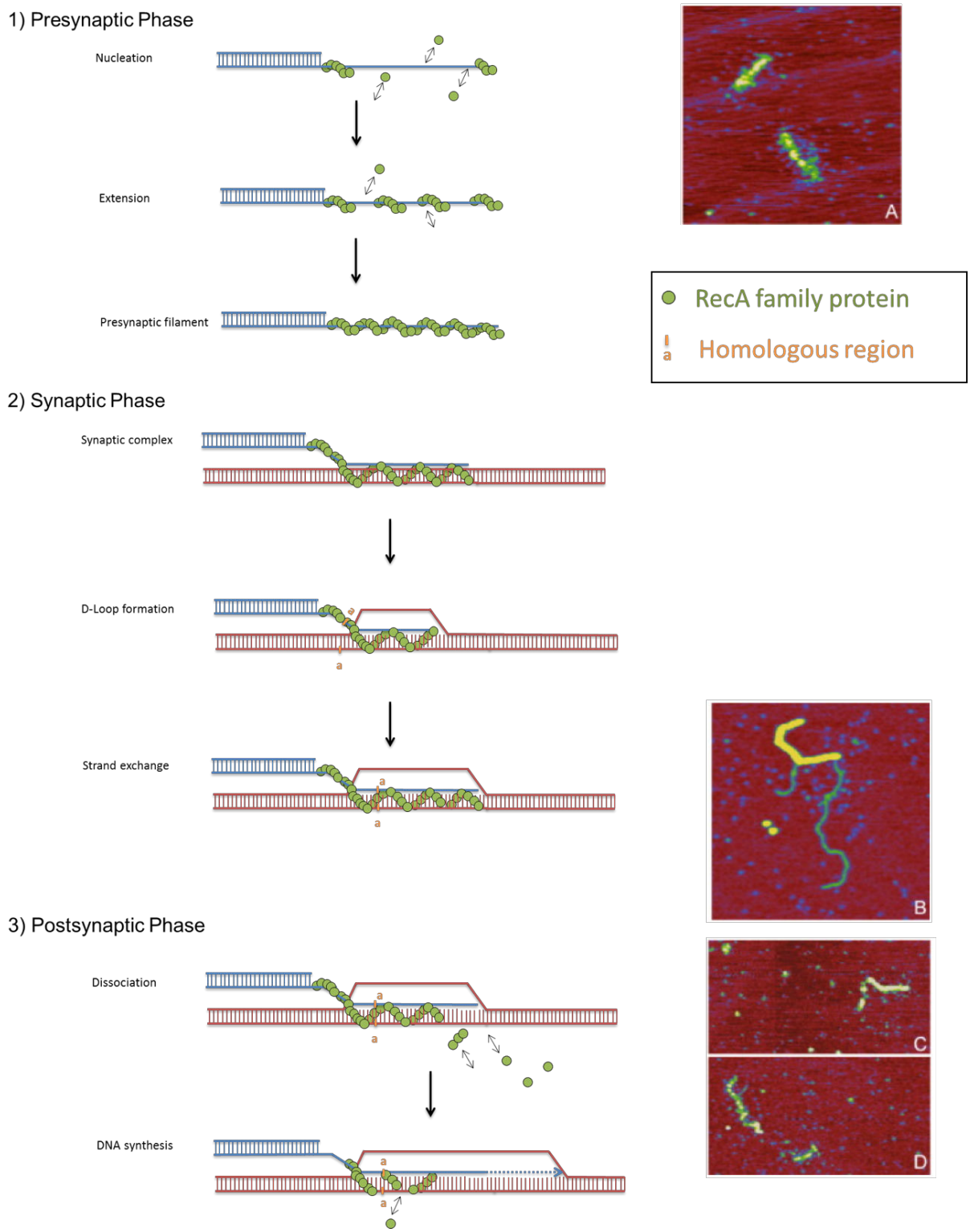

Figure 51 : Schematic representation of the functions of RecA family protein in HR (study from **(Sung & Klein, 2006; Holthausen *et al*, 2010; Sung *et al*, 2003; Krejci *et al*, 2012)**). In the panels on the left: RecA family proteins function in all three phases: 1) Presynaptic phase: formation of nucleoprotein filament by RecA family proteins loading on ssDNA; 2) Synaptic phase: formation of three-stranded intermediate and D-loop, in order to realize strand exchange between the invading DNA substrate and homologous duplex DNA template; 3) Postsynaptic phase: DNA synthesis in using 3'end of invading DNA as primer, and RecA family proteins dissociated from DNA in ATP-hydrolysis dependent manner. In the panel on the right: SFM (structure from motion) images of human Rad51-DNA complex at the different phases: (A) formation of nucleoprotein filament; (B) Strand exchange; (C) and (D) earlier and later of Rad51 filaments disassembling from DNA.

3) Postsynaptic phase. During this phage, RecA family proteins dissociate from dsDNA in an ATP-hydrolysis dependent manner, to expose the 3'-OH end of invaded ssDNA. This invading 3'end will be used as primer to realize the subsequent DNA synthesis (Krejci *et al*, 2012; van der Heijden *et al*, 2007; Holthausen *et al*, 2010). Indeed, the filament disassociation starts from the end when the terminal Rad51 hydrolyses ATP. The disassembly occurs in bursts of varying numbers of monomers interspersed by long pauses. Even if the internal Rad51 monomers simultaneously hydrolyze ATP, they stay upon the filament through protein-protein interactions. The terminal Rad51 has only one interface with its neighbor, therefore, its hydrolysis of ATP ruptures this interface to disassemble the Rad51 protein assembly (Modesti *et al*, 2007; van Mameren *et al*, 2009). In *Sulfolobus solfataricus*, this ATP hydrolysis-mediated RadA disassembly from ssDNA can occur only in the presence of magnesium and ssDNA under a high temperature (65°C-85°C).

Globally, *in vitro* ATP binding, but not hydrolysis, is necessary for the formation of nucleoprotein helical filaments, formation of synaptic complex, formation D-loop and strand exchange by RecA family proteins. ATP hydrolysis is obligatory for the dissociation of RecA family proteins from DNA. Although ATP hydrolysis is not required for presynaptic complex formation, it could occurr also during the formation of nucleoprotein filaments, which results in dissociation of recombinase and destabilization of the filament (Holthausen *et al*, 2010; Chi *et al*, 2006). Moreover, reducing the ATP hydrolysis rate can promote DNA strand exchange activity of hRad51 (Bugreev & Mazin, 2004). So, we can suppose that *in vivo*, some mediator proteins should temporarily inhibit ATPase activity of RecA family proteins to stabilize nucleoprotein filament formation and stimulate strand exchange process during the DNA repair by HR.

Furthermore, genetic studies have demonstrated that *rad*A gene is important. Deletion of *rad*A gene in *Holoferax volcanii* is not lethal but augments its sensibility to DNA damage agent, such as UV light. This means that *radA* gene is not essential for survival of this archaeaon in laboratory condition, but it is important for the DNA repair mechanism. In contrast, in hyperthermophilic archaea, *Sulfolobus islandicus, Thermococcus kodakarensis* and *Pyrococcus furiosus*, the deletion of this gene is lethal, meaning that *radA* gene is essential for survival in these microorganisms which grow at high temperature (Haldenby *et al*, 2009; Farkas *et al*, 2012; Zhang *et al*, 2013).

II. Hypotheses for biological functions of primase/recombinase association

The molecular mechanisms by which homologous recombination repairs DSBs have been extensively studied and are now well characterized in bacteria and eukaryotes. More and more studies have shown that HR is a pivotal pathway in the maintenance of genome integrity. The mechanisms by which HR contribute to DNA replication in bacteria and eukaryotes have been reported (Cox, 2001, 2007; West, 2003; Costes & Lambert, 2012; Ait Saada *et al*, 2018), but in archaea these mechanisms are poorly understood. From the highly-connected sub-network encompassing four proteins from *Pyrococcus abyssi*: RadA, RadB, small subunit p41 of DNA Primase and DNA ligase, we try to understand better how homologous recombination acts to protect, restart and repair replication forks. Two main hypotheses have been proposed based on several reported studies from bacteria and eukaryotes:

1. Lesion site bypass by cooperation between RadA and Primase

Bacteria possess special translesion synthesis polymerases, such as Pol II, IV, V from *E. coli.* Several studies have shown that recombinase RecA proteins are essential for activating DNA polymerase V (UmuD'$_2$C) to catalyze TLS on AP-site DNA damage both *in vivo* and *in vitro* (Patel *et al*, 2010). The last model of RecA-PolV TLS function revealed that RecA filament (RecA*) is required to directly activate PolV, by transferring a molecule of RecA with ATP from the 3'-proximal tip of RecA filament to form an activated "PolV-RecA-ATP" complex. This activated form can catalyze TLS without RecA filament (Jiang *et al*, 2009) (Figure 52).

*Pfu*Primase has been shown to display TLS activity but is strongly inhibited at before AP-sites (Jozwiakowski *et al*, 2015). Hence, we thought that the interaction between *Pab*RadA and *Pab*Primase could have TLS activity on AP-site DNA damage.

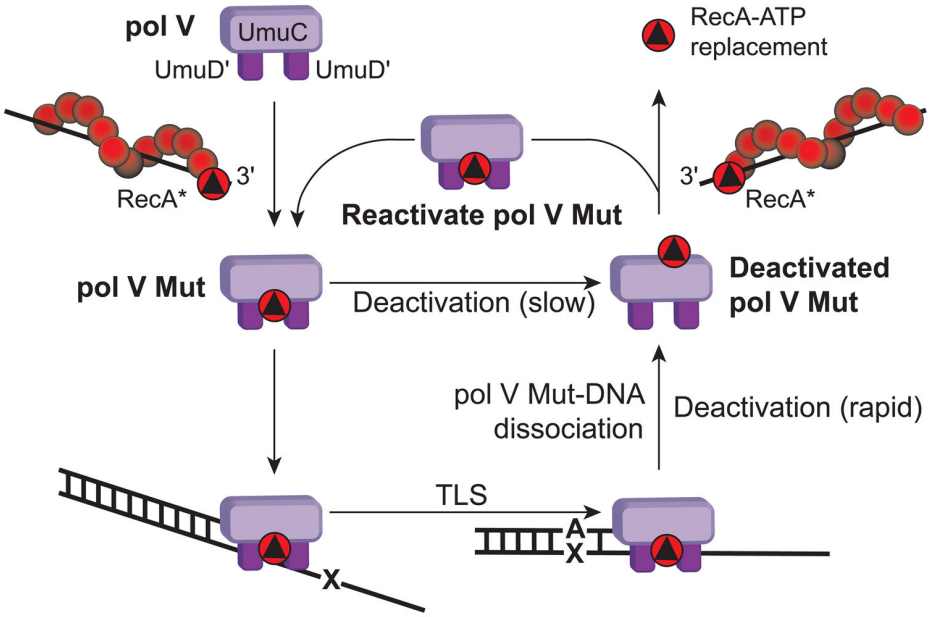

Figure 52 : Model for pol V Mut function (Patel *et al*, 2010). Transfer of an ATP-bound RecA subunit from RecA filament (RecA*) creates the active pol V Mut (PolV-RecA-ATP). PolV Mut can migrate to a template-primer site where its activity is required (such as AP-site) and extend the primer and insert nucleotides opposite any lesion encountered (TLS). Upon dissociation, pol V Mut is inactivated.

2. RadA-mediated intermediate extension by DNA polymerase

In Bacteria, translesion DNA polymerase Pol IV is preferentially recruited to RecA-mediated D-loop and promotes D-loop intermediate extension (Figure 53A) (Pomerantz *et al*, 2013). McIlwraith et *al* have demonstrated similarly that human recombinase Rad51 proteins interact with DNA polymerase η (Pol η, one of TLS polymerases in eukaryote). Rad51 proteins target the Polη to the primer in D-loop substrate and stimulates its DNA extension activity, suggesting that Polη functions at stalled replication forks for the reinitiation of DNA synthesis by HR repair (McIlwraith *et al*, 2005) (Figure 53B).

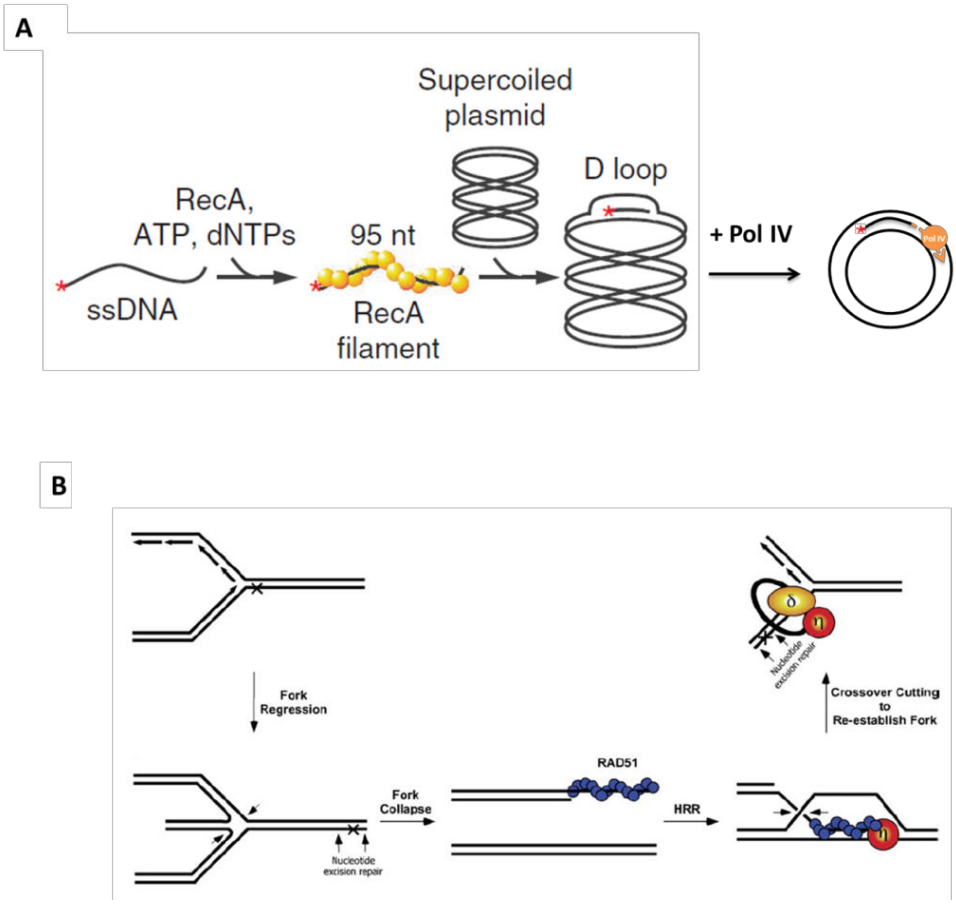

Figure 53 : (A) Model for D-loop extension by Pol IV in Bacteria (Modified from **(Pomerantz *et al*, 2013)**). ssDNA is incubated with RecA, ATP and dNTPs, promoting RecA filament formation. A supercoiled plasmid containing the same sequence as the ssDNA is then added, facilitating D-loop formation. And then Pol IV is recruited by D-loop and extends the D-Loop. **(B) Model for pol V Mut function** (Modified from **(McIlwraith *et al*, 2005)**). Replication fork may regress to form a "chicken foot" structure when it stalls at a DNA lesion. This "chicken foot" structure can undergo nucleolytic cleavage (indicated by arrows) by either HJ resolvase or a flap endonuclease. Fork regression allows subsequent nucleotide excision repair processes to remove the blocking lesion. The double-strand break formed by fork collapse serves as a substrate for Rad51 (indicated in blue) binding and the inintaiton of HR repair. When the lesion is present on the leading strand, 5'→3' resection at the DSB will be required to form an extended 3' single strand for RAD51 binding and subsequent HRR. RAD51 mediates the formation of a D-loop that serves as a primer for DNA synthesis by polη. RAD51 may play an active role in polη recruitment. In subsequent steps, the crossover strands need to be cut to reestablish a replication fork.

This model is unknown in archaea, but as mentionned above, *Pfu*Primase has TLS activity, so we want to test if primase from *P. abysii* could extend the D-loop intermediate in the presence of RadA, as observed in eukaryotic model. Nevertheless, the same study has shown that D-loop intermediate extension cannot be promoted by the replicative DNA polymerase δ or by another TLS polymerase such as polι (McIlwraith *et al*, 2005). So, we are curious to know wether the two replicative polymerases B and D in archaea could perform D-loop intermediate elongation with RadA.

This study was conducted in three phases: firstly, we have produced and purified the proteins RadA from *P. abyssi* and *P. furiosus* with two different purification methods, small subunit of Primase (Primase-P41) and Primase complex (p41-p46) from *Pyrococcus abyssi*.

Physical interaction between RadA and Primase is in progress by Gaëlle Hogrel (Post-doc in Lab). The test CoIP was utilized in the first time to confirm the physical interaction. Unfortunately, the obtained results cannot conclude the physical interaction. Then the detection was initiated by immunodetecton of *Pab*P46 and *Pab*RadA from cellular extract after separation by ultracentrifugation on a 5-25% sucrose gradient. Interestingly, the preliminary result (Figure 54) shown that *Pab*P46 accumulated in fractions at higher molecular weight (F5 to F9) than primase complex alone (P41/46 was expected around 86 kDa). Co-sedimentation of *Pab*P46-RadA was observed in fraction 9 which may correspond to a macromolecular assembly, suggesting that *Pab*Primase complex physically interact with *Pab*RadA.

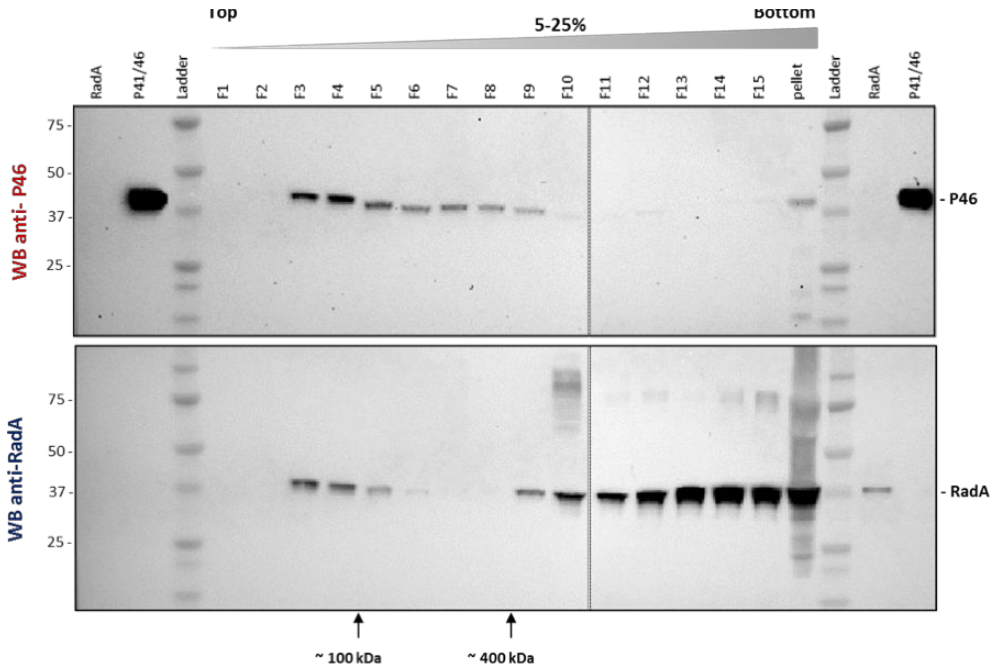

Figure 54: Localization of native P46 and RadA in 5-25 % sucrose gradient. *P. abyssi* cellular extract was fractionated on a 5-25% sucrose gradient after ultracentrifugation at 210 000 g during 20 hours. Proteins of interest were revealed by western-blot with their specific antibodies.

Once physical interaction was detected, we have then confirmed their enzymatic activities, such as DNA binding activity, D-loop formation and DNA strand exchange acivity of *Pab*RadA compared with *Pfu*RadA ; and primer extension activity by *Pab*P41 compared with *Pab*Primase.

Secondly, we have tried to test which type of DNA damage could stop the DNA synthesis by P41 or Primase and if RadA could help to perform DNA damage bypass.

Finally, to answer if RadA mediates DNA synthesis from strand invasion intermediates of HR, we tested the DNA polymerasion activity of both P41 and Primase on substrates mimicking D-loop substrates, and then added RadA in different conditions. Similar experimental design was also used to look at D-loop substrate extension by Polymerases B and D from *P. abyssi*, and test the effect of RadA on this activity.

III. Materials & Methods

1) Protein

The *radA* gene of *Pyrococcus abyssi*, with the His6-tag at the N-terminal region, was inserted into a *pFO4 (Amp^R)* vector (Marine Express (Groisillier *et al*, 2010)). The *radA* gene of *Pyrococcus furiosus,* without tag (plasmid provided by Y. Ishino, (Komori *et al*, 2000b)), was inserted into *pET21a*. The *p41* gene of *Pyrococcus abyssi*, with the His6-tag at the N-terminal region, was inserted into a *pQE80-L (Amp^R)* vector (Le Breton *et al*, 2007), and the *p46* gene of *Pyrococcus abyssi*, without tag, was inserted into a *pET26b+ (Kan^R)* vector (Le Breton *et al*, 2007). All of targeted genes were expressed in *Escherichia coli* Rostta pLysS. The *p41* gene and *p46* gene were expressed together in the same strain (*E.coli* Rosetta pLysS) to form *Pab*P41_P46 complex (*Pab*Primase).

Cells were grown at 37°C to an OD_{600} 0,7-0,8, and the protein expression was induced with 1 mM IPTG. Four hours after induction, cells were harvested by centrifugation (8000G), and resuspended in lysis buffer containing (i) for *Pab*RadA : 50 mM Tris-HCl pH8; 1 mM DTT, 300 mM NaCl; 10mM Imidazole, (ii) for *Pfu*RadA: 50mM Tris-HCl pH8; 0,5 mM DTT, 400 mM NaCl; 0,1 mM EDTA, supplemented by an EDTA-Free protease inhibitor (Roche), (iii) for *Pab*P41 : 50 mM Tris-HCl pH8; 500 mM NaCl; 10 mM Imidazole, 1 mM DTT, (iv) for *Pab*Primase : 50 mM MES pH6 ; 200 mM NaCl; 20 mM Imidazole, 1 mM DTT, . Cells were sonicated on ice, 20 seconds on, 30 seconds off, at 35% amplitude, repeated 5 times. Protein supernatant was collected by centrifugation (10000rpm) during 20min and incubated at 80°C for 15 or 20 min.

For three proteins from *Pyrococcus* abyssi, after centrifugation (10000 rpm during 30 min), soluble fractions were loaded onto a nickel resin column “HiTrap Chelating HP” (CE Healthcare) and connected with second heparin column “HiTrap Heparin” (CE Healthcare). After the washing stage of nickel column, proteins were eluted with a linear gradient from 0 mM to 500 mM or 1 M imidazole, and injected directly to heparin column, and eluted with a linear gradient from 0 mM to 500 mM or 1M NaCl. Peak fractions were run on 15% SDS-PAGE gel with migration buffer MOPS-SDS at 180V for 50min. For *Pab*RadA and *Pab*P41, proteins were pooled and dialyzed using “Cellu-Sep T2” (6000-8000 MWCO, membrane Filtration Products, Inc) at 14°C in

conservation buffer (i) for *Pab*RadA: 50 mM Tris-HCl pH8, 200 mM NaCl, 0,1 mM EDTA, 0,5 mM DTT, complemented with 20% glycerol and stored at -20°C, (ii) for *Pab*P41: 50mM Tris-HCl pH8, 300mM NaCl, 1mM DTT, complemented with 20% glycerol and stored at -20°C. For *Pab*Primase, the peak fractions were pooled before running on a "Superdex 200 10/300 GL" column (CE Healthcare). *Pab*Primase proteins were eluted, concentrated and dialyzed at 14°C in conservation buffer (50 mM MES pH6, 600 mM NaCl, 1 mM DTT), and then complemented with 40% glycerol and stored at -20°C.

Table 16 : Composition of elution buffers during protein purification

	***Pab*RadA**	***PabP41***	***Pab*Primase**
Nickel column elution buffer	50 mM Tris-HCl pH8 300 mM NaCl 500 mM Imidazole 1 mM DTT	50 mM Tris-HCl, pH 8 300 mM NaCl 1 M imidazole 1 mM DTT	50 mM MES pH 6 200 mM NaCl 1 M Imidazole 1 mM DTT
Heparin column elution buffer	50 mM Tris-HCl pH8 1 M NaCl 1 mM DTT	50 mM Tris-HCl, pH 8 1 M NaCl 0,5 mM DTT	50 mM MES pH 6 1M NaCl 1 mM DTT

The purification protocol of *Pfu*RadA was modified from that described by (Komori *et al*, 2000b). In brief, after centrifugation (10000 rpm, 30 min), soluble fractions were mixed with polyethylenimine (Polyethylenimine 50% (W/V), sigma) at a final concentration of 0,5%. Protein pellets was obtained after centrifugation (10000 rpm, 20 min) and *Pfu*RadA proteins in pellets were eluted with 0.3 M ammonium sulfate in buffer A (50 mM Tris-HCl, pH 8.0, 0.1 mM EDTA, 0.5 mM DTT, 5% glycerol) from the precipitate after polyethylenimine treatment. After centrifugation (10000 rpm, 20 min) the supernatant was mixed with an equal volume of 2 M ammonium sulfate and applied onto a phenyl-sepharose column "Hiprep 16/10 phenyl FF (lowsub)" (CE Healthcare) (substrates are separated on the basis of their different hydrophobicity according to a hydrophobic interaction). *Pfu*RadA proteins were eluted with a linear gradient from 1 M to 0 M ammonium sulfate (Elution buffer: 50 mM Tris-HCl, pH 8.0, 0.1 mM EDTA, 0.5 mM DTT, 5% glycerol). The fractions were dialyzed in buffer containing 50 mM

Tris-HCl, pH 8.0, 200 mM NaCl, 0.1 mM EDTA, 0.5 mM DTT, 5% glycerol. The dialysate was applied onto heparin column “Hitrap heparin” (CE Healthcare), and *Pfu*RadA proteins were eluted at high salt concentration (~0,7 M NaCl) (Elution buffer: 50 mM Tris-HCl, pH 8.0, 1 M NaCl, 0.1 mM EDTA, 0.5 mM DTT, 5% glycerol) . The fractions were mixed with the same volume of buffer A and were applied onto a “Mono Q HR 5/5” column (CE Healthcare). *Pfu*RadA proteins were eluted with a linear gradient from 1 M to 0,5 M ammonium sulfate (Elution buffer: 50 mM Tris-HCl, pH 8.0, 1 M NaCl, 0.1 mM EDTA, 0.5 mM DTT, 5% glycerol). *Pfu*RadA proteins were dialyzed at 14°C in conservation buffer (50 mM Tris-HCl, pH 8.0, 450 mM NaCl, 0.1 mM EDTA, 0.5 mM DTT, 5% glycerol) and stored at -20°C.

All proteins were quantified using absorbance measurement at 280nm by Nanodrop. All molar concentrations indicated in this study corresponded to the monomeric form of *Pab*RadA, *Pfu*RadA, *PabP41* and *Pab*Primase.

2) DNA substrates

Table 17 : List of oligonucleotide and DNA substrate

Oligonucleotides		Size (base)	Label (5'Cy5 Or 5'FAM)	Sequences (5'-3')
1	L17*	17 nt	x	TGCCAAGCTTGCATGCC
2	L17**	17 nt	x	TGCCAAGCTTGCATGCC
3	L32*	32 nt	x	TGCCAAGCTTGCATGCCTGCAGGTCGACTCTA
4	L50	50 nt		CATCTGGCCTGTCTTACACAGTGCTACAGACTGGAACAAAAACCCTGC-AG
5	L87	87 nt		CAGGAAACAGCTATGACCATGATTACGAATTCGAGCTCGGTACCCGGG-GATCCTCTAGAGTCGACCTGCAGGCATGCAAGCTTGGCA
6	L87*	87 nt	x	CAGGAAACAGCTATGACCATGATTACGAATTCGAGCTCGGTACCCGGG-GATCCTCTAGAGTCGACCTGCAGGCATGCAAGCTTGGCA
7	L87 RC	87 nt		TGCCAAGCTTGCATGCCTGCAGGTCGACTCTAGAGGATCCCCGGGTAC-CGAGCTCGAATTCGTAATCATGGTCATAGCTGTTTCCTG
8	L87_AP	87 nt		CAGGAAACAGCTATGACCATGATTACGAATTCGAGCTCGGTACCCGGG-GATCCTXTAGAGTCGACCTGCAGGCATGCAAGCTTGGCA
9	L87_8oxoG	87 nt		CAGGAAACAGCTATGACCATGATTACGAATTCGAGCTCGGTACCCGGG-GATCCTXTAGAGTCGACCTGCAGGCATGCAAGCTTGGCA
10	L87_uracil	87 nt		CAGGAAACAGCTATGACCATGATTACGAATTCGAGCTCGGTACCCGGG-GATCCTXTAGAGTCGACCTGCAGGCATGCAAGCTTGGCA
11	M13mp18 RF I DNA	7250		M13mp18 RF I DNA (BioLabs, N4018S)
12	DL_Trap60	60		AAGATGTCCTAGCAAGGCACCCTAGTAGCGTGGTAGAATTCGGCAGCG-TCATGCGACGGC
13	DL_Sca1	91		GCCAGGGACGGGGTGAACCTGCAGGTGGGCGGCTGCTCATCGTAGGT-TAGTATCGACCTATTGGTAGAATTCGGCAGCGTCATGCGACGGC
14	DL_Sca2	91		GCCGTCGCATGACGCTGCCGAATTCTACCACGCTACTAGGGTGCCTTG-CTAGGACATCTTTGCCCACCTGCAGGTTCACCCCGTCCCTGGC
15	DL_intFAM	29	x	AAGATGTCCTAGCAAGGCACCCTAGTAGC

Modified nucleotide is noted in en "X" in orange

DNA Substrate	Primer / Template (N° / N°)	schematic
L87/87	6 / 7	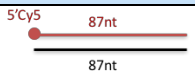
L17/87	1 / 5	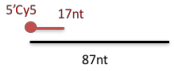
L32/87	3 / 5	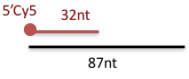
L17/87_AP	1 / 8	
L17/87_oxoG	1 / 9	
L17/87_Uracil	1 / 10	
D-Loop	13/14/15	

Oligonucleotides were purchased from Eurogentec and were purified by RP-HPLC or PAGE, and Double-stranded circular DNA M13mp18 RF I DNA was purchased from BioLabs. Annealing reactions were done in presence of 10mM Tris-HCl pH8, 100nM NaCl by heating to 95°C for 5 min, and then cooling to room temperature over-night. Final concentration of dsDNA substrate is 1µM. The D-loop complexes were further purified by gel electrophoresis. Labeled DNA substrates were constructed with the following sequences in table 18.

3) EMSA (Electrophoretic Mobility Shift Assay)

For the DNA binding analysis, *Pab*RadA, *Pab*P41 and *Pab*Primase proteins were incubated with different DNA substrates, as indicated in figures. in 10µL reactions containing fixation buffer (20 mM Tris-HCl pH 8, 150 mM NaCl, 2mM DTT, 50 µg/mL BSA, 0,5% Triton-X100), 10 mM $MgCl_2$, complemented with 2,5 mM ATP (when indicated). 10 nM DNA substrates were incubated with increasing proteins concentration (i) *Pab*RadA was 0; 6,25; 12,5; 25; 50; 100; 200; 400; 800 and 1250 nM; (ii) *Pab*P41: 0; 20; 40; 80; 100; 160 and 200 nM; (iii) *Pab*Primase: 0; 10; 20; 40; 80; 100; 200 nM), the mix was incubated for 10 min at 65°C for *Pab*RadA or 55°C for *Pab*P41 and *Pab*Primase. After being mixed with 10µL Ficoll 20%, the samples were resolved by electrophoresis (60V, for 2h) through a 0,75% agarose gel in 1X Tris Borate EDTA (TBE) buffer. Labeled fragments were analyzed with a fluorimager Typhoon 9500 (GE Healthcare) and quantified with Image Quant software.

4) D-loop formation assay

For D-loop reactions with *Pab*RadA, in 20µL reaction, 2 nM ssDNA L87 (Oligo N°6) was preincubated with an increasing concentration of RadA (0, 2, 16, 100 nM) at 65°C in the reaction buffer containing 20 mM Tris-HCl pH8, 50 µg/mL BSA, 1 mM DTT, 150 mM NaCl, 10 mM $MgCl_2$ or 1 mM $CaCl_2$ complemented with 2,5 mM ATP (when presented). After 10 min, reactions were started by the addition of 5 nM M13 double-stranded plasmid (N°13), and incubation continued for an additional 30 min at 65°C. Reactions were stopped by addition of stop buffer (50 µg/mL Proteinase K, 0,5% SDS and 40 mM EDTA) and were further incubated for 15 min at 37°C. The reaction products were separated by agar gel electrophoresis (0,75%, 130 V, 120 min, 4°C) in 1X TBE buffer. Labeled fragments were analyzed with a fluorimager Typhoon 9500 (GE Healthcare).

5) Strand exchange assay

For strand exchange assays, in 20 µL reaction, 25 nM ssDNA L87 was incubated at 65°C for 10 min with *Pab*RadA or *Pfu*RadA proteins at increasing concentrations (0, 150, 375, 750, 1250 nM) in a reaction buffer (20 mM Tris-HCl pH8, 50 µg/mL BSA, 1 mM DTT, 150 mM NaCl, 10 mM $MgCl_2$) complemented with ATP (when indicated). After addition of 62,5 nM dsDNA substrates (substrate L87/87), the strand exchange reaction was allowed to proceed during 30 min at 65°C. The reaction aliquots were stopped by addition of stop buffer (50 µg/mL Proteinase K, 0,5% SDS and 40 mM EDTA) and were further incubated for 15 min at 37°C. The reaction products were separated by non-denaturing polyacrylamide gel electrophoresis (6%, 130 V, 150 min, 4°C) in 1X TBE buffer. Labeled fragments were analyzed with a fluorimager Typhoon 9500 (GE Healthcare) and quantified with Image Quant software.

6) DNA Synthesis assay

For DNA synthesis reactions with different DNA polymerases (*Pab*P41, *Pab*Primase, *Pab*Pol B exo- and *Pab*Pol D exo- (two last proteins were already available in the lab)) in the condition: (i) without RadA and (ii) with RadA. In 10 µL reaction, (i) 50 nM DNA substrates (indicated in figure) were incubated with an increasing concentration of proteins (0, 50, 100, 200, 400 nM) at 55°C; or (ii) 50 nM DNA substrate 17/87 was preincubated with an increasing concentration of *Pfu*RadA (0, 400, 1250, 2500 nM) in reaction buffer at 55°C. After 10 min, 400 nM DNA polymerase was added. in the reaction buffer containing 20 mM Tris-HCl pH8, 10 mM $MgCl_2$, 150 mM NaCl, 200 µM dNTP, 50 µg/mL BSA, 1 mM DTT. After 60 min incubation, reactions were stopped by addition of stop buffer (86% deionized formamid, 0,01 N NaOH, 10 mM EDTA, 2 µM Trap) and by heating samples at 95°C for 5 min. The reaction products were separated by electrophoresis on a gel composed of 18% polyacrylamide 19:1, 7 M urea, 16% deionized formamide and 1x TBE. Labeled fragments were analyzed with a fluorimager Typhoon 9500 (GE Healthcare).

7) TLS (Translesion DNA synthesis) assay

Translesion DNA synthesis reactions were carried out in two conditions: (i) without ssDNA and (ii) with ssDNA, in a reaction buffer consisting of 20 mM Tris-HCl pH8, 10 mM $MgCl_2$, 150 mM NaCl, 200 µM dNTP, 50 µg/mL BSA, 1 mM DTT and 2,5 mM ATP / ATPγS (Sigma).

In 10 µL reaction, for (i): 50 nM DNA L17/87_AP was preincubated with an increasing concentration of *Pfu*RadA (0, 400, 1250, 2500 nM) in reaction buffer at 55°C. After 10 min, 400 nM *Pab*P41 or *Pab*Primase were added. For (ii): 125 nM ssDNA L17 or L50 were preincubated with saturated amount of *Pfu*RadA (2,5 µM) with ATP at 55°C; at the same time, 400 nM *Pab*P41 or *Pab*Primase were pre-incubated also with ATP at 55°C. After 10 min, 50 nM DNA substrates D, *Pfu*RadA and *Pab*P41 or *Pab*Primase were added in reaction buffer, to initiate primer extension. Then the incubation continued for an additional 60 min at 55°C. The reactions were stopped by addition of stop buffer (86% deionized formamid, 0,01 N NaOH, 10 mM EDTA, 2 µM Trap) and by heating samples at 95°C for 5 min. The reaction products were separated by electrophoresis on a gel composed of 18% polyacrylamide 19:1, 7 M urea, 16% deionized formamide and 1x TBE. Labeled fragments were analyzed with a fluorimager Typhoon 9500 (GE Healthcare).

IV. Results and discussion

1) Protein purification

To study the functional interaction between RadA and P41 subunit of DNA primase, we have purified the proteins RadA from *Pyrococcus abyssi* and *Pyrococcus furiosus,* as well as Primase complex (P41/p46) and isolated P41 subunit from *Pyrococcus abyssi* (Figure 55).

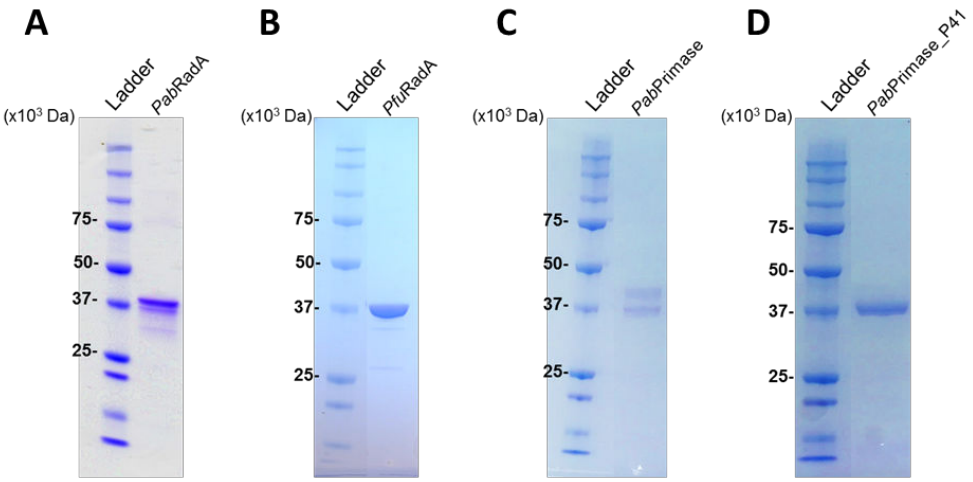

Figure 55: Purification of proteins. Purification of *Pab*RadA (A), *Pfu*RadA (B), *Pab*Primase (C) and *Pab*P41 (D). Coomassie stained SDS-PAGE gel (15%) of purified protein. Lane Ladder, molecular weight marker (molecular mass indicated in kiloDaltons).

All the purified proteins migrated at their expected sizes. However, additional faint bands of lower molecular weights were present in *Pab*RadA pattern, indicative of potential degradation occurring during the purification. The difference in size between *Pab*RadA and *Pfu*RadA corresponds to an additional His-tag located at the N-ter of *Pab*RadA. The proteins were considered to be pure enough and were in sufficient amount to follow on with biochemical characterizations

2) Biochemical characterization

a) RadA DNA binding, DNA pairing and strand exchange activities

Archaeal Recombinases possess DNA binding, DNA pairing and strand exchange activities (Komori *et al*, 2000b). Using electrophoretic mobility shift assay (EMSA), we first tested DNA binding abilities of *Pab*RadA.

Figure 56 showed that *Pab*RadA bound ssDNA in a ATP-independent manner (Figure 56) as observed for archaeal *Pfu*RadA (Komori *et al*, 2000b); bacterial RecA (Menetski & Kowalczykowski, 1985) and human Rad51 (Morozumi *et al*, 2013). In presence or absence of ATP, *Pab*RadA started to bind to ssDNA from concentration of 50 nM (ratio ssDNA:*Pab*RadA is 1:5, Figure 56, lane 5 and 15), and the total protein-DNA complexes were formed with 400 nM *Pab*RadA (ratio ssDNA:*Pab*RadA is 1:40, Figure 63, lane 8 and 18).

In addition, we tested *Pab*RadA DNA binding activity on different lengths and different types of DNA substrates in presence of ATP (Figure 57 A-E). Quantitative analysis of the gel retardation assays clearly indicated that *Pab*RadA preferentially binds to ssDNA, in comparaison to dsDNA and primed DNA (Figure 57 F right panel) and display higher affinity to long ssDNA oligonucleotide (Figure 57 F left panel). This result is in contradiction with the reported lack of preference of *Pfu*RadA between dsDNA and ssDNA (Komori *et al*, 2000b). EMSA was performed in conditions similar to that reported for *Pfu*RadA, however, *Pab*RadA possesses additional His-tag and the purified sample of *Pab*RadA contained more DNA contaminants compared to *Pfu*RadA sample. These differences might explain the difference observed regarding DNA substrate preference. Still, that *Pab*RadA displays affinity towards dsDNA, a prerequisite to test strand exchange activity.

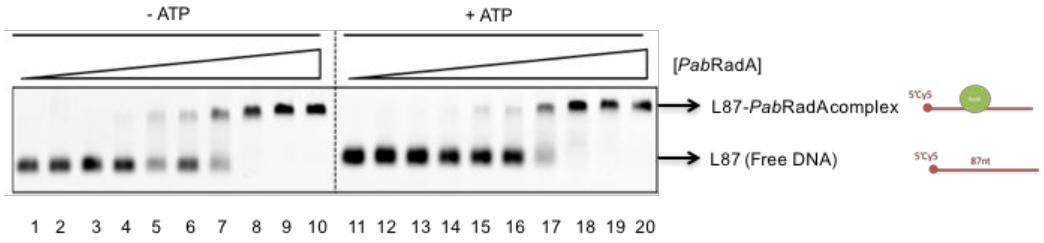

Figure 56 : ATP-independent DNA binding activity of *Pab*RadA. *Pab*RadA (0; 6,25; 12,5; 25; 50; 100; 200; 400; 800 and 1250 nM) and 10 nM ssDNA (87nt) were incubated with or without 2,5 mM ATP at 65°C for 10 min. reaction products were analyzed by 0,75% agar gel electrophoresis in 1X TBE buffer, and the bands were detected by autoradiography.

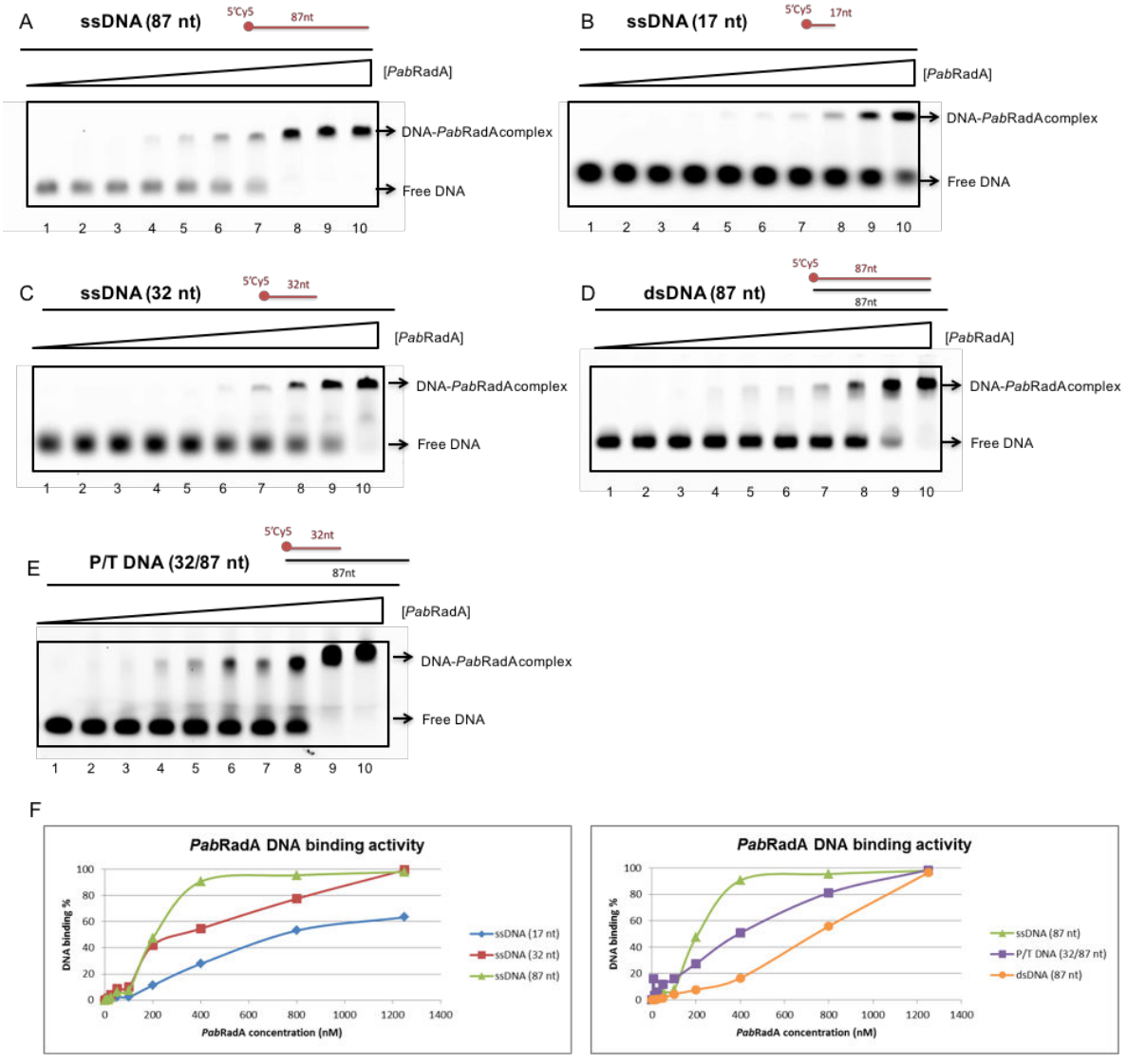

Figure 57 : DNA length-/substrate-dependent binding activity of *Pab*RadA. *Pab*RadA (0; 6,25; 12,5; 25; 50; 100; 200; 400; 800 and 1250 nM) and 10 nM different DNA substrates were incubated with 2,5 mM ATP at 65°C for 10 min. Reaction products were analyzed by 0,75% agar gel electrophoresis in 1X TBE buffer, and the bands were detected by autoradiography (A)-(E). (F) the gels shown in (A)-(E) were subjected to image analysis to obtain data points for a graphical representation of the results.

b) D-loop formation assay

Prior to determine the strand exchange activity of *Pab*RadA, we have tested its strand invasion property, which means the D-loop formation ability. For that purpose, Supercoiled M13 DNA was incubated with a complementary labeled 87nt ssDNA, in absence or presence of *Pab*RadA. The reaction products were then resolved in a native gel. As shown in Figure 58, when supercoiled M13 was added in the reaction, in absence of RadA (lane 1), in addition to the labeled 87nt ssDNA at the bottom of the gel, a smear was observed in the middle of the gel, likely corresponding to non-specific association of supercoiled DNA with 87nt oligonucleotide. However, in presence of increasing concentration of RadA (Figure 58, lanes 2 to 4) a specific product was observed, corresponding to the invasion of deoxyoligonucleotide into the supercoiled M13 replicative form. This product appeared at concentration of RadA starting from 16 nM (stoichiometry ratio ssDNA/RadA is 1:8). This result confirmed that *Pab*RadA is capable to promote the invasion of ssDNA (87 nt) into the circular double-stranded M13, to form D-loop. In addition, we confirmed that this activity is ATP-dependent (Figure 58, compare lanes 4 and 5) as described for recombinases from Archaea, Eukaryotes and Bacteria (Sigurdsson *et al*, 2001; Chi *et al*, 2006; Seitz *et al*, 1998; Komori *et al*, 2000a). Strand invasion was also enhanced when Mg^{2+} divalent cation in reaction buffer was replaced by Ca^{2+} (Figure 58, lane 6 to 9) as observed for human Rad51 (Bugreev & Mazin, 2004).

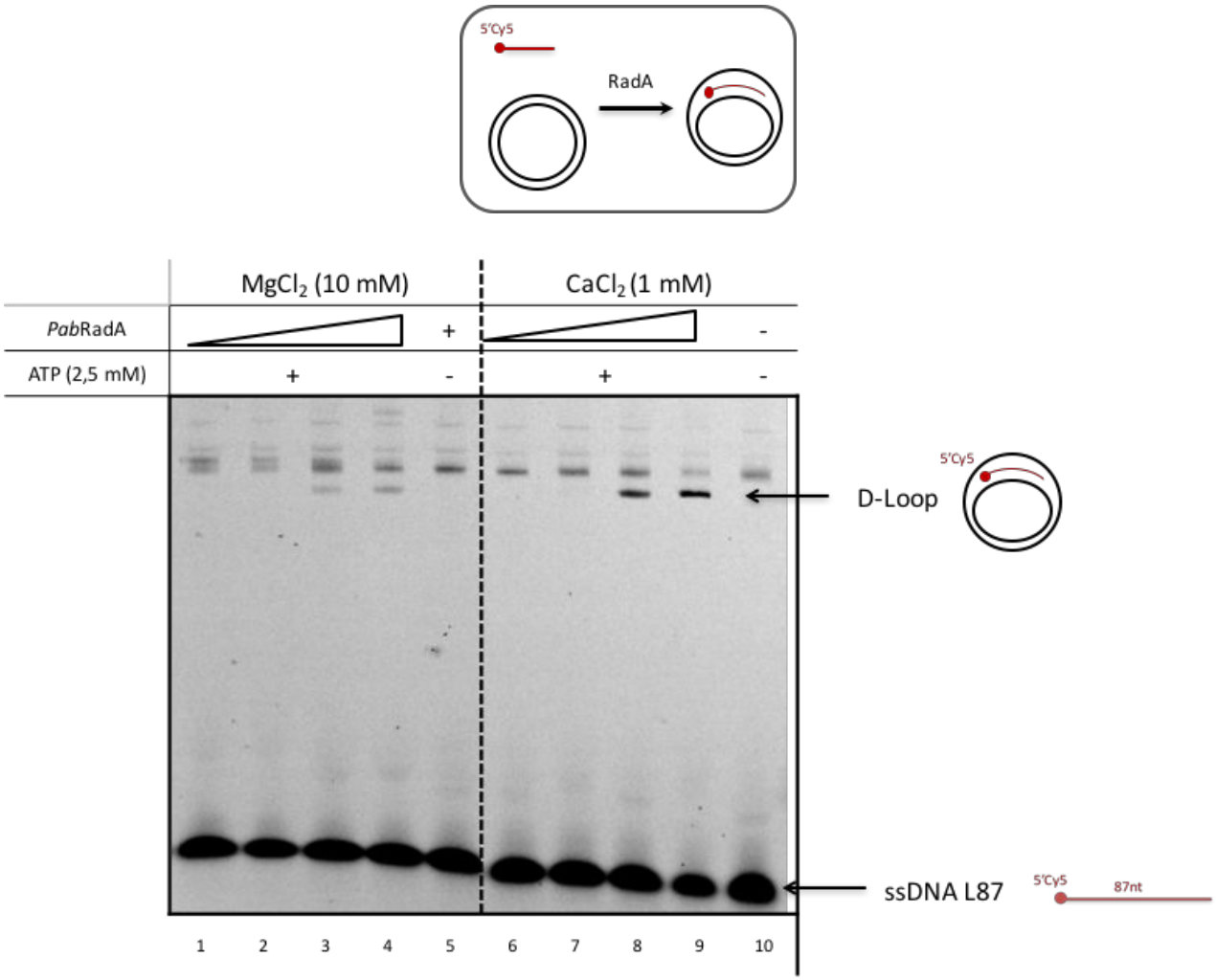

Figure 58 : D-loop formation activity of *Pab*RadA. *Pab*RadA (0, 2, 16, 100 nM) was pre-incubated with 2 nM 87nt ssDNA at 65°C for 10 min, and then 5 nM double-stranded circular DNA substrate M13 were added and incubated with or without 2,5 mM ATP with either 10 mM MgCl2 or 1 mM CaCl2 at 65°C for 30 min. Reaction was stopped by addition of Proteinase K, SDS and EDTA. Reaction products were resolved in 0,75% agar gel electrophoresis and fluorescence revealed using Typhoon 9500 (GE Healthcare).

c) Strand exchange assay

Next we investigated DNA strand exchange activity of *Pab*RadA and *Pfu*RadA by three-strand exchange assay using labeled DNA duplex and homologous ssDNA, represented on top of Figure 59. Using this assay, displacement of the labeled strand within the duplex DNA is followed by native gel electrophoresis.

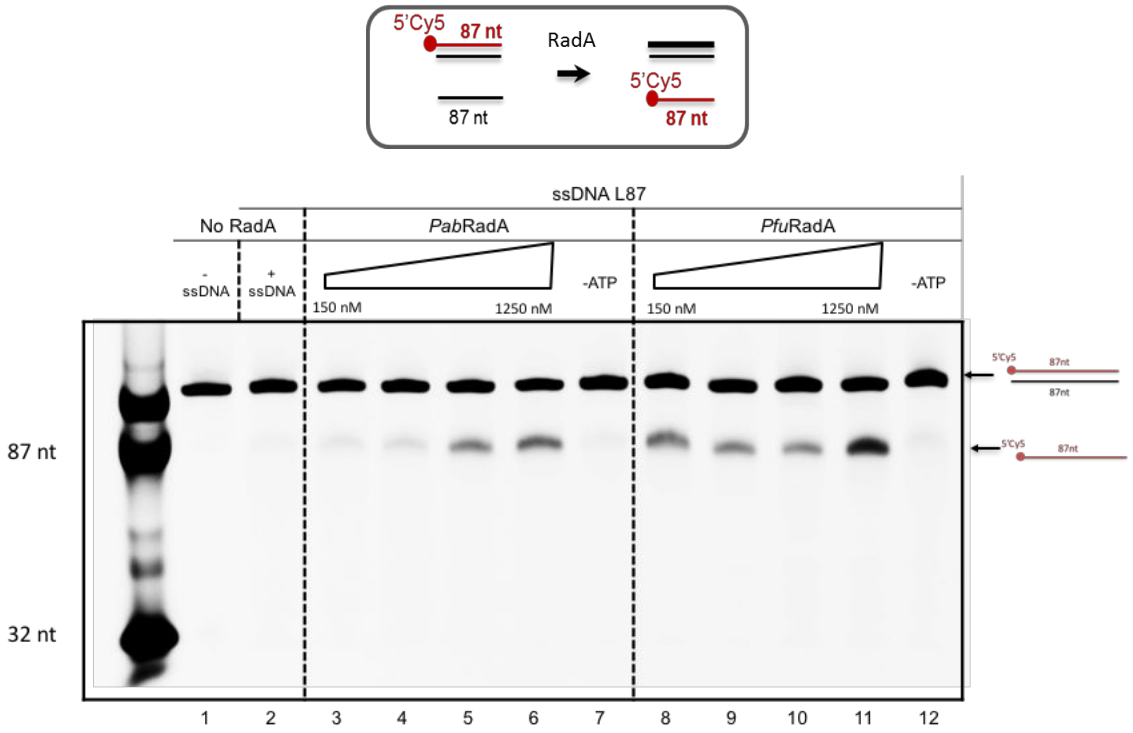

Figure 59 : DNA strand exchange activity of RadA. *Pab*RadA or *Pfu*RadA (0, 150, 375, 750, 1250 nM) was pre-incubated with 25 nM ssDNA (L87) at 65°C for 10 min, and then 62,5 nM double-stranded DNA substrate (Substrate 87/87) were added and incubated with or without 2,5 mM ATP with 10 mM MgCl2 at 65°C for 30 min. Reaction was stopped by addition of Proteinase K, SDS and EDTA. Reaction products were resolved in 6% polyacrylamide non-denaturant gel electrophoresis and fluorescence revealed using Typhoon 9500 (GE Healthcare).

In the absence of *Pab*RadA, the labeled DNA fragment is not displaced from the DNA duplex (Figure 59, lane 2). In contrast, when *Pab*RadA is present a band corresponding to the labeled displaced fragment is observed at expected size (87 nt) indicating that *Pab*RadA is active and promote strand exchange (Figure 59, lane 3-6). We obtained similar results with *Pfu*RadA, however the protein from *P. furiosus* showed higher efficiency (Figure 59, lane 8-12). This difference of efficiency between *Pab*RadA and *Pfu*RadA might be related to the higher ratio of DNA contamination in the *Pab*RadA sample, as mentioned above. ATP dependence of strand exchange reactions was also confirmed for both RadA proteins (Figure 59, lane 6 vs 7 and lane 11 vs 12), as already reported for *Pfu*RadA (Komori *et al*, 2000b).

d) Primase/P41 DNA binding activity

We then checked the biochemical properties of DNA primase complex and isolated p41 subunit of *P. abyssi*. DNA binding activities of both *Pab*P41 and *Pab*Primase have been detected using gel retardation assay. The binding affinity of *Pab*Primase to single-stranded DNA and primer/template DNA was much higher than that of *Pab*P41 (Figure 60A vs 60B). At the maximum concentration (200 nM) of proteins, *Pab*P41did not show a strong DNA binding activity (Figure 60A, lane 7 and 14). In contrast, with the same amount of the *Pab*Primase, there is a clear shifted band with different mobility (Figure 60B), indicating that the subunit *Pab*P46 subunit probably increases DNA affinity of the *Pab*Primase to DNA by forming a complex with the catalytic subunit *Pab*P41. These results are in line with the reported properties of *Pfu*Primase and its catalytic subunit p41 (Liu *et al*, 2001). The same study also revealed that the large subunit of *Pfu*Primase displays high affinity for dsDNA.

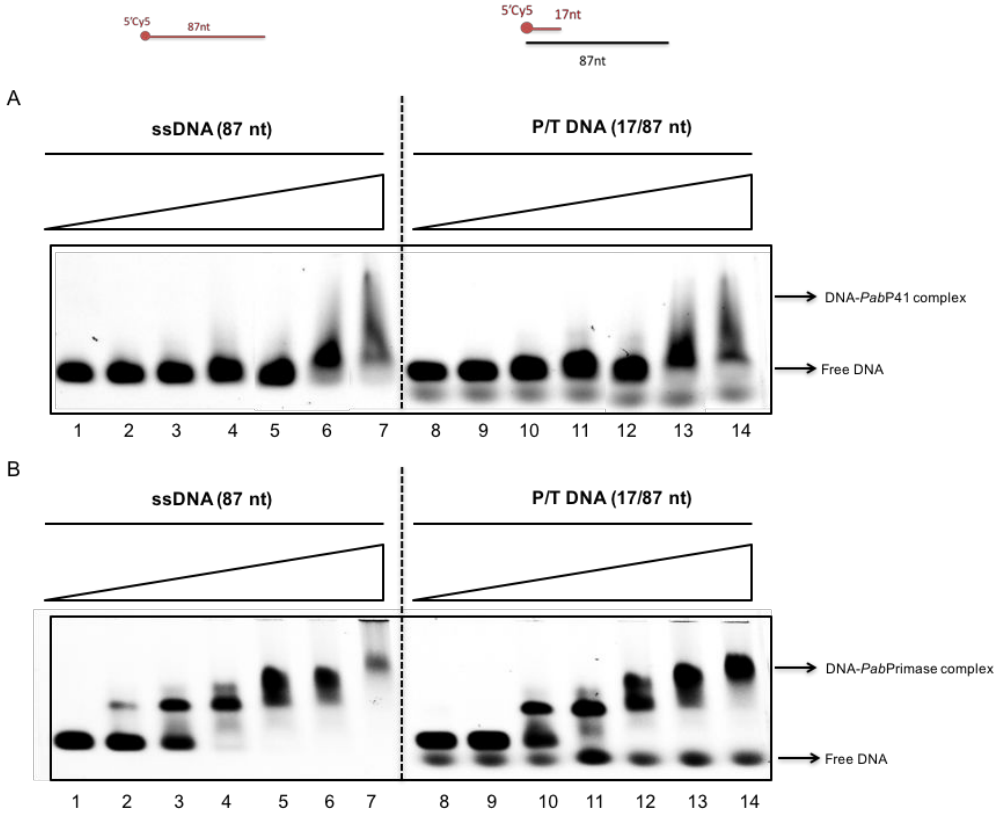

Figure 60 : DNA binding activity of *Pab*P41and *Pab*Primase. *Pab*P41 (0; 20; 40; 80; 100; 160 and 200 nM) or *Pab*Primse (0; 10; 20; 40; 80; 100; 200 nM) and 10 nM different DNA substrates were incubated without ATP at 55°C for 10 min. Reaction products were analyzed by 0,75% agar gel electrophoresis in 1X TBE buffer, and the bands were detected by autoradiography (A) for DNA-*Pab*P41 complex; (B) for DNA-*Pab*Primase complex.

e) DNA Synthesis

Ability to extend primer/template substrate was then investigated for *Pab*Primase and *Pab*P41. Archaeal DNA primase is an enzyme involved in the replication of DNA, *Pfu*P41 subunit utilizes preferentially dNTPs than rNTPs *in vitro* for the *de novo* synthesis (Liu *et al*, 2001). The primer-elongation activities of DNA primase and the p41 subunit were analyzed in the presence of 5′-end-labeled DNA primers (17nt) hybridized to a short single-stranded DNA template of 87 bases (Figure 61). As shown in Figure 67 A and B, *Pab*P41 and the *Pab*Primase complex were able to elongate DNA primers. Nevertheless, the elongation was not complete and efficiency was higher with the *Pab*Primase complex. This is consistent with previous report of *Pab*Primase characterization (Le Breton *et al*, 2007).

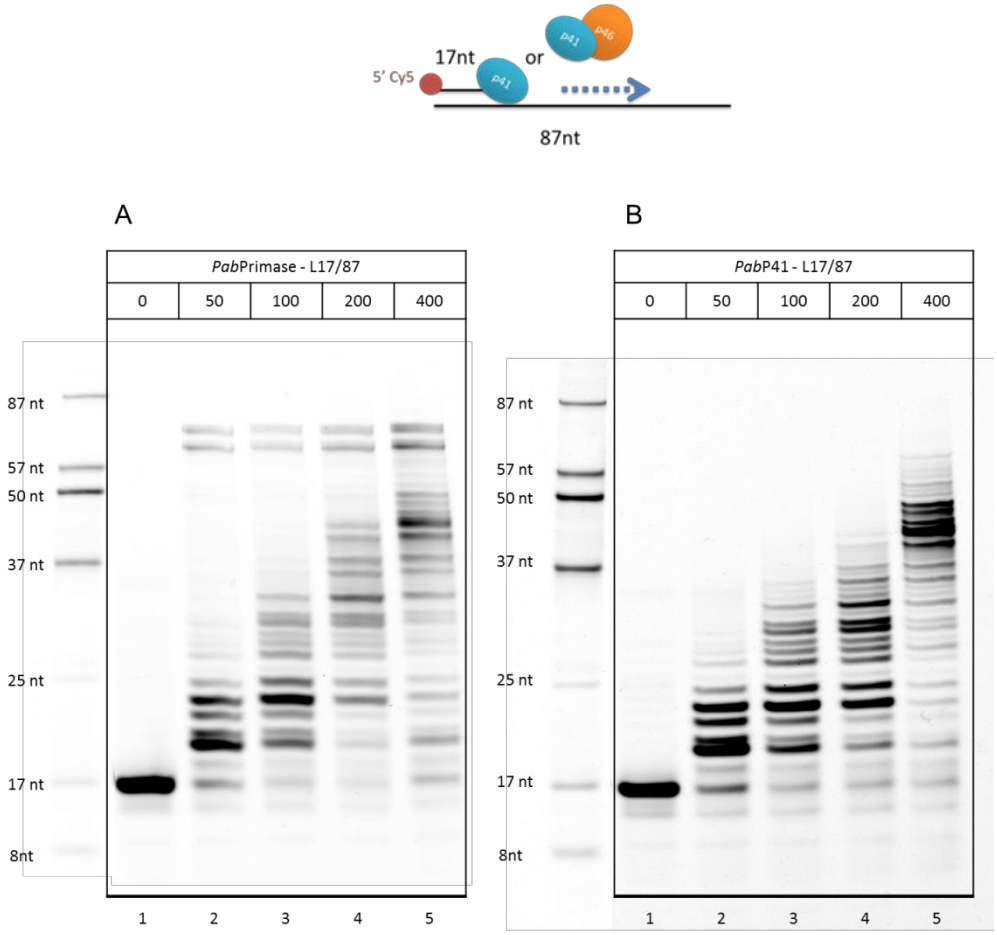

Figure 61 : DNA synthesis activity by *Pab*Primase or *Pab*P41. *Pab*Primase *or Pab*P41 (0, 50, 100, 200, 400 nM) was incubated with 50 nM primed DNA substrate (substrate 17/87) at 55°C for 60 min without ATP. Reaction products were resolved in 18% PAGE and fluorescence revealed using Typhoon 9500 (GE Healthcare).

f) Lesions bypass synthesis

It has already been reported that both isolated p41 subunits and p41-p46 complex from *Archaeoglobus fulgidus,* or p41-p46 complex from *P. furiosus* display translesion abilities to bypass common oxidative DNA lesions, such as 8-Oxo-2-deoxyguanosines (8-oxo dG) and UV light-induced DNA damage (Jozwiakowski *et al*, 2015). In this regard, we checked whether the corresponding enzymes from *P. abyssi* showed similar properties. To this aim, we tested whether *Pab*Primase and *Pabp*41 could traverse 8-oxo dG and deoxyuracil (dU) on templates containing damages at position 33nt. Figure 62 clearly showed that subunit p41 and the primase holoenzyme could readily bypass dU damage, they could also bypass 8-oxo dG damage but with a marked pausing site at the position of the lesion. This result was still in accordance with the reported behavior of primase from *A. fulgidus and P. furiosus* (Jozwiakowski *et al*, 2015). In the same paper, the authors also demonstrated that Euryarchaeal primases were blocked by abasic site lesion.

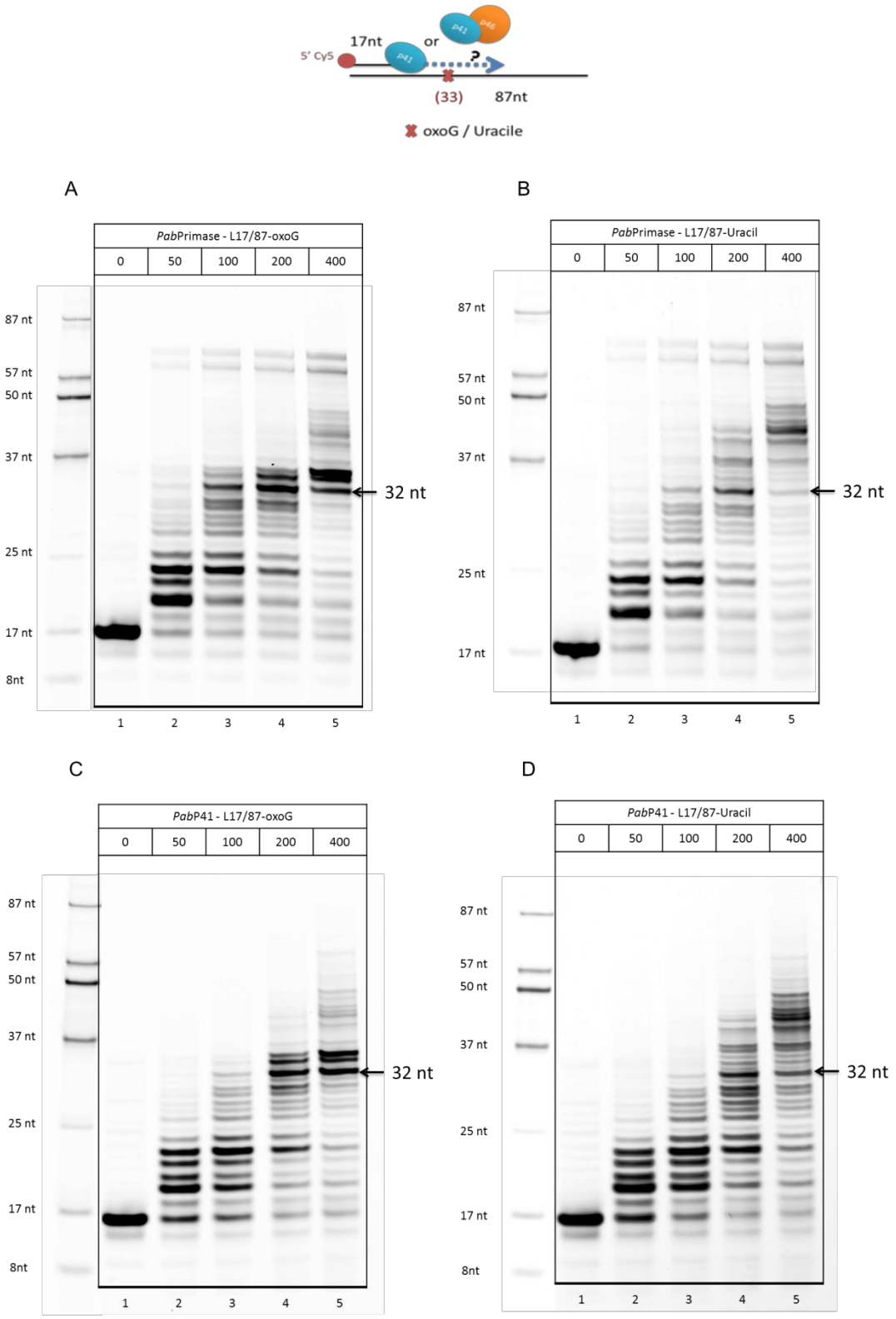

Figure 62 : Translesion synthesis past 8-oxo-dG, dUs. *Pab*Primase *or Pab*P41 (0, 50, 100, 200, 400 nM) was incubated with 50 nM primed DNA substrate with different DNA damages (8-oxo dG or dU) at 55°C for 60 min without ATP. Reaction products were resolved in 18% PAGE and fluorescence revealed using Typhoon 9500 (GE Healthcare).

Indeed, thermophilic archaea are subjected to increased levels of oxidative stress, promoting depurination of 8-oxo dG to apurinic site (AP) and we demonstrated in the laboratory that endogenous AP sites persist in the genome of *P. abyssi* and at a slightly higher level compared with *Escherichia coli* (Palud *et al*, 2008). Figure 63 showed that, consistent with previous report, primase and p41 subunit from *P. abyssi* could not bypass this type of lesion. Notably, we previously demonstrated that presence of AP sites strongly inhibited the DNA polymerizing activity of the only two DNA polymerases from *P. abyssi*, *Pab*PolB and *Pab*PolD, which raises the question of how *P. abyssi* can cope with abasic lesions present in the genome?

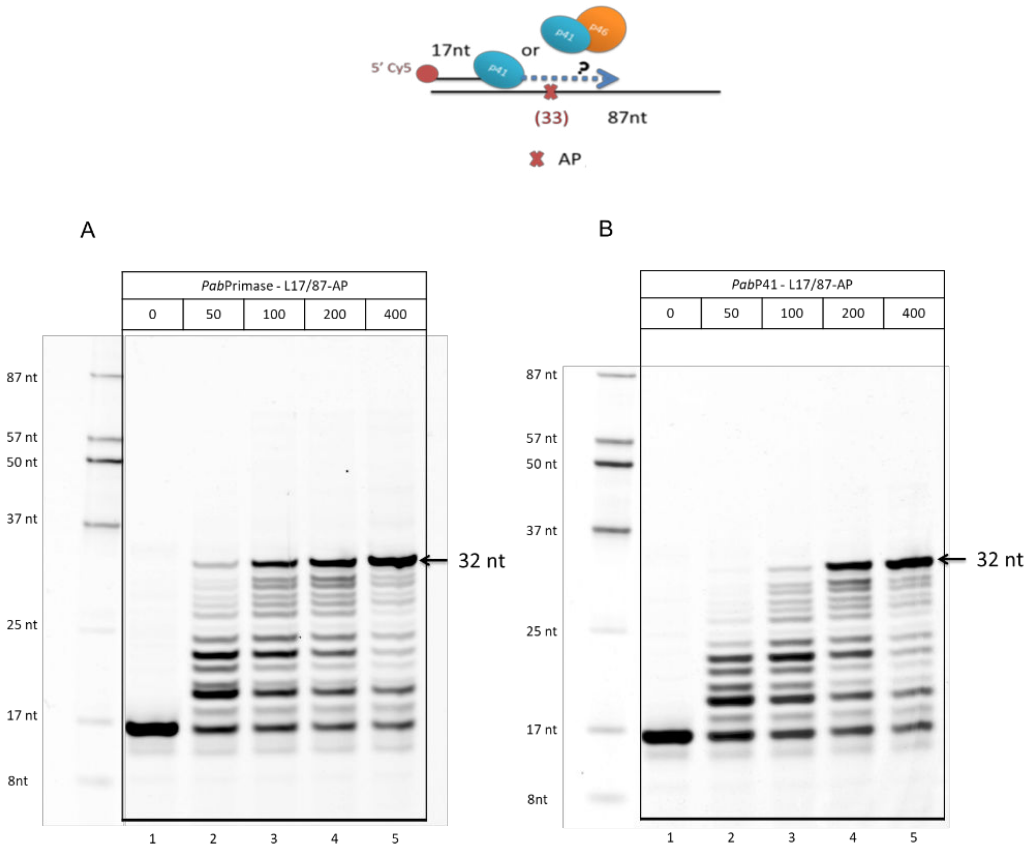

Figure 63 : Translesion synthesis past an abasic site. *Pab*Primase or *Pab*P41 (0, 50, 100, 200, 400 nM) was incubated with 50 nM primed DNA substrate with AP site at 55°C for 60 min without ATP. Reaction products were resolved in 18% PAGE and fluorescence revealed using Typhoon 9500 (GE Healthcare).

3) Could RadA help Primase to perform Translesion Synthesis?

At that point, we confirmed that the primase and recombinase, produced and purified, displayed the expected activities. We then sought to study a potential functional interplay between these proteins. The first hypothesis tested was the possibility that RadA might help primase to bypass damages, and more particularly AP sites, as we demonstrated, *in vitro,* that neither DNA polymerases nor DNA primase from *P. abyssi* are able to bypass this kind of lesion, detected in the genome (Palud *et al*, 2008). The rational basis for the exploration of such a hypothesis also stems from the description of a comparable association in *E. coli*, where DNA polymerase V, activated by a RecA nucleoprotein filament (RecA*), catalyzes translesion DNA synthesis.

Pol V is a low-fidelity DNA polymerase induced as part of the SOS regulation in *E. coli* in response to DNA damage. The replicative polymerase, pol III, typically stalls when it encounters a DNA template lesion. One pathway that enables restoration of fork movement involves pol V, which replaces pol III and catalyzes translesion DNA synthesis. After TLS, pol III resumes normal replication. Both *in vitro* and *in vivo*, pol V TLS activity requires the assembly of an active RecA filament on single-stranded (ss) DNA, termed RecA* (The active form of DNA polymerase V is UmuD′2C–RecA–ATP (Jiang *et al*, 2009). In addition, an *in vitro* system has been reconstituted containing PolV subunit and RecA that demonstrated replicative bypass of a single AP DNA lesion (Rajagopalan *et al*, 1992). Although polV from *E. coli* is obviously not a DNA primase, it was tempting to speculate that an association of primase and RadA could play a similar function in bypassing DNA lesions in Archaea.

To this aim, we used the same experimental design, as described above, to test the abilities of primase and p41 subunit to bypass AP site in presence of RadA. In this case, however, we used RadA from *P. furiosus*, as the protein was produced in greater amount and was more efficient than *Pab*RadA in strand exchange reaction. Similar results were obtained when *PabRadA* was used instead of *PfuRadA* (data not shown). Figure 64 showed that in absence of RadA protein, the DNA synthesis by primase and p41 subunit was blocked, as expected (Lane 3 of Figure 64 A and B). When RadA was added in the reaction, we could not observe DNA synthesis above the damaged site indicating that, in these conditions, RadA could not mediate translesion synthesis by

primase or p41 subunit. On the contrary, increasing concentration of RadA resulted in strong inhibition of DNA synthesis for both enzymes (Lane 4-6 of Figure 64 A and B). We demonstrated above that RadA can bind to primer template substrate (Figure 57E), we thus suppose that excess of RadA might saturate the DNA substrate and prevent access to the primase. One study has demonstrated that higher concentration of RecA were highly inhibitory for PolV-mediated DNA synthesis (Pham *et al*, 2001).

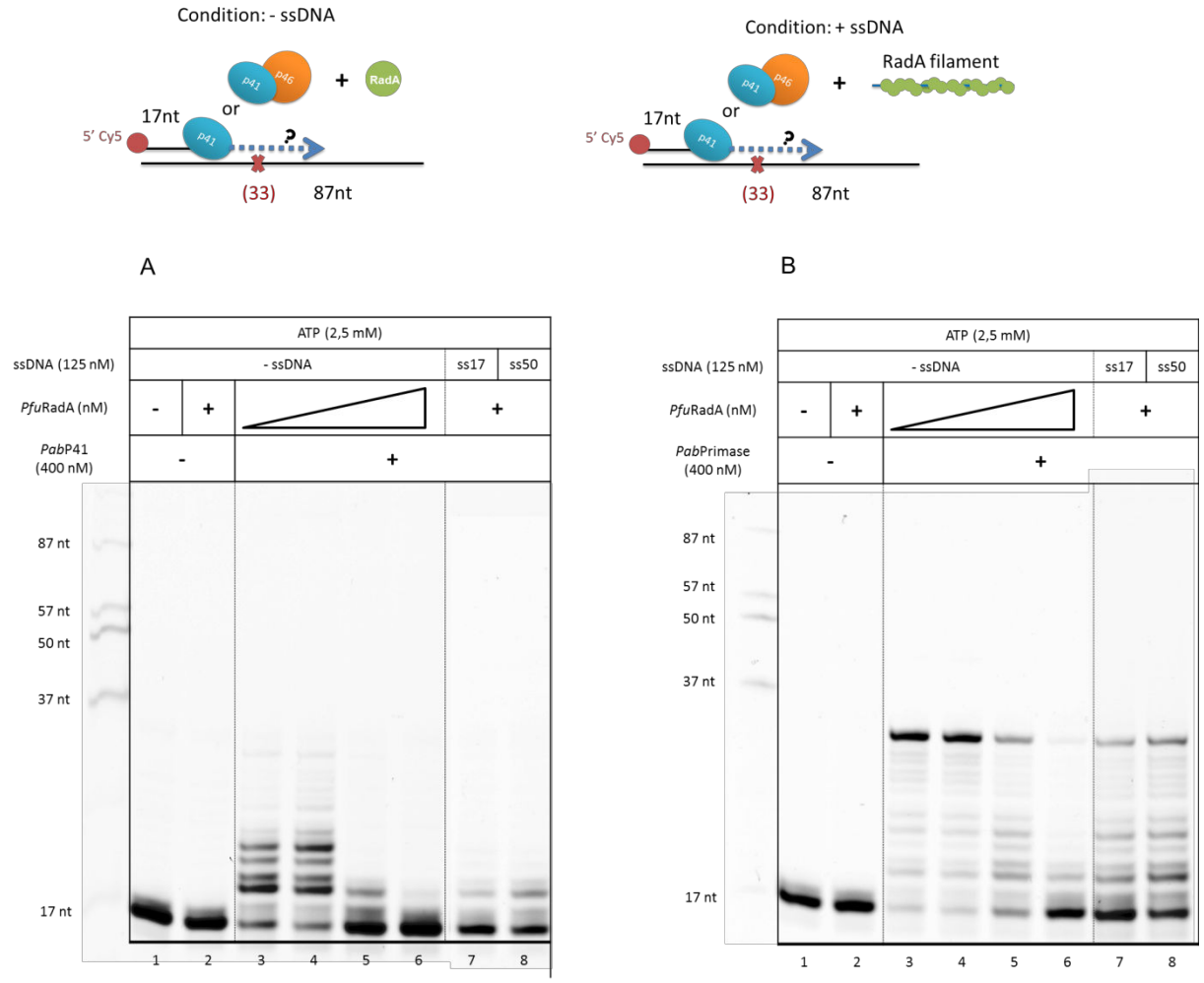

Figure 64 : No TLS effect by P41 or Primase in the presence of RadA. (i)*Pfu*RadA (0, 400, 1250, 2500 nM) was pre-incubated with 50 nM primed DNA substrate containing AP site, or (ii) 2500 nM *Pfu*RadA was pre-incubated with 125 nM ssDNA for 10 min at 55°C, then (i) 400 nM *Pab*Primase or *Pab*PP41, or (ii) 50 nM primed DNA substrate and 400 nM *Pab*Primase or *Pab*P41 were added and incubated at 55°C for 60 min with 2,5 mM ATP. Reaction products were resolved in 18% PAGE and fluorescence revealed using Typhoon 9500 (GE Healthcare).

Several studies have shown that a trans-activated RecA nucleoprotein filament is required for activation of its PolV-catalyzed TLS *in vitro* (Schlacher *et al*, 2006; Jiang *et al*, 2009). In this context, we added ssDNA in the reaction. We used two types of ssDNA, one was homologous to the template, corresponding to the region of the primer/template, the other oligonucleotide is a mixed sequence without homology with the substrate. We wanted to see whether DNA filament formation or strand exchange activity were necessary for the activation of TLS activity of DNA primase. The ssDNA was pre-incubated with an excess of RadA to form a saturated amount of nucleation filament, and then primase and damaged primed DNA were added into the reaction. Once again, we could not observe TLS activity, in these conditions, for both *Pab*Primase and *Pab*P41 (Figure 64A & B, Lane 7-8).

4) Which DNA polymerase promotes DNA synthesis from strand invasion intermediates of HR

We were disappointed by these results but decided to investigate the potential association of primase and RadA in a different context. Indeed, this detected association could also indicate that DNA primase might have a role in DNA recombination pathway. The most obvious hypothesis would be that Primase or p41 subunit could be in charge of DNA synthesis from strand Invasion Intermediates of homologous recombination. Indeed, it has been shown in Eucaryotes and Bacteria, that specialized translesion-synthesis DNA polymerases (polη and pol IV, respectively) can extend DNA synthesis from D-loop recombination intermediates in which an invading strand serves as the primer (as mentioned in Figure 53, Page 128) (McIlwraith *et al*, 2005; Pomerantz *et al*, 2013).

In contrast, this question, of which polymerase has the ability to extend D loop recombination intermediates, is still pending for the Archaea. However, answering this question turns out to be crucial in the context of recent findings demonstrating that in euryarchaea *Haloferax volcanii* and *Thermococcus kodakarensis*, origins of replication are not essential and deletion of all known origins of replication does not result in growth defects (Hawkins *et al*, 2013). It has thus been suggested that origin-depleted cells depended upon the recombination machinery to initiate DNA replication. Most surprisingly, under normal growth conditions, even when the putative origin is present, *T. Kodakarensis* did not utilize the origin, and initiation occurred at many sites along the chromosome (Gehring *et al*, 2017). These different reports emphasize the importance of studies aiming to highlight interplay between DNA recombination and DNA replication mechanisms in Archaea.

In this regard, we looked at the performance of DNA polymerases B and D as well as primase and p41 subunit from *P. abyssi* on synthetic substrates mimicking D-loop recombination intermediates. For that purpose, we used the exonuclease-deficient versions of PolB and PolD to concentrate first on the extension activities of these enzymes. Purified PolB exo- and Pold exo- were already available in the laboratory.

We started with the study of extension activities by the polymerases on a simple 17nt/87nt primer/template substrate in absence or presence of RadA. To unify the reaction condition, we used the same reaction buffer of *Pab*41 and *Pab*Primase to test the DNA synthesis activity of *Pab*PolB and *Pab*PolD. Figure 65 showed that addition of RadA in primer extension reactions did not drastically change the extension capabilities of the enzymes. Increase of PolD exo- efficiency and slight inhibition of p41 subunit (Figure 65 A and B, lane 12 and 6), at high concentration of RadA, were only observed once and it is thus difficult to conclude on a robust effect of RadA in these conditions.

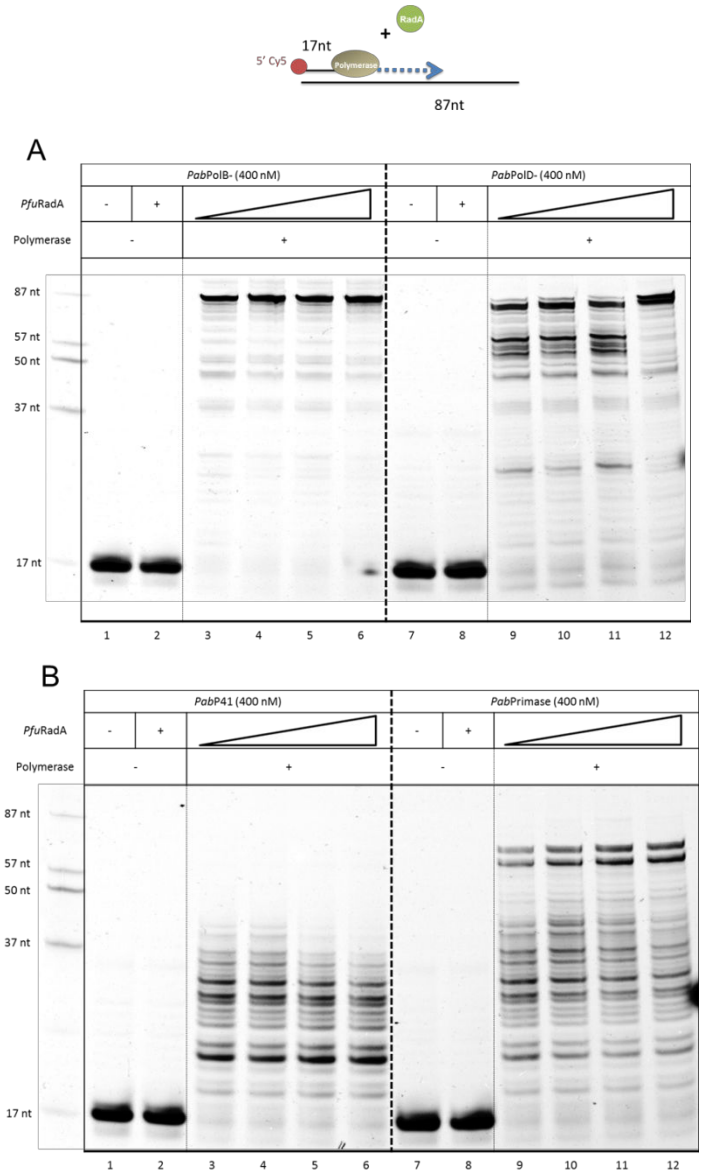

Figure 65 : RadA has no significative effect on DNA extension by different polymerases. *Pfu*RadA (0, 400, 1250, 2500 nM) was pre-incubated with 50 nM primed DNA substrate (substrate 17/87) for 10 min at 55°C, then 400 nM *Pab*PolB, *Pab*PolD, *Pab*Primase or *Pab*P41were added and incubated at 55°C for 60 min without ATP. Reaction products were resolved in 18% PAGE and fluorescence revealed using Typhoon 9500 (GE Healthcare).

To go further, we put the four polymerases to the test to extend D-loop intermediates. This substrate consisted of three distinct oligonucleotides forming D-loop after annealing. In this structure, the two strands of a double-stranded DNA molecule are separated for a stretch and held apart by a third FAM-labeled strand of DNA, which extension can be followed by migration of the reaction products in denaturating PAGE (Figure 66, top). We first observed an already reported phenomenon when primase and p41 subunit were in presence of labeled ssDNA (control lanes 1 in Figure 66 A and B). Indeed, these two enzymes displayed 3'-terminal nucleotidyl-transferase activity, being able to incorporate nucleotides at the 3' end of synthetic oligonucleotides in a non-templated manner. This property was already reported for the DNA primase of *Sulfolobus solfataricus* (De Falco *et al*, 2004; Lao-Sirieix & Bell, 2004). This peculiar activity might indicate that Archeal DNA primase may play a role in DNA repair. We then observed that both DNA primase holenzyme and PolB were able to extend the intermediate to completion (61nt, Figure 66A and C). DNA polB was particularly proficient in synthesizing the full product, as equimolar ratio of enzyme/DNA was sufficient to observe both synthesis of 61nt product and nearly complete use of the template. This result is to be linked with the reported PolB's endowment of strand displacement (Henneke, 2012). In contrast, PolD could not elongate the primer to produce a full product (Figure 66D lanes 4-7), however it could incorporate 3-4 nucleotides and increasing concentrations of PolD did not improve this extension activity. The p41 subunit of primase displayed low efficiency on primer/template and was not able to synthesize a full product (figure 66B lane 2). When RadA was added to the reaction, p41 subunit, as well as primase holoenzyme, could incorporate one nucleotide, however in the case of p41, increasing concentrations only slightly improve incorporation activity (Figure 66B, lanes 4-7).

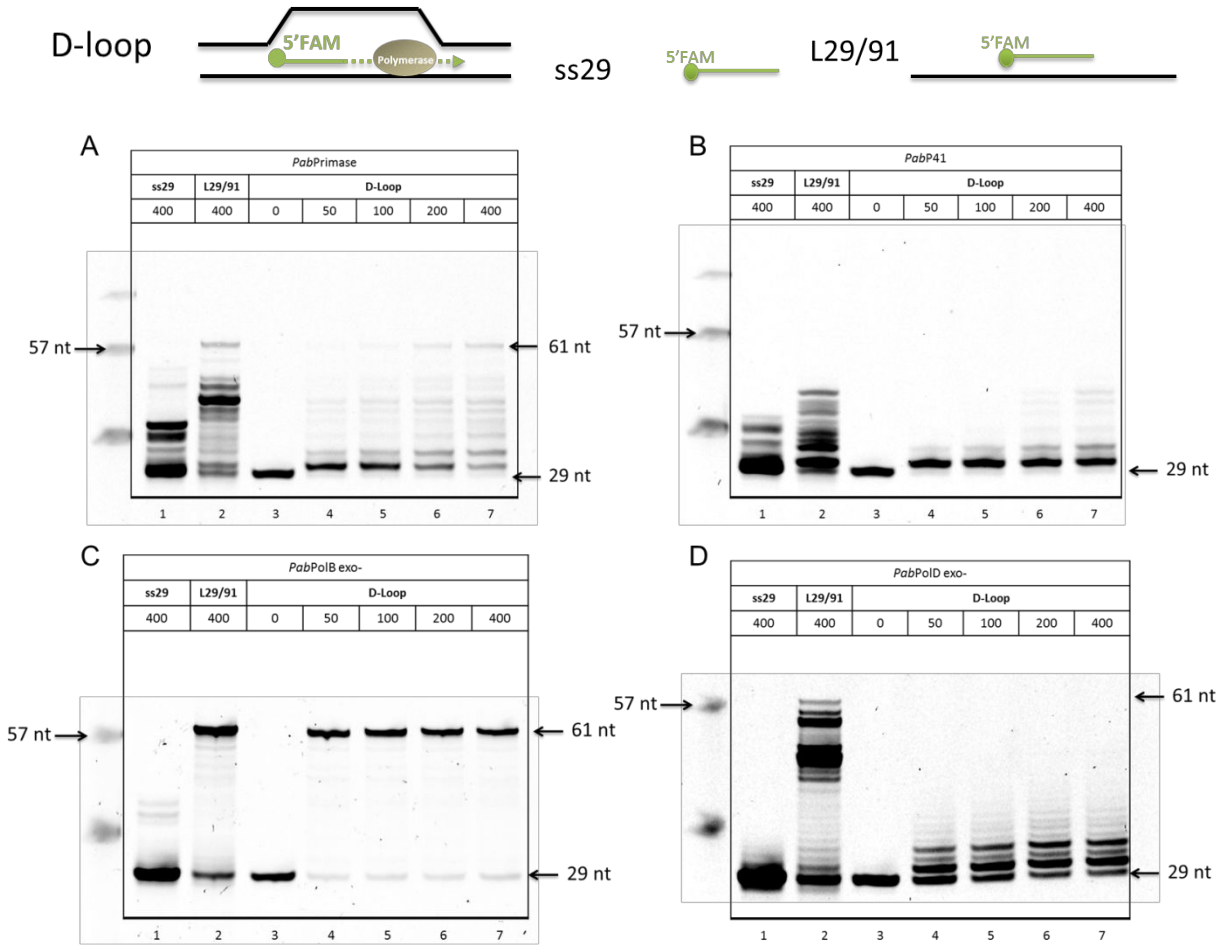

Figure 66 : DNA extension on D-loop by different DNA polymerases from *Pyrococcus abyssi*. *Pab*PolB, *Pab*PolD, *Pab*Primase *or Pab*P41(0, 50, 100, 200, 400 nM) were incubated with 50 nM synthetic DNA D-loop substrate at 55°C for 60 min in the absence of ATP. Reaction products were resolved in 18% PAGE and fluorescence revealed using Typhoon 9500 (GE Healthcare).

Altogether, these results indicate that, in these conditions, PolB seems to be the best candidate to take charge of D-loop extension. However, these results are still preliminary; repetitions are needed to confirm these data. Indeed, as I was running out of time at the end of my PhD I could not repeat these last experiments and neither could I perform the additional experiments that were planned to investigate further the functional interplay between recombinase and polymerases in the context of D-loop extension. In the next chapter, I will describe what would be, in my opinion, the follow up experiments to perform in order to have a better molecular understanding of this process in Archaea.

General conclusion

In thesis, I have studied two functional interactions between proteins potentially involved in homologous recombination in hyperthermophilic Thermococcales.

In Chapter I, we studied the physical and functional interplay between PCNA and Mre11-rad50 complex from *P. furiosus*. We have identified a physical association between PCNA and MR complex. In addition, we have demonstrated functional interplay *in vitro* between *Pfu*MR complex and *Pfu*PCNA in the DNA end resection. At physiological ionic strength, PCNA stimulates MR nuclease activities for DNA end resection and promotes an endonucleolytic incision proximal to the 5' strand of DNA DSBs. In our conditions, we have shown that *Pfu*PCNA/MR don't have DNA helicase activity, however, in condition suitable for DNA cleavage, the endonucleasic cleavage product (27-29 nt) was displaced from the initial dsDNA substrate. Hence, we propose that *Pfu*PCNA stimulates *Pfu*MR DNA end processing leading to an internal cleavage coupled with 5' end removal, to free 3'overhang ssDNA for the subsequent step in HR pathway. Furthermore, the genetic study of the PIP motif deletion in *T. barophilus* gave a preliminary result, suggesting that interaction of PCNA with MR complex may be essential for cells viability. Altogether, our findings indicate that the both physical and functional interactions between *Pfu*MR complex and *Pfu*PCNA consist with an end resection process for the HR pathway.

To sum up the main results obtained in the context of homologous recombination, we propose a revised model for this pathway in hyperthermophilic archaea (Figure 67). We propose that once DNA from HA suffers DSBs, MR/PCNA complex will be recruited to DNA ends, and perform a endonuclease cleavage at 5' end of DNA and displace this 5' fragment to free a 3'overhang in size of 27-29 nt. Interestingly, we demonstrated in the laboratory that at least 20 nt are required for binding one *Pab*RPA trimer onto DNA efficiently. This means that the product of nuclease/unwinding activity of PCNA/MR complex could be bound by RPA in order to prevent ssDNA nuclease degradation. In a following step, NurA/HerA complex could load on the protected 3'overhang substrate to trigger 5'→3' exonucleasic degradation to produce a long 3'end that is used for the strand invasion step. In support to this hypothesis, it has been

shown that HerA/NurA complex preferentially processes short overhang substrates, either 3' or 5', in comparison to blunt DNA substrates (Blackwood *et al*, 2012). However, up to now, there is no mechanistic evidence to suggest how the HerA/NurA helicase–nuclease works in conjunction with the Mre11-Rad50 complex.

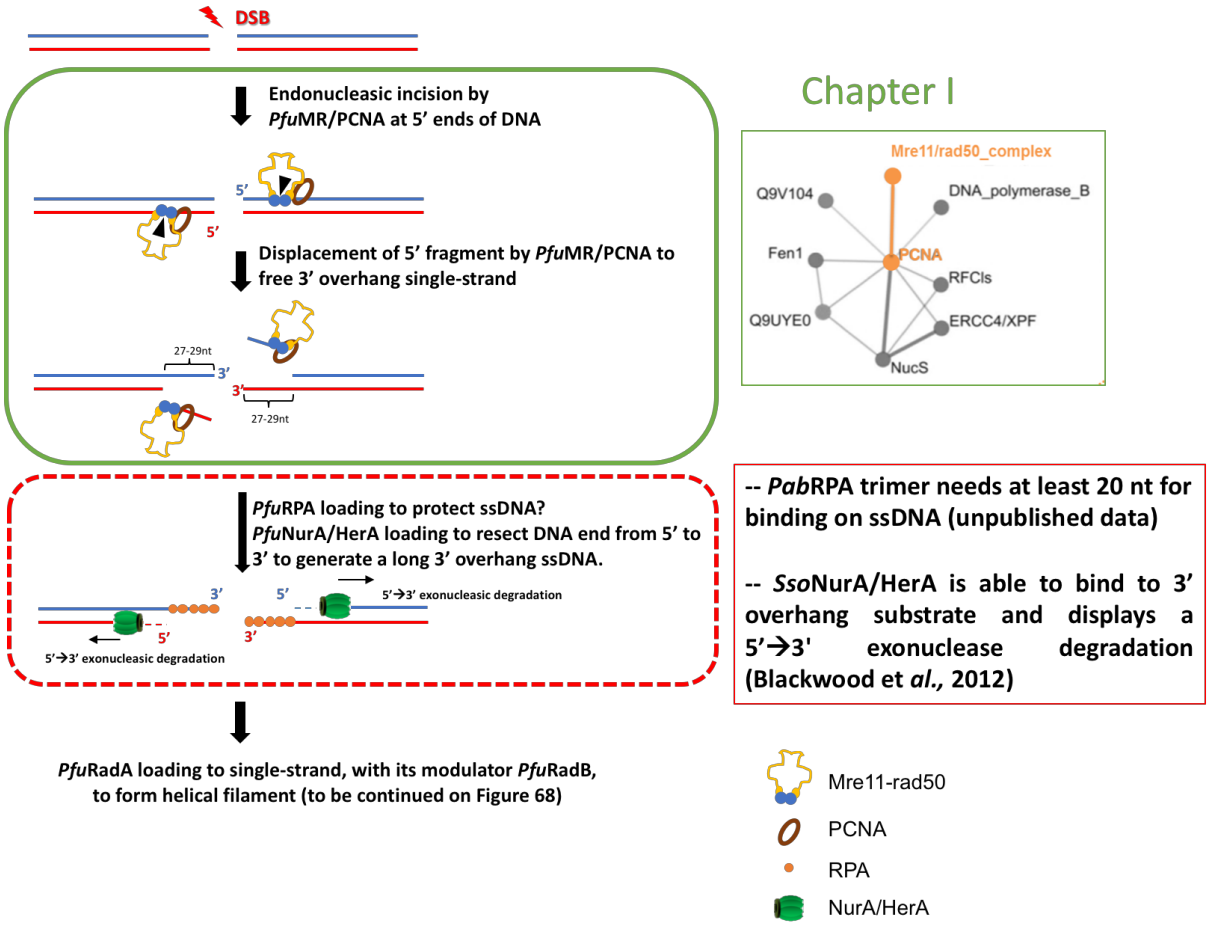

Figure 67: Model of initiation of homologous recombination in hyperthermophilic archaea. Adapetd from (Blackwood *et al*, 2012; Hogrel *et al*, 2018)**.** Green solid box : confirmed results from chapter I ; Red boxes: speculative mechanism (dotted line) and supporting findings (solid line) . *Pab: Pyrococcus.abyssi; Sso: Sulfolobus solfataricus; Pfu: Pyrococcus furiosus*.

In chapter II, we explored the functional interplay between DNA Primase and recombinase RadA from *P. abyssi* or *P. furiosus*. In the first time, we have successfully produced and purified different proteins required: *Pab*RadA, *Pfu*RadA, *Pab*P41 (catalytic subunit of Primase) and *Pab*Primase (or *Pab*p41_p46 complex). Enzymatic activities of each protein were tested subsequently. Our results have shown that all of enzymes bound different DNA substrate (ssDNA, dsDNA and primed DNA) in an ATP-independent manner. *Pab*RadA preferentially binds to ssDNA in comparison to others. We also demonstrated that *Pab*RadA/*Pfu*RadA possesses both D-loop formation and strand exchange abilities in ATP-dependent manner. Both *Pab*P41 and *Pab*Primase have primer-elongation activities. Then we tested biological function of Primase/RadA association. The first hypothesis regarding a potential function in TLS synthesis did not prove to be accurate as, in the condition tested, primer-elongation by *Pab*Primase holoenzyme or P41 subunit alone was blocked by abasic site lesion in the absence or presence of *Pfu*RadA. We then tested DNA synthesis from strand invasion intermediates. We have shown that in our condition without ATP with a simple primer/template substrate, RadA doesn't have significant effect on primer extension by PolD exo-, PolB exo-, Primase and P41, although there is an augmentation of PolD exo- efficiency and a slight inhibition of *Pab*p41; however, these observations need to be conformed. With the mimic D-loop substrate, we have observed that both *Pab*PolB and *Pab*Primase can perform a complete primer extension, but *Pab*PolB has a much higher efficiency than *Pab*Primase. In contrast, *Pab*P41 displayed a low efficiency on mimic D-loop substrate, while *Pab*PolD incorporated only 3 or 4 nucleotides.

To replace these findings in the model of HR in hyperthermophilic archaea, we propose that polymerase (PolB or Primase) could extend the D-loop intermediate, and DNA ligase could be recruited by PCNA or primase to ligate the nick. Simultaneously, strand exchange results in the formation of holiday junctions that can branch migrate, possibly catalyzed by the Hjm. Hjm is stimulated by PCNA, and can interact with the junction-resolving enzymes Hjc, which can form a functional complex with PCNA. Finally, DNA ligase will seal the resultant nicked duplexes (Figure 68).

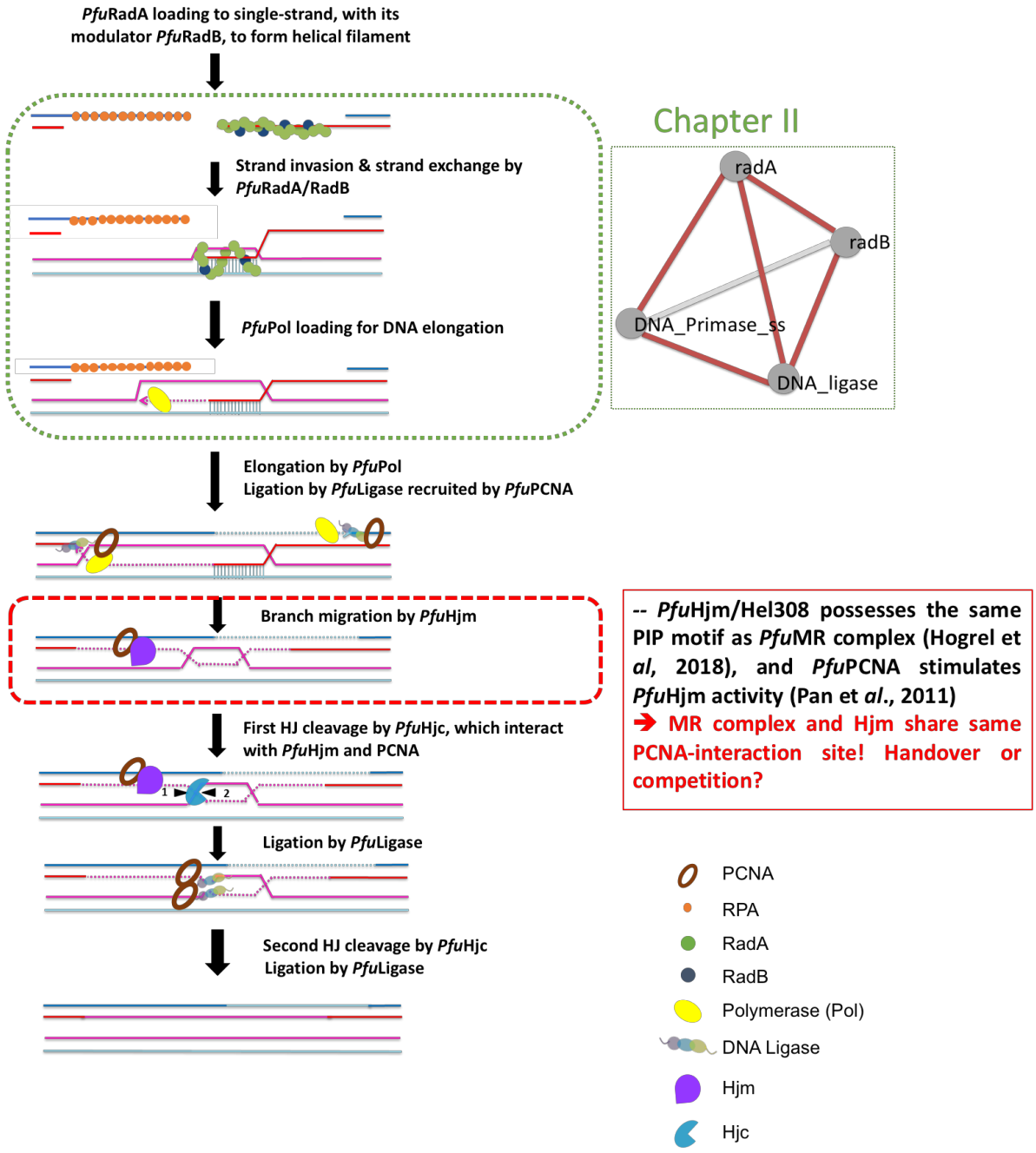

Figure 68: Model of homologous recombination after initiation in hyperthermophilic archaea. Study from (Hogrel *et al*, 2018; Pan *et al*, 2011). Green dotted box : obtained results from chapter II ; Red box: Observed mechanism (dotted line) and supporting links between observed mechanism and Chapter I's findings (solid line): *Pfu: Pyrococcus furiosus*

This model is still speculative, but we believe that it could serve as a basis to address pending questions in order to get a comprehensive understanding of HR pathway in Archaea. In particular, this model highlights the following questions:

Is there a coordination between MR complex and HerA/NurA complex at dsDNA break to achieve generation of long 3'overhang substrate necessary for RadA loading ?

Which polymerase is in charge of extension of D-loop intermediates?

Perspectives:

To answer these questions, the effect of RPA on distinct activities of MR complex should be looked at. Indeed, we could consider the possibility that RPA could improve both the endonucleolytic cut promoted by PCNA/MR and the observed local unwinding activity. In support to this hypothesis, we have shown in the laboratory that RPA displayed limited unwinding ability. In addition, we should also perform nuclease assays for PCNA/MR complex in the presence of NurA/HerA complex to detect the generation of long 3'overhang products that might reflect a concerted work between the two complexes. To this aim it would be beneficial to carry out these assays using linear plasmids. In addition, the inactive mutant versions of all these key players should prove to be beneficial to dissect enzymatic contributions of these proteins to deliver the proper DNA substrate for RadA loading.

To answer the other question regarding the identity of polymerase involved in elongation of HR intermediates, the next step could be to see the activity of polymerases, but this time in presence of RadA, on synthetic D-loop substrate. Finally, the test will be applied in the model that RadA-induced strand exchange between ssDNA and double-stranded circular DNA, and then Primase-induced extension from the invaded primer (Figure 69). From this experimental design, we can explore if primase, or other polymerases is able to load on invaded ssDNA strand and initiate primer extention. The length of primer extension could help us to decide the function of primase in this model is used for "primer synthesis" or "primer elongation".

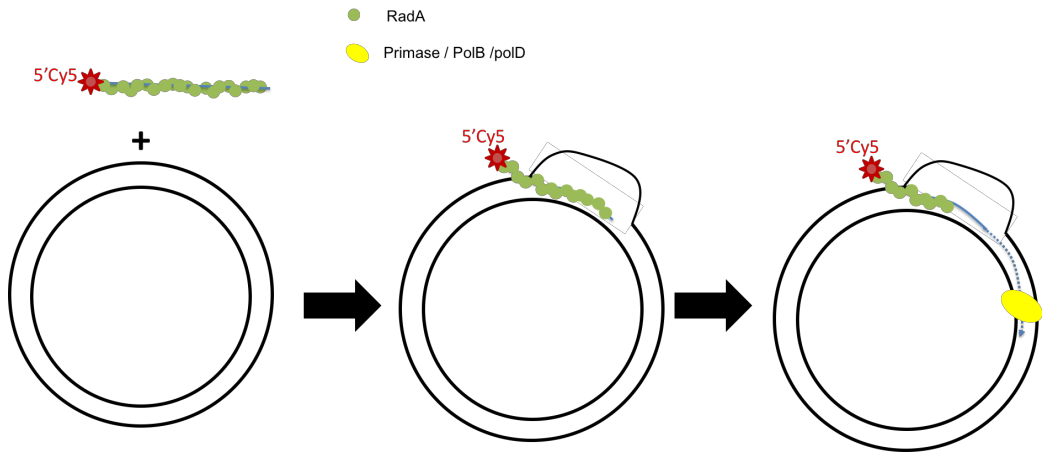

Figure 69: Proposed test to study Primase exention from RadA-induced invaded strand.

In the sub-network of chapter II, RadB and Ligase are two other proteins identified with RadA and Primase.

RadB is a paralogous of RadA, which is only found in euryarchaeota, not in crenarchaeota (Haldenby *et al*, 2009; McRobbie *et al*, 2009). Archaeal RadB is involved in homologous recombination in modulating RadA activity by direct interaction *in vitro* and *in vivo*. For exemple, *Pfu*RadB inhibits RadA-induced strand exchange activity (Komori *et al*, 2000b), or *Hvo*RadB plays a role in stabilizing RadA filaments (Wardell *et al*, 2017). RadB can interact with other protein involved in HR, for example, *Pfu*RadB interacts with Holliday junction resolvase (Hjc). *Pfu*RadB is able to stimulate Holliday junction cleavage activity of Hjc (Komori *et al*, 2000b). *Pfu*RadB interacts also with the small subunit DP1 of PolD; it suggested that RadB might play a minor role in DNA replication (Hayashi *et al*, 1999).

*Pfu*Ligase is a strict ATP-dependent ligase, the main function of DNA ligase is to catalyze the phosphodiester bond formation. Interestingly, *Pfu*Ligase alone cannot bind to a nicked DNA substrate at a high salt concentration; it needs *Pfu*PCNA to form a DNA Ligase-PCNA-DNA complex and to stimulate its enzymatic activity (Kiyonari *et al*, 2006; Ishino & Ishino, 2012) .

Purification of *Pab*RadB and *Pab*Ligase and then characterization of their functional activities should be performed also. Then try to detect the effect of RadB on RadA or add RadB and Ligase in the reaction to explore more functional effect among these four proteins.

We will continue to identify activities and molecular interactions of individual enzymes that have a plausible connection with DNA repair and replication fidelity, however the best route to understanding biologica function will be whether the proposed contribution to genome maintenance can be confirmed in living archaeal cells. Unfortunately, as already stated in this document, the genes for DNA recombination proteins in HA are essential. In the long term of these two studies, we can try to develop conditional mutants or fluorescent-labeled proteins *in vivo*, leading to observe the co-localization of fluorescent proteins (such as PCNA/MR, RadA/Primase, RadA/RadB, RadB/Primase etc) during cells growth, or after inducing different DNA damage, using UV that induces DSB, or Hydroxyurea that induces stalled replication forks, to confirm a precise role of these proteins in HR involved in DNA replication and repair mechanism.

Reference

A

Achenbach-Richter L, Gupta R, Stetter KO & Woese CR (1987) Were the original eubacteria thermophiles? *Syst. Appl. Microbiol.* **9:** 34–39

Adams MW (1998) The biochemical diversity of life near and above 100°C in marine environments. *J. Appl. Microbiol.* **85 Suppl 1:** 108S-117S

Adelman CA, De S & Petrini JHJ (2009) Rad50 is dispensable for the maintenance and viability of postmitotic tissues. *Mol. Cell. Biol.* **29:** 483–492

Ahdash Z, Lau AM, Byrne RT, Lammens K, Stüetzer A, Urlaub H, Booth PJ, Reading E, Hopfner K-P & Politis A (2017) Mechanistic insight into the assembly of the HerA–NurA helicase–nuclease DNA end resection complex. *Nucleic Acids Res* **45:** 12025–12038

Ait Saada A, Lambert SAE & Carr AM (2018) Preserving replication fork integrity and competence via the homologous recombination pathway. *DNA Repair (Amst.)*

Akanuma S, Nakajima Y, Yokobori S, Kimura M, Nemoto N, Mase T, Miyazono K, Tanokura M & Yamagishi A (2013) Experimental evidence for the thermophilicity of ancestral life. *Proc Natl Acad Sci U S A* **110:** 11067–11072

Anand R, Ranjha L, Cannavo E & Cejka P (2016) Phosphorylated CtIP Functions as a Co-factor of the MRE11-RAD50-NBS1 Endonuclease in DNA End Resection. *Mol. Cell* **64:** 940–950

Aparicio T, Baer R & Gautier J (2014) DNA double-strand break repair pathway choice and cancer. *DNA Repair (Amst.)* **19:** 169–175

Aravind L & Koonin EV (2001) Prokaryotic homologs of the eukaryotic DNA-end-binding protein Ku, novel domains in the Ku protein and prediction of a prokaryotic double-strand break repair system. *Genome Res.* **11:** 1365–1374

Arezi B & Kuchta RD (2000) Eukaryotic DNA primase. *Trends Biochem. Sci.* **25:** 572–576

Armstrong AA, Mohideen F & Lima CD (2012) Recognition of SUMO-modified PCNA requires tandem receptor motifs in Srs2. *Nature* **483:** 59–63

Assenmacher N & Hopfner K-P (2004) MRE11/RAD50/NBS1: complex activities. *Chromosoma* **113:** 157–166

Augustin MA, Huber R & Kaiser JT (2001) Crystal structure of a DNA-dependent RNA polymerase (DNA primase). *Nat. Struct. Biol.* **8:** 57–61

B

Bakermans C (2015) Microbial Evolution under Extreme Conditions Berlin, Boston: De Gruyter

Barfoot T, Herdendorf TJ, Behning BR, Stohr BA, Gao Y, Kreuzer KN & Nelson SW (2015) Functional Analysis of the Bacteriophage T4 Rad50 Homolog (gp46) Coiled-coil Domain. *J. Biol. Chem.* **290:** 23905–23915

Barry ER & Bell SD (2006) DNA Replication in the Archaea. *Microbiol. Mol. Biol. Rev.* **70:** 876–887

Bartlett EJ, Brissett NC & Doherty AJ (2013) Ribonucleolytic resection is required for repair of strand displaced nonhomologous end-joining intermediates. *Proc. Natl. Acad. Sci. U.S.A.* **110:** E1984-1991

Bartlett EJ, Brissett NC, Plocinski P, Carlberg T & Doherty AJ (2016) Molecular basis for DNA strand displacement by NHEJ repair polymerases. *Nucleic Acids Res* **44:** 2173–2186

Becerra A, Delaye L, Lazcano A & Orgel LE (2007) Protein disulfide oxidoreductases and the evolution of thermophily: was the last common ancestor a heat-loving microbe? *J. Mol. Evol.* **65:** 296–303

Beck K & Lipps G (2007) Properties of an unusual DNA primase from an archaeal plasmid. *Nucleic Acids Res.* **35:** 5635–5645

Berquist BR, DasSarma P & DasSarma S (2007) Essential and non-essential DNA replication genes in the model halophilic Archaeon, Halobacterium sp. NRC-1. *BMC Genet.* **8:** 31

Bhaskara V, Dupré A, Lengsfeld B, Hopkins BB, Chan A, Lee J-H, Zhang X, Gautier J, Zakian V & Paull TT (2007) Rad50 adenylate kinase activity regulates DNA tethering by Mre11/Rad50 complexes. *Mol. Cell* **25:** 647–661

Bianchi J, Rudd SG, Jozwiakowski SK, Bailey LJ, Soura V, Taylor E, Stevanovic I, Green AJ, Stracker TH, Lindsay HD & Doherty AJ (2013) PrimPol bypasses UV photoproducts during eukaryotic chromosomal DNA replication. *Mol. Cell* **52:** 566–573

Birien T, Thiel A, Henneke G, Flament D, Moalic Y & Jebbar M (2018) Development of an Effective 6-Methylpurine Counterselection Marker for Genetic Manipulation in Thermococcus barophilus. *Genes (Basel)* **9:**

Blackwood JK, Rzechorzek NJ, Abrams AS, Maman JD, Pellegrini L & Robinson NP (2012) Structural and functional insights into DNA-end processing by the archaeal HerA helicase–NurA nuclease complex. *Nucleic Acids Res* **40:** 3183–3196

Blackwood JK, Rzechorzek NJ, Bray SM, Maman JD, Pellegrini L & Robinson NP (2013) End-resection at DNA double-strand breaks in the three domains of life. *Biochem Soc Trans* **41:** 314–320

Bocquier AA, Liu L, Cann IKO, Komori K, Kohda D & Ishino Y (2001) Archaeal primase: bridging the gap between RNA and DNA polymerases. *Current Biology* **11:** 452–456

Boehm EM & Washington MT (2016) R.I.P. to the PIP: PCNA-binding motif no longer considered specific. *Bioessays* **38:** 1117–1122

Borde V (2007) The multiple roles of the Mre11 complex for meiotic recombination. *Chromosome Res.* **15:** 551–563

Boussau B, Blanquart S, Necsulea A, Lartillot N & Gouy M (2008) Parallel adaptations to high temperatures in the Archaean eon. *Nature* **456:** 942–945

Bowater R & Doherty AJ (2006) Making Ends Meet: Repairing Breaks in Bacterial DNA by Non-Homologous End-Joining. *PLoS Genet* **2:**

Brandt S, Samartzis EP, Zimmermann A-K, Fink D, Moch H, Noske A & Dedes KJ (2017) Lack of MRE11-RAD50-NBS1 (MRN) complex detection occurs frequently in low-grade epithelial ovarian cancer. *BMC Cancer* **17:**

Brooks DJ, Fresco JR & Singh M (2004) A novel method for estimating ancestral amino acid composition and its application to proteins of the Last Universal Ancestor. *Bioinformatics* **20:** 2251–2257

Bruning JB & Shamoo Y (2004) Structural and thermodynamic analysis of human PCNA with peptides derived from DNA polymerase-delta p66 subunit and flap endonuclease-1. *Structure* **12:** 2209–2219

Bruskov VI, Malakhova LV, Masalimov ZK & Chernikov AV (2002) Heat-induced formation of reactive oxygen species and 8-oxoguanine, a biomarker of damage to DNA. *Nucleic Acids Res.* **30:** 1354–1363

Bubeck D, Reijns MAM, Graham SC, Astell KR, Jones EY & Jackson AP (2011) PCNA directs type 2 RNase H activity on DNA replication and repair substrates. *Nucleic Acids Res* **39:** 3652–3666

Bugreev DV & Mazin AV (2004) Ca2+ activates human homologous recombination protein Rad51 by modulating its ATPase activity. *Proc. Natl. Acad. Sci. U.S.A.* **101:** 9988–9993

C

Cai J, Wang Y, Liu D, Zeng Y, Xue Y, Ma Y & Feng Y (2007) Fervidobacterium changbaicum sp. nov., a novel thermophilic anaerobic bacterium isolated from a hot spring of the Changbai Mountains, China. *Int. J. Syst. Evol. Microbiol.* **57:** 2333–2336

Cann IK, Ishino S, Hayashi I, Komori K, Toh H, Morikawa K & Ishino Y (1999) Functional interactions of a homolog of proliferating cell nuclear antigen with DNA polymerases in Archaea. *J. Bacteriol.* **181:** 6591–6599

Cann IK, Komori K, Toh H, Kanai S & Ishino Y (1998) A heterodimeric DNA polymerase: evidence that members of Euryarchaeota possess a distinct DNA polymerase. *Proc. Natl. Acad. Sci. U.S.A.* **95:** 14250–14255

Cannavo E & Cejka P (2014) Sae2 promotes dsDNA endonuclease activity within Mre11–Rad50–Xrs2 to resect DNA breaks. *Nature* **514:** 122–125

Cannavo E, Cejka P & Kowalczykowski SC (2013) Relationship of DNA degradation by Saccharomyces cerevisiae exonuclease 1 and its stimulation by RPA and Mre11-Rad50-Xrs2 to DNA end resection. *Proc. Natl. Acad. Sci. U.S.A.* **110:** E1661-1668

Cannon B, Kuhnlein J, Soo-Hyun Yang, Cheng A, Schindler D, Stark J m., Russell R & Paull T t. (2013) Visualization of local DNA unwinding by Mre11/Rad50/ Nbs1 using single-molecule FRET. *Proceedings of the National Academy of Sciences of the United States of America* **110:** 18868–18873

Cannone G, Xu Y, Beattie TR, Bell SD & Spagnolo L (2015) The architecture of an Okazaki fragment-processing holoenzyme from the archaeon Sulfolobus solfataricus. *Biochem. J.* **465:** 239–245

Cassani C, Gobbini E, Vertemara J, Wang W, Marsella A, Sung P, Tisi R, Zampella G & Longhese MP (2018) Structurally distinct Mre11 domains mediate MRX functions in resection, end-tethering and DNA damage resistance. *Nucleic Acids Res.* **46:** 2990–3008

Ceccaldi R, Rondinelli B & D'Andrea AD (2016) Repair Pathway Choices and Consequences at the Double-Strand Break. *Trends in Cell Biology* **26:** 52–64

Cejka P (2015) DNA End Resection: Nucleases Team Up with the Right Partners to Initiate Homologous Recombination. *J Biol Chem* **290:** 22931–22938

Chan MK, Mukund S, Kletzin A, Adams MW & Rees DC (1995) Structure of a hyperthermophilic tungstopterin enzyme, aldehyde ferredoxin oxidoreductase. *Science* **267:** 1463–1469

Chapman JR, Taylor MRG & Boulton SJ (2012) Playing the End Game: DNA Double-Strand Break Repair Pathway Choice. *Molecular Cell* **47:** 497–510

Chemnitz Galal W, Pan M, Kelman Z & Hurwitz J (2012) Characterization of DNA primase complex isolated from the archaeon, Thermococcus kodakaraensis. *J. Biol. Chem.* **287:** 16209–16219

Chen L-T, Ko T-P, Chang Y-C, Lin K-A, Chang C-S, Wang AH-J & Wang T-F (2007a) Crystal structure of the left-handed archaeal RadA helical filament: identification of a functional motif for controlling quaternary structures and enzymatic functions of RecA family proteins. *Nucleic Acids Res.* **35:** 1787–1801

Chen L-T, Ko T-P, Chang Y-W, Lin K-A, Wang AH-J & Wang T-F (2007b) Structural and functional analyses of five conserved positively charged residues in the L1 and N-terminal DNA binding motifs of archaeal RADA protein. *PLoS ONE* **2:** e858

Chen X, Paudyal SC, Chin R-I & You Z (2013) PCNA promotes processive DNA end resection by Exo1. *Nucl. Acids Res.* **41:** 9325–9338

Chen Z, Yang H & Pavletich NP (2008) Mechanism of homologous recombination from the RecA-ssDNA/dsDNA structures. *Nature* **453:** 489–484

Cheng KC, Cahill DS, Kasai H, Nishimura S & Loeb LA (1992) 8-Hydroxyguanine, an abundant form of oxidative DNA damage, causes G----T and A----C substitutions. *J. Biol. Chem.* **267:** 166–172

Chi P, Van Komen S, Sehorn MG, Sigurdsson S & Sung P (2006) Roles of ATP binding and ATP hydrolysis in human Rad51 recombinase function. *DNA Repair (Amst.)* **5:** 381–391

Chiruvella KK, Liang Z & Wilson TE (2013) Repair of Double-Strand Breaks by End Joining. *Cold Spring Harb Perspect Biol* **5:** a012757

Clark AJ & Margulies AD (1965) ISOLATION AND CHARACTERIZATION OF RECOMBINATION-DEFICIENT MUTANTS OF ESCHERICHIA COLI K12*. *Proc Natl Acad Sci U S A* **53:** 451–459

Cohen GN (2014) Microbial Biochemistry Dordrecht: Springer Netherlands

Cohen GN, Barbe V, Flament D, Galperin M, Heilig R, Lecompte O, Poch O, Prieur D, Quérellou J, Ripp R, Thierry J-C, Van der Oost J, Weissenbach J, Zivanovic Y & Forterre P (2003) An integrated analysis of the genome of the hyperthermophilic archaeon Pyrococcus abyssi. *Molecular Microbiology* **47:** 1495–1512

Coker JA (2016) Extremophiles and biotechnology: current uses and prospects. *F1000Res* **5:**

Connelly JC & Leach DR (1996) The sbcC and sbcD genes of Escherichia coli encode a nuclease involved in palindrome inviability and genetic recombination. *Genes Cells* **1:** 285–291

Connelly JC & Leach DRF (2002) Tethering on the brink: the evolutionarily conserved Mre11-Rad50 complex. *Trends Biochem. Sci.* **27:** 410–418

Connelly JC, de Leau ES & Leach DR (1999) DNA cleavage and degradation by the SbcCD protein complex from Escherichia coli. *Nucleic Acids Res.* **27:** 1039–1046

Connelly JC, de Leau ES & Leach DRF (2003) Nucleolytic processing of a protein-bound DNA end by the E. coli SbcCD (MR) complex. *DNA Repair (Amst.)* **2:** 795–807

Connelly JC, de Leau ES, Okely EA & Leach DR (1997) Overexpression, purification, and characterization of the SbcCD protein from Escherichia coli. *J. Biol. Chem.* **272:** 19819–19826

Constantinesco F, Forterre P & Elie C (2002) NurA, a novel 5'–3' nuclease gene linked to rad50 and mre11 homologs of thermophilic Archaea. *EMBO Rep* **3:** 537–542

Constantinesco F, Forterre P, Koonin EV, Aravind L & Elie C (2004) A bipolar DNA helicase gene, herA, clusters with rad50, mre11 and nurA genes in thermophilic archaea. *Nucleic Acids Res.* **32:** 1439–1447

Costanzo V, Robertson K, Bibikova M, Kim E, Grieco D, Gottesman M, Carroll D & Gautier J (2001) Mre11 protein complex prevents double-strand break accumulation during chromosomal DNA replication. *Mol. Cell* **8:** 137–147

Costes A & Lambert SAE (2012) Homologous recombination as a replication fork escort: fork-protection and recovery. *Biomolecules* **3:** 39–71

Cox MM (2001) Recombinational DNA repair of damaged replication forks in Escherichia coli: questions. *Annu. Rev. Genet.* **35:** 53–82

Cox MM (2007) Motoring along with the bacterial RecA protein. *Nat. Rev. Mol. Cell Biol.* **8:** 127–138

Čuboňová L, Richardson T, Burkhart BW, Kelman Z, Connolly BA, Reeve JN & Santangelo TJ (2013) Archaeal DNA Polymerase D but Not DNA Polymerase B Is Required for Genome Replication in Thermococcus kodakarensis. *J Bacteriol* **195:** 2322–2328

D

Dahm R (2005) Friedrich Miescher and the discovery of DNA. *Dev. Biol.* **278:** 274–288

Das D, Moiani D, Axelrod HL, Miller MD, McMullan D, Jin KK, Abdubek P, Astakhova T, Burra P, Carlton D, Chiu H-J, Clayton T, Deller MC, Duan L, Ernst D, Feuerhelm J, Grant JC, Grzechnik A, Grzechnik SK, Han GW, et al (2010) Crystal structure of the first eubacterial Mre11 nuclease reveals novel features that may discriminate substrates during DNA repair. *J. Mol. Biol.* **397:** 647–663

De Falco M, Fusco A, De Felice M, Rossi M & Pisani FM (2004) The DNA primase of Sulfolobus solfataricus is activated by substrates containing a thymine-rich bubble and has a 3'-terminal nucleotidyl-transferase activity. *Nucleic Acids Res.* **32:** 5223–5230

Decottignies A (2013) Alternative end-joining mechanisms: a historical perspective. *Front Genet* **4:** 48

Delmas S, Duggin IG & Allers T (2013) DNA damage induces nucleoid compaction via the Mre11-Rad50 complex in the archaeon Haloferax volcanii. *Mol. Microbiol.* **87:** 168–179

Delong EF & Pace NR. (2001) Environmental Diversity of Bacteria and Archaea. *Syst. Biol.* **50:** 470–478

Deshpande RA, Lee J-H, Arora S & Paull TT (2016) Nbs1 Converts the Human Mre11/Rad50 Nuclease Complex into an Endo/Exonuclease Machine Specific for Protein-DNA Adducts. *Mol. Cell* **64:** 593–606

Deshpande RA, Lee J-H & Paull TT (2017) Rad50 ATPase activity is regulated by DNA ends and requires coordination of both active sites. *Nucleic Acids Res.* **45:** 5255–5268

Deshpande RA, Williams GJ, Limbo O, Williams RS, Kuhnlein J, Lee J-H, Classen S, Guenther G, Russell P, Tainer JA & Paull TT (2014) ATP-driven Rad50 conformations regulate DNA tethering, end resection, and ATM checkpoint signaling. *EMBO J.* **33:** 482–500

Desogus G, Onesti S, Brick P, Rossi M & Pisani FM (1999) Identification and characterization of a DNA primase from the hyperthermophilic archaeon Methanococcus jannaschii. *Nucleic Acids Res.* **27:** 4444–4450

Di Giulio M (2000) The universal ancestor lived in a thermophilic or hyperthermophilic environment. *J. Theor. Biol.* **203:** 203–213

Di Giulio M (2003) The universal ancestor was a thermophile or a hyperthermophile: tests and further evidence. *J. Theor. Biol.* **221:** 425–436

Dionne I, Brown NJ, Woodgate R & Bell SD (2008) On the mechanism of loading the PCNA sliding clamp by RFC. *Mol. Microbiol.* **68:** 216–222

Doherty AJ, Jackson SP & Weller GR (2001) Identification of bacterial homologues of the Ku DNA repair proteins. *FEBS Lett.* **500:** 186–188

Dorazi R, Götz D, Munro S, Bernander R & White MF (2007) Equal rates of repair of DNA photoproducts in transcribed and non-transcribed strands in Sulfolobus solfataricus. *Mol. Microbiol.* **63:** 521–529

Dorazi R, Parker JL & White MF (2006) PCNA Activates the Holliday Junction Endonuclease Hjc. *Journal of Molecular Biology* **364:** 243–247

E

Eme L, Spang A, Lombard J, Stairs CW & Ettema TJG (2017) Archaea and the origin of eukaryotes. *Nature Reviews Microbiology* **15:** 711–723

Erauso G, Reysenbach AL, Godfroy A, Meunier JR, Crump B, Partensky F, Baross JA, Marteinsson V, Barbier G, Pace NR. & Prieur D (1993) Pyrococcus abyssi sp. nov., a new hyperthermophilic archaeon isolated from a deep-sea hydrothermal vent (English). *Archives of microbiology* **160:** 338–349

Errico A & Costanzo V (2012) Mechanisms of replication fork protection: a safeguard for genome stability. *Crit. Rev. Biochem. Mol. Biol.* **47:** 222–235

F

Fan J, Otterlei M, Wong H-K, Tomkinson AE & Wilson DM (2004) XRCC1 co-localizes and physically interacts with PCNA. *Nucleic Acids Res* **32:** 2193–2201

Farkas J, Stirrett K, Lipscomb GL, Nixon W, Scott RA, Adams MWW & Westpheling J (2012) Recombinogenic properties of Pyrococcus furiosus strain COM1 enable rapid selection of targeted mutants. *Appl. Environ. Microbiol.* **78:** 4669–4676

Fiala G & Stetter KO (1986) Pyrococcus furiosus sp. nov. represents a novel genus of marine heterotrophic archaebacteria growing optimally at 100°C. *Arch. Microbiol.* **145:** 56–61

Forterre P (2013) The common ancestor of archaea and eukarya was not an archaeon. *Archaea* **2013:** 372396

Forterre P, Brochier C & Philippe H (2002) Evolution of the Archaea. *Theoretical Population Biology* **61:** 409–422

Frick DN & Richardson CC (2001) DNA primases. *Annu. Rev. Biochem.* **70:** 39–80

Fujikane R, Ishino S, Ishino Y & Forterre P (2010) Genetic analysis of DNA repair in the hyperthermophilic archaeon, Thermococcus kodakaraensis. *Genes Genet. Syst.* **85:** 243–257

Fujikane R, Shinagawa H & Ishino Y (2006) The archaeal Hjm helicase has recQ-like functions, and may be involved in repair of stalled replication fork. *Genes to Cells* **11:** 99–110

Fukui T, Atomi H, Kanai T, Matsumi R, Fujiwara S & Imanaka T (2005) Complete genome sequence of the hyperthermophilic archaeon Thermococcus kodakaraensis KOD1 and comparison with Pyrococcus genomes. *Genome Res* **15:** 352–363

G

Galtier N & Lobry JR (1997) Relationships between genomic G+C content, RNA secondary structures, and optimal growth temperature in prokaryotes. *J. Mol. Evol.* **44:** 632–636

Galtier N, Tourasse N & Gouy M (1999) A nonhyperthermophilic common ancestor to extant life forms. *Science* **283:** 220–221

Garcia V, Phelps SEL, Gray S & Neale MJ (2011) Bidirectional resection of DNA double-strand breaks by Mre11 and Exo1. *Nature* **479:** 241–244

García-Gómez S, Reyes A, Martínez-Jiménez MI, Chocrón ES, Mourón S, Terrados G, Powell C, Salido E, Méndez J, Holt IJ & Blanco L (2013) PrimPol, an archaic primase/polymerase operating in human cells. *Mol. Cell* **52:** 541–553

Gehring AM, Astling DP, Matsumi R, Burkhart BW, Kelman Z, Reeve JN, Jones KL & Santangelo TJ (2017) Genome Replication in Thermococcus kodakarensis Independent of Cdc6 and an Origin of Replication. *Front Microbiol* **8:** 2084

Gelot C, Magdalou I & Lopez BS (2015) Replication stress in Mammalian cells and its consequences for mitosis. *Genes (Basel)* **6:** 267–298

Gérard E, Jolivet E, Prieur D & Forterre P (2001) DNA protection mechanisms are not involved in the radioresistance of the hyperthermophilic archaea Pyrococcus abyssi and P. furiosus. *Mol. Genet. Genomics* **266:** 72–78

Gibbs E, Kelman Z, Gulbis JM, O'Donnell M, Kuriyan J, Burgers PM & Hurwitz J (1997) The influence of the proliferating cell nuclear antigen-interacting domain of p21(CIP1) on DNA synthesis catalyzed by the human and Saccharomyces cerevisiae polymerase delta holoenzymes. *J. Biol. Chem.* **272:** 2373–2381

Gill S, Krupovic M, Desnoues N, Béguin P, Sezonov G & Forterre P (2014) A highly divergent archaeo-eukaryotic primase from the Thermococcus nautilus plasmid, pTN2. *Nucleic Acids Res.* **42:** 3707–3719

Gilljam KM, Feyzi E, Aas PA, Sousa MML, Müller R, Vågbø CB, Catterall TC, Liabakk NB, Slupphaug G, Drabløs F, Krokan HE & Otterlei M (2009) Identification of a novel, widespread, and functionally important PCNA-binding motif. *J. Cell Biol.* **186:** 645–654

Gomez F (2014) Extreme Environment. In *Encyclopedia of Astrobiology* pp 1–3. Springer, Berlin, Heidelberg

Gouge J, Ralec C, Henneke G & Delarue M (2012) Molecular recognition of canonical and deaminated bases by P. abyssi family B DNA polymerase. *J. Mol. Biol.* **423:** 315–336

Gouge J, Rosario S, Romain F, Poitevin F, Béguin P & Delarue M (2015) Structural basis for a novel mechanism of DNA bridging and alignment in eukaryotic DSB DNA repair. *EMBO J.* **34:** 1126–1142

Grabowski B & Kelman and Z (2003) Archaeal DNA Replication: Eukaryal Proteins in a Bacterial Context. *Annual Review of Microbiology* **57:** 487–516

Grasso S & Tell G (2014) Base excision repair in Archaea: Back to the future in DNA repair. *DNA Repair* **21:** 148–157

Grogan DW (2015) Understanding DNA Repair in Hyperthermophilic Archaea: Persistent Gaps and Other Reasons to Focus on the Fork. *Archaea* **2015:** 942605

Grogan DW, Carver GT & Drake JW (2001) Genetic fidelity under harsh conditions: Analysis of spontaneous mutation in the thermoacidophilic archaeon Sulfolobus acidocaldarius. *PNAS* **98:** 7928–7933

Groisillier A, Hervé C, Jeudy A, Rebuffet E, Pluchon PF, Chevolot Y, Flament D, Geslin C, Morgado IM, Power D, Branno M, Moreau H, Michel G, Boyen C & Czjzek M (2010) MARINE-EXPRESS: taking advantage of high throughput cloning and expression strategies for the post-genomic analysis of marine organisms. *Microb Cell Fact* **9:** 45

Gueguen Y, Rolland JL, Lecompte O, Azam P, Le Romancer G, Flament D, Raffin JP & Dietrich J (2001) Characterization of two DNA polymerases from the hyperthermophilic euryarchaeon Pyrococcus abyssi. *Eur. J. Biochem.* **268:** 5961–5969

H

Haldenby S, White MF & Allers T (2009) RecA family proteins in archaea: RadA and its cousins. *Biochemical Society Transactions* **37:** 102–107

Hasan MN, Hagedoorn PL & Hagen WR (2002) Pyrococcus furiosus ferredoxin is a functional dimer. *FEBS Letters* **531:** 335–338

Hashimoto H, Inoue T, Nishioka M, Fujiwara S, Takagi M, Imanaka T & Kai Y (1999) Hyperthermostable protein structure maintained by intra and inter-helix ion-pairs in archaeal O6-methylguanine-DNA methyltransferase. *J. Mol. Biol.* **292:** 707–716

Hashimoto Y, Puddu F & Costanzo V (2011) RAD51 and MRE11 dependent reassembly of uncoupled CMG helicase complex at collapsed replication forks. *Nat Struct Mol Biol* **19:** 17–24

Hawkins M, Malla S, Blythe MJ, Nieduszynski CA & Allers T (2013) Accelerated growth in the absence of DNA replication origins. *Nature* **503:** 544–547

Hayashi I, Morikawa K & Ishino Y (1999) Specific interaction between DNA polymerase II (PolD) and RadB, a Rad51/Dmc1 homolog, in Pyrococcus furiosus. *Nucleic Acids Res.* **27:** 4695–4702

Heider MR, Burkhart BW, Santangelo TJ & Gardner AF (2017) Defining the RNaseH2 enzyme-initiated ribonucleotide excision repair pathway in Archaea. *J. Biol. Chem.* **292:** 8835–8845

van der Heijden T, Seidel R, Modesti M, Kanaar R, Wyman C & Dekker C (2007) Real-time assembly and disassembly of human RAD51 filaments on individual DNA molecules. *Nucleic Acids Res* **35:** 5646–5657

Henneke G (2012) In vitro reconstitution of RNA primer removal in Archaea reveals the existence of two pathways. *Biochem. J.* **447:** 271–280

Henneke G, Flament D, Hübscher U, Querellou J & Raffin J-P (2005) The Hyperthermophilic Euryarchaeota Pyrococcus abyssi Likely Requires the Two DNA Polymerases D and B for DNA Replication. *Journal of Molecular Biology* **350:** 53–64

Henneke G, Gueguen Y, Flament D, Azam P, Querellou J, Dietrich J, Hübscher U & Raffin J-P (2002) Replication Factor C from the Hyperthermophilic Archaeon Pyrococcus abyssi Does Not Need ATP Hydrolysis for Clamp-loading and Contains a Functionally Conserved RFC PCNA-binding Domain. *Journal of Molecular Biology* **323:** 795–810

Herdendorf TJ, Albrecht DW, Benkovic SJ & Nelson SW (2011) Biochemical Characterization of Bacteriophage T4 Mre11-Rad50 Complex. *J Biol Chem* **286:** 2382–2392

Hileman TH & Santangelo TJ (2012) Genetics Techniques for Thermococcus kodakarensis. *Front Microbiol* **3:** 195

Hirose S, Hiraga S & Okazaki T (1983) Initiation site of deoxyribonucleotide polymerization at the replication origin of the Escherichia coli chromosome. *Mol. Gen. Genet.* **189:** 422–431

Hishiki A, Hashimoto H, Hanafusa T, Kamei K, Ohashi E, Shimizu T, Ohmori H & Sato M (2009) Structural basis for novel interactions between human translesion synthesis polymerases and proliferating cell nuclear antigen. *J. Biol. Chem.* **284:** 10552–10560

Hjort K & Bernander R (2001) Cell cycle regulation in the hyperthermophilic crenarchaeon Sulfolobus acidocaldarius. *Mol. Microbiol.* **40:** 225–234

Hogrel G, Lu Y, Laurent S, Henry E, Etienne C, Phung DK, Dulermo R, Bossé A, Pluchon P-F, Clouet-d'Orval B & Flament D (2018) Physical and functional interplay between PCNA DNA clamp and Mre11–Rad50 complex from the archaeon Pyrococcus furiosus. *Nucleic Acids Res* **46:** 5651–5663

Holthausen JT, Wyman C & Kanaar R (2010) Regulation of DNA strand exchange in homologous recombination. *DNA Repair (Amst.)* **9:** 1264–1272

Holzer S, Yan J, Kilkenny ML, Bell SD & Pellegrini L (2017) Primer synthesis by a eukaryotic-like archaeal primase is independent of its Fe-S cluster. *Nature Communications* **8:** 1718

Hong Y, Chu M, Li Y, Ni J, Sheng D, Hou G, She Q & Shen Y (2012) Dissection of the functional domains of an archaeal Holliday junction helicase. *DNA Repair (Amst.)* **11:** 102–111

Hopfner K-P, Craig L, Moncalian G, Zinkel RA, Usui T, Owen BAL, Karcher A, Henderson B, Bodmer J-L, McMurray CT, Carney JP, Petrini JHJ & Tainer JA (2002) The Rad50 zinc-hook is a structure joining Mre11 complexes in DNA recombination and repair. *Nature* **418:** 562–566

Hopfner K-P, Karcher A, Craig L, Woo TT, Carney JP & Tainer JA (2001) Structural Biochemistry and Interaction Architecture of the DNA Double-Strand Break Repair Mre11 Nuclease and Rad50-ATPase. *Cell* **105:** 473–485

Hopfner K-P, Karcher A, Shin D, Fairley C, Tainer JA & Carney JP (2000a) Mre11 and Rad50 from Pyrococcus furiosus: Cloning and Biochemical Characterization Reveal an Evolutionarily Conserved Multiprotein Machine. *J Bacteriol* **182:** 6036–6041

Hopfner K-P, Karcher A, Shin DS, Craig L, Arthur LM, Carney JP & Tainer JA (2000b) Structural Biology of Rad50 ATPase: ATP-Driven Conformational Control in DNA Double-Strand Break Repair and the ABC-ATPase Superfamily. *Cell* **101:** 789–800

Hopfner K-P & Tainer JA (2003) Rad50/SMC proteins and ABC transporters: unifying concepts from high-resolution structures. *Curr. Opin. Struct. Biol.* **13:** 249–255

Hopkins BB & Paull TT (2008) The P. furiosus Mre11/Rad50 complex promotes 5' strand resection at a DNA double-strand break. *Cell* **135:** 250–260

Hu J, Guo L, Wu K, Liu B, Lang S & Huang L (2012) Template-dependent polymerization across discontinuous templates by the heterodimeric primase from the hyperthermophilic archaeon Sulfolobus solfataricus. *Nucleic Acids Res.* **40:** 3470–3483

Huang Q, Li Y, Zeng C, Song T, Yan Z, Ni J, She Q & Shen Y (2015a) Genetic analysis of the Holliday junction resolvases Hje and Hjc in Sulfolobus islandicus. *Extremophiles* **19:** 505–514

Huang Q, Liu L, Liu J, Ni J, She Q & Shen Y (2015b) Efficient 5'-3' DNA end resection by HerA and NurA is essential for cell viability in the crenarchaeon Sulfolobus islandicus. *BMC Mol. Biol.* **16:** 2

Hurst LD & Merchant AR (2001) High guanine-cytosine content is not an adaptation to high temperature: a comparative analysis amongst prokaryotes. *Proc. Biol. Sci.* **268:** 493–497

Hyrien O (2000) Mechanisms and consequences of replication fork arrest. *Biochimie* **82:** 5–17

I

Indiani C & O'Donnell M (2006) The replication clamp-loading machine at work in the three domains of life. *Nat. Rev. Mol. Cell Biol.* **7:** 751–761

Ishino S, Nishi Y, Oda S, Uemori T, Sagara T, Takatsu N, Yamagami T, Shirai T & Ishino Y (2016) Identification of a mismatch-specific endonuclease in hyperthermophilic Archaea. *Nucleic Acids Res* **44:** 2977–2986

Ishino Y & Ishino S (2012) Rapid progress of DNA replication studies in Archaea, the third domain of life. *Sci China Life Sci* **55:** 386–403

Ito K, Murayama Y, Takahashi M & Iwasaki H (2018) Two three-strand intermediates are processed during Rad51-driven DNA strand exchange. *Nat. Struct. Mol. Biol.* **25:** 29–36

Ito N, Matsui I & Matsui E (2007) Molecular basis for the subunit assembly of the primase from an archaeon Pyrococcus horikoshii. *FEBS J.* **274:** 1340–1351

Ito N, Nureki O, Shirouzu M, Yokoyama S & Hanaoka F (2003) Crystal structure of the Pyrococcus horikoshii DNA primase-UTP complex: implications for the mechanism of primer synthesis. *Genes Cells* **8:** 913–923

Iyer LM, Koonin EV, Leipe DD & Aravind L (2005) Origin and evolution of the archaeo-eukaryotic primase superfamily and related palm-domain proteins: structural insights and new members. *Nucleic Acids Res.* **33:** 3875–3896

J

de Jager M, Dronkert ML, Modesti M, Beerens CE, Kanaar R & van Gent DC (2001) DNA-binding and strand-annealing activities of human Mre11: implications for its roles in DNA double-strand break repair pathways. *Nucleic Acids Res.* **29:** 1317–1325

de Jager M, Wyman C, van Gent DC & Kanaar R (2002) DNA end-binding specificity of human Rad50/Mre11 is influenced by ATP. *Nucleic Acids Res.* **30:** 4425–4431

Jain R, Rivera MC, Moore JE & Lake JA (2002) Horizontal Gene Transfer in Microbial Genome Evolution. *Theoretical Population Biology* **61:** 489–495

Jiang Q, Karata K, Woodgate R, Cox MM & Goodman MF (2009) The active form of DNA polymerase V is UmuD'(2)C-RecA-ATP. *Nature* **460:** 359–363

Jolivet E, Matsunaga F, Ishino Y, Forterre P, Prieur D & Myllykallio H (2003) Physiological responses of the hyperthermophilic archaeon 'Pyrococcus abyssi' to DNA damage caused by ionizing radiation. *J. Bacteriol.* **185:** 3958–3961

Jones RM & Petermann E (2012) Replication fork dynamics and the DNA damage response. *Biochemical Journal* **443:** 13–26

Jónsson ZO, Hindges R & Hübscher U (1998) Regulation of DNA replication and repair proteins through interaction with the front side of proliferating cell nuclear antigen. *The EMBO Journal* **17:** 2412–2425

Jorda J & Yeates TO (2011) Widespread disulfide bonding in proteins from thermophilic archaea. *Archaea* **2011:** 409156

Jozwiakowski SK, Borazjani Gholami F & Doherty AJ (2015) Archaeal replicative primases can perform translesion DNA synthesis. *Proc. Natl. Acad. Sci. U.S.A.* **112:** E633-638

K

Kantidze OL, Velichko AK, Luzhin AV & Razin SV (2016) Heat Stress-Induced DNA Damage. *Acta Naturae* **8:** 75–78

Karshikoff A & Ladenstein R (2001) Ion pairs and the thermotolerance of proteins from hyperthermophiles: a 'traffic rule' for hot roads. *Trends Biochem. Sci.* **26:** 550–556

Kashiwagi S, Kuraoka I, Fujiwara Y, Hitomi K, Cheng QJ, Fuss JO, Shin DS, Masutani C, Tainer JA, Hanaoka F & Iwai S (2010) Characterization of a Y-Family DNA Polymerase eta from the Eukaryotic Thermophile Alvinella pompejana. *J Nucleic Acids* **2010:**

Keck JL, Roche DD, Lynch AS & Berger JM (2000) Structure of the RNA polymerase domain of E. coli primase. *Science* **287:** 2482–2486

Keen BA, Jozwiakowski SK, Bailey LJ, Bianchi J & Doherty AJ (2014) Molecular dissection of the domain architecture and catalytic activities of human PrimPol. *Nucleic Acids Res* **42:** 5830–5845

Kelman LM & Kelman Z (2014) Archaeal DNA Replication. *Annual Review of Genetics* **48:** 71–97

Kelman LM & Kelman Z (2018) Do Archaea Need an Origin of Replication? *Trends Microbiol.* **26:** 172–174

Kelman Z & White MF (2005) Archaeal DNA replication and repair. *Curr. Opin. Microbiol.* **8:** 669–676

Kil YV, Baitin DM, Masui R, Bonch-Osmolovskaya EA, Kuramitsu S & Lanzov VA (2000) Efficient strand transfer by the RadA recombinase from the hyperthermophilic archaeon Desulfurococcus amylolyticus. *J. Bacteriol.* **182:** 130–134

Kim JH, Grosbart M, Anand R, Wyman C, Cejka P & Petrini JHJ (2017) The Mre11-Nbs1 Interface Is Essential for Viability and Tumor Suppression. *Cell Rep* **18:** 496–507

Kirkland PA & Maupin-Furlow JA (2009) Stabilization of an archaeal DNA-sliding clamp protein, PCNA, by proteasome-activating nucleotidase gene knockout in Haloferax volcanii. *FEMS Microbiol. Lett.* **294:** 32–36

Kiyonari S, Takayama K, Nishida H & Ishino Y (2006) Identification of a novel binding motif in Pyrococcus furiosus DNA ligase for the functional interaction with proliferating cell nuclear antigen. *J. Biol. Chem.* **281:** 28023–28032

Klapstein K, Chou T & Bruinsma R (2004) Physics of RecA-mediated homologous recognition. *Biophys. J.* **87:** 1466–1477

Kobayashi K, Ehrlich SD, Albertini A, Amati G, Andersen KK, Arnaud M, Asai K, Ashikaga S, Aymerich S, Bessieres P, Boland F, Brignell SC, Bron S, Bunai K, Chapuis J, Christiansen LC, Danchin A, Débarbouille M, Dervyn E, Deuerling E, et al (2003) Essential Bacillus subtilis genes. *Proc. Natl. Acad. Sci. U.S.A.* **100:** 4678–4683

Kobayashi K, Guilliam TA, Tsuda M, Yamamoto J, Bailey LJ, Iwai S, Takeda S, Doherty AJ & Hirota K (2016) Repriming by PrimPol is critical for DNA replication restart downstream of lesions and chain-terminating nucleosides. *Cell Cycle* **15:** 1997–2008

Koga Y (2012) Thermal adaptation of the archaeal and bacterial lipid membranes. *Archaea* **2012:** 789652

Komori K, Miyata T, Daiyasu H, Toh H, Shinagawa H & Ishino a Y (2000a) Domain analysis of an archaeal RadA protein for the strand exchange activity. *J. Biol. Chem.* **275:** 33791–33797

Komori K, Miyata T, DiRuggiero J, Holley-Shanks R, Hayashi I, Cann IK, Mayanagi K, Shinagawa H & Ishino Y (2000b) Both RadA and RadB are involved in homologous recombination in Pyrococcus furiosus. *J. Biol. Chem.* **275:** 33782–33790

Kondratova A, Watanabe T, Marotta M, Cannon M, Segall AM, Serre D & Tanaka H (2015) Replication fork integrity and intra-S phase checkpoint suppress gene amplification. *Nucleic Acids Res.* **43:** 2678–2690

Koonin EV, Mushegian AR, Galperin MY & Walker DR (1997) Comparison of archaeal and bacterial genomes: computer analysis of protein sequences predicts novel functions and suggests a chimeric origin for the archaea. *Molecular Microbiology* **25:** 619–637

Koonin EV, Wolf YI, Kondrashov AS & Aravind L (2000) Bacterial homologs of the small subunit of eukaryotic DNA primase. *J. Mol. Microbiol. Biotechnol.* **2:** 509–512

Kottemann M, Kish A, Iloanusi C, Bjork S & DiRuggiero J (2005) Physiological responses of the halophilic archaeon Halobacterium sp. strain NRC1 to desiccation and gamma irradiation. *Extremophiles* **9:** 219–227

Krejci L, Altmannova V, Spirek M & Zhao X (2012) Homologous recombination and its regulation. *Nucleic Acids Res* **40:** 5795–5818

Krwawicz J, Arczewska KD, Speina E, Maciejewska A & Grzesiuk E (2007) Bacterial DNA repair genes and their eukaryotic homologues: 1. Mutations in genes involved in base excision repair (BER) and DNA-end processors and their implication in mutagenesis and human disease. *Acta Biochim. Pol.* **54:** 413–434

Kumar S & Nussinov R (2001) How do thermophilic proteins deal with heat? *Cell. Mol. Life Sci.* **58:** 1216–1233

Kuriyan J & O'Donnell M (1993) Sliding clamps of DNA polymerases. *J. Mol. Biol.* **234:** 915–925

Kusakabe T, Hine AV, Hyberts SG & Richardson CC (1999) The Cys4 zinc finger of bacteriophage T7 primase in sequence-specific single-stranded DNA recognition. *Proc. Natl. Acad. Sci. U.S.A.* **96:** 4295–4300

L

Lafrance-Vanasse J, Williams GJ & Tainer JA (2015) Envisioning the dynamics and flexibility of Mre11-Rad50-Nbs1 complex to decipher its roles in DNA replication and repair. *Progress in Biophysics and Molecular Biology* **117:** 182–193

Lamarche BJ, Orazio NI & Weitzman MD (2010) The MRN complex in Double-Strand Break Repair and Telomere Maintenance. *FEBS Lett* **584:** 3682–3695

Lammens K, Bemeleit DJ, Möckel C, Clausing E, Schele A, Hartung S, Schiller CB, Lucas M, Angermüller C, Söding J, Sträßer K & Hopfner K-P (2011) The Mre11:Rad50 Structure Shows an ATP-Dependent Molecular Clamp in DNA Double-Strand Break Repair. *Cell* **145:** 54–66

Lao-Sirieix S & Bell SD (2004) The Heterodimeric Primase of the Hyperthermophilic Archaeon Sulfolobus solfataricus Possesses DNA and RNA Primase, Polymerase and 3'-terminal Nucleotidyl Transferase Activities. *Journal of Molecular Biology* **344:** 1251–1263

Lao-Sirieix S-H, Nookala RK, Roversi P, Bell SD & Pellegrini L (2005a) Structure of the heterodimeric core primase. *Nat. Struct. Mol. Biol.* **12:** 1137–1144

Lao-Sirieix S-H, Pellegrini L & Bell SD (2005b) The promiscuous primase. *Trends Genet.* **21:** 568–572

Le Breton M, Henneke G, Norais C, Flament D, Myllykallio H, Querellou J & Raffin J-P (2007) The Heterodimeric Primase from the Euryarchaeon Pyrococcus abyssi: A Multifunctional Enzyme for Initiation and Repair? *Journal of Molecular Biology* **374:** 1172–1185

Leach DR, Lloyd RG & Coulson AF (1992) The SbcCD protein of Escherichia coli is related to two putative nucleases in the UvrA superfamily of nucleotide-binding proteins. *Genetica* **87:** 95–100

Lebel M, Spillare EA, Harris CC & Leder P (1999) The Werner Syndrome Gene Product Co-purifies with the DNA Replication Complex and Interacts with PCNA and Topoisomerase I. *J. Biol. Chem.* **274:** 37795–37799

Lehmann AR (2006a) Translesion synthesis in mammalian cells. *Experimental Cell Research* **312:** 2673–2676

Lehmann AR (2006b) New Functions for Y Family Polymerases. *Molecular Cell* **24:** 493–495

Leigh JA, Albers S-V, Atomi H & Allers T (2011) Model organisms for genetics in the domain Archaea: methanogens, halophiles, Thermococcales and Sulfolobales. *FEMS Microbiology Reviews* **35:** 577–608

Leuko S, Raftery MJ, Burns BP, Walter MR & Neilan BA (2009) Global protein-level responses of Halobacterium salinarum NRC-1 to prolonged changes in external sodium chloride concentrations. *J. Proteome Res.* **8:** 2218–2225

Li X, Fu L, Li Z, Ma X, Xiao X & Xu J (2015) Genetic tools for the piezophilic hyperthermophilic archaeon Pyrococcus yayanosii. *Extremophiles* **19:** 59–67

Li Z, Huang RY-C, Yopp DC, Hileman TH, Santangelo TJ, Hurwitz J, Hudgens JW & Kelman Z (2014) A novel mechanism for regulating the activity of proliferating cell nuclear antigen by a small protein. *Nucleic Acids Res.* **42:** 5776–5789

Lieber MR (2010) The Mechanism of Double-Strand DNA Break Repair by the Nonhomologous DNA End Joining Pathway. *Annu Rev Biochem* **79:** 181–211

Lieph R, Veloso FA & Holmes DS (2006) Thermophiles like hot T. *Trends Microbiol.* **14:** 423–426

Lim CT, Lai PJ, Leach DRF, Maki H & Furukohri A (2015) A novel mode of nuclease action is revealed by the bacterial Mre11/Rad50 complex. *Nucleic Acids Res* **43:** 9804–9816

Lim HS, Kim JS, Park YB, Gwon GH & Cho Y (2011) Crystal structure of the Mre11–Rad50–ATPγS complex: understanding the interplay between Mre11 and Rad50. *Genes Dev* **25:** 1091–1104

Lin Z, Nei M & Ma H (2007) The origins and early evolution of DNA mismatch repair genes—multiple horizontal gene transfers and co-evolution. *Nucleic Acids Res* **35:** 7591–7603

Lindahl T (1993) Instability and decay of the primary structure of DNA. *Nature* **362:** 709–715

Lindahl T & Nyberg B (1974) Heat-induced deamination of cytosine residues in deoxyribonucleic acid. *Biochemistry* **13:** 3405–3410

Lipps G, Röther S, Hart C & Krauss G (2003) A novel type of replicative enzyme harbouring ATPase, primase and DNA polymerase activity. *EMBO J.* **22:** 2516–2525

Lipscomb GL, Stirrett K, Schut GJ, Yang F, Jenney FE, Scott RA, Adams MWW & Westpheling J (2011) Natural Competence in the Hyperthermophilic Archaeon Pyrococcus furiosus Facilitates Genetic Manipulation: Construction of Markerless Deletions of Genes Encoding the Two Cytoplasmic Hydrogenases. *Appl Environ Microbiol* **77:** 2232–2238

Liu B, Ouyang S, Makarova KS, Xia Q, Zhu Y, Li Z, Guo L, Koonin EV, Liu Z-J & Huang L (2015) A primase subunit essential for efficient primer synthesis by an archaeal eukaryotic-type primase. *Nat Commun* **6:** 7300

Liu L, Komori K, Ishino S, Bocquier AA, Cann IK, Kohda D & Ishino Y (2001) The archaeal DNA primase: biochemical characterization of the p41-p46 complex from Pyrococcus furiosus. *J. Biol. Chem.* **276:** 45484–45490

Liu Y, Sung S, Kim Y, Li F, Gwon G, Jo A, Kim A-K, Kim T, Song O, Lee SE & Cho Y (2016) ATP-dependent DNA binding, unwinding, and resection by the Mre11/Rad50 complex. *The EMBO Journal* **35:** 743–758

van Loenhout MTJ, van der Heijden T, Kanaar R, Wyman C & Dekker C (2009) Dynamics of RecA filaments on single-stranded DNA. *Nucleic Acids Res.* **37:** 4089–4099

Lopez P, Philippe H, Myllykallio H & Forterre P (1999) Identification of putative chromosomal origins of replication in Archaea. *Mol. Microbiol.* **32:** 883–886

Lydeard JR, Lipkin-Moore Z, Sheu Y-J, Stillman B, Burgers PM & Haber JE (2010) Break-induced replication requires all essential DNA replication factors except those specific for pre-RC assembly. *Genes Dev.* **24:** 1133–1144

M

MacNeill SA (2011) Protein-protein interactions in the archaeal core replisome. *Biochem. Soc. Trans.* **39:** 163–168

MacNeill SA (2016) PCNA-binding proteins in the archaea: novel functionality beyond the conserved core. *Curr Genet* **62:** 527–532

Maga G & Hübscher U (2003) Proliferating cell nuclear antigen (PCNA): a dancer with many partners. *Journal of Cell Science* **116:** 3051–3060

Mailand N, Gibbs-Seymour I & Bekker-Jensen S (2013) Regulation of PCNA-protein interactions for genome stability. *Nat. Rev. Mol. Cell Biol.* **14:** 269–282

Majka J, Alford B, Ausio J, Finn RM & McMurray CT (2012) ATP hydrolysis by RAD50 protein switches MRE11 enzyme from endonuclease to exonuclease. *J. Biol. Chem.* **287:** 2328–2341

van Mameren J, Modesti M, Kanaar R, Wyman C, Peterman EJG & Wuite GJL (2009) Counting RAD51 proteins disassembling from nucleoprotein filaments under tension. *Nature* **457:** 745–748

Manzan A, Pfeiffer G, Hefferin ML, Lang CE, Carney JP & Hopfner K-P (2004) MlaA, a hexameric ATPase linked to the Mre11 complex in archaeal genomes. *EMBO Rep.* **5:** 54–59

Marguet E & Forterre P (1994) DNA stability at temperatures typical for hyperthermophiles. *Nucleic Acids Res.* **22:** 1681–1686

Marguet E & Forterre P (1998) Protection of DNA by salts against thermodegradation at temperatures typical for hyperthermophiles. *Extremophiles* **2:** 115–122

Marteinsson VT, Birrien JL, Reysenbach AL, Vernet M, Marie D, Gambacorta A, Messner P, Sleytr UB & Prieur D (1999) Thermococcus barophilus sp. nov., a new barophilic and hyperthermophilic archaeon isolated under high hydrostatic pressure from a deep-sea hydrothermal vent. *Int. J. Syst. Bacteriol.* **49 Pt 2:** 351–359

Maser RS, Mirzoeva OK, Wells J, Olivares H, Williams BR, Zinkel RA, Farnham PJ & Petrini JH (2001) Mre11 complex and DNA replication: linkage to E2F and sites of DNA synthesis. *Mol. Cell. Biol.* **21:** 6006–6016

Matsui E, Nishio M, Yokoyama H, Harata K, Darnis S & Matsui I (2003) Distinct domain functions regulating de novo DNA synthesis of thermostable DNA primase from hyperthermophile Pyrococcus horikoshii. *Biochemistry* **42:** 14968–14976

Matsumi R, Manabe K, Fukui T, Atomi H & Imanaka T (2007) Disruption of a sugar transporter gene cluster in a hyperthermophilic archaeon using a host-marker system based on antibiotic resistance. *J. Bacteriol.* **189:** 2683–2691

Matsumiya S, Ishino Y & Morikawa K (2001) Crystal structure of an archaeal DNA sliding clamp: proliferating cell nuclear antigen from Pyrococcus furiosus. *Protein Sci.* **10:** 17–23

Matsuoka S, Yamaguchi M & Matsukage A (1994) D-type cyclin-binding regions of proliferating cell nuclear antigen. *J. Biol. Chem.* **269:** 11030–11036

McGeoch AT & Bell SD (2005) Eukaryotic/archaeal primase and MCM proteins encoded in a bacteriophage genome. *Cell* **120:** 167–168

McGeoch AT & Bell SD (2008) Extra-chromosomal elements and the evolution of cellular DNA replication machineries. *Nat. Rev. Mol. Cell Biol.* **9:** 569–574

McIlwraith MJ, McIlwraith MJ, Vaisman A, Liu Y, Fanning E, Woodgate R & West SC (2005) Human DNA polymerase eta promotes DNA synthesis from strand invasion intermediates of homologous recombination. *Mol. Cell* **20:** 783–792

McRobbie A-M, Carter LG, Kerou M, Liu H, McMahon SA, Johnson KA, Oke M, Naismith JH & White MF (2009) Structural and functional characterisation of a conserved archaeal RadA paralog with antirecombinase activity. *J. Mol. Biol.* **389:** 661–673

Menetski JP & Kowalczykowski SC (1985) Interaction of recA protein with single-stranded DNA. Quantitative aspects of binding affinity modulation by nucleotide cofactors. *J. Mol. Biol.* **181:** 281–295

Meslet-Cladiére L, Norais C, Kuhn J, Briffotaux J, Sloostra JW, Ferrari E, Hübscher U, Flament D & Myllykallio H (2007) A novel proteomic approach identifies new interaction partners for proliferating cell nuclear antigen. *J. Mol. Biol.* **372:** 1137–1148

Michel B (2000) Replication fork arrest and DNA recombination. *Trends Biochem. Sci.* **25:** 173–178

Michel B & Bernander R (2014) Chromosome replication origins: do we really need them? *Bioessays* **36:** 585–590

Mimitou EP & Symington LS (2008) Sae2, Exo1 and Sgs1 collaborate in DNA double-strand break processing. *Nature* **455:** 770–774

Mirzoeva OK & Petrini JHJ (2003) DNA replication-dependent nuclear dynamics of the Mre11 complex. *Mol. Cancer Res.* **1:** 207–218

Möckel C, Lammens K, Schele A & Hopfner K-P (2012) ATP driven structural changes of the bacterial Mre11:Rad50 catalytic head complex. *Nucleic Acids Res.* **40:** 914–927

Modesti M, Ristic D, van der Heijden T, Dekker C, van Mameren J, Peterman EJG, Wuite GJL, Kanaar R & Wyman C (2007) Fluorescent human RAD51 reveals multiple nucleation sites and filament segments tightly associated along a single DNA molecule. *Structure* **15:** 599–609

Moldovan G-L, Pfander B & Jentsch S (2007) PCNA, the maestro of the replication fork. *Cell* **129:** 665–679

Moncalian G, Lengsfeld B, Bhaskara V, Hopfner K-P, Karcher A, Alden E, Tainer JA & Paull TT (2004) The rad50 signature motif: essential to ATP binding and biological function. *J. Mol. Biol.* **335:** 937–951

Moreno-Herrero F, de Jager M, Dekker NH, Kanaar R, Wyman C & Dekker C (2005) Mesoscale conformational changes in the DNA-repair complex Rad50/Mre11/Nbs1 upon binding DNA. *Nature* **437:** 440–443

Morita R, Nakane S, Shimada A, Inoue M, Iino H, Wakamatsu T, Fukui K, Nakagawa N, Masui R & Kuramitsu S (2010) Molecular Mechanisms of the Whole DNA Repair System: A Comparison of Bacterial and Eukaryotic Systems. *J Nucleic Acids* **2010:**

Morozumi Y, Ino R, Ikawa S, Mimida N, Shimizu T, Toki S, Ichikawa H, Shibata T & Kurumizaka H (2013) Homologous pairing activities of two rice RAD51 proteins, RAD51A1 and RAD51A2. *PLoS ONE* **8:** e75451

Mosig G (1998) Recombination and recombination-dependent DNA replication in bacteriophage T4. *Annu. Rev. Genet.* **32:** 379–413

Mueser TC, Hinerman JM, Devos JM, Boyer RA & Williams KJ (2010) Structural analysis of bacteriophage T4 DNA replication: a review in the Virology Journal series on bacteriophage T4 and its relatives. *Virol. J.* **7:** 359

Myler LR, Gallardo IF, Soniat MM, Deshpande RA, Gonzalez XB, Kim Y, Paull TT & Finkelstein IJ (2017) Single-Molecule Imaging Reveals How Mre11-Rad50-Nbs1 Initiates DNA Break Repair. *Mol. Cell* **67:** 891-898.e4

Myllykallio H, Lopez P, López-García P, Heilig R, Saurin W, Zivanovic Y, Philippe H & Forterre P (2000) Bacterial Mode of Replication with Eukaryotic-Like Machinery in a Hyperthermophilic Archaeon. *Science* **288:** 2212–2215

N

Nakabeppu Y (2014) Cellular Levels of 8-Oxoguanine in either DNA or the Nucleotide Pool Play Pivotal Roles in Carcinogenesis and Survival of Cancer Cells. *International Journal of Molecular Sciences* **15:** 12543–12557

Naryzhny SN (2008) Proliferating cell nuclear antigen: a proteomics view. *Cell. Mol. Life Sci.* **65:** 3789–3808

Nicolette ML, Lee K, Guo Z, Rani M, Chow JM, Lee SE & Paull TT (2010) Mre11-Rad50-Xrs2 and Sae2 promote 5' strand resection of DNA double-strand breaks. *Nat. Struct. Mol. Biol.* **17:** 1478–1485

Nucleic Acids - Biology - OpenStax CNX Available at: https://cnx.org/contents/GFy_h8cu@9.87:yxeAKc4X@8/Nucleic-Acids

O

Oh J, Al-Zain A, Cannavo E, Cejka P & Symington LS (2016) Xrs2 Dependent and Independent Functions of the Mre11-Rad50 Complex. *Mol. Cell* **64:** 405–415

Ohshita K, Fukui K, Sato M, Morisawa T, Hakumai Y, Morono Y, Inagaki F, Yano T, Ashiuchi M & Wakamatsu T (2017) Archaeal MutS5 tightly binds to Holliday junction similarly to eukaryotic MutSγ. *FEBS J.* **284:** 3470–3483

Olaisen C, Kvitvang HFN, Lee S, Almaas E, Bruheim P, Drabløs F & Otterlei M (2018) The role of PCNA as a scaffold protein in cellular signaling is functionally conserved between yeast and humans. *FEBS Open Bio* **8:** 1135–1145

Oren A (2010) Industrial and environmental applications of halophilic microorganisms. *Environ Technol* **31:** 825–834

P

Pace NR (1991) Origin of life--facing up to the physical setting. *Cell* **65:** 531–533

Palud A, Villani G, L'Haridon S, Querellou J, Raffin J-P & Henneke G (2008) Intrinsic properties of the two replicative DNA polymerases of Pyrococcus abyssi in replicating abasic sites: possible role in DNA damage tolerance? *Molecular Microbiology* **70:** 746–761

Pan H & Wigley DB (2000) Structure of the zinc-binding domain of Bacillus stearothermophilus DNA primase. *Structure* **8:** 231–239

Pan M, Kelman LM & Kelman Z (2011) The archaeal PCNA proteins. *Biochem. Soc. Trans.* **39:** 20–24

Park YB, Hohl M, Padjasek M, Jeong E, Jin KS, Krężel A, Petrini JHJ & Cho Y (2017) Eukaryotic Rad50 functions as a rod-shaped dimer. *Nat. Struct. Mol. Biol.* **24:** 248–257

Patel M, Jiang Q, Woodgate R, Cox MM & Goodman MF (2010) A New Model for SOS-induced Mutagenesis: How RecA Protein Activates DNA Polymerase V. *Crit Rev Biochem Mol Biol* **45:** 171–184

Paull TT (2018) 20 Years of Mre11 Biology: No End in Sight. *Mol. Cell* **71:** 419–427

Paull TT & Gellert M (1998) The 3′ to 5′ Exonuclease Activity of Mre11 Facilitates Repair of DNA Double-Strand Breaks. *Molecular Cell* **1:** 969–979

Paull TT & Gellert M (1999) Nbs1 potentiates ATP-driven DNA unwinding and endonuclease cleavage by the Mre11/Rad50 complex. *Genes Dev* **13:** 1276–1288

Peak MJ, Robb FT & Peak JG (1995) Extreme resistance to thermally induced DNA backbone breaks in the hyperthermophilic archaeon Pyrococcus furiosus. *J. Bacteriol.* **177:** 6316–6318

Pellegrini L (2012) The Pol α-primase complex. *Subcell. Biochem.* **62:** 157–169

Pellegrini L, Yu DS, Lo T, Anand S, Lee M, Blundell TL & Venkitaraman AR (2002) Insights into DNA recombination from the structure of a RAD51-BRCA2 complex. *Nature* **420:** 287–293

Petermann E & Helleday T (2010) Pathways of mammalian replication fork restart. *Nat. Rev. Mol. Cell Biol.* **11:** 683–687

Pham P, Bertram JG, O'Donnell M, Woodgate R & Goodman MF (2001) A model for SOS-lesion-targeted mutations in Escherichia coli. *Nature* **409:** 366–370

Pichler T (2009) Marine shallow-water hydrothermal systems as natural laboratories. *FOG - Freiberg Online Geoscience* **22:** 77–81

Pluchon P-F, Fouqueau T, Crezé C, Laurent S, Briffotaux J, Hogrel G, Palud A, Henneke G, Godfroy A, Hausner W, Thomm M, Nicolas J & Flament D (2013) An Extended Network of Genomic Maintenance in the Archaeon Pyrococcus abyssi Highlights Unexpected Associations between Eucaryotic Homologs. *PLoS One* **8:**

Podar M, Makarova KS, Graham DE, Wolf YI, Koonin EV & Reysenbach A-L (2013) Insights into archaeal evolution and symbiosis from the genomes of a nanoarchaeon and its inferred crenarchaeal host from Obsidian Pool, Yellowstone National Park. *Biol. Direct* **8:** 9

Pomerantz RT, Kurth I, Goodman MF & O'Donnell ME (2013) Preferential D-loop extension by a translesion DNA polymerase underlies error-prone recombination. *Nat. Struct. Mol. Biol.* **20:** 748–755

Postel-Vinay S, Vanhecke E, Olaussen KA, Lord CJ, Ashworth A & Soria J-C (2012) The potential of exploiting DNA-repair defects for optimizing lung cancer treatment. *Nat Rev Clin Oncol* **9:** 144–155

Prado F (2014) Genetic instability is prevented by Mrc1-dependent spatio-temporal separation of replicative and repair activities of homologous recombination: homologous recombination tolerates replicative stress by Mrc1-regulated replication and repair activities operating at S and G2 in distinct subnuclear compartments. *Bioessays* **36:** 451–462

Prakash S, Johnson RE & Prakash L (2005) Eukaryotic translesion synthesis DNA polymerases: specificity of structure and function. *Annu. Rev. Biochem.* **74:** 317–353

R

Rajagopalan M, Lu C, Woodgate R, O'Donnell M, Goodman MF & Echols H (1992) Activity of the purified mutagenesis proteins UmuC, UmuD', and RecA in replicative bypass of an abasic DNA lesion by DNA polymerase III. *Proc. Natl. Acad. Sci. U.S.A.* **89:** 10777–10781

Ramadan K, Shevelev I & Hübscher U (2004) The DNA-polymerase-X family: controllers of DNA quality? *Nat. Rev. Mol. Cell Biol.* **5:** 1038–1043

Rampelotto PH (2010) Resistance of Microorganisms to Extreme Environmental Conditions and Its Contribution to Astrobiology. *Sustainability* **2:** 1602–1623

Ravoitytė B & Wellinger RE (2017) Non-Canonical Replication Initiation: You're Fired! *Genes (Basel)* **8:**

Raymann K, Forterre P, Brochier-Armanet C & Gribaldo S (2014) Global phylogenomic analysis disentangles the complex evolutionary history of DNA replication in archaea. *Genome Biol Evol* **6:** 192–212

Reginato G, Cannavo E & Cejka P (2017) Physiological protein blocks direct the Mre11-Rad50-Xrs2 and Sae2 nuclease complex to initiate DNA end resection. *Genes Dev.* **31:** 2325–2330

Rinke C, Schwientek P, Sczyrba A, Ivanova NN, Anderson IJ, Cheng J-F, Darling A, Malfatti S, Swan BK, Gies EA, Dodsworth JA, Hedlund BP, Tsiamis G, Sievert SM, Liu W-T, Eisen JA, Hallam SJ, Kyrpides NC, Stepanauskas R, Rubin EM, et al (2013) Insights into the phylogeny and coding potential of microbial dark matter. *Nature* **499:** 431–437

Robb FT, Maeder DL, Brown JR, DiRuggiero J, Stump MD, Yeh RK, Weiss RB & Dunn DM (2001) Genomic sequence of hyperthermophile, Pyrococcus furiosus: Implications for physiology and enzymology. In *Methods in Enzymology* pp 134–157. Academic Press

Rojowska A, Lammens K, Seifert FU, Direnberger C, Feldmann H & Hopfner K-P (2014) Structure of the Rad50 DNA double-strand break repair protein in complex with DNA. *EMBO J.* **33:** 2847–2859

Rolland J, Gueguen Y, Persillon C, Masson J-M & Dietrich J (2004) Characterization of a thermophilic DNA ligase from the archaeon Thermococcus fumicolans. *FEMS Microbiol. Lett.* **236:** 267–273

Rothschild LJ & Mancinelli RL (2001) Life in extreme environments. *Nature*

Rouillon C, Henneke G, Flament D, Querellou J & Raffin J-P (2007) DNA polymerase switching on homotrimeric PCNA at the replication fork of the euryarchaea Pyrococcus abyssi. *J. Mol. Biol.* **369:** 343–355

Rouillon C & White MF (2011) The evolution and mechanisms of nucleotide excision repair proteins. *Research in Microbiology* **162:** 19–26

Rowen L & Kornberg A (1978) Primase, the dnaG protein of Escherichia coli. An enzyme which starts DNA chains. *J. Biol. Chem.* **253:** 758–764

Rzechorzek NJ, Blackwood JK, Bray SM, Maman JD, Pellegrini L & Robinson NP (2014) Structure of the hexameric HerA ATPase reveals a mechanism of translocation-coupled DNA-end processing in archaea. *Nat Commun* **5:** 5506

S

Sachadyn P (2010) Conservation and diversity of MutS proteins. *Mutation Research/Fundamental and Molecular Mechanisms of Mutagenesis* **694:** 20–30

Samuels M, Gulati G, Shin J-H, Opara R, McSweeney E, Sekedat M, Long S, Kelman Z & Jeruzalmi D (2009) A biochemically active MCM-like helicase in Bacillus cereus. *Nucleic Acids Res* **37:** 4441–4452

Sancar A, Lindsey-Boltz LA, Ü nsal-Kaccedil;maz K & Linn S (2004) Molecular Mechanisms of Mammalian Dna Repair and the Dna Damage Checkpoints. *Annual Review of Biochemistry* **73:** 39–85

Sanchez-Berrondo J, Mesa P, Ibarra A, Martínez-Jiménez MI, Blanco L, Méndez J, Boskovic J & Montoya G (2012) Molecular architecture of a multifunctional MCM complex. *Nucleic Acids Res.* **40:** 1366–1380

Santangelo TJ, Cubonová L & Reeve JN (2010) Thermococcus kodakarensis genetics: TK1827-encoded beta-glycosidase, new positive-selection protocol, and targeted and repetitive deletion technology. *Appl. Environ. Microbiol.* **76:** 1044–1052

Sarmiento F, Long F, Cann I & Whitman WB (2014) Diversity of the DNA Replication System in the Archaea Domain. *Archaea* **2014:**

Sarmiento F, Mrázek J & Whitman WB (2013) Genome-scale analysis of gene function in the hydrogenotrophic methanogenic archaeon Methanococcus maripaludis. *Proc. Natl. Acad. Sci. U.S.A.* **110:** 4726–4731

Sartori AA & Jiricny J (2003) Enzymology of base excision repair in the hyperthermophilic archaeon Pyrobaculum aerophilum. *J. Biol. Chem.* **278:** 24563–24576

Sartori AA, Lukas C, Coates J, Mistrik M, Fu S, Bartek J, Baer R, Lukas J & Jackson SP (2007) Human CtIP promotes DNA end resection. *Nature* **450:** 509–514

Sauguet L, Raia P, Henneke G & Delarue M (2016) Shared active site architecture between archaeal PolD and multi-subunit RNA polymerases revealed by X-ray crystallography. *Nat Commun* **0:**

Schlacher K, Cox MM, Woodgate R & Goodman MF (2006) RecA acts in trans to allow replication of damaged DNA by DNA polymerase V. *Nature* **442:** 883–887

Scholz S, Sonnenbichler J, Schäfer W & Hensel R (1992) Di-myo-inositol-1,1'-phosphate: a new inositol phosphate isolated from Pyrococcus woesei. *FEBS Lett.* **306:** 239–242

Seifert FU, Lammens K, Stoehr G, Kessler B & Hopfner K-P (2016) Structural mechanism of ATP-dependent DNA binding and DNA end bridging by eukaryotic Rad50. *EMBO J.* **35:** 759–772

Seitz EM, Brockman JP, Sandler SJ, Clark AJ & Kowalczykowski SC (1998) RadA protein is an archaeal RecA protein homolog that catalyzes DNA strand exchange. *Genes Dev* **12:** 1248–1253

Seitz EM, Haseltine CA & Kowalczykowski SC (2001) DNA recombination and repair in the Archaea. In, Microbiology B-A in A (ed) pp 101–169. Academic Press

Sharples GJ & Leach DR (1995) Structural and functional similarities between the SbcCD proteins of Escherichia coli and the RAD50 and MRE11 (RAD32) recombination and repair proteins of yeast. *Mol. Microbiol.* **17:** 1215–1217

Shibata A (2017) Regulation of repair pathway choice at two-ended DNA double-strand breaks. *Mutat. Res.* **803–805:** 51–55

Shibata A & Jeggo PA (2014) DNA double-strand break repair in a cellular context. *Clin Oncol (R Coll Radiol)* **26:** 243–249

Shibata A, Moiani D, Arvai AS, Perry J, Harding SM, Genois M-M, Maity R, van Rossum-Fikkert S, Kertokalio A, Romoli F, Ismail A, Ismalaj E, Petricci E, Neale MJ, Bristow RG, Masson J-Y, Wyman C, Jeggo PA & Tainer JA (2014) DNA Double-Strand Break Repair Pathway Choice Is Directed by Distinct MRE11 Nuclease Activities. *Molecular Cell* **53:** 7–18

Shiloh Y (2003) ATM and related protein kinases: safeguarding genome integrity. *Nat. Rev. Cancer* **3:** 155–168

Shin DS, Pellegrini L, Daniels DS, Yelent B, Craig L, Bates D, Yu DS, Shivji MK, Hitomi C, Arvai AS, Volkmann N, Tsuruta H, Blundell TL, Venkitaraman AR & Tainer JA (2003) Full-length archaeal Rad51 structure and mutants: mechanisms for RAD51 assembly and control by BRCA2. *EMBO J* **22:** 4566–4576

Shin DS, Pratt AJ & Tainer JA (2014) Archaeal Genome Guardians Give Insights into Eukaryotic DNA Replication and Damage Response Proteins. *Archaea* **2014:**

Shiraishi M, Ishino S, Yoshida K, Yamagami T, Cann I & Ishino Y (2016) PCNA is involved in the EndoQ-mediated DNA repair process in Thermococcales. *Sci Rep* **6:**

Shull ERP, Lee Y, Nakane H, Stracker TH, Zhao J, Russell HR, Petrini JHJ & McKinnon PJ (2009) Differential DNA damage signaling accounts for distinct neural apoptotic responses in ATLD and NBS. *Genes Dev.* **23:** 171–180

Sigurdsson S, Trujillo K, Song B, Stratton S & Sung P (2001) Basis for avid homologous DNA strand exchange by human Rad51 and RPA. *J. Biol. Chem.* **276:** 8798–8806

Soler N, Marguet E, Cortez D, Desnoues N, Keller J, van Tilbeurgh H, Sezonov G & Forterre P (2010) Two novel families of plasmids from hyperthermophilic archaea encoding new families of replication proteins. *Nucleic Acids Res.* **38:** 5088–5104

Spang A, Caceres EF & Ettema TJG (2017) Genomic exploration of the diversity, ecology, and evolution of the archaeal domain of life. *Science* **357:**

Spies M, Kil Y, Masui R, Kato R, Kujo C, Ohshima T, Kuramitsu S & Lanzov V (2000) The RadA protein from a hyperthermophilic archaeon Pyrobaculum islandicum is a DNA-dependent ATPase that exhibits two disparate catalytic modes, with a transition temperature at 75 °C. *European Journal of Biochemistry* **267:** 1125–1137

Sriskanda V, Kelman Z, Hurwitz J & Shuman S (2000) Characterization of an ATP-dependent DNA ligase from the thermophilic archaeon Methanobacterium thermoautotrophicum. *Nucleic Acids Res.* **28:** 2221–2228

Sterner R & Liebl W (2001) Thermophilic adaptation of proteins. *Crit. Rev. Biochem. Mol. Biol.* **36:** 39–106

Stetter KO (2002) Hyperthermophilic Microorganisms. In *Astrobiology: The Quest for the Conditions of Life*, Horneck G & Baumstark-Khan C (eds) pp 169–184. Berlin, Heidelberg: Springer Berlin Heidelberg

Stetter KO (2006a) History of discovery of the first hyperthermophiles. *Extremophiles* **10:** 357–362

Stetter KO (2006b) Hyperthermophiles in the history of life. *Philos Trans R Soc Lond B Biol Sci* **361:** 1837–1843

Stetter KO, Thomm M, Winter J, Wildgruber G, Huber H, Zillig W, Jané-Covic D, König H, Palm P & Wunderl S (1981) Methanothermus fervidus, sp. nov., a novel extremely thermophilic methanogen isolated from an Icelandic hot spring. *Zentralblatt für Bakteriologie Mikrobiologie und Hygiene: I. Abt. Originale C: Allgemeine, angewandte und ökologische Mikrobiologie* **2:** 166–178

Stojkovič G, Makarova AV, Wanrooij PH, Forslund J, Burgers PM & Wanrooij S (2016) Oxidative DNA damage stalls the human mitochondrial replisome. *Sci Rep* **6:** 28942

Stracker TH & Petrini JHJ (2011) The MRE11 complex: starting from the ends. *Nat Rev Mol Cell Biol* **12:** 90–103

Sung P & Klein H (2006) Mechanism of homologous recombination: mediators and helicases take on regulatory functions. *Nat. Rev. Mol. Cell Biol.* **7:** 739–750

Sung P, Krejci L, Van Komen S & Sehorn MG (2003) Rad51 recombinase and recombination mediators. *J. Biol. Chem.* **278:** 42729–42732

Sung P & Stratton SA (1996) Yeast Rad51 recombinase mediates polar DNA strand exchange in the absence of ATP hydrolysis. *J. Biol. Chem.* **271:** 27983–27986

Sung S, Li F, Park YB, Kim JS, Kim A-K, Song O, Kim J, Che J, Lee SE & Cho Y (2014) DNA end recognition by the Mre11 nuclease dimer: insights into resection and repair of damaged DNA. *EMBO J* **33:** 2422–2435

Syed A & Tainer JA (2018) The MRE11-RAD50-NBS1 Complex Conducts the Orchestration of Damage Signaling and Outcomes to Stress in DNA Replication and Repair. *Annu. Rev. Biochem.* **87:** 263–294

Symington LS & Gautier J (2011) Double-strand break end resection and repair pathway choice. *Annu. Rev. Genet.* **45:** 247–271

Szalkai B, Scheer I, Nagy K, Vértessy BG & Grolmusz V (2014) The Metagenomic Telescope. *PLoS ONE* **9:** e101605

T

Tainer JA, McCammon JA & Ivanov I (2010) Recognition of the Ring-Opened State of Proliferating Cell Nuclear Antigen by Replication Factor C Promotes Eukaryotic Clamp-Loading. *J Am Chem Soc* **132:** 7372–7378

Takai K, Nakamura K, Toki T, Tsunogai U, Miyazaki M, Miyazaki J, Hirayama H, Nakagawa S, Nunoura T & Horikoshi K (2008) Cell proliferation at 122 degrees C and isotopically heavy CH4 production by a hyperthermophilic methanogen under high-pressure cultivation. *Proc. Natl. Acad. Sci. U.S.A.* **105:** 10949–10954

Taylor AMR, Groom A & Byrd PJ (2004) Ataxia-telangiectasia-like disorder (ATLD)-its clinical presentation and molecular basis. *DNA Repair (Amst.)* **3:** 1219–1225

Thiel A, Michoud G, Moalic Y, Flament D & Jebbar M (2014) Genetic Manipulations of the Hyperthermophilic Piezophilic Archaeon Thermococcus barophilus. *Appl Environ Microbiol* **80:** 2299–2306

Thompson MJ & Eisenberg D (1999) Transproteomic evidence of a loop-deletion mechanism for enhancing protein thermostability. *J. Mol. Biol.* **290:** 595–604

Tittel-Elmer M, Alabert C, Pasero P & Cobb JA (2009) The MRX complex stabilizes the replisome independently of the S phase checkpoint during replication stress. *EMBO J.* **28:** 1142–1156

Tittel-Elmer M, Lengronne A, Davidson MB, Bacal J, François P, Hohl M, Petrini JHJ, Pasero P & Cobb JA (2012) Cohesin association to replication sites depends on rad50 and promotes fork restart. *Mol. Cell* **48:** 98–108

Trakselis MA & Benkovic SJ (2001) Intricacies in ATP-dependent clamp loading: variations across replication systems. *Structure* **9:** 999–1004

Trenz K, Smith E, Smith S & Costanzo V (2006) ATM and ATR promote Mre11 dependent restart of collapsed replication forks and prevent accumulation of DNA breaks. *EMBO J.* **25:** 1764–1774

Trujillo KM, Roh DH, Chen L, Van Komen S, Tomkinson A & Sung P (2003) Yeast xrs2 binds DNA and helps target rad50 and mre11 to DNA ends. *J. Biol. Chem.* **278:** 48957–48964

Trujillo KM & Sung P (2001) DNA structure-specific nuclease activities in the Saccharomyces cerevisiae Rad50*Mre11 complex. *J. Biol. Chem.* **276:** 35458–35464

Trujillo KM, Yuan SS, Lee EY & Sung P (1998) Nuclease activities in a complex of human recombination and DNA repair factors Rad50, Mre11, and p95. *J. Biol. Chem.* **273:** 21447–21450

U

Uchisaka N, Takahashi N, Sato M, Kikuchi A, Mochizuki S, Imai K, Nonoyama S, Ohara O, Watanabe F, Mizutani S, Hanada R & Morio T (2009) Two Brothers with Ataxia-Telangiectasia-like Disorder with Lung Adenocarcinoma. *The Journal of Pediatrics* **155:** 435–438

V

Velichko AK, Petrova NV, Razin SV & Kantidze OL (2015) Mechanism of heat stress-induced cellular senescence elucidates the exclusive vulnerability of early S-phase cells to mild genotoxic stress. *Nucleic Acids Res.* **43:** 6309–6320

Vieille C & Zeikus GJ (2001) Hyperthermophilic Enzymes: Sources, Uses, and Molecular Mechanisms for Thermostability. *Microbiol Mol Biol Rev* **65:** 1–43

W

Waltes R, Kalb R, Gatei M, Kijas AW, Stumm M, Sobeck A, Wieland B, Varon R, Lerenthal Y, Lavin MF, Schindler D & Dörk T (2009) Human RAD50 Deficiency in a Nijmegen Breakage Syndrome-like Disorder. *Am J Hum Genet* **84:** 605–616

Wang W, Daley JM, Kwon Y, Krasner DS & Sung P (2017) Plasticity of the Mre11–Rad50–Xrs2–Sae2 nuclease ensemble in the processing of DNA-bound obstacles. *Genes Dev.* **31:** 2331–2336

Wang X, Lim HJ & Son A (2014) Characterization of denaturation and renaturation of DNA for DNA hybridization. *Environ Health Toxicol* **29:**

Warbrick E (2000) The puzzle of PCNA's many partners. *Bioessays* **22:** 997–1006

Wardell K, Haldenby S, Jones N, Liddell S, Ngo GHP & Allers T (2017) RadB acts in homologous recombination in the archaeon Haloferax volcanii, consistent with a role as recombination mediator. *DNA Repair (Amst.)* **55:** 7–16

Warters RL & Brizgys LM (1987) Apurinic site induction in the DNA of cells heated at hyperthermic temperatures. *J. Cell. Physiol.* **133:** 144–150

Weller GR & Doherty AJ (2001) A family of DNA repair ligases in bacteria? *FEBS Lett.* **505:** 340–342

West SC (2003) Molecular views of recombination proteins and their control. *Nat. Rev. Mol. Cell Biol.* **4:** 435–445

White MF (2011) Homologous recombination in the archaea: the means justify the ends. *Biochemical Society Transactions* **39:** 15–19

Williams GJ, Lees-Miller SP & Tainer JA (2010) Mre11-Rad50-Nbs1 conformations and the control of sensing, signaling, and effector responses at DNA double-strand breaks. *DNA Repair (Amst)* **9:** 1299–1306

Williams GJ, Williams RS, Williams JS, Moncalian G, Arvai A, Limbo O, Guenther G, SilDas S, Hammel M, Russell P & Tainer JA (2011) ABC ATPase signature helices in Rad50 link nucleotide state to Mre11 interface for DNA repair. *Nat Struct Mol Biol* **18:** 423–431

Williams RS, Moncalian G, Williams JS, Yamada Y, Limbo O, Shin DS, Groocock LM, Cahill D, Hitomi C, Guenther G, Moiani D, Carney JP, Russell P & Tainer JA (2008) Mre11 Dimers Coordinate DNA End Bridging and Nuclease Processing in Double-Strand-Break Repair. *Cell* **135:** 97–109

Wilson TE, Topper LM & Palmbos PL (2003) Non-homologous end-joining: bacteria join the chromosome breakdance. *Trends in Biochemical Sciences* **28:** 62–66

Woese CR (1987) Bacterial evolution. *Microbiol. Rev.* **51:** 221–271

Woese CR & Fox GE (1977) Phylogenetic structure of the prokaryotic domain: the primary kingdoms. *Proc Natl Acad Sci U S A* **74:** 5088–5090

Woese CR, Kandler O & Wheelis ML (1990) Towards a natural system of organisms: proposal for the domains Archaea, Bacteria, and Eucarya. *Proc Natl Acad Sci U S A* **87:** 4576–4579

Woods WG & Dyall-Smith ML (1997) Construction and analysis of a recombination-deficient (radA) mutant of Haloferax volcanii. *Mol. Microbiol.* **23:** 791–797

Wu Y, He Y, Moya IA, Qian X & Luo Y (2004) Crystal structure of archaeal recombinase RADA: a snapshot of its extended conformation. *Mol. Cell* **15:** 423–435

Wu Z, Liu J, Yang H & Xiang H (2014) DNA replication origins in archaea. *Front Microbiol* **5:**

X

Xu H, Zhang P, Liu L & Lee MYWT (2001) A Novel PCNA-Binding Motif Identified by the Panning of a Random Peptide Display Library. *Biochemistry* **40:** 4512–4520

Xu L & Marians KJ (2003) PriA mediates DNA replication pathway choice at recombination intermediates. *Mol. Cell* **11:** 817–826

Xu X, Yan C, Kossmann BR & Ivanov I (2016) Secondary Interaction Interfaces with PCNA Control Conformational Switching of DNA Polymerase PolB from Polymerization to Editing. *J Phys Chem B* **120:** 8379–8388

Y

Yamagishi A, Kon T, Takahashi G & Oshima T (1998) From the common ancestor of all living organisms to protoeukaryotic cell. In *Thermophiles: the keys to molecular evolution and the origin of Life ?* pp 287–295. London: Taylor & Francis: Juergen Wiegel, Adams W.W. Michael

Yamtich J & Sweasy JB (2010) DNA Polymerase Family X: Function, Structure, and Cellular Roles. *Biochim Biophys Acta* **1804:** 1136–1150

Yang S, VanLoock MS, Yu X & Egelman EH (2001a) Comparison of bacteriophage T4 UvsX and human Rad51 filaments suggests that RecA-like polymers may have evolved independently. *J. Mol. Biol.* **312:** 999–1009

Yang S, Yu X, Seitz EM, Kowalczykowski SC & Egelman EH (2001b) Archaeal RadA protein binds DNA as both helical filaments and octameric rings11Edited by M. Belfort. *Journal of Molecular Biology* **314:** 1077–1085

Yang W (2000) Structure and function of mismatch repair proteins. *Mutation Research/DNA Repair* **460:** 245–256

Yao N, Turner J, Kelman Z, Stukenberg PT, Dean F, Shechter D, Pan ZQ, Hurwitz J & O'Donnell M (1996) Clamp loading, unloading and intrinsic stability of the PCNA, beta and gp45 sliding clamps of human, E. coli and T4 replicases. *Genes Cells* **1:** 101–113

Yeeles JTP, Poli J, Marians KJ & Pasero P (2013) Rescuing Stalled or Damaged Replication Forks. *Cold Spring Harb Perspect Biol* **5:** a012815

Yip KS, Britton KL, Stillman TJ, Lebbink J, de Vos WM, Robb FT, Vetriani C, Maeder D & Rice DW (1998) Insights into the molecular basis of thermal stability from the analysis of ion-pair networks in the glutamate dehydrogenase family. *Eur. J. Biochem.* **255:** 336–346

Z

Zaremba-Niedzwiedzka K, Caceres EF, Saw JH, Bäckström D, Juzokaite L, Vancaester E, Seitz KW, Anantharaman K, Starnawski P, Kjeldsen KU, Stott MB, Nunoura T, Banfield JF, Schramm A, Baker BJ, Spang A & Ettema TJG (2017) Asgard archaea illuminate the origin of eukaryotic cellular complexity. *Nature* **541:** 353–358

Zhang C, Tian B, Li S, Ao X, Dalgaard K, Gökce S, Liang Y & She Q (2013) Genetic manipulation in Sulfolobus islandicus and functional analysis of DNA repair genes. *Biochem. Soc. Trans.* **41:** 405–410

Zhang S, Wei T, Hou G, Zhang C, Liang P, Ni J, Sheng D & Shen Y (2008) Archaeal DNA helicase HerA interacts with Mre11 homologue and unwinds blunt-ended double-stranded DNA and recombination intermediates. *DNA Repair (Amst.)* **7:** 380–391

Zheng T, Huang Q, Zhang C, Ni J, She Q & Shen Y (2012) Development of a simvastatin selection marker for a hyperthermophilic acidophile, Sulfolobus islandicus. *Appl. Environ. Microbiol.* **78:** 568–574

Zhou Y, Caron P, Legube G & Paull TT (2014) Quantitation of DNA double-strand break resection intermediates in human cells. *Nucleic Acids Res* **42:** e19

Zhu Z, Chung W-H, Shim EY, Lee SE & Ira G (2008) Sgs1 helicase and two nucleases Dna2 and Exo1 resect DNA double-strand break ends. *Cell* **134:** 981–994

Zobell CE (1952) Bacterial Life at the Bottom of the Philippine Trench. *Science* **115:** 507–508

Annexes

I. Polymerase B and Polymerase D from *Pyrococcus abyssi*

*Pab*PolB is a monomeric DNA polymerase and the crystal structure of *Pab*PolB shown that is looks like a "hand" (Figure 70A). The "Palm" domain (in orange) contains the catalytic site (5'→3' DNA polymerization activity); the "finger" domain (in pink) has nucleotides recognition activity; the "Thumb" domain (in red) is for DNA binding; the N-terminal (in green) is responsible for recognizing and binding deaminated bases 4 nt upstream the primer-template junction during DNA replication; and the last domain of *Pab*PolB is "exonuclease domain" (in blue) which carries a 3'→5' exonuclease proofreading activity (Gouge *et al*, 2012; Gueguen *et al*, 2001).

*Pab*PolD is a heterodimeric DNA polymerase which is composed of a large subunit (DP2) and a small subunit (DP1). The subunit DP2 possess the 5'→3' polymerization activity, and the subunit DP1 is responsible for 3'→5' exonuclease activity (Cann *et al*, 1998; Gueguen *et al*, 2001). Recently, the crystal structures of these two subunits of *Pab*PolD have been determined (Figure 70B). The study revealed that the catalytic core of DP1 is different from all other known DNA polymerase, but possesses a catalytic site similar to RNA polymerase family. Interestingly, the subunit DP1has a structure similar to Mre11 which has also a 3'→5' exonuclease activity (Sauguet *et al*, 2016).

Biochemical studies have demonstrated that both *Pab*PolB and *Pab*PolD are primer-directed DNA polymerase, but *Pol*PolB recognizes only DNA primer, while *Pab*PolD recognizes both DNA and RNA primer, and preferentially to primed template compared to *Pab*PolB. Hence, it is suggesting that *Pab*PolB might function upon leading strand while *Pab*PolD could be involved in the synthesis of both lagging strand and leading strand. In addition, both *Pab*PolB and *Pab*PolD harbor DNA strand displacement activity (Henneke *et al*, 2005; Henneke, 2012). In addition, archaeal PolB is not only used for DNA replication, but also implicated in DNA repair pathways. For example, PolB from *T. kodakarensis* was involved in RER (ribonucleotide excision repair) pathway to remove the ribonucleotide inserted in DNA (Heider *et al*, 2017).

Moreover, genetic studies have shown that archaeal PolD enzyme is always essential, but not for PolB. For example, in *Halobacterium sp. NRC-1*, both PolB and PolD are essential for cellular survival (Berquist *et al*, 2007). In contrast, in *T. kodakarensis* and *Methanococcus maripaludis S2*, it is unable to introduce *polD* mutation *in vivo*, however, cellules lacking PolB can grow normally but with an increased sensitivity to UV irradiation (Čuboňová *et al*, 2013; Sarmiento *et al*, 2013)(Čuboňová *et al*, 2013; Sarmiento *et al*, 2013).

.

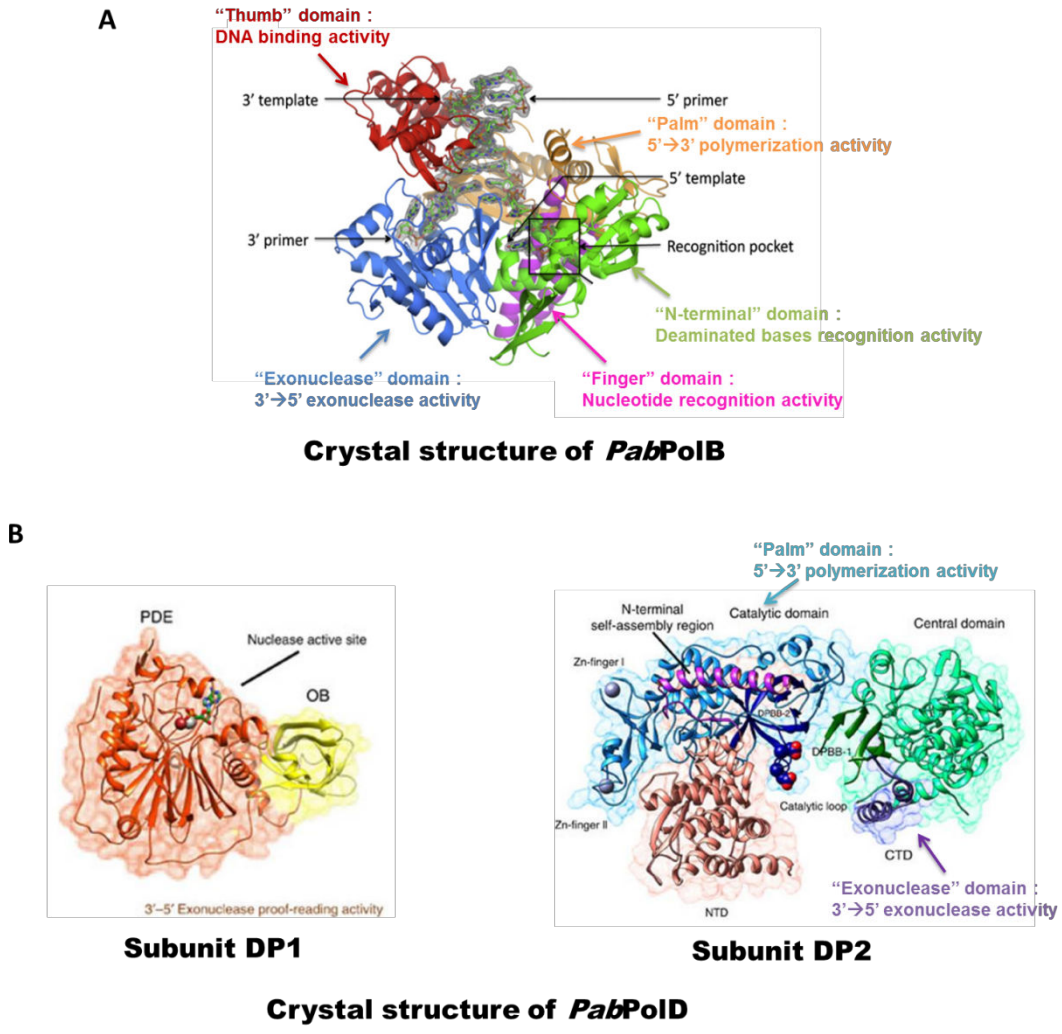

Figure 70: Crystal structure of *Pab*PolB and *Pab*PolD

II. Materials and Methods of Supplementary data of article "Physical and functional interplay between PCNA DNA clamp and Mr11-Rad50 complex from the archaeon Pyrococcus furiosus" (Hogrel et al, 2018)

MATERIAL AND METHODS (Supplementary data)

SPR experiments

Data were obtained using a Reichert SR7000DC spectrometer instrument (Reichert Iinc., Buffalo, NY). The running buffer was 25 mM HEPES pH 7.0, 150 or 300 mM NaCl, 1 mM DTT, 0.05 % Tween 20, and the flow rate was 25 µl/min. *Pfu*PCNA was immobilized on a mixed self-assembled monolayer (10 % C11-(OEG)6-COOH: 90 % C11-(OEG)3-OH), Reichert Inc.) *via* classical amine coupling chemistry and the chip was stabilized after serial injections of 100 mM H_3PO_4 (3 x 30 s). Each curve displayed was double referenced with a set of blank buffer injections. When the interaction with Mre11 PIP-like peptide was analysed, a concentration range from 0.37 µM to 30 µM of peptide was injected on the *Pfu*PCNA chip at 25°C. Acquisitions with *Pfu*MR were performed as described above, with a running buffer containing 25 mM HEPES pH 7.0, 300 mM NaCl, 1 mM DTT, 0.05 % Tween 20 and a concentration range of *Pfu*MR from 1.56 nM to 50 nM. Data were then fitted using a global analysis method with Scrubber 2.0a software (Biologic Software, Australia). Kinetic constants for binding were calculated using global fitting analysis that accounts for both association and dissociation phases as well as the maximal level of complex formation.

Co-immunoprecipitation experiments

Experiments were performed as described in the "materials and methods" section, except for the following steps. In 20 µl reaction, 1µg *Pfu*PCNA alone was incubated 10 min at 4°C with anti-PCNA Dynabeads prepared in 20 mM Tris-HCl pH 8.0, 150 mM NaCl, 1 mM DTT). Beads were washed with binding buffer (25 mM HEPES pH 7.0, 150 mM NaCl, 1 mM DTT, 0.05 % Tween 20). Then in 20 µl reaction, 5 µg *Pfu*MR or *Pfu*MR ∆PIP complex were added to *Pfu*PCNA in binding buffer 150 or 300 mM NaCl. The resulting protein complexes were incubated 15 min at 4°C. Beads were washed 3 times with 100 µl binding buffer 150 mM or 300 mM NaCl before final elution. Fractions bound to the beads were analysed either by Western-blotting (using His-tag antibody) or Coomassie blue staining as indicated in figure legends.

DNA substrates

Labelled dsDNA substrates were constructed with the following sequences. Phosphorothiate bonds are indicated by "s" between nucleotides.

S50/50:

5'Cy5-CTGCAGGGTTTTTGTTCCAGTCTGTAGCACTGTGTAAGACAGGCCAGATG -3'

5'-CATCTGGCCTG-TCTTACACAGTGCTACAGACTGGAACAAAAACCCTGCAG-3'

Biotine_S50/50s

5'Cy5-C**T(biotin)**GCAGGGTTTTTGTTCCAGTCTGTAGCACTGTGTAAGACAGGCCAGATG -3'

5'-CATCTGGCCTGTCTTACACAGTGCTACAGACTGGAACAAAAACCCsTsGsCsAsG-3'.

3'Cy5_S50/50s

5'-CTGCAGGGTTTTTGTTCCAGTCTGTAGCACTGTGTAAGACAGGCCAGATG-3'Cy5

5'-CATCTGGCCTGTCTTACACAGTGCTACAGACTGGAACAAAAACCCsTsGsCsAsG-3'.

3'Cy5_S50s/50s

5’-CTGCAGGGTTTTTGTTCCAGTCTGTAGCACTGTGTAAGACAGGCCsAsGsAsTsG-3’Cy5

5’-CATCTGGCCTGTCTTACACAGTGCTACAGACTGGAACAAAAACCCsTsGsCsAsG-3’.

S50/50s:

5’Cy5-CTGCAGGGTTTTTGTTCCAGTCTGTAGCACTGTGTAAGACAGGCCAGATG-3’

5’-CATCTGGCCTGTCTTACACAGTGCTACAGACTGGAACAAAAACCCsTsGsCsAsG-3’.

S50s/50s:

5’Cy5-CTGCAGGGTTTTTGTTCCAGTCTGTAGCACTGTGTAAGACAGGCCsAsGsAsTsG-3’

5’-CATCTGGCCTGTCTTACACAGTGCTACAGACTGGAACAAAAACCCsTsGsCsAsG-3’.

S87/87s:

5’Cy5-CAGGAAACAGCTATGACCATGATTACGAATTCGAGCTCGGTACCCGGGGATCCTCTAGAG
TCGACCTGCAGGCATGCAAGCTTGGCA-3’

5’-TGCCAAGCTTGCATGCCTGCAGGTCGACTCTAGAGGATCCCCGGGTACCGAGCTCGAATTCG
TAATCATGGTCATAGCTGTTsTsCsCsTsG-3’

S87s/87s:

5’Cy5-CAGGAAACAGCTATGACCATGATTACGAATTCGAGCTCGGTACCCGGGGATCCTCTAGAG
TCGACCTGCAGGCATGCAAGCTsTsGsGsCsA-3’

5’-TGCCAAGCTTGCATGCCTGCAGGTCGACTCTAGAGGATCCCCGGGTACCGAGCTCGAATTCG
TAATCATGGTCATAGCTGTTsTsCsCsTsG-3’

RQ-S87s/87s:

5’FAM- CAGGAAACAGCTATGACCATGATTACGAATTCGAGCTCGGTACCCGGGGATCCTCTAGA
GTCGACCTGCAGGCATGCAAGCTsTsGsGsCsA-3’

5’-TGCCAAGCTTGCATGCCTGCAGGTCGACTCTAGAGGATCCCCGGGTACCGAGCTCGAA
TTCGTAATCATGGTCATAGCTGTTs**Ts(BHQ1)**CsCsTsG-3’

RQ23-S87s/87s:

5’CAGGAAACAGCTATGACCATGA**T(FAM)**TACGAATTCGAGCTCGGTACCCGGGGATCCTCTAGA
GTCGACCTGCAGGCATGCAAGCTsTsGsGsCsA-3’

5’- TGCCAAGCTTGCATGCCTGCAGGTCGACTCTAGAGGATCCCCGGGTACCGAGCTCGAATTCG
TAA**T(BHQ1)**CATGGTCATAGCTGTTsTsCsCsTsG-3’

The following oligonucleotides were used as reverse complement to avoid re-annealing of DNA product onto the dsDNA substrate.

Trap RC50:

5’-CTGCAGGGTTTTTGTTCCAGTCTGTAGCACTGTGTAAGACAGGCCAGATG-3’

Trap RC87:

5’-CAGGAAACAGCTATGACCATGATTACGAATTCGAGCTCGGTACCCGGGGATCCTCTAGAGTCG
ACCTGCAGGCATGCAAGCTTGGCA-3’

Trap 3’87RC

5’-CAGGAAACAGCTATGACCATGATTACGAAT-3’

Electrophoretic mobility shift assays (EMSAs)

In 10 µl reaction, 25 nM DNA substrate S50/50s were pre-incubated with 50 or 200 nM *Pfu*PCNA, when indicated, in a DNA binding buffer (25 mM HEPES pH, 7.0, 150 or 300 mM NaCl, 1 mM DTT, 0.5 mg/ml

BSA, 0.1% Triton-X100) complemented with 1 mM ATP, 5 mM $MgCl_2$ and 5 mM $MnCl_2$ at ambient temperature for 5 min. DNA substrate or DNA/*Pfu*PCNA complex were then incubated with a concentration range from 0 nM to 1000 nM of *Pfu*MR at ambient temperature for 15 min. Samples were loaded on a 0.75% agarose gel and run for 4 hrs at 60 V at 4°C with running buffer 1X TBE. Gels were imaged with fluorimager Typhoon 9500 (GE Healthcare) and quantified with Image Quant software.

ATPase assays

Pre-incubation of 200 nM *Pfu*MR wt or ΔPIP with 400 nM *Pfu*PCNA (when indicated) was performed at 65°C for 10 min. Proteins were then incubated at 65°C for 30 min in 15 µl buffer containing 25 mM HEPES pH 7.0, 300 mM NaCl, 1 mM DTT, 0.5 mg/ml BSA, 5 mM $MgCl_2$ complemented with 200 nM dsDNA S50s/50s, when indicated, before adding 1 mM ATP and ATP γ32P (62.5 nCi/µl) for 60 min. Two microliters of reaction solution were collected at various time points and spotted on TLC plates (PEI-cellulose, Nagel). ATP, ADP and Pi were separated by TLC using 250 mM KH_2PO_4. Products were analysed by autoradiography and level of Pi generated was quantified by MultiGauge (Version 3.0) software to quantify ATPase activity. Three independent experiments were performed to measure ATPase activities.

Native gel DNA unwinding assays

Reactions were performed as described in "Real time fluorescence DNA unwinding assays" section of the materials and methods, except that at the end of incubation at 55°C, the samples were loaded onto an electrophoresis gel composed of 10% polyacrylamide 19:1 and 1X TBE in a running buffer (1X TBE) for 3h at 120 V. Labelled fragments were analysed with fluorimager Typhoon 9500 (GE Healthcare) and quantified with Image Quant software.

FIGURE LEGENDS – SUPPLEMENTAL DATA

Figure S1. (A) Purified recombinant *P. furiosus* PCNA, Mre11-Rad50 and truncated constructs of Mre11 and Rad50. (B) Construct schematics for *Pfu*Mre11 and *Pfu*Rad50 (adapted from (1)). *Pfu*Rad50-link constructs contain Gly-Ser repeat sequences to link Rad50 N and C terminal lobes. In *Pfu*Mre11 sequence, dotted arrow indicates a disordered region. In *Pfu*Rad50 sequences, black arrows show region binding with Mre11 RBD, the shortened version *Pfu*Rad50^{link2} lacks several amino acids required for Mre11 binding. (C) Influence of co-factors on the physical interaction between *Pfu*PCNA and *Pfu*MR. Co-immunoprecipitaion experiments were performed as described in the "Material and methods" section using beads coated with PCNA antibodies. *Pfu*PCNA and *Pfu*Mre11 were revealed through His-tag detection by western-blotting. The experiment was performed in condition containing 150 mM NaCl.

Figure S2. Mre11 and Hel308/Hjm proteins of order *Thermococcales* harbour a PIP-like motif. Alignment of selected C-terminal domains from archaeal proteins using ScanProsite with the pattern [PK]-x-[KRNA]-x-[GSPNK]-x(1,3)-[IL]-x(2)-[WFY]-[ILV] as anchor on archaeal proteins. The figure was generated using EsPript server and similar highlighted positions were determined using BLOSUM62 similarity matrix. Abbreviations: *Pfu*, Pyrococcus furiosus ; *Pab*, Pyrococcus abyssi ; *Pho*, Pyrococcus horikoshii ; *PspNA2*, Pyrococcus sp. NA2 ; *Pya*, Pyrococcus yayanosii ; *PspST04*, Pyrococcus sp.

ST04 ; *Pfe*, Palaeococcus ferrophilus ; *Ppa*, Palaeococcus pacificus DY20341 ; *Tga*, Thermococcus gammatolerans ; *TspAM4*, Thermococcus sp. AM4 ; *Tna*, Thermococcus nautili ; *Ton*, Thermococcus onnurineus ; *Teu*, Thermococcus eurythermalis ; *Tko*, Thermococcus kodakarensis ; *Tzi*, Thermococcus zilligii ; *Tpa*, Thermococcus paralvinellae ; *Tli*, Thermococcus litoralis ; *TspPK*, Thermococcus sp. PK ; *Tsi*, Thermococcus sibiricus MM 739 ; *Tsp4557*, Thermococcus sp. 4557 ; *Tcl*, Thermococcus cleftensis.

Figure S3. PIP-like motif of *Pfu*MR complex plays a key role in interaction with *Pfu*PCNA (A) Surface plasmon sensograms for binding of Mre11 PIP-like peptide onto immobilised *Pfu*PCNA with a concentration range from 0.37 µM to 30 µM of peptide and 30 µM of non-interacting peptide. The experiment was performed with running buffer containing 150 mM NaCl. (B) Left panel, SDS-PAGE of purified *Pfu*MR and *Pfu*MR ΔPIP proteins, right panel,co-immunoprecipitation assays with *Pfu*MR (wt or ΔPIP and *Pfu*PCNA in binding buffer with 150 or 300 mM NaCl. 1 µg of protein was loaded on SDS-PAGE as Input. IP corresponds to the immunoprecipitation assays in presence of beads coated with PCNA antibodies. Fractions bound to the beads were analysed by Coomassie blue staining. (C) Surface plasmon sensograms for binding of *Pfu*MR complex to immobilised *Pfu*PCNA from a concentration range from 1.56 nM to 50 nM of *Pfu*MR complex. Experimental curves were fitted with a model describing a PCNA:MR stoichiometry of 1:1 and a binding reaction with two events of distinct kinetic constants. Experiments were performed in condition containing 300 mM NaCl.

Figure S4. dsDNA end resection by *Pfu*MR nuclease activities. Reactions in (A) and (B) were performed in same conditions as Figure 3B and 3D, except that reaction buffer contained 150 mM NaCl. (C) Time course experiments. Reactions included 25 nM of dsDNA S50/50s incubated with 25 nM *Pfu*MR (left panel) at 70°C from 0 to 90 min and complemented by 50 nM *Pfu*PCNA (right panel). (D) 25 nM of DNA substrate were incubated at 70°C, 30 min with increasing concentrations of *Pfu*MR ΔPIP. (E) 25 nM of DNA substrate were pre-incubated with indicated concentrations of *Pfu*PCNA at room temperature for 5 min before adding 25 nM *Pfu*MR ΔPIP. Reactions were performed for 30 min at 70°C. Reaction buffer contained 300 mM NaCl.

Figure S5. *Pfu*PCNA and salinity do not influence DNA binding activity of *Pfu*MR. 25 nM of S50/50s DNA substrate incubated with an increasing concentration of *Pfu*MR complex at ambient temperature for 15 min complemented by 50 or 200 nM *Pfu*PCNA, when indicated, in condition containing 150 or 300 mM NaCl. Experiments were performed in triplicate and error bars correspond to standard deviation.

Figure S6. Influence of co-factors on the functional interaction between *Pfu*MR and *Pfu*PCNA. Reactions included 25 nM dsDNA S50/50s incubated 30 min at 70°C with 25 nM *Pfu*MR, complemented with 50 nM *Pfu*PCNA, 1 mM ATP, 5 mM $MgCl_2$ and 5 mM $MnCl_2$, when indicated. All experiments were performed in condition containing 300 mM NaCl.

Figure S7. Comparison of DNA resection by *Pfu*PCNA/MR wt and ΔPIP on different dsDNA substrates. DNA substrates are illustrated on top of the figures. 25 nM dsDNA substrates were pre-

incubated with 50 nM of *Pfu*PCNA at room temperature for 5 min before adding 25 nM *Pfu*MR. The reactions were performed for 30 min at 70°C.

Figure S8. DNA unwinding activity of *Pfu*PCNA/MR complex at 55°C. Reactions included 25 nM RQ-S87s/87s **(A)** or RQ23-S87s/87s **(B)** DNA substrates incubated 30 min at 55°C with 25 nM *Pfu*MR wt or ΔPIP, complemented with 50 nM *Pfu*PCNA, 1 mM ATP and 5 mM $MgCl_2$, 5 mM $MnCl_2$, when indicated. All experiments were performed in condition containing 300 mM NaCl.

Figure S9. *Pfu*PCNA has no effect on ATPase activity of *Pfu*MR. ATPase assays were carried out at 65°C with 200 nM *Pfu*MR wt or ΔPIP in presence of 1 mM ATP, 5 mM $MgCl_2$, and complemented with 200 nM dsDNA S50s/50s and 400 nM *Pfu*PCNA when indicated. Experiments were performed in triplicate and error bars correspond to standard deviation.

REFERENCE

1. Williams, G.J., Williams, R.S., Williams, J.S., Moncalian, G., Arvai, A.S., Limbo, O., Guenther, G., SilDas, S., Hammel, M., Russell, P. *et al.* (2011) ABC ATPase signature helices in Rad50 link nucleotide state to Mre11 interface for DNA repair. *Nature Structural & Molecular Biology*, **18**, 423-431.

UNIVERSITE SCIENCES BRETAGNE DE LA MER LOIRE ET DU LITTORAL

UBO Université de Bretagne Occidentale

Titre : **Études fonctionnelles des nouvelles interactions protéine-protéine impliquées potentiellement dans la recombinaison homologue chez les archées hyperthermophiles**

Mots clés : Archée hyperthermophile, Réparation/réplication/recombinaison de l'ADN, complexe PCNA/Mre11-Rad50, DNA Primase, recombinase RadA

Résumé : Les archées hyperthermophiles ont une température optimale de croissance supérieure à 80°C. Les cellules exposées à un stress thermique subissent une augmentation de la sensibilité aux agents induisant des cassures double brin de l'ADN. Les études sur les eucaryotes et bactéries ont démontré que la recombinaison homologue joue un rôle essentiel non seulement dans la réparation de l'ADN, mais aussi dans le redémarrage des arrêts de la fourche de réplication. Les enzymes associées aux étapes initiales de la recombinaison homologue chez les archées sont homologues à celles des eucaryotes, et différentes des analogues bactériens. De plus, plusieurs études ont démontré que les protéines impliquées dans la recombinaison homologue sont essentielles chez les archées hyperthermophiles, soulignant l'importance biologique de cette voie de réparation chez ces organismes particuliers. Le rôle de la recombinaison homologue pour la stabilité génomique a été bien étudié chez les eucaryotes et les bactéries, cependant, peu de ses propriétés fonctionnelles ont été étudiées chez les archées hyperthermophiles.

Pour mieux comprendre le mécanisme de recombinaison homologue impliquée au niveau de la maintenance génomique chez les archées, un réseau d'interactions protéine-protéines a été révélé précédemment au laboratoire à partir des protéines de *Pyrococcus abyssi*. Ces travaux ont démontré de nouvelles interactions où interviennent les protéines de la réplication et les protéines de la recombinaison de l'ADN. L'objet de cette étude de thèse est de présenter deux interactions : PCNA/Mre11-rad50 (MR) complexe et Primase/RadA. Pour la première fois chez *P. furiosus,* une interaction physique et fonctionnelle a été démontré entre le PCNA et le complexe MR (l'initiateur de HR). Un motif, situé en position C-terminale de Mre11, permet l'interaction avec PCNA. PCNA stimule l'activité endonucléase du complexe MR à distance proche de l'extrémité 5' d'une cassure double brin. Cette propriété est en accord avec l'intervention ultérieure des enzymes assurant la suite du mécanisme de réparation par recombinaison homologue. Par ailleurs, les protéines RadA, Primase et P41 ont été produites et purifiées. Leurs fonctions enzymatiques ont été confirmé. Cependant, nous n'avons pas pu caractériser la fonction de l'association de RadA/Primase.

Title : **Functional studies of new protein-protein interactions potentially involved in homologous recombination in hyperthermophilic archaea**

Keywords: Hyperthermophilic archaea, DNA repair/replication/recombination, PCNA/MR complex, Primase/RadA

Abstract: Hyperthermophilic archaea (HA) are found in high-temperature environments and grow optimally above 80°C. Usually, cells exposed to heat stress display an increased sensitivity to agents inducing double-stranded DNA breaks (DSBs). Studies in Eukaryotes and Bacteria have revealed that homologous recombination (HR) plays a crucial role not only in DNA DSBs repair, but also in the collapsed/stalled DNA replication fork restart. Recombinase and various HR-associated enzymes in archaea specifically resemble the eukaryotic homologues, rather than bacterial homologues. Furthermore, several studies have demonstrated the necessity of HR proteins in HA, suggesting that, HR is an important mechanism in HA. HR influencing genome stability has been well studied in Eukaryotes and Bacteria, however, few of its functional properties have been studied in HA.

To better understand how HR mechanism is involved in the archaeal genome maintenance process, a previous work proposed a protein-protein interaction network based on *Pyrococcus abyssi* proteins. Through the network, new interactions involving proteins from DNA replication and DNA recombination were highlighted. The targets of the study presented here for two protein interaction are: PCNA/Mre11-rad50 complex (MR complex) and Primase/RadA. For the first time in *P. furiosus*, we showed both physical and functional interactions between PCNA (*Maestro* in DNA replication) and MR complex (initiator of HR). we have identified a PCNA-interaction motif (PIP) located in the C-terminal of Mre11, and shown that PCNA stimulated MR complex endonuclease cleavage proximal to the s' strand of DNA DSBs at physiological ionic strength. For the second interaction, we have purified the proteins *Pab*RadA/*Pfu*RadA, *Pab*Primase and *Pab*P41, and confirmed its enzymatic functions. However, we were not able to characterize the function of Primase/RadA association.